



**ROBERT GORDON  
UNIVERSITY•ABERDEEN**

## **OpenAIR@RGU**

### **The Open Access Institutional Repository at Robert Gordon University**

<http://openair.rgu.ac.uk>

#### **Citation Details**

**Citation for the version of the work held in 'OpenAIR@RGU':**

PESTANA, C. J., 2012. Monitoring and regulating cyanobacterial metabolites (microcystins and geosmin) in aquatic systems. Available from *OpenAIR@RGU*. [online]. Available from: <http://openair.rgu.ac.uk>

#### **Copyright**

Items in 'OpenAIR@RGU', Robert Gordon University Open Access Institutional Repository, are protected by copyright and intellectual property law. If you believe that any material held in 'OpenAIR@RGU' infringes copyright, please contact [openair-help@rgu.ac.uk](mailto:openair-help@rgu.ac.uk) with details. The item will be removed from the repository while the claim is investigated.

**Monitoring and regulating cyanobacterial  
metabolites (microcystins and geosmin) in  
aquatic systems**

**By  
Carlos João Pestana**

**A thesis submitted in partial fulfilment of the  
degree of Doctor of Philosophy**

**Robert Gordon University  
April 2012**

# TABLE OF CONTENTS

---

## Contents

Cover page .....	i
Table of contents.....	ii
Declaration.....	v
Dedication.....	vi
Acknowledgements.....	vii
Abbreviations.....	viii
Abstract.....	1
1 Introduction.....	4
1.1 Origins and distribution of cyanobacteria .....	4
1.2 Cyanobacterial blooms: cause and effect.....	6
1.3 Cyanobacterial secondary metabolites.....	11
1.3.1 Cyanotoxins.....	12
1.3.2 Taste and odour compounds.....	26
1.4 Water treatment options for cyanobacterial secondary metabolites (microcystins, geosmin, and 2-methylisoborneol).....	30
1.4.1 Conventional water treatment methods .....	31
1.4.2 Advanced water treatment.....	37
1.5 Semi-conductor photocatalysis.....	42
1.6 Aims.....	47
2 Pheromonal activity of microcystin-LR in understanding the control of microcystins in water.....	51
2.1 Introduction .....	51

2.2	Materials and Methods .....	55
2.2.1	Cultures .....	55
2.2.2	Media.....	55
2.2.3	Cell enumeration by flow cytometry .....	56
2.2.4	Analysis of microcystins.....	57
2.2.4.1	HPLC-PDA analysis of microcystins .....	57
2.2.4.2	HPLC-MS analysis of microcystins.....	58
2.2.4.3	UPLC-MS analysis of microcystins.....	59
2.2.5	Elucidation of growth characteristics of four different <i>M. aeruginosa</i> strains	60
2.2.6	Stable isotope labelling microcystins with <sup>15</sup> N.....	61
2.2.7	Assessing the impact of microcystin as a pheromone.....	64
2.3	Results .....	70
2.3.1	Elucidation of growth characteristics of four different <i>M. aeruginosa</i> strains	70
2.3.2	Assessing the impact of microcystin as a pheromone.....	82
2.4	Discussion.....	105
3	Photocatalytic Water Treatment.....	119
3.1	Introduction .....	119
3.2	Materials and methods.....	125
3.2.1	Reagents.....	125
3.2.2	HPLC-PDA detection of analytes (pollutants and microcystins)..	125

3.2.3	Photocatalytic destruction of microcystin-LR with Degussa P25.	127
3.2.4	Photocatalytic destruction of microcystin-LR with TiO <sub>2</sub> Photospheres™ 15µm.....	128
3.2.5	Photocatalytic destruction of microcystin-LR with Degussa P25, Photospheres™ 15µm, and Photospheres™ MTO/0131.....	129
3.2.6	Light and scanning electron microscopic investigation of Photosphere™ samples.....	131
3.2.7	Evaluation of the removal of fines from Photospheres™ preparations and weight adjustment.....	131
3.2.8	Photocatalytic destruction of microcystin-LR with three different Photospheres™ preparations and influence of catalyst load.....	132
3.2.9	Photocatalytic destruction of different microcystin variants and nodularin with Photospheres™ 40µm .....	132
3.2.10	Investigation of photosphere™ 40µm reuse .....	133
3.2.11	Evaluation of the use of light emitting diodes (LEDs) in the photocatalytic destruction of microcystin-LR.....	134
3.2.12	Evaluation of Photospheres™ 40µm for the removal of waste water pollutants .....	135
3.3	Results .....	138
3.3.1	Photocatalytic destruction of microcystin-LR with Photospheres™ and Degussa P25.....	138
3.3.2	Photocatalytic destruction of microcystin-LR with Photospheres™ 15µm, Photospheres™ MTO/0131 and P25.....	141

3.3.3	Light and scanning electron microscopic investigation of Photosphere™ samples.....	144
3.3.4	Effects of a fines-removal step and weight adjustment of different types of Photospheres™ and the effect of catalyst load .....	149
3.3.5	Photocatalytic destruction of 11 different microcystin variants with Photospheres™40µm.....	155
3.3.6	Evaluation of the use of light emitting diodes (LEDs) in the photocatalytic destruction of microcystin-LR.....	158
3.3.7	Photocatalysis of waste water pollutants .....	161
3.4	Discussion.....	173
4	Monitoring and controlling the cyanobacterial metabolites 2-MIB and GSM	194
4.1	Introduction .....	194
4.2	Materials and methods.....	204
4.2.1	Reagents.....	204
4.2.2	Optimised method for GC-MS analysis.....	204
4.2.3	SPE method development for the recovery of 2-MIB and GSM from water	208
4.2.4	Optimised method for SPE .....	214
4.2.5	Analysis of environmental samples - Rescobie Loch and fishfarm	214
4.2.6	Stability of 2-MIB and GSM stored on SPE cartridges.....	215
4.2.7	Photocatalysis of 2-MIB and GSM.....	216

4.2.8	Development of passive sampling for GSM and 2-MIB.....	223
4.3	Results .....	228
4.3.1	Optimisation of GC-MS method.....	228
4.3.2	Optimisation of SPE method .....	230
4.3.3	Analysis of environmental samples: Rescobie Loch and fishfarm 239	
4.3.4	Stability of 2-MIB and GSM on SPE cartridges.....	241
4.3.5	Photocatalysis of 2-MIB and GSM.....	242
4.3.6	Development of passive sampling for 2-MIB and GSM.....	246
4.4	Discussion.....	252
5	Conclusions.....	276
5.1	Introduction .....	276
5.2	5.2 Pheromonal activity of microcystin-LR in the control of microcystins in water.....	276
5.3	Photocatalytic water treatment.....	278
5.4	Monitoring and controlling of the cyanobacterial metabolites 2-MIB and GSM 280	
6	References.....	284
7	Appendix.....	325
8	Scientific Output.....	337

# DECLARATION

---

I declare that the work presented in this thesis is my own, except where otherwise acknowledged, and has not been submitted in any form for another degree or qualification at any other academic institution.

Information derived from the published or unpublished work of others has been acknowledged in the text and a list of references is given.

.....

Carlos Pestana



# **DEDICATION**

---

**Für meine Mama**

## **ACKNOWLEDGEMENTS**

---

Most of all, I would like to thank my mother for her continuing support and love, without which I would not be where I am now.

All my thanks go to my supervisory team Professor Linda Lawton, Dr. Christine Edwards, Dr. Radhakrishna Prabhu, and Dr. Craig McKenzie. Thank you for your guidance, support, help and camaraderie.

Not only would I like to extend my thanks to the people in our research group, Kostas, Aakash, Vijith, Arif, Shaista, and Radisti, but also to all the wonderful people I had the good fortune to work with: Fiona, Szymon, Nathan, Leszek, Ben, Peter, Jean Claude, Audrey, Olu, John, Alec, Kirstin, Marie, Heather, Beth, Yusuf, Iain, Emily, Kyari, Ann, and Eoin.

Dear Mandy, Sholto, Adam, and Clare thank you for your friendship over the years.

I am also very grateful to the Institute of Innovation, Design & Sustainability Research and Nanoparticulate Surface Adhesion Ltd. for their financial assistance.

## ABBREVIATIONS

---

2-MIB	2-methylisoborneol
Adda	3-amino-9-methoxy-2,6,8-trimethyl-10-phenyldeca-4,6-dienoic acid
AO	Acid Orange 74
AOP	Advanced oxidation process
ARMCANZ	Agriculture and Resource Management Council of Australia and New Zealand
ATSDR	American Agency for Toxic Substances and Disease Registry
CLLE	Continuous liquid-liquid extraction
CP	2-chlorophenol
EC	End capped
EDX	Energy dispersive x-ray spectroscopy
EPA	Environmental Protection Agency
GAC	Granular activated carbon
GC	Gas chromatography
GSM	Geosmin
HPLC	High performance liquid chromatography
LED	Light emitting diode
LOD	Limit of detection
LOQ	Limit of quantification
LVI	Large volume injection
MC	Microcystin
MF	Micro filtration

MS	Mass spectroscopy
MWCO	Molecular weight cut off
NBR	Non bio recirculation system
NF	Nano filtration
NHMRC	National Health and Medical Research Council
NOD	Nodularin
NOM	Natural organic matter
NSA	Nanoparticulate Surface Adhesion
Ox	Oxidation
PAC	Powder activated carbon
PDA	Photo diode array
POCIS	Polar organic chemical integrative samplers
PSP	Paralytic shellfish poison
PS™	Photospheres™
PTFE	Polytetrafluoroethylene
Red	Reduction
RO	Reverse osmosis
RS 1	Recirculation system 1
RS 2	Recirculation system 2
RT	Room temperature
SBSE	Stir bar sorptive extraction
SD	Standard deviation
SEM	Scanning electron microscope
SPE	Solid phase extraction
SPMD	Semi-permeable membrane device
SPME	Solid phase micro extraction

SRM	Silicone rubber membrane
TCA	Trichloroanisole
TCE	Trichloroethylene
UF	Ultra filtration
UPLC	Ultra performance liquid chromatography
USADLLME	Ultra sound assisted dispersive liquid liquid micro extraction
UV	Ultra violet
V1	Version 1
V2	Version 2
WHO	World Health Organisation
WTP	Water treatment plant

## Abstract

---

Cyanobacterial secondary metabolites can cause serious harm to animals and humans (cyanotoxins) and can have a major financial impact on the potable water and aquaculture industries (taste and odour compounds). Understanding the factors that affect cyanotoxin production can help in exploring means for the control of these secondary metabolites. One of the most prominent cyanotoxins are microcystins and their sister compound nodularin. The biological role of microcystins is poorly understood. A pheromonal effect was observed applying a novel stable isotope labelling ( $^{15}\text{N}$ ) method. Microcystin-LR has been shown to stimulate culture growth, limit microcystin synthesis, and affect the distribution of microcystin-LR between the intra- and extra-cellular matrices. Furthermore the control of microcystins in potable water has been explored applying photocatalysis over titanium dioxide. A novel product called Photospheres™ was assessed in its photocatalytic efficiency in the destruction of 12 microcystin analogues and nodularin. The photocatalytic efficiency of the Photospheres™ was further explored in the degradation of four common waste water pollutants (2-chlorophenol, p-cresol, Acid Orange 74, and trichloroethylene) and in a custom built reactor using light emitting diodes as source of irradiation. The monitoring and regulation of cyanobacterial taste and odour compounds, especially geosmin and 2-methylisoborneol is important in the potable water and aquaculture industries. A rapid, robust, sensitive, and cost-effective analysis method using SPE-GC-MS has been developed and is capable of detecting both compounds to sub nano gram levels. The method was successfully applied on spiked laboratory and environmental samples (loch and fishfarm waters). The photocatalytic

destruction of both 2-methylisoborneol and geosmin was explored with a custom built flow reactor that was able to degrade > 95 % of both compounds in spiked and environmental samples. Furthermore the application of silicone rubber membranes as passive samplers was explored in spiked and environmental samples, demonstrating that silicone rubber membranes can successfully be used in environmental applications to deliver rapid and accurate determinations of both 2-methylisoborneol and geosmin.

## **Chapter 1**

---

# **Introduction**



## **1 Introduction**

### **1.1 Origins and distribution of cyanobacteria**

Cyanobacteria are an immensely diverse group of prokaryotic organisms that have successfully conquered a wide variety of habitats, some of which present extreme living conditions. Cyanobacteria first appeared around 2.8 to 3.5 billion years ago and are considered responsible for turning early earth's atmosphere from anaerobic to an aerobic one (Adams, 1997; Summons *et al.*, 1999). Fossilised records of primitive precursors of cyanobacteria have been found that suggest that today's higher plant's chloroplasts are derived from an endosymbiotic relationship between cyanobacterial precursors and early higher plants (Raven and Allen, 2003).

Cyanobacteria, were in the past commonly known as "blue-green algae", and are sometimes, mistakenly, still called thus. The misnomer stems from the fact that their morphology is similar to that of eukaryotic algae and also from their ability to photosynthesise. The descriptor of "blue-green" originates from the colour that cyanobacterial blooms can display, which is due to two photosynthetic pigments, namely phycocyanins and chlorophyll *a* (Mur *et al.*, 1999). In fact even the scientific name of cyanobacteria means nothing other than blue-green bacteria (Greek, cyano = blue-green). Even though cyanobacteria are still, mistakenly, referred to as eukaryotic algae, their intracellular arrangement and protein synthesis apparatus is very close to that of prokaryotes. Cyanobacteria lack cell nuclei and membrane encapsulated organelles, but also have lipopolysaccharide layers encompassing the cell contents. These features have made their phylogenetic classification a challenge. The most accepted classification is the grouping of cyanobacteria with the

eubacteria forming their own subgroup called cyanophyceae (Castenholz and Waterbury, 1989).

Cyanobacteria have successfully conquered a multitude of different aquatic and terrestrial habitats. Cyanobacteria can be found in all types of bodies of water be they marine or brakish of nature, or fresh water. Colonies of cyanobacteria have been observed in deserts (Liu *et al.*, 2011) as well as in the arctic and in Antarctica (Varin *et al.*, 2011). Cyanobacteria can be found in extreme conditions of salinity and over a wide range of temperatures (Varin *et al.*, 2011; Krienitz *et al.*, 2012). Agrawal and Singh (2001) have shown that various species of cyanobacteria are able to withstand water stress, survive extreme heat and UV exposure.

Cyanobacteria are capable of fixing nitrogen due to certain morphological changes of cells within a filament called heterocysts (Franche *et al.*, 2009). These heterocysts are placed at (semi-) regular intervals in the filament and supply their neighbouring cells with nitrogen in the form of ammonia, while the surrounding cells supply the heterocyst with other nutrients (Franche *et al.*, 2009). This ability makes cyanobacteria attractive symbionts for other uni-cellular organisms as well as higher plants. Evidence of symbiotic relationships of cyanobacteria with diatoms can be found for as far back as the oceans of the Eocene (34 to 56 x 10<sup>6</sup> a ago) and Pleistocene (11.7 x 10<sup>3</sup> to 2.6 x 10<sup>6</sup> a ago) ages (Bauersachs *et al.*, 2010) and continues to this day with diatoms in the open oceans (Foster *et al.*, 2011). Symbiotic relationships with higher plants are also well documented. Probably the most well known symbiotic relationship exists between *Azolla* spp. and *Anabaena azollae*

(Lumpkin and Plucknett, 1980). *Azolla* is a companion plant grown with rice in Asia, Africa and the Americas, due to the capability of fixing nitrogen through its association with cyanobacteria it can increase rice yield significantly. *Azolla* forms a lawn of plants on the surface of the water, thus blocking out light, stopping undesirable plants from growing and once dead it can act as a green fertilizer for the rice plants. Association with higher animals is also not unknown. Wujek and Licoln (1988) discovered a new species of *Oscillatoria* growing on *Bradypus variegates* (Brown-throated three-toed sloth) (figure 1.1).



**Figure 1.1:** *Bradypus variegates* (Brown-throated three-toed sloth) in Panama. Note the green discolouration of the fur caused by micro algae and cyanobacterial species (National Geographic, 2012; used with permission).

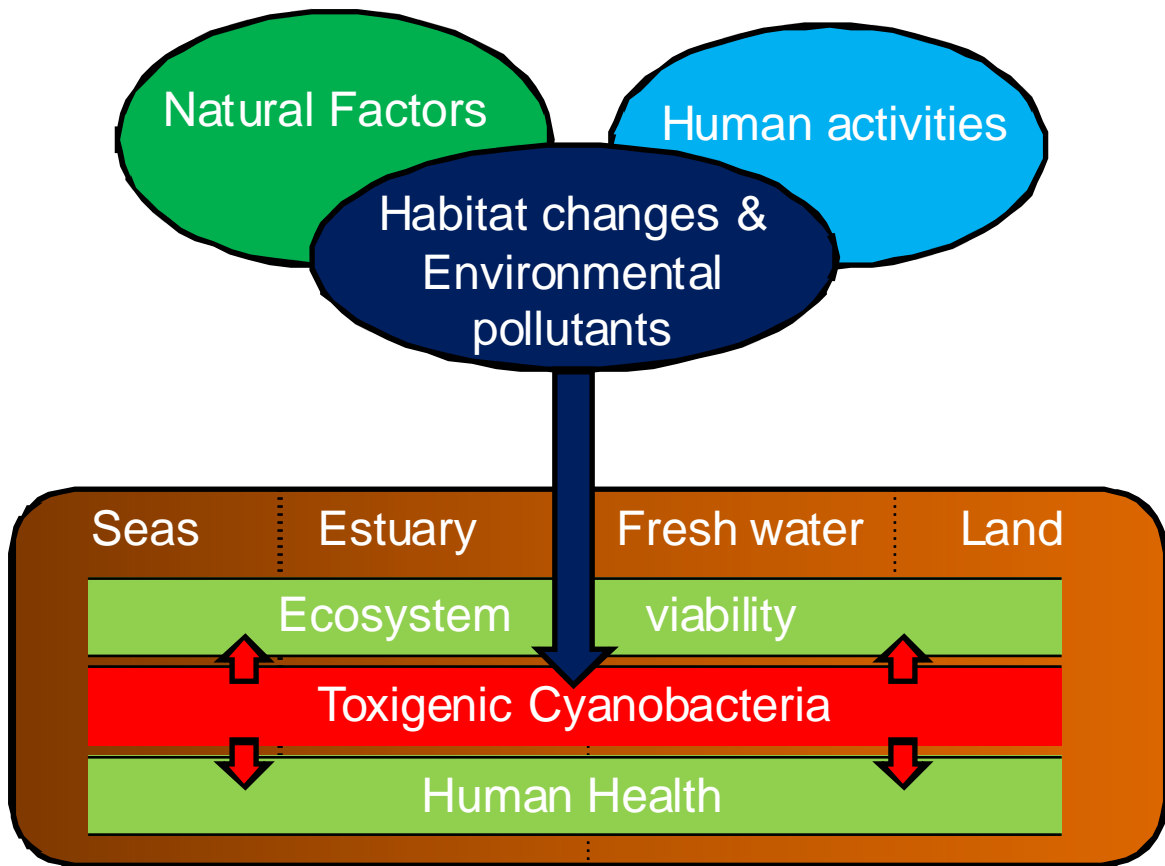
Symbiosis with other animals such as sponges is also documented (Vacelet, 1971).

## **1.2 Cyanobacterial blooms: cause and effect**

Cyanobacteria are known to experience explosive increases in biomass under certain conditions, the mass appearances are called blooms. Certain

environmental factors contribute to these blooms, most notably eutrophication of water bodies (Mur *et al.*, 1999). This relationship between eutrophication and increase of cyanobacterial biomass has been documented in boreal, temperate, subtropical and tropical ecosystems (Havens, 2005). In blooms, cyanobacteria successfully supplant the other phytoplanktonic species and become dominant. The length of a given bloom depends on many factors such as phosphate and nitrate concentrations, mean depth, mixing, flushing rate, and water temperature. Paerl (1988) was able to demonstrate a positive correlation between dissolved nutrient content (phosphates and nitrates) and the occurrences of cyanobacterial blooms in lakes, rivers and coastal waters. In a later publication Paerl and Huisman (2008) also positively link global warming to an increase in occurrences of cyanobacterial blooms. Bloom formation thus is the result of a number of factors; human-caused and natural (figure 1.2).

Cyanobacterial blooms demonstrate large temporal variations. Some bodies of water have seasonal blooms (usually in the summer), some have persistent blooms throughout all seasons, and some display extreme peaks and crashes over the year, with individual blooms lasting from a few days to a number of weeks (Haven, 2005). An extreme example for these short but intense blooms is Hartbeespoort Dam, South Africa, where high sun irradiance in the surface layers and low winds (thus little mixing) conspire to create short-lived hyper-scums of *Microcystis aeruginosa* (Zohary *et al.*, 1995).



**Figure 1.2:** Diagram showing the synergistic contribution of natural forces and human activities that leads to cyanobacterial bloom formation, especially in rivers, lakes (fresh water) and estuary waters, and the resultant problems arising from cyanobacterial blooms (adapted from ISOC-HAB, 2005).

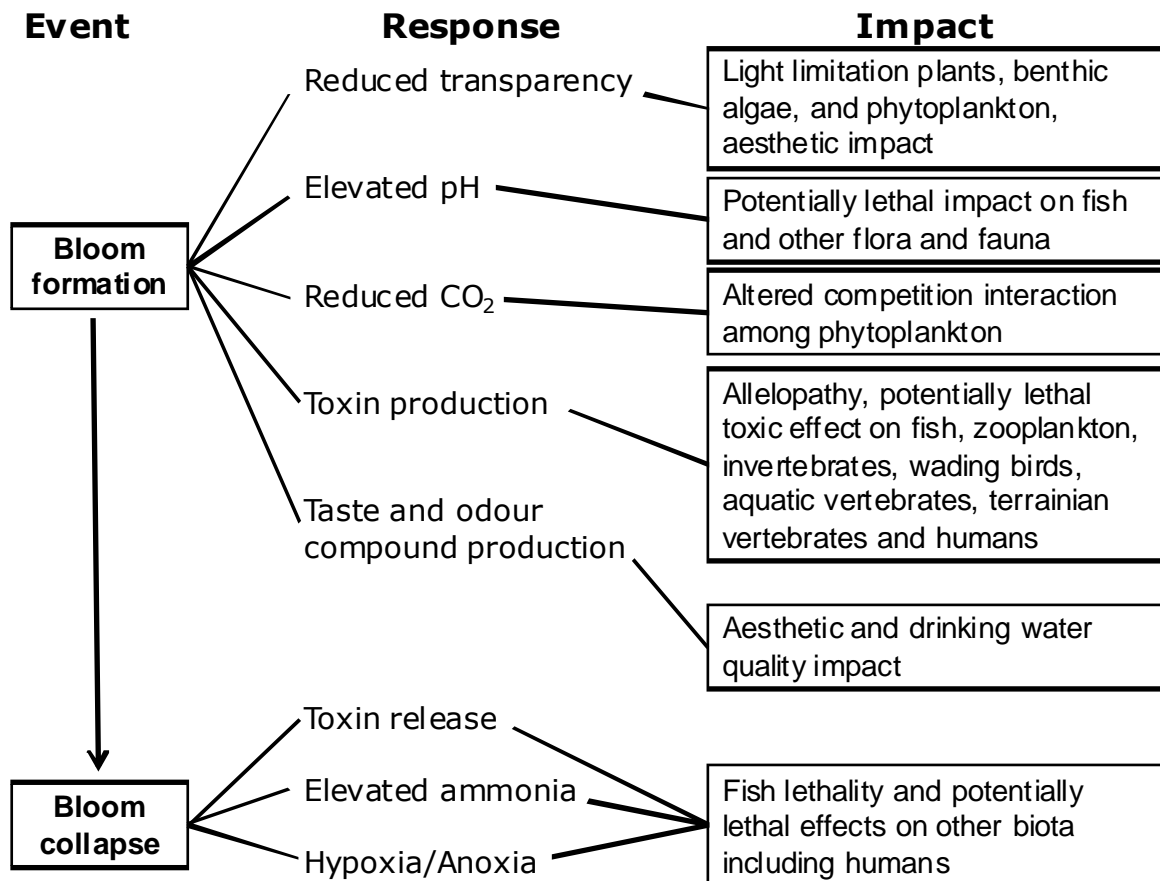
When cyanobacterial blooms occur, the biological impact on the relevant water body is significant. Increased cyanobacterial biomass causes reduced water transparency, thus reducing irradiance in the water column, which results in decreased growth of producers that cannot maintain a position high enough in the water column, this especially impacts on benthic algae and rooted plants. Scheffer *et al.* (1993) have shown that a shift from plant dominance to phytoplankton dominance can happen very quickly in a eutrophic lake.

The photosynthetic activity of cyanobacteria during a bloom depletes the free dissolved CO<sub>2</sub> in the water which, in turn, leads to an increase in pH (Mur *et al.*, 1999). Kann and Smith (1999) have shown that elevated pH can be the

cause of fish death or at least negatively impact fish well-being. It has been observed (Jones, 1987) that the ammonia content of the water increases during blooms and was able to correlate snail mortality to increased levels of ammonia and decreased levels of oxygen following an *Anabaena circinalis* bloom collapse. Another, potentially the most detrimental, side-effect of cyanobacterial blooms is the potential production and eventual release of cyanotoxins. The production of a variety of toxins by certain cyanobacterial strains (e.g. *Anabaena circinalis*, *Aphanizomenon flos-aquae*, *Cylindrospermopsis raciborskii*, and *Microcystis aeruginosa*) can have a variety of biological impacts on the aquatic ecosystem. The presence of the toxin may have effects on other flora and/or fauna (Suikkanen *et al.*, 2004). Toxins may act as signalling compounds affecting other species' behaviour, potentially detrimentally, such as suppression of zooplankton grazing (Gilbert, 1990), decreased grow-rates and reproductive rates (Ferrao-Filho *et al.*, 2000), or changes in dominance (Ghadouani *et al.*, 2003). Anderson *et al.* (1993) have shown hepatotoxic effects of microcystin on fish. Gerard and Poullain (2005) have shown that the presence of microcystins negatively affects the growth and fertility of snails in laboratory exposures. Bioaccumulation of the toxins (microcystins) is a further problem that has been shown to exist in both fish (Magalhaes *et al.*, 2001) and in invertebrates (Liras *et al.*, 1998; Lehtiniemi *et al.*, 2002). Prepas *et al.* (1997) have postulated that the accumulation of microcystin in the tissue of fresh water clams is the route of toxicity for the muskrat (*Ondatra zibethicus*). Waterfowl are also negatively affected by blooms as illustrated by the mass-mortality of ducks coinciding with a *Microcystis* bloom in Japan (Matsunaga *et al.*, 1999). The amounts of toxin available in the water increase when the blooms collapse, the cells lyse and

their contents are spilled into the surrounding matrix, as most cyanobacterial toxins are of an intra-cellular nature (Wiegand and Pflugmacher, 2005). Another issue related to cyanobacterial blooms is the production of taste and odour compounds by the cyanobacteria or other bacterial species present. Graham *et al.* (2010) have found in an investigation of blooms in 23 lakes in the United States that in 91 % of blooms taste and odour compounds were present when toxins were present as well. Taste and odour compounds especially pose a problem when the water body that presents the bloom is used as a potable water source in areas where insufficient ground water sources cannot cover that need.

In summary the formation of cyanobacterial blooms can be an indicator of the state of a body of water, one that is experiencing eutrophication for example. The effects of blooms can be detrimental to the flora and fauna of the water in question and can have serious health implications for humans as well (figure 1.3).



**Figure 1.3:** A summary of ecological responses and impacts associated with blooms of cyanobacteria in lakes, rivers, and estuaries (adapted from Havens, 2005).

### 1.3 Cyanobacterial secondary metabolites

Cyanobacteria produce a wide variety of secondary metabolites that can have toxic effects on other biota or that can represent a nuisance. There is a wide range of cyanobacterial toxins that can target a range of organs (table 1.2). The ecological role of these secondary metabolites to date remains unclear (Lawton and Edwards, 2001). Several roles have been proposed including defence mechanisms, cell signalling, and to gain ecological advantages over food competitors (Kaebernick and Neilan, 2001).



**Table 1.1:** List of cyanotoxins, the organisms that produce them and the primary target organ (adapted from Wiegand and Pflugmacher, 2005)

<b>Toxin group</b>	<b>Producers</b>	<b>Target organ</b>
Microcystins	<i>Microcystis, Anabaena, Planktothrix</i>	Liver
Nodularin	<i>Nodularia</i>	Liver
Cylindrospermopsin	<i>Cylindrospermopsis, Anabaena, Planktothrix, Raphidiopsis</i>	Liver
Anatoxin	<i>Anabaena, Aphanizomenon, Cylindrospermopsis, Planktothrix</i>	Nerve synapse
Anatoxin-a(s)	<i>Anabaena</i>	Nerve synapse
Saxitoxins	<i>Aphanizomenon, Lyngbya, Anabaena, Cylindrospermopsis</i>	Nerve synapse
Lipopolysaccharide	all cyanobacteria	Endotoxin that can affect all exposed tissue

### 1.3.1 Cyanotoxins

Cyanobacterial secondary metabolites can be classed into three groups, hepatotoxins, neurotoxins and lipopolysaccharide endotoxins. Of these all but the lipopolysaccharides are intra-cellular and generally only find their way into the extracellular matrix upon cell lysis. These toxins tend to have a target organ that suffers when intoxication with the secondary metabolite occurs. Lipopolysaccharides are present on the outside of the cyanobacterial cell and can affect any tissue they get in contact with.

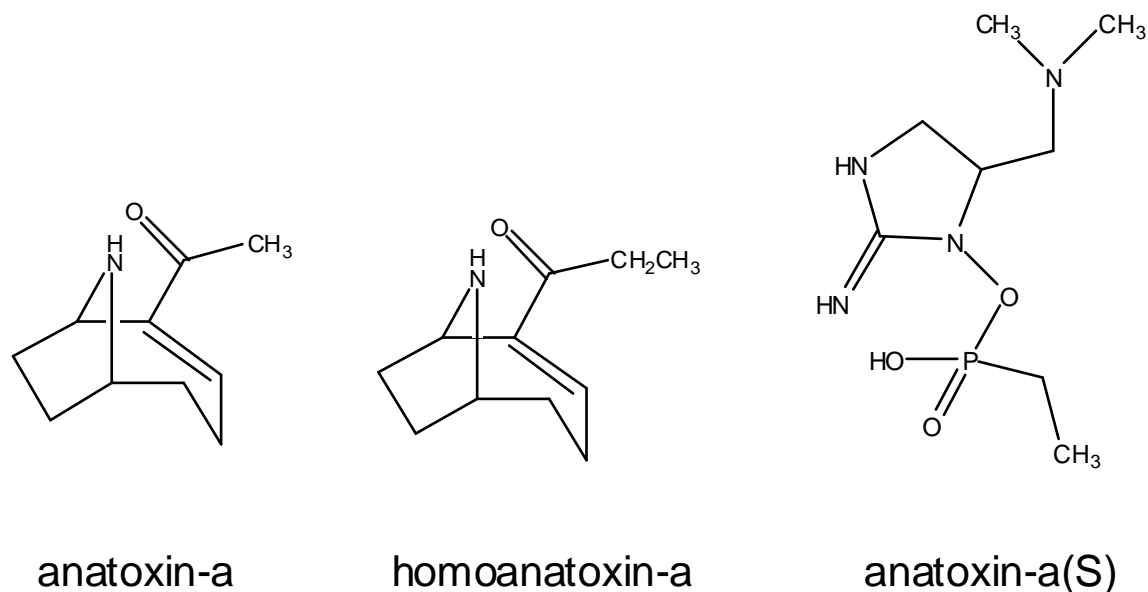
### **1.3.1.1 Cyanobacterial alkaloids: anatoxin-a, anatoxin-a(S), saxitoxin, and cylindrospermopsin**

One group of cyanotoxins are chemically defined as alkaloids, this group has four members, anatoxin-a, anatoxin-a(S), saxitoxins which are all neurotoxins and the hepatotoxin cylindrospermopsin.

Anatoxin-a is a secondary amine (165 Da) and has one analogue, homoanatoxin-a (179 Da). It was first isolated from *Anabaena flos-aquae* in 1977 by Devlin *et al.* (figure 1.4). Lawton and Edwards (2009) report the production of this toxin also by *Oscillatoria*, *Aphanizomenon*, and *Raphidiopsis*. In birds and mammals anatoxin-a acts as neurotoxin, mimicking acetylcholine (a neurotransmitter) by binding irreversibly to the acetylcholine receptors causing muscle contraction (Wiegand and Pflugmacher, 2005). Receptors that are affected thus, cannot be deactivated by acetylcholinesterase, this means continuous contraction stimuli are created, resulting in over-stimulation (Carmichael, 1997). This is harmful to the target organism because it can lead to paralysis due to the fact that no further neural transmissions can occur. This can lead to death if the respiratory apparatus is affected (Van Appeldoorn *et al.* 2007).

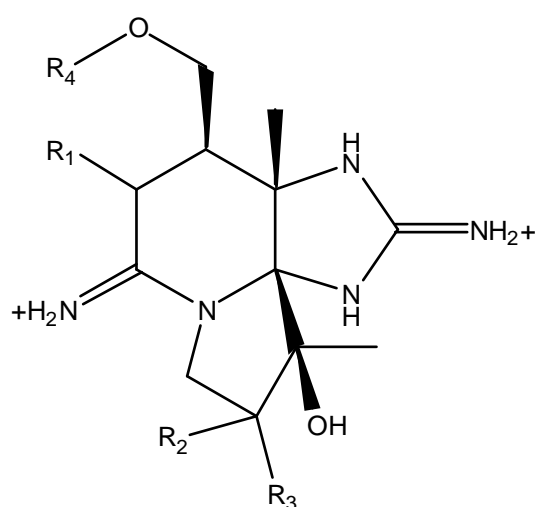
Anatoxin-a(S) (252 Da) was also isolated from *A. flos-aquae* and also acts as neurotoxin by inhibiting cholinesterases (figure 1.4) (Van Appeldoorn *et al.*, 2007). Its mode of toxicity is different to that of anatoxin-a, it does not block the acetylcholine receptor like anatoxin-a does, but prevents the removal of the acetylcholine from the receptor by acetylcholinesterases (Carmichael,

1997), this results in the overstimulation of the receptor just as in the case of anatoxin-a.



**Figure 1.4:** General chemical structure of cyanobacterial alkaloids anatoxin-a, homoanatoxin-a, and anatoxin-a(S)

Another member of the groups of cyanotoxin alkaloids are the saxitoxins, which are produced by cyanobacteria (*Lyngbya* sp., *Anabaena* sp., *Aphanizomenon* sp, and *Cylindrospermopsis raciborskii*; table 1.1), as well as by a number of dinoflagellates (Carmichael, 1997; Chorus and Bartram, 1999). Saxitoxins have a unique structure (figure 1.4) and 13 analogues have been identified to date (table 1.2). Saxitoxins have been given the byname of paralytic shellfish poisons (PSPs) because the toxin has been found to bioaccumulate in mussels and clams by their ingestion of saxitoxin-producing dinoflagellates. Ingestion of these is the major route of toxicosis in humans (Wiegand and Pflugmacher, 2005). Toxicity in mammals is caused by binding of the saxitoxins to the sodium channels of nerve cells resulting in paralysis due to a lack in stimulation and ultimately respiratory arrest (Su *et al.*, 2004).



**Figure 1.5:** General chemical structure of cyanobacterial alkaloid saxitoxin

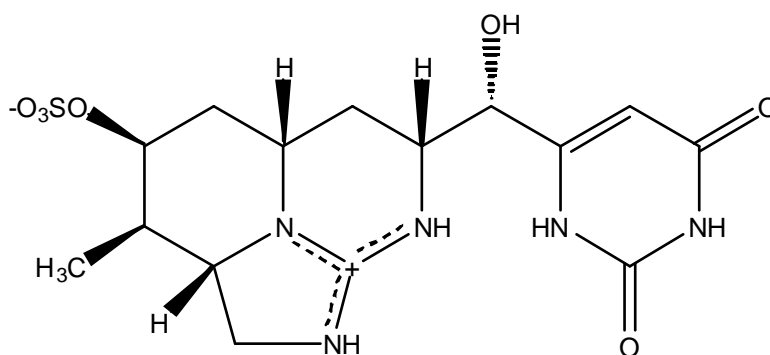
**Table 1.2:** Variable groups in cyanobacterial alkaloid saxitoxin analogues (adapted from Van Appeldoorn *et al.*, 2007)

<b>Variant</b>	<b>R<sub>1</sub></b>	<b>R<sub>2</sub></b>	<b>R<sub>3</sub></b>	<b>R<sub>4</sub></b>
Saxitoxin	H	H	H	CONH <sub>2</sub>
NEOSTX	OH	H	H	CONH <sub>2</sub>
GTX1	OH	H	OSO <sub>3</sub> <sup>-</sup>	CONH <sub>2</sub>
GTX2	H	H	OSO <sub>3</sub> <sup>-</sup>	CONH <sub>2</sub>
GTX3	H	OSO <sub>3</sub> <sup>-</sup>	H	CONH <sub>2</sub>
GTX4	OH	OSO <sub>3</sub> <sup>-</sup>	H	CONH <sub>2</sub>
GTX5	H	H	H	CONHSO <sub>3</sub> <sup>-</sup>
GTX6	OH	H	H	CONHSO <sub>3</sub> <sup>-</sup>
C1	H	H	OSO <sub>3</sub> <sup>-</sup>	CONHSO <sub>3</sub> <sup>-</sup>
C2	H	OSO <sub>3</sub> <sup>-</sup>	H	CONHSO <sub>3</sub> <sup>-</sup>
dcSTX	H	H	H	H
dcGTX2	H	H	OSO <sub>3</sub> <sup>-</sup>	H
dcGTX3	H	OSO <sub>3</sub> <sup>-</sup>	H	H

STX – saxitoxin; NEOSTX – neosaxitoxin; GTX – gonyautoxins; C – c-toxins; dc - decarbamoyl

The final member of the group of cyanobacterial alkaloids is cylindrospermopsin (figure 1.6). It is produced by a number of cyanobacteria including *Cylindrospermopsis*, *Planktothrix*, *Raphidiopsis*, and *Anabaena* (table 1.1). In mammals cylindrospermopsin's primary target organ is the liver

(Chorus and Bartram, 1999), however it has also been found to irreversibly inhibit protein synthesis and thus can have an effect on a variety of organs (Froscio *et al.*, 2003). The toxicity of this alkaloid originates from the pyrimidine group which interacts with the cytochrome P450 system (Froscio *et al.*, 2003). Ingestion of cylindrospermopsin can cause necrosis of the liver and kidney. Cylindrospermopsin has been linked to the "Palm Island Mystery Disease" that occurred on Palm Island, Australia in 1979 (table 1.5).

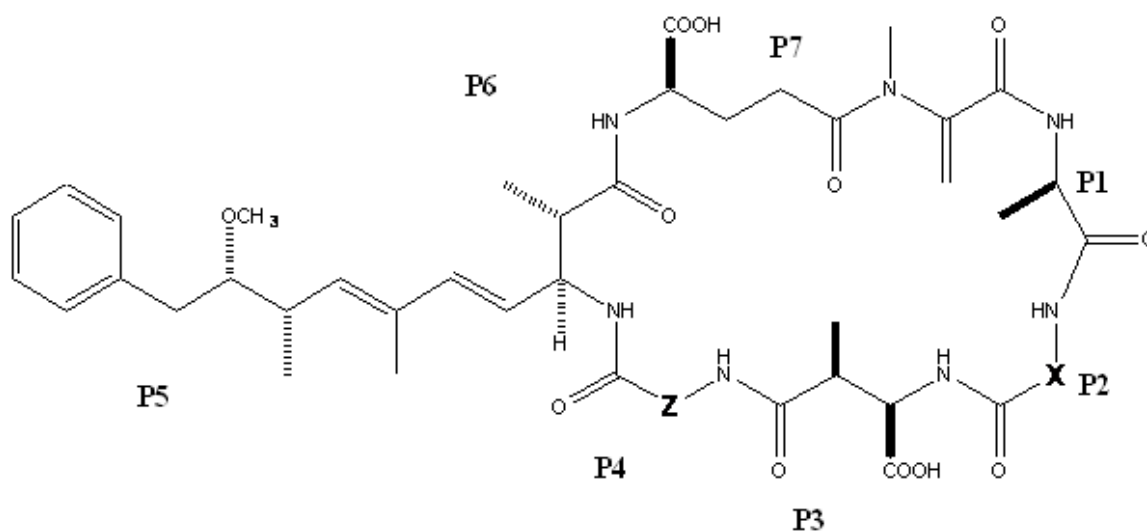


**Figure 1.6:** General structure of the cyanobacterial alkaloid cylindrospermopsin

### 1.3.1.2 Cyanobacterial cyclic peptides: microcystins and nodularins

A variety of cyanobacterial toxins are chemically classed as cyclic peptides, these are called microcystins and, their related compounds, nodularin (Carmichael, 1994). The effects of these toxins were first described by Francis in 1878 where an algal bloom in Lake Alexandrina, in Australia, was connected to sheep deaths. It was later found that nodularin was responsible for the livestock lethality (Dawson, 1998). Microcystins and nodularin are hepatotoxic cyclic peptides, with relative molecular weights of  $\approx 800 - 1100$  Da. These compounds tend to be water soluble (Sivonen, 1996). Microcystins are produced by a number of strains of cyanobacteria most prominently by

*Microcystis*, *Anabaena*, *Planktothrix* but also by strains of *Nostoc*, *Anabaenopsis* and *Radiocystis* (Viera *et al.*, 2003; Mohamed and Sheri, 2009). All microcystins have common structural characteristics (figure 1.7): three D-amino acids, which are alanine (position 1), aspartic acid (position 3), and glutamic acid (position 6). There are two L-amino acids (positions 2 and 4) which are variable and are responsible for naming the particular MC variant. The one letter amino acid code is used for the naming, thus, a microcystin molecule with leucine (L) and arginine (R), would be called microcystin-LR (Sivonen, 1996; Sivonen and Jones, 1999). There is methyldehydroalanine (position 7) and, the highly unusual and characteristic for microcystins, amino acid that is abbreviated Adda (position 5, 3-amino-9-methoxy-2,6,8-trimethyl-10-phenyldeca-4,6-dienoic acid) (McElhiney and Lawton, 2005; Sivonen and Jones, 1999).



**Figure 1.7:** General chemical structure of microcystin with respective positions of amino acids and variables (X and Z) indicated. P1) d-alanine; P2) variable amino acid; P3) d-aspartic acid, P4) variable amino acid; P5) Adda; P6) glutamic acid; P7) methyldehydroalanine

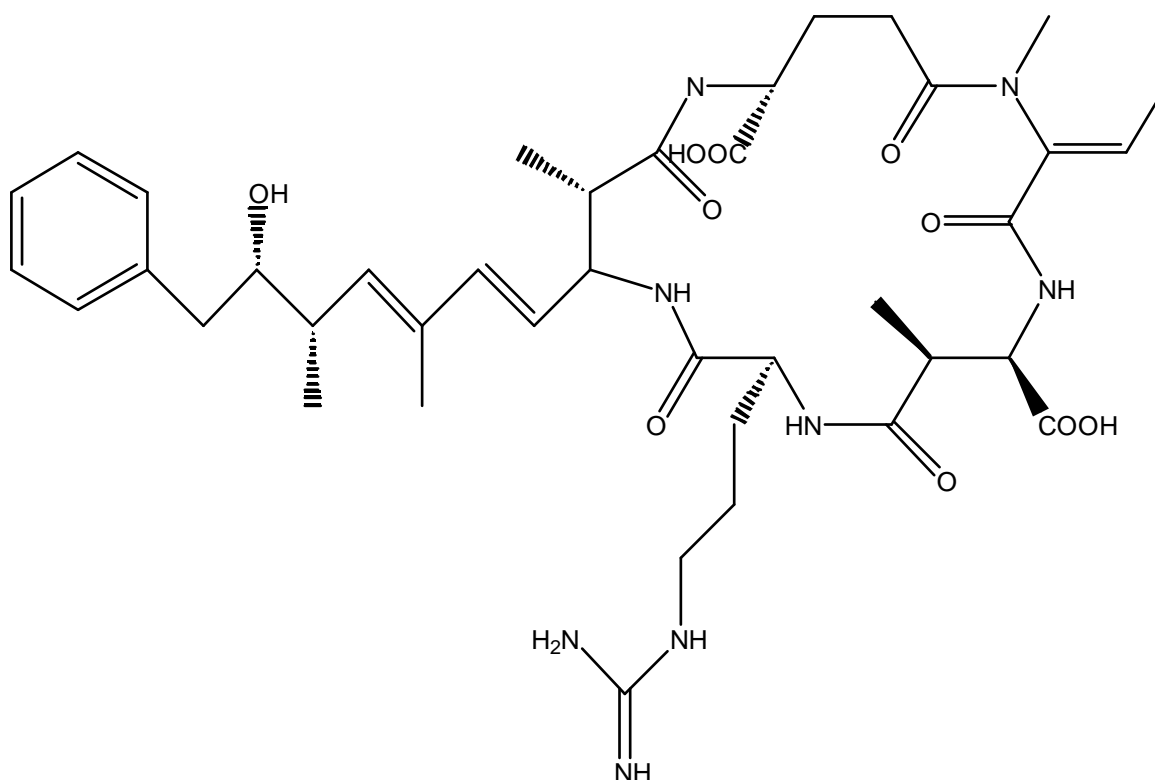
There are more than 80 MC variants that have been characterised (Wood *et al.*, 2008). The differences between the variants usually stem from the variety

in the L-amino acids, structural changes in the Adda amino acid and the amount of methylation and demethylation (Sivonen, 1996; Sivonen and Jones, 1999) (table 1.3).

**Table 1.3:** List of 17 microcystin analogues, their variable amino acids, and their respective molecular weight (adapted from Zurawell, 2002).

<b>Microcystin analogue</b>	<b>Variable amino acids</b>	<b>Molecular weight / Da</b>
Microcystin-LA	Leucine, Alanine	910
Microcystin-LAba	Leucine, L-aminobutyric acid	923
Microcystin-AR	Alanine, Arginine	953
Microcystin-RA	Arginine, Alanine	953
Microcystin-YA	Tyrosine, Alanine	959
Microcystin-LF	Leucine, Phenylalanine	985
Microcystin-LR	Leucine, Arginine	996
Microcystin-LY	Leucine, Tyrosine	1002
Microcystin-HilR	L-homoisoleucine, Arginine	1008
Microcystin-FR	Phenylalanine, Arginine	1028
Microcystin-M(O)R	Methionine S-oxide, Arginine	1028
Microcystin-HtyR	L-homotyrosine, Arginine	1030
Microcystin-YM(O)	Tyrosine, methionine S-oxide	1035
Microcystin-RR	Arginine, Arginine	1038
Microcystin-YR	Tyrosine, Arginine	1045
Microcystin-(H4)YR	1,2,3,4-tetrahydrotyrosine, Arginine	1048
Microcystin-WR	Tryptophan, Arginine	1068

Another member of the microcystin family is the mono cyclic pentapeptide nodularin, which is almost exclusively produced by *Nodularia spumigena* in brackish waters (Sivonen and Jones, 1999). Rinehard *et al.* (1988) first structurally characterised nodularin (figure 1.8)



**Figure 1.8:** Structure of the cyanobacterial cyclic pentapeptide nodularin.

Nodularin is structurally very similar to microcystin including the characteristic unusual amino acid, Adda (Mazur-Marzec *et al.*, 2009). Due to the similarities with microcystin, nodularin can be analytically determined with the same methods as microcystins (Edwards and Lawton, 2010). The main points in which it varies from microcystin is the lack of the amino acids D-Ala in position 1, the variable amino acid X at position 2, the variable amino acid at position Z is replaced with arginine, and the substitution of the Mdha with MDhb in position 7 (Rantala *et al.*, 2004). Rantala *et al.* (2004) have also identified slight variants of nodularin: nodularin-Har which replaces the arginine in position 4 with homoarginine.

To date, the ecological role for both microcystin and nodularin remains unknown. However, the negative impact of these toxins on both flora and



fauna, including humans has been universally established. Microcystins have been shown to affect a wide range of organisms from micro algae to higher animals and plants. The toxicity of microcystins and nodularin both operate on a similar mechanism in mammals. Both inhibit the protein phosphatases (PP) PP1 and PP2 (Imanishi and Harada, 2004). The importance of PPs stems from their role in reversible protein dephosphorylation which is a mechanism inherent in many cellular activities. Addition of phosphate activates many types of enzyme and the removal of phosphate (the role of protein phosphatases) deactivates them again (Seeger and Krebs, 1995). The toxicity of both microcystins and nodularin originates from the adda amino acid Dawson, 1998). The toxicity of both microcystins and nodularin is selective for the liver in mammals (table 1.3). The disruption of protein phosphatases in the liver leads to a breakdown of the hepatocytes structure which leads to an enlargement of the liver, liver bleeding and ultimately to haemorrhagic shock and death (Dow and Swoboda, 2000). Protein phosphatases have been determined to be tumour suppressing in addition to their cell regulatory role hence disruption of PPs can lead to a promotion of liver cancer in mammals (Ito *et al.*, 1997). In fact, in China the chronic consumption of microcystins in drinking water and fish has been proven to be directly linked to human hepatocellular carcinoma (Yu *et al.*, 1989). Mikhailov *et al.* (2003) have also found that microcystins bind to ATP synthetases and inhibit that enzyme's role leading to uncontrolled cell apoptosis. The toxicity of nodularin operates on a similar principle as that of microcystins, due to the effect of the Adda amino acid. However the type of attachment to the PPs is different compared to that of microcystins, it lacks the D-alanine and N-methyldehydroalanine amino acids that are involved in the covalent binding of microcystins to the PPs.

Due to the serious health implications of microcystins, a number of regulatory bodies have determined guideline values of microcystin-LR in drinking water, which, however, in most cases, fails to take into account the existence of the several microcystin analogues with differing toxicity (table 1.4).

**Table 1.4:** Summary of toxicity of microcystin analogues and nodularin in mice ( $\mu\text{g kg}^{-1}$ ) and microcystin human health based exposure guide lines (adapted from: U.S. EPA, 1998; WHO, 1998; Gilroy *et al.*, 2000; Camichael, 2001; NHMRC and ARMCANZ, 2011; Health Canada, 2002; Zurawell, 2002)

<b>Microcystin analogue</b>	<b>Toxicity in mice (LD<sub>50</sub>) (<math>\mu\text{g kg}^{-1}</math>)</b>
Microcystin-AR	250
Microcystin-FR	250
Microcystin-HilR	100
Microcystin-HtyR	80-100
Microcystin-LA	50
Microcystin-LR	50
Microcystin-LY	90
Microcystin-M(O)R	700-800
Mirocystin-RR	500-800
Microcystin-WR	150-200
Microcystin-YA	60-70
Microcystin-YM(O)	56-110
Microcystin-YR	150-200
Nodularin	30-50
<b>Regulatory body</b>	<b>Recommended maximum concentration (<math>\mu\text{g L}^{-1}</math>)</b>
World Health Organisation (WHO)	1.0 <sup>1</sup>
Australia	1.3 <sup>2</sup>
Canada	1.5 <sup>3</sup>
New Zealand	1.0
Oregon, USA	1.0 $\mu\text{g g}^{-1}$ (algal food supplements)

<sup>1</sup> free microcystin-LR; <sup>2</sup> total, free and cell bound, also this value counts for microcystin-LR toxicity equivalents, i.e. variants are converted to equivalent microcystin-LR toxicity and summed; <sup>3</sup> total microcystin-LR, free and cell bound

The first recorded human intoxication with cyanobacterial toxins dates back approximately 1000 years, when General Zhu Ge-Ling noticed that troops

drinking from a green river in Southern China died (Chorus and Bartram, 1999). Since then a number of episodes with human health impact have been recorded in most cases either microcystins, or in the cases where the causative agent could not yet be determined, *Microcystis* spp. have been involved (table 1.5).

**Table 1.5:** Confirmed and suspected cyanobacterial episodes with human health impact (adapted from Svrček and Smith, 2004)

<b>Location</b>	<b>Year</b>	<b>Case</b>	<b>Organism(s)</b>	<b>Toxin</b>
Ohio River, U.S.	1931	gastroenteritis	Unknown cyanobacteria	unknown
Harare, Zimbabwe	1966	gastroenteritis	<i>M. aeruginosa</i>	Unknown
Sewickley, Pa., U.S.	1976	gastroenteritis	<i>Schizotrix calcicola, Plectonema, Phormidium, Lyngbya</i>	Unknown
Armidale, Australia	1983	Liver damage, constipation, dysentery, renal damage	<i>M. aeruginosa</i>	Unknown
Palm Island	1983	hepatoenteritis	<i>C. raciborskii</i>	Cylindrospermopsin
Rudyard Reservoir, UK	1989	Vomiting, dermatitis, pneumonia, diarrhoea	<i>M. aeruginosa</i>	Microcystin-LR
Itaparica Dam, Brazil	1993	88 deaths, gastroenteritis	<i>Anabaena sp., Microcystis sp.</i>	Unknown
Nandong District, Jiangsu Province, Nanhui/Shanghai Fusui, China	1994- 1995	Primary liver cancer correlation	<i>M. aeruginosa, Planktothrix agardhii, Anabaena sp., Lyngbya sp.</i>	Microcystins
Caruaru, Brazil	1996	52 deaths	<i>Aphanizomenon sp., Oscillatoria sp.</i>	Micorcystins, cylindrospermopsin

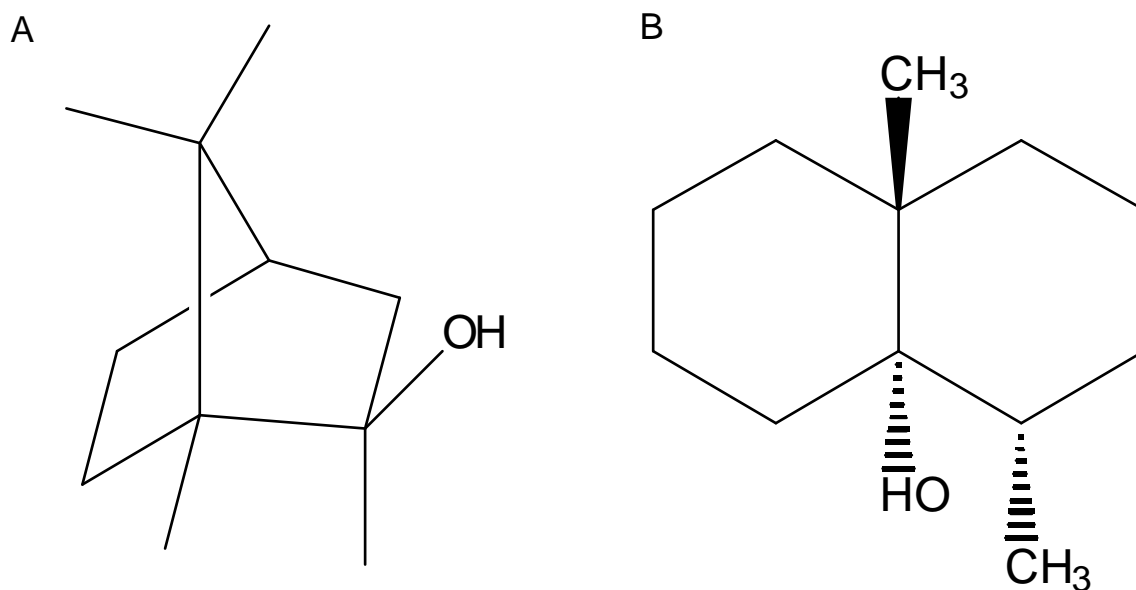
Microcystins are very stable compounds possibly due to their cyclic nature. They are able to withstand a range of pH and temperatures, many hours of boiling and persist for a number of years when dried at room temperature. Furthermore, microcystins can withstand hydrolysis by a number of common enzymes such as chymotrypsin, trypsin, and pepsin. Due to their high molecular weight and high water solubility they are not volatile (Cousins *et al.*, 1996; Harada and Tsuji, 1998; Lawton and Robertson, 1999).

The ecological role of microcystins is unclear, one proposed role is that of signalling compounds (including pheromonal roles). According to Leão *et al.* (2009) evidence for signalling of cyanobacteria has been known since 1948 (Lefèvre and Nisbet 1948) or possibly as early as 1917 (Harder). Very few of the cyanobacterial secondary metabolites have been identified as definitely possessing signalling properties. One of the most prominent ones is fischerellin, a signalling compound that was first isolated from *Fischerella muscicola* by Gross *et al.* in 1991. This compound has photosystem-II inhibiting properties and displays antifungal, herbicidal, and algicidal properties (Hagmann and Jüttner 1996, and Papke *et al.* 1997). There are other studies that present effects of cyanobacterial signalling, among them Engelke *et al.* (2003) who showed a connection between a, mostly structurally unidentified, sulphur containing peptide from *Planktothrix agardhii* on the toxin production in *Microcystis aeruginosa*. While many studies have explored the influence of typical physico-chemical parameters (e.g. N, P, temperature and light intensity) on microcystin production, few have reported effects of signalling

compounds. Engelke *et al.* (2003) clearly demonstrated stimulation in toxin production when cultures of *M. aeruginosa* were exposed to a highly polar signalling compound from *Planktothrix agardhii*. While this demonstrated an inherent effect on toxin levels, actual production levels of microcystin could not be determined and the bioassay used required many weeks before a clear result was obtained. This compound warrants further investigation as it may greatly enhance understanding of the factors which influence bloom toxicity. Also the effect of cyanobacteria on diatom growth has been studied (Keating 1978), where it was found that chemicals released from cyanobacterial blooms can inhibit growth in diatoms. However microbes are not the only target of signalling compounds from cyanobacteria, there are a number of studies about the effect of these on higher plants and animals, among these are Jang *et al.* (2007), who showed a reciprocal relationship between *M. aeruginosa* and *Lemna japonica* (duckweed), where one inhibits the growth of the other. Apart from the signalling effect on other species, another aspect that should be mentioned is the pheromonal (effect on the own species) activity of those secondary metabolites. There are few publications on the topic, and in regards to MC very little is known about potential pheromonal effects. A recent study failed to identify any function of MC for the cyanobacterium *M. aeruginosa* (Rohrlack and Heyenstrand 2007). However further studies are required to understand and possibly utilise the pheromonal effects of cyanobacterial secondary metabolites in controlling their detrimental effects on the ecosystem and humans.

### 1.3.2 Taste and odour compounds

The smell of freshly ploughed soil is very distinct and recognisable. In the late 19<sup>th</sup> century the odour of soil was first scientifically described by Berthelot and André (1892), who noticed that the typically musty, earthy odour of soil could be extracted from soil by steam, and was characterised as a volatile compound. In the 1930s Thaysen and Thaysen, as well as Pentelow (in Gerber and Lechevalier, 1965) were able to identify actinomyces as the causative organism that produced the odour compound and eventually identified it as geosmin (Greek "ge" = earth and "osme" = smell) (systematic name: *trans*-1,10-dimethyl-*trans*-9-decalol). They also performed the first test on fish and found that the compound accumulated in the fish's fatty tissue through uptake either through the mouth or the gills but not the skin. They also described that the only way to rid the fish of the smell was to keep it alive in an environment with fresh running water. Since then a number of other organisms, such as cyanobacteria (Izaguirre *et al.* 1982) and fungi, have been identified to be producing geosmin (GSM) and also 2-methylisoborneol (2-MIB), another taste and odour compound with a musty, earthy, muddy smell (figure 1.9).



**Figure 1.9:** The chemical structures of A) 2-methylisoborneol (2-MIB) and B) *trans*-1,10-dimethyl-*trans*-9-decalol – geosmin (GSM)

Geosmin is an alicyclic alcohol, it has semi-volatile characteristics, a molecular weight of 182, its boiling point is 270 °C, it exists as an oil at room temperature and has an aqueous solubility of 150 mg L<sup>-1</sup> (Pirbazi *et al.*, 1992; Budavari, 2001). It is produced by a number of cyanobacteria (*Oscillatoria*, *Anabaena*) and actinomycetes (Persson, 1982; Matsumoto and Tsuchiya, 1988; Glöckner *et al.*, 2000). Geosmin's taste and odour is described as musty, earthy, and mouldy (Suffet *et al.*, 1999). The taste and odour thresholds in humans vary but Howgate (2004) suggested a value of 15 ng L<sup>-1</sup>, based on a number of publications. The other taste and odour compound that often appears in conjunction with geosmin is 2-methylisoborneol. Chemically it is characterised as a terpene with a molecular weight of 168. It exists as white crystals at room temperature with a boiling point of 198 °C and a water solubility of 195 mg L<sup>-1</sup>. It is produced by the cyanobacteria *Oscillatoria* (Persson, 1982) and *Phormidium* (Negoro *et al.*, 1988) and a number of actinomycetes



(Glöckner *et al.*, 2000). 2-MIB is described in similar terms as GSM where taste and odour are concerned, differentiation between the two compounds is difficult. The mean human taste and odour threshold was defined by Howgate (2004) as around 35 ng L<sup>-1</sup>.

Studies relating to the toxicology of 2-MIB and GSM are limited. Diogini *et al.* (1993) have found no mutagenic response for either compound in *Salmonella typhimurium* assay up to concentrations leading to cytotoxicity, six orders of magnitude higher than the recognised taste and odour threshold. Nakajima *et al.* (1996) have found the IC<sub>50</sub> (50 % inhibitory concentration) to be 17 and 69 mg L<sup>-1</sup> for GSM and 2-MIB respectively in sea urchin embryos. These results are comparable to the Diogini *et al.* study from 1993. Gagné *et al.* (1999) have found no cytotoxicity in rainbow trout hepatocytes for GSM, for 2-MIB they were able to determine a cytotoxic effect at 45 mg L<sup>-1</sup>, many times the taste and odour threshold. However, they were able to observe DNA damage at 0.45 and 10 mg L<sup>-1</sup> for GSM and 2-MIB respectively. This DNA damage can lead to mutations and eventually carcinoma.

A number of research groups have proposed that GSM and, to a lesser degree, 2-MIB could be used as an indicator for the presence of other cyanobacterial metabolites, especially cyanotoxins (Yagi *et al.*, 1988; Blaha *et al.*, 2004). However, Blaha *et al.* (2004) have not found a direct correlation in their study. A similar proposition was made by Graham *et al.* (2010) who investigated blooms in 23 American lakes and found GSM and/or 2-MIB present in 91 % of cases that also presented with

cyanotoxins (mostly microcystins), which indicates that while maybe no direct correlation exists, the presence of taste and odour compounds can serve as a warning indicator for the presence of cyanotoxins.

Both 2-MIB and GSM can be considered nuisance compounds that can have significant financial impacts on both the potable water industry and aquaculture (Hanson, 2004). Research shows that taste and odour of water serves as a criterion of quality for many customers (McGuire, 1995; Jardine *et al.*, 1999). In South Korea and Japan a maximum allowable level of 2-MIB and GSM was set at 10 ng L<sup>-1</sup> each, as an aesthetics guideline (Jo *et al.*, 2011). A series of investigations also proved that 2-MIB and GSM are a major factor impacting on the aquaculture industry. Robertson *et al.* (2006) have shown that both 2-MIB and GSM bioaccumulate in farmed rainbow trout. Howgate (2004) proposed that one means of ridding the fish of the flavour is depuration as already stipulated by Thaysen and Thaysen, and Pentelow (in Gerber and Lechevalier, 1965) in the 1930s. This, however, presents the fish farmer with a dilemma, since, as a rule, fish in depuration tanks are not fed, i.e. starved. As a result of that, depending on how long the fish have to remain in the depuration tanks, the fish lose weight which has negative impacts on the net profit the fish farmer can achieve per fish. Furthermore the farmer must supply and maintain uncontaminated water for that duration of time, which involves further cost and complications. The other option is attempting to sell the contaminated fish, which can result in customer rejection and loss of confidence in the product of farmed fish.

#### **1.4 Water treatment options for cyanobacterial secondary metabolites (microcystins, geosmin, and 2-methylisoborneol)**

There are several standard and some more advanced water treatment options when it comes to the removal of secondary cyanobacterial metabolites, especially of microcystins and the two taste and odour compounds geosmin and 2-methylisoborneol. A number of studies are focussing on singled out aspects of the water treatment process, but only few investigate combined treatment approaches and examine the efficiency of several combined methods as one would find in a water treatment plant (WTP). The efficiency of removal of different treatment methods will be examined in regards to their removal of cyanobacterial secondary metabolites.

One approach of treating mass occurrences in source water is the use of algicides. The use of algicides is detrimental to the removal of cyanobacterial secondary metabolites due to the fact that most algicidal agents operate on the principle of cell lyses, which by lysing the cells, i.e. physically destroying it the free toxin concentration in the water is *de facto* increased (Jones and Orr, 1994). Free toxin is able to persist in water for a number of weeks or even months (Jones *et al.*, 1995). A water treatment strategy needs to be devised. It needs to be decided whether to remove the cells that contain the toxin intact or whether to propagate the release of the toxin into the water and deal with the dissolved toxin (Hart *et al.*, 1998).

### **1.4.1 Conventional water treatment methods**

Flocculation and coagulation are often the first step in water treatment. In flocculation gentle mixing is applied to aggregate dispersed particles, including cyanobacterial cells, which eventually leads to larger flocs which subsequently can be removed by sedimentation. Coagulation is a similar process, here, however, chemicals are applied to facilitate the aggregation of the dispersed particles, these chemicals include aluminium and ferric iron salts or synthetic polymers (Mouchet and Bonn elye, 1998). The success of removal, especially of cyanobacteria depends largely on the dosage of the chemical and pH of the water (Bernhardt and Clasen, 1991). These treatment options are more suited to the removal of the intact cyanobacterial cells rather than the dissolved toxin, or taste and odour compounds. However, there is a number of studies that have, unsuccessfully, attempted to remove dissolved toxins (Rositano and Nicholson, 1994) and taste and odour compounds (McGuire and Gatson, 1988) from the water with these processes.

Clarification is a process that allows the removal of floc from the water. Static clarifiers allow the floc to settle and remove the supernatant, while sludge blanket clarifiers filter the floc out by passing the water through a layer of sludge. Mouchet and Bonn elye (1998) have found that the sludge blanket type is more successful in removing cyanobacterial cells. However it has been found that the cyanobacterial cells lyse in the sludge releasing their toxin into the sludge and water, making sludge management paramount and still poses the issue of dissolved toxin in the water (Drikas *et al.*, 2001).

Another basic process in water treatment is the filtration. This process allows the removal of suspended particulates, including cyanobacterial cells, by passing the water through a series of granulated media that filter out the suspended particulates (Letterman, 1999).

Rapid sand filters can be employed with clarified waters or directly with contaminated water. It has been found that rapid sand filters are more effective in treating pre-treated waters compared to direct treatment (Mouchet and Bonn elye, 1998). But even pre-treated water achieves unsatisfactory removal of microcystins (14 to 60 %) in water that had undergone coagulation – flocculation and then passed through a sand-anthracite filter (Lambert *et al.*, 1996). Dissolved toxins cannot be removed by sand filtration (Lambert *et al.*, 1996). The success of removal in the above study relates to intra-cellular toxins, i.e. the successful retention of cyanobacterial cells. A danger relating to rapid sand filters is the entrapment of cyanobacterial cells in the filter, when these cells die and lyse dissolved toxin will be released in the filtrate. Yagi *et al.* (1983) and Hattori (1988) have shown that rapid sand filtration is unsuccessful in the removal of both taste and odour compounds.

Slow sand filtration operates on a similar principle as rapid sand filtration with two major differences. The flow rates applied in slow sand filtration are approximately fifty times lower than those used in rapid sand filtration (Kiely, 1998), and in slow sand filtration, biofilms develop on the filter medium, referred to as *Schmutzdecke* (German, lit. dirt blanket). This

*Schmutzdecke* allows for biodegradation to occur on the filter as the filtrate is passed through. Biodegradation of both microcystins and taste and odour compounds in biofilms is well documented (Yagi *et al.*, 1983; Sumitomo *et al.*, 1992; Jones and Orr, 1994; Rapala *et al.*, 1994; Christoffersen *et al.*, 2002).

Bank filtration is a process in which surface water sources are in part filtered by natural soil banks. Miller and Fallowfield (2001) have found some removal of cyanobacterial hepatotoxins but the difficulty with bank filtration lies in optimising it, as little can be done apart from site selection.

Activated carbon is a means of water treatment that is separated into two general types that have different applications. Powder activated carbon (PAC), which is used as and when required as an additional clean-up means, and granular activated carbon (GAC) which is in permanent use (Letterman, 1999). The efficiency of a given type of activated carbon depends on the pore size, this is especially true for microcystins which present rather large molecules with an estimated diameter of 1.2 to 2.6 nm. Most activated carbons are microporous (< 2 nm), with some mesopores (2 to 50 nm) are present as well. The presence of mesopores greatly depends on the starting material (wood, charcoal, coconut shell) (Letterman, 1999). Fawell *et al.* (1993) found wood based activated carbon to be the most effective in the removal of microcystins. This was later corroborated by Donati *et al.* (1994) and Warhurst *et al.* (1997). Both PAC and GAC have been found to be effective in the removal of

microcystins (Hoffman, 1976; Bruchet *et al.*, 1998). Cook and Newcombe (2002) proved that adsorption efficiencies are quite different for different microcystin analogues (microcystin-RR > -YR > -LR > -LA). The same group also showed (2002b) that nodularin follows a similar adsorption pattern to microcystin-LR. Both PAC and GAC have also been shown to successfully remove both taste and odour compounds from water (Ng *et al.*, 2002; Jung *et al.*, 2004; Orr *et al.*, 2004). In the case of the taste and odour compounds pore size is of little importance as both molecules are comparatively small. The drawbacks of the treatment of microcystins, and taste and odour compound with activated carbon is the fact that other natural organic matter (NOM) present in the raw water will compete for adsorption sites on the carbon particles (Donati *et al.*, 1994; Bruchet *et al.*, 1998; Hepplewhite *et al.*, 2004; Ho and Newcombe, 2005). A further drawback of the use of activated carbon (either PAC or GAC) is the fact that efficacy reduces over time, as fewer and fewer active adsorption sites become available until the removal of cyanobacterial secondary metabolites suffers to an extent as to render the application of activated carbon useless. The time until such saturation is reached greatly depends on the NOM content of the water that is passed over the carbon (Hattori, 1988; Hart *et al.*, 1998). The bed-life can be as short as 30 d or last up to 5 to 6 m (Hart *et al.*, 1998). Once the activated carbon is saturated few options remain. PAC is usually destroyed (usually incinerated) or disposed of in landfills, the same option are present for GAC as well, in addition it can also be regenerated (usually in an inert environment at 800 °C), however, regeneration can be very cost intensive (San Miguel *et al.*, 2001; Chestnutt *et al.*, 2007). Another option for GAC is to allow the

formation of biofilms to occur (Biologically activated carbon). Hart (1998) was able to show complete removal of microcystin-LR on a biologically active GAC bed with a contact time of 15 min.

The previously described methods are all physical means of removing either cyanobacterial cells and/or their metabolites from the water. There are a number of chemical treatments that mostly aim at the destruction of the free metabolites in the water. Potassium permanganate ( $\text{KMnO}_4$ ) has been used in water treatment since 1913, when it was introduced in London, England (Galvin and Mellado, 1998). Since the 1960s it has been in large scale use both in the U.S. and in Europe (Letterman, 1999). It works as an oxidising agent (Lawton and Robertson, 1999). It has been successfully used in raw and clarified water to remove microcystin-LR (Fawell *et al.*, 1993; Rositano *et al.*, 1998). In 2001 Karner *et al.* have successfully applied it in a large scale test at several WTP in Wisconsin, U.S.A.. In comparison to microcystin, the removal of taste and odour compounds with potassium permanganate is largely ineffective (Nerenberg *et al.*, 2000; Tung *et al.*, 2004).

Chlorine is the chemical most often applied in WTP in North America. It has, however, been shown that chlorination of microcystins is largely ineffectual (Hoffman, 1976; Keijola *et al.*, 1988; Himberg *et al.*, 1989). It was found that both the pH of the water as well as present NOM interferes with the chlorination of microcystin. The same holds true for the taste and odour compounds with both Nerenberg *et al.* (2000) and Tung *et al.* (2004) finding chlorination an ineffective means for the removal of 2-MIB



or GSM due to the high concentrations and increased contact time needed for removal.

There are few studies investigating the effect of a combination of the above mentioned conventional water treatment options on the total removal of microcystins and even fewer focussing on the taste and odour compounds. The first such study was carried out by Hoffman (1976) he combined coagulation - flocculation - sedimentation - filtration - chlorination and could not achieve a significant decrease of bioactivity. This was later corroborated by Keijola *et al.* (1988) and Himberg *et al.* (1989) who used coagulation-flocculation-sand filtration-chlorination to achieve 11 to 32 % and 9 -16 % removal respectively. Much later Schmidt *et al.* (2002) tested different combined methods with differing successes. Karner *et al.* (2001) applied yet another combination of treatment methods with great success (table 1.6). No such investigations regarding combined treatment methods for 2-2-MIB and GSM exist. However, Nerenberg *et al.* (2000) have combined ozonation with biofiltration to successfully decrease 2-MIB concentration to below threshold values.

**Table 1.6:** Treatment trains of conventional water treatment trains aimed at the removal of microcystin-LR from waste water (Kamer *et al.*, 2001; Schmidt *et al.*, 2002).

<b>Treatment</b>	<b>Microcystin-LR removal (%)</b>	<b>Reference</b>
Coagulation-flocculation-filtration	87-94	
Permanganate-coagulation-flocculation-filtration	31-59	
PAC-coagulation-flocculation-filtration	92-99	Schmidt <i>et al.</i> , 2002
Ozonation-coagulation-flocculation-filtration	73-93	
Ozonation-PAC-coagulation-flocculation-filtration	95-97	
Pretreatment*-PAC-coagulation-flocculation-sedimentation-recarbonisation-rapid sand filtration-fluoridation-chlorination	90-99	Karner <i>et al.</i> , 2001

\*not further specified

### 1.4.2 Advanced water treatment

Membrane filtration is a physical separation process that applies semi-permeable membranes to divide a water stream into a permeate (what passes through the membrane) and a retentate (what is retained) (Scrcsek and Smith, 2004). There are four types of membranes applied in WTPs: microfiltration (MF), ultrafiltration (UF), nanofiltration (NF), and reverse osmosis (RO) (Zhou and Smith, 2001). MF and UF apply low pressure to

pass the water stream through and NF and RO apply high pressure. MF and UF are more suited to remove cyanobacterial cells as opposed to dissolved toxins and/or taste and odour compounds, while NF and RO have low molecular weight cut offs (MWCO) with 200 and 100 Da respectively, and can be applied to filter out the dissolved metabolites. Neuman and Weckesser (1998) successfully removed 95 and 99 % of dissolved microcystin-LR and -RR respectively using RO membranes. Vouri *et al.* (1997) achieved similar results with RO membranes and nodularin. Muntisov and Trimboli (1996) have used NF to completely remove microcystin-LR and nodularin from spiked river water. MF and UF membranes were assessed by Chow *et al.* (1997). They found removal of at least 98 % of *M. aeruginosa* cells from the incoming water flow. However they also found that subsequently it was hard to remove the cyanobacterial cells from the membranes again which can cause similar problems as cyanobacterial cells trapped in sand filters, resulting in the release of dissolved toxin into the water. NF membrane filtration has also been successfully applied to the removal of both taste and odour compounds (Reiss *et al.*, 1999; Smith *et al.*, 2003). Due to the relatively low molecular weights of 2-MIB and GSM (169 and 182 Da respectively) it is important to apply membranes with a low MWCO.

If a molecule absorbs ultra violet (UV) irradiation, the absorbed energy can cause one or more of the chemical bonds within the molecule to break. Since the 1970s UV irradiation has been used as a means of reducing the presence of microorganisms on surfaces (Svrcek and Smith, 2004). According to Zhou and Smith (2001) UV lamps with a spectral

output of 200 to 300 nm are used and the UV dose, usually defined as irradiation in a given area (typically  $\text{J cm}^{-2}$ ). A dose in the range of  $0.04 \text{ J cm}^{-2}$  is used to remove inactivation of harmful biota (Zhou and Smith, 2001). In principle UV photolysis could be successfully employed to render microcystins non-toxic. As mentioned before the toxicity of microcystins arises from the Adda amino acid group. Lawton and Robertson (1999) have shown that photoisomerisation of either of the unsaturated bonds in the ring structure, present in the Adda group, is promoted to an elevated orbital resulting in a rotation around the new single bond. Another means that could render the Adda group non-functional is the internal photosensitised cycloaddition, however, whether this is actually physically possible is still under debate (Kaya and Sano 1998, Goldberg *et al.*, 1995, Lawton and Robertson, 1999). It is interesting to note that the presence of phycocyanins, a group of photosynthetically active pigments inherent in cyanobacterial cells, can act as a sensitiser in the photolysis of microcystins (Tsuji *et al.*, 1994). Under natural sunlight the degradation of microcystins was negligible until phycocyanins were added (Tsuji *et al.*, 1994). In practice, however, UV photolysis without the use of sensitisers (catalysts) is inapplicable in WTP, because, as Tsuji *et al.* (1995) report, the required UV dose for the destruction of microcystin-LR is  $1.5 \text{ J cm}^{-2}$ . Rosenfeldt *et al.* (2005) have investigated the photolysis of 2-MIB and GSM and found that a UV dose of  $1 \text{ J cm}^{-2}$  was capable of removing around 10 % and between 25 and 50 % respectively (starting concentration  $50 \text{ ng L}^{-1}$ ). However, Agus *et al.* (2011) only found about 5 % degradation of either compound in a study with the same starting concentration.

Advanced oxidation processes (AOPs) apply the oxidative capacity of a compound to facilitate rapid breakdown of target analytes (table 1.7).

According to Glaze *et al.* (1987), AOP have been defined as:

“near ambient temperature and pressure water treatment processes which involve the generation of hydroxyl radicals in sufficient quantity to effect water purification”.

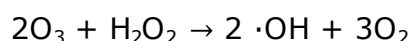
**Table 1.7:** List of advanced oxidation processes in potable water treatment and their mode of action (Svrcek and Smith, 2004)

<b>Process</b>	<b>Mode of action</b>
Ozonation	Decomposition of ozon creates ·OH radicals
Ozonation with H <sub>2</sub> O <sub>2</sub>	H <sub>2</sub> O <sub>2</sub> facilitates the more rapid breakdown of ozone
UV lysis with H <sub>2</sub> O <sub>2</sub>	UV lysis decomposes H <sub>2</sub> O <sub>2</sub> into 2 ·OH radicals
Semi-conductor photocatalysis	Under UV radiation the semi-conductor facilitates the formation of ·OH radicals

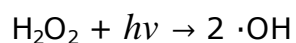
One application of AOPs is the introduction of ozone (O<sub>3</sub>) into the drinking water. Ozone is a gas that can be dispersed into the water. It is unstable and tends to the formation of hydroxyl radicals. Ozone can react directly where an oxidation of the target compound is achieved with molecular ozone or through the formation of hydroxyl radicals (·OH) that were created by the decomposition of ozone. Keijola *et al.* (1988), Himberg *et al.* (1989), Rositano *et al.* (2001), and Hart *et al.* (1998) have all reported the successful decomposition of microcystin-LR by ozonation. In these studies it has also been found that the decomposition of microcystin-LR is ozone-dose dependant. Rositano *et al.* (1998) also determined that an alkaline environment is detrimental to the oxidation of microcystin-LR,

probably due to a decreased oxidising potential at higher pH. In that same study it was also found that NOM competes with microcystin as oxidation by hydroxyl radicals is non-specific. Koch *et al.* (1992) have shown that 2-MIB and GSM can be successfully removed by ozonation. The limitation of ozonation is the operating cost, according to Kiely (1998) it is three times higher than that of chlorination.

Hydrogen peroxide (H<sub>2</sub>O<sub>2</sub>) is another compound that can be applied in AOPs. While in itself rather ineffective in the degradation of microcystin-LR, it can greatly improve other AOPs. To demonstrate, Rositano and Nicholson (1994) found 17 % degradation after 60 minutes with high amounts of H<sub>2</sub>O<sub>2</sub> (20 mg L<sup>-1</sup>), while Fawell *et al.* (1993) and a later study by Rositano *et al.* (1998) found virtually no microcystin-LR degradation at low levels of H<sub>2</sub>O<sub>2</sub> (2 mg L<sup>-1</sup>). Ozonation is one of these processes, the speed of formation of ·OH radicals is greatly enhanced (Zhou and Smith, 2001):



Rositano *et al.* (1998) have shown that microcystin removal can be facilitated by the H<sub>2</sub>O<sub>2</sub>-O<sub>3</sub> combination. In their study 1 mg L<sup>-1</sup> of microcystin-LR was completely removed after 30 min with the combination of 0.1 mg L<sup>-1</sup> H<sub>2</sub>O<sub>2</sub> and 0.2 mg L<sup>-1</sup> of O<sub>3</sub>. But ozonation is not the only AOP that can be enhanced by the addition of hydrogen peroxide. UV photolysis and hydrogen peroxide can be used in a synergistic system, due to the fact the UV irradiation promotes the formation of ·OH radicals from H<sub>2</sub>O<sub>2</sub> (Zhou and Smith, 2001):



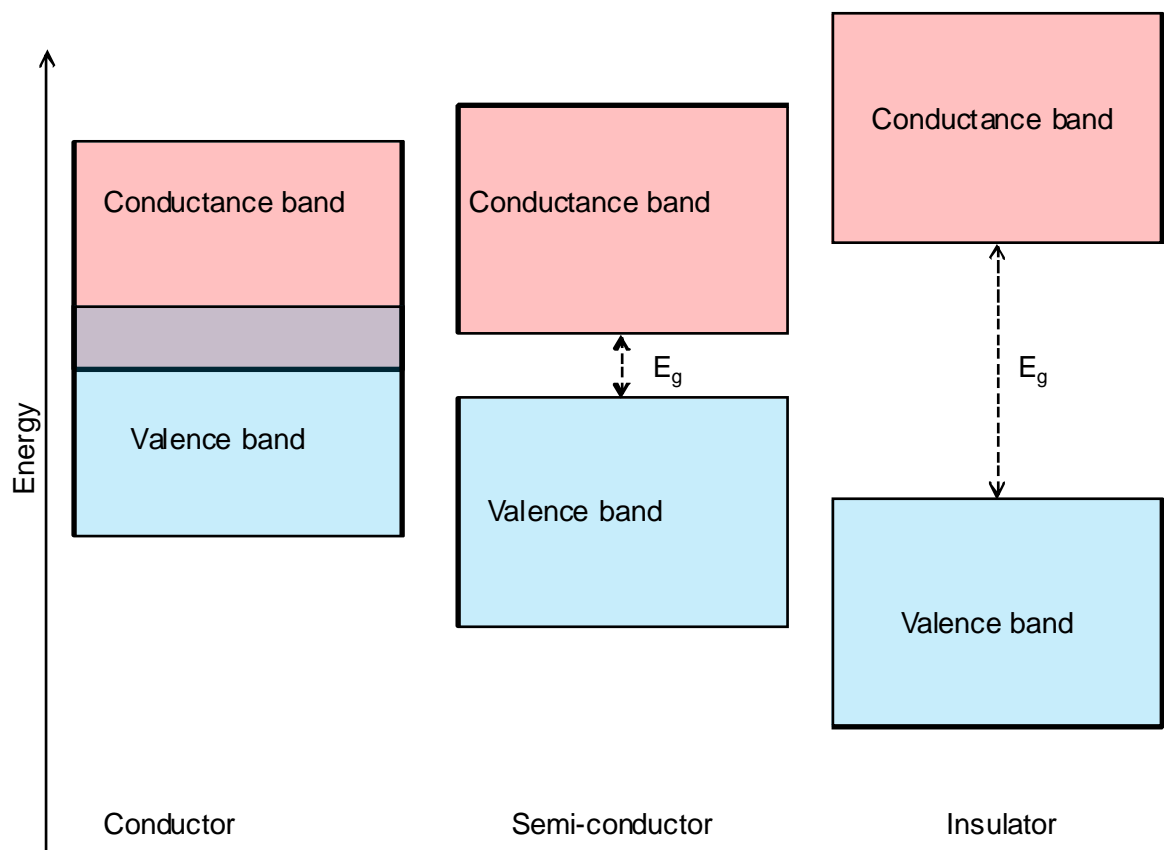
Rositano and Nicholson (1994) achieved 50 % removal of microcystin-LR with UV-H<sub>2</sub>O<sub>2</sub> after 30 minutes. Cornish *et al.* (2000) showed greater than 90 % toxin (microcystin-LR) reduction in the same timeframe. Both Jo *et al.* (2011) and Agus *et al.* (2011) achieved good degradation of 2-MIB and GSM with the UV-H<sub>2</sub>O<sub>2</sub> combination. Jo *et al.* achieved GSM degradation of 90 % and 2-MIB degradation of 60 % with H<sub>2</sub>O<sub>2</sub> assisted photolysis with a UV dose of 1.2 J cm<sup>-2</sup>, which is higher than what can be achieved by WTPs. The Agus *et al.* study combined RO with UV-H<sub>2</sub>O<sub>2</sub> and achieved complete removal of both odorants.

Another AOP that promises to be a useful tool in the degradation of cyanobacterial metabolites is UV photolysis over a semi-conductor photocatalyst, such as titanium dioxide.

### **1.5 Semi-conductor photocatalysis**

According to the band theory all solids can be described as possessing two energetic bands, the low-energy valence band (completely filled with electrons at 0 °K) and the high-energy conductance band (empty at 0 °K) (Sobczyński and Dobosz, 2001). The energetic distance between the bands, i.e. the energy required to promote one electron from the valence to the conductance band is called band gap ( $E_g$ ). The electric conductivity of a given solid is determined by the width of  $E_g$ , this determines whether a given solid is a conductor, a semi-conductor, or an insulator (figure 1.7). If the electric bands of the solid overlap, the solid is characterised as a

conductor, most metals are conductors. If there is a small band gap, that can be bridged by an electron with sufficient power input, then the solid is characterised as a semi-conductor and if the band gap cannot be bridged or if exorbitant amounts of energy are required the solid is characterised as an insulator (Sobczyński and Dobosz, 2001). Semi-conductor photocatalysis is a chemical process, during which, upon irradiation of light with an appropriate wavelength (the energy of the irradiation must be greater than the band gap ( $E_g$ ) energy), electrons are promoted from the valence to the conductance band (figure 1.7), which results in a positively charged hole in the valence band.

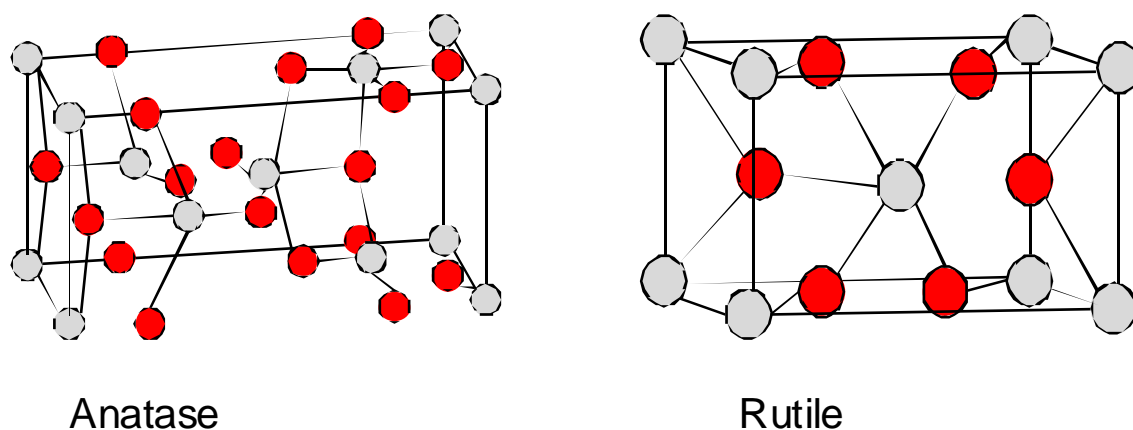


**Figure 1.10:** Simplified representation of the electric band structure of solids that act as conductors, semi-conductors and insulator respectively.



This facilitates the formation of hydroxyl radicals ( $\cdot\text{OH}$ ), which, in turn, can facilitate the decomposition of other compounds present (Carp *et al.*, 2004).

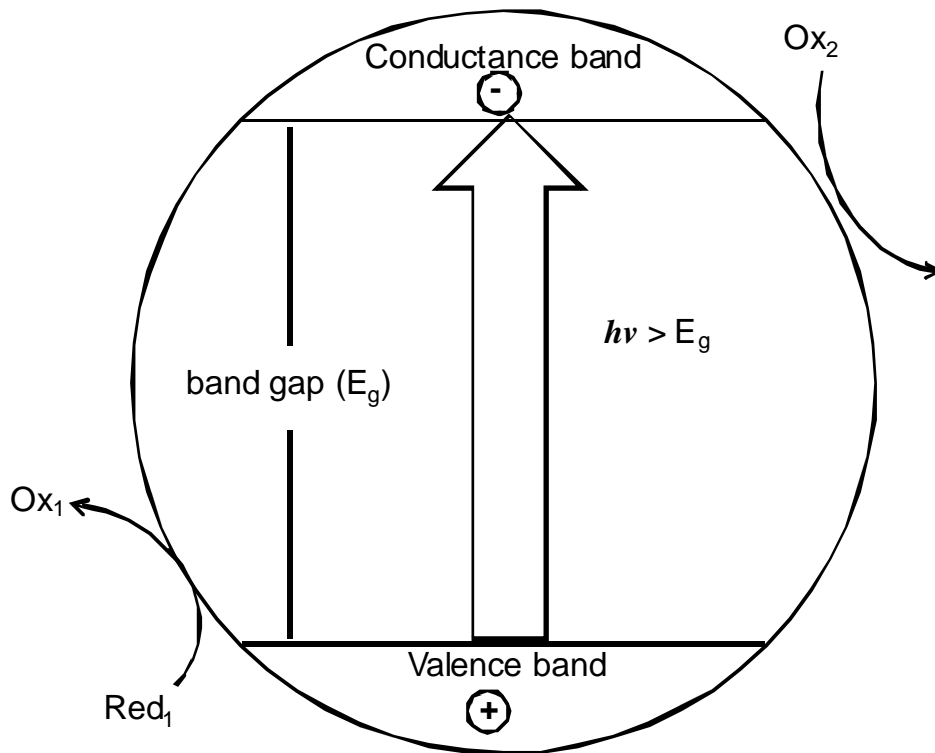
The holes created in the valence band are strong oxidants and the electrons that are promoted to the conduction band are strong reductants (Robertson *et al.*, 1997). One of the most commonly used semi-conductor photocatalysts is titanium dioxide ( $\text{TiO}_2$ ), to its almost ideal properties as photocatalyst. It is photoactive, but at the same time photostable, i.e. it is not liable to photocorrosion (holes generated by incoming irradiation that might cause the oxidation of the photocatalyst itself), it is both chemically and biologically inert, and relatively inexpensive (Mills and Le Hunte, 1997). Titanium dioxide occurs in nature in three crystal configurations, called anatase, rutile and brookite forms (figure 1.8). Of these three types only anatase and rutile display photocatalytic activity (Hanaor and Sorrell, 2011).



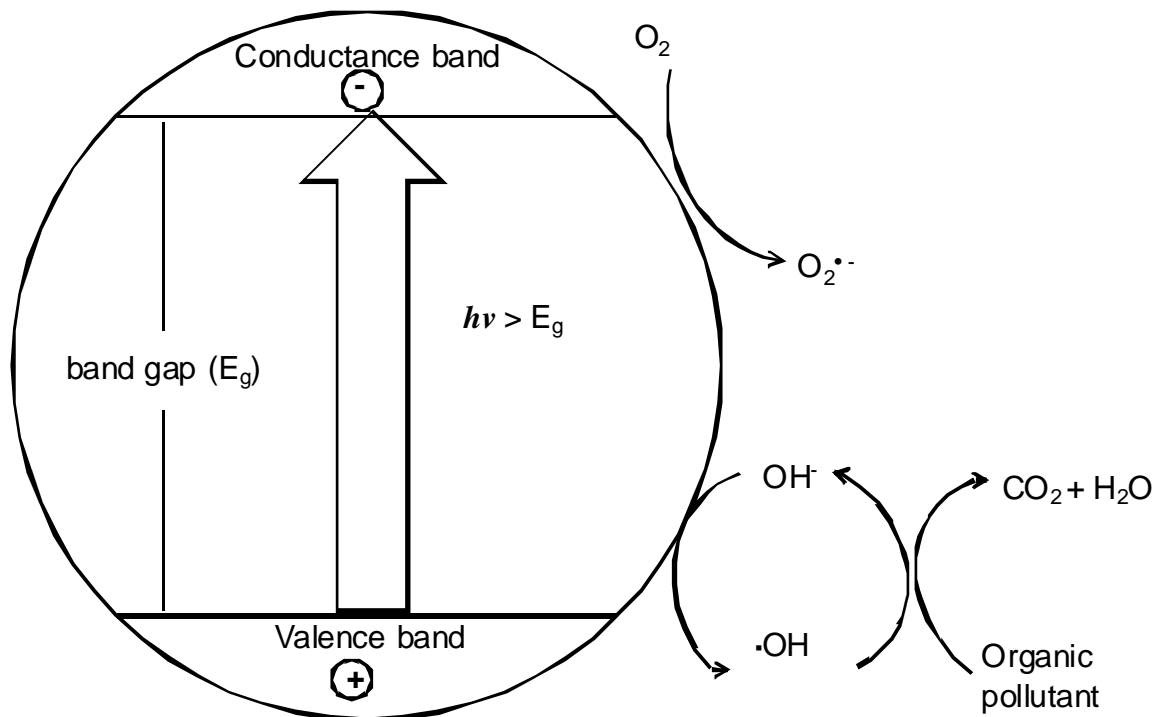
**Figure 1.11:** Simplified crystal structure representation of the two photocatalytically active types of titanium dioxide.

The bandwidth ( $E_g$ ) of the anatase type is 3.2 eV, while that of the rutile type is 3.0 eV. This means that if the semi-conductor is hit with light of the appropriate wavelength to gap  $E_g$ , i.e.  $h\nu > E_g$ , then electrons can be promoted from the valence to the conductance band (figure 1.9).

Semi-conductor photocatalysis over  $\text{TiO}_2$  can be applied to water splitting and semi-conductor films for the degradation of pollutants in the gas phase (Mills and Le Hunte, 1997). However, by far the largest area of study involves semi-conductor photocatalysis over  $\text{TiO}_2$  in the oxidation of organic pollutants, especially in water (Mills *et al.*, 1993; Hoffmann *et al.*, 1995; Byrne *et al.*, 1998). Turchi and Ollis (1990), have proposed that the generation of hydroxyl radicals created by the redox reactions on the surface of the catalyst facilitates the mineralisation of the chemical species in solution with the photocatalyst (figure 1.10).



**Figure 1.12:** Irradiance of a semi-conductor at an appropriate wavelength promoting an electron from the valence band to the conduction band. Reduced and oxidised forms of solution species also shown (adapted from Sobczyński and Dobosz, 2001).



**Figure 1.13:** Proposed mechanism of the mineralisation of an organic pollutant in water by semi-conductor photocatalysis over titanium dioxide (adapted from Mills and Le Hunte, 1993)

To date there are no semi-conductor photocatalytic processes established in WTPs (Svrcek and Smith, 2004). Semi-conductor photocatalysis shows promise as a supplementary step to water treatment in WTPs in regards to the removal of cyanobacterial secondary metabolites such as microcystins and odorous compounds, however, a number of inherent limitations need to be addressed if it is to develop its full potential. These drawbacks include separation of the catalyst from water that traditionally has been problematic (Liu *et al.*, 2009) and the prohibitive cost of retrofitting UV arrays necessary for semi-conductor photocatalysis over titanium dioxide.

## **1.6 Aims**

Cyanobacteria and their metabolites can cause serious harm to humans and can constitute a significant problem in potable water treatment and aquaculture alike, attempts to monitor and control these metabolites cost both industries large sums of money annually (Hanson, 2004). The aim of this study is to find means to alleviate the impact of cyanobacterial secondary metabolites by exploring the effects of microcystin-LR as a signalling compound on microcystin production with the aim of limiting *de novo* toxin synthesis in cultures of *Microcystis aeruginosa*, one of the prime producers of microcystins. Stable isotope labelling ( $^{15}\text{N}$ ) will be employed to monitor *de novo* toxin synthesis under different growth conditions, including cell density and putative pheromonal effects of microcystin-LR. However, in instances where altering the growth conditions is not feasible or where dissolved microcystins are already present in the water, means of removing the dissolved toxin will be

explored. UV assisted photocatalysis over titanium dioxide will be investigated applying a novel product, called Photospheres™. These titania covered, buoyant, hollow silica spheres may mitigate the inherent limitation of powder catalysts (difficulty of separation from water, Liu *et al.*, 2009) and pellet catalysts (decreased effectiveness, Liu *et al.*, 2009), by combining the advantages of both types (ease of removal, similar effectiveness as powder catalyst). After examining the effectiveness of Photospheres™ in the removal of microcystins, their universal applicability will be tested in the removal of four common organic water pollutants (2-chlorophenol, *p*-cresol, Acid Orange 74, and trichloroethylene). To alleviate the financial and environmental impact of applying UV light arrays the feasibility of applying UV light emitting diodes in the photocatalytic degradation of microcystin-LR over Photospheres™ will be explored.

Apart from cyanotoxins, off-flavour compounds like 2-methylisoborneol and geosmin are also produced by cyanobacteria. Both compounds contribute significantly to off-flavour episodes in drinking water and aquaculture produce. The human olfactory and gustatory recognition of these compounds is very sensitive and can lead to customer rejection of the product (water or aquaculture produce). Monitoring and controlling the levels of 2-MIB and GSM in water are necessary to avoid financial loss. An analytical method will be developed that is capable of determining the concentrations of both compounds below the human taste and odour threshold. For this a preconcentration method based on solid phase extraction will be optimised to achieve the required detection sensitivity.

Laboratory and environmental samples will be assessed with the method to ensure it is fit for purpose. With this method solid phase extraction could be carried out *in situ* and cartridges could be stored for future analysis in instances where immediate analysis is unfeasible or impractical, such as *in situ* at a fishfarm or on a research vessel. Based on this method the controlling of 2-MIB and GSM will be assessed with a continuous flow photocatalytic reactor that will degrade both compounds to concentrations below the human taste and odour threshold. After laboratory testing the method will be employed to remove both compounds from fishfarm waters that are known to contain 2-MIB and GSM. Furthermore a practical means of monitoring the concentration of both compounds will be evaluated. The use of silicone rubber membranes (SRMs) that are deployed in contaminated water and onto which the both 2-MIB and GSM adhere will be assessed in both laboratory and environmental samples. The use of SRMs would allow the determination of both compounds by the operators of a fishfarm or a water treatment plant and send the exposed membranes to a laboratory for analysis without having to have a laboratory on site. The use of SRMs on research vessels where space is at a premium with subsequent analysis in a remote laboratory would also be beneficial.

**Pheromonal activity of  
microcystin-LR in  
understanding the control  
of microcystins in water**

## **2 Pheromonal activity of microcystin-LR in understanding the control of microcystins in water**

### **2.1 Introduction**

Cyanobacteria can be present in water in mass occurrences called blooms (de Figueiredo, *et al.*, 2004). When these blooms collapse, i.e. the majority of cyanobacterial cells die, the cells lyse and toxic secondary metabolites are released into the water, which can lead to serious health implications in both humans and animals alike (Chorus and Batram, 1999). The monitoring and especially regulation of these cyanotoxins is important for human health and safety. This is illustrated by WHO guidelines ( $1 \mu\text{g L}^{-1}$  of microcystin-LR) regarding one of the most prominent cyanotoxins, the microcystins. Many studies have focussed on the environmental factors (light, oxidative stress, trace-metals, phosphate, nitrate, sulphate, temperature) that affect microcystin production (Lukac and Aegerter, 1993; Rapala and Sivonen, 1997; Jacoby *et al.*, 2000; Zilliges *et al.*, 2011; Jähnichen *et al.*, 2011; Briand *et al.*, 2012), however, there are few studies that have investigated the effect of potential semiochemicals (signalling compounds) or culture density on microcystin synthesis. Engelke *et al.* (2003) found increased microcystin and nodularin production in cultures grown in medium that had spent growth medium of another cyanobacterium (*Planktothrix agardhii*). The putative signalling compounds (a thiol-containing peptide) was isolated but not yet fully characterised. Bártová *et al.* (2011) found that extracts from a *Microcystis* bloom affected cellular differentiation in the filamentous cyanobacterium *Trichormus variabilis*, the extracts forced a decrease in heterocyst formation thus limiting *T. variabilis*' ability to fix nitrogen. The



findings in these examples, however, while involving semiochemicals, are classed as kairomonal in the case of the Engelke *et al.* (2003) study (i.e. benefitting the receiver) and allelomonal in the case of the Bártová *et al.* (2011) study (i.e. benefitting the sender). To date there are few studies investigating the pheromonal (having an effect on the same species) activity of cyanobacterial secondary metabolites, Fisher and Wolk (1976) demonstrated that sporulation in *Cylindrospermum licheniforme*, Kütz can be induced without the usual lag of 5 days when cultured in spent medium in which sporulation of *C. licheniforme*, Kütz had already occurred once, indicating the presence of a signalling compound dissolved in the extra-cellular matrix. Schatz *et al.* (2004) have shown that the presence of MC-LR and/or cell extracts from *M. aeruginosa* can lead to an up-regulation of the expression of the *mcyB* gene (part of the cluster encoding MC synthesis) and increase the amounts of intra-cellular MC-LR. More recently Gan *et al.* (2011) have shown that the addition of MC-RR and MC-LR to the growth medium of five different *Microcystis* sp. strains can lead to an increase of colony diameter, while the addition of MC-degrading bacteria (which reduced the concentration of the exogenous dissolved MCs in the medium) lead to the colony diameter reducing in size again. There are also a number of studies that, while not directly reporting on pheromonal effects of MCs further support the evidence for their putative role as semiochemicals. Pearson *et al.* (2004) have identified a gene that might encode a protein that can act as an active transporter of MCs from the intra- to the extra-cellular matrix. They could furthermore show that knocking out that gene led to a loss of toxigenicity in the *M. aeruginosa* strain (PCC 7806) tested. Zilliges *et al.* (2008) have identified an extra-

cellular glycoprotein that is associated with the outside of the cell wall, which may act as MC receptor. In addition they were able to show that this protein was only produced in toxigenic bacteria indicating that, if MCs are semiochemicals, a role as pheromone is very likely as only other MC-producing bacteria are able to produce this putative semiochemical.

Due to the potentially harmful effects of dissolved microcystins in potable water, it is important to understand factors affecting microcystin synthesis. Semiochemicals may present a way of understanding the control of microcystin concentrations in water. It is therefore important to elucidate the potential pheromonal effects of MC-LR on microcystin synthesis. In order to be able to monitor any potential semiochemical effects on MC synthesis a means of differentiating between *de novo*, i.e. newly produced toxin, and toxin that is present at the beginning of the experiment in the cells, is required. To achieve this two variables need to be closely monitored: cell density and *de novo* toxin production. In the past, studies that have monitored cell growth and microcystin synthesis have done this by counting cells with a haemocytometer, chlorophyll estimation, or cell dry weight (Chorus and Bartram, 1999), all of these approaches, however, have limitations. Dry weight and chlorophyll determinations cannot differentiate between living and dead cells and cell numbers can only be approximated from the results achieved. The use of a haemocytometer is time consuming and may be imprecise depending on the operator. A more time effective and reproducible approach is the use of a flow cytometer. Flow cytometry achieves reproducible results and allows the differentiation between living and dead cells (Veldhuis and

Kraay, 2000). In addition to monitor cell growth a means of differentiating between already present toxin and newly synthesised toxin is required. Stable isotope labelling with  $^{15}\text{N}$  nitrogen allows the monitoring of *de novo* production. The nitrogen source in the growth medium is replaced with  $^{15}\text{N}$  as sole source of nitrogen, the cyanobacterial cells will utilise the labelled nitrogen in the synthesis of MC. When determining the MC concentrations in a culture by liquid chromatography coupled with mass spectrometry, based on the molecular weight of the molecule it can be differentiated between labelled and unlabelled microcystin. Sano *et al.* (2011) have applied this method to create  $^{15}\text{N}$ -MC-LR LC-MS standards.

Utilising flow cytometry and stable isotope labelling with  $^{15}\text{N}$ , the effects of cell density, and potential pheromonal effects of MC-LR on microcystin production will be elucidated. After the selection of a suitable microcystin-producing strain of *Microcystis aeruginosa* the effects of exogenously added MC-LR will be assessed. Furthermore the effects of cell density and detailed pheromonal effects of MC-LR will be explored, especially in regards to toxin distribution (intra-cellular versus extra-cellular matrix). Finally the fate of exogenously added MC-LR will be investigated by applying stable isotope labelled ( $^{15}\text{N}$ ) MC-LR.

## **2.2 Materials and Methods**

### **2.2.1 Cultures**

Five different strains of *Microcystis aeruginosa* were used: PCC 7820, PCC 7813, PCC 7806, B2666, and NIES 1099. Of these PCC 7820, PCC 7813 and PCC 7806 were acquired from the Pasteur Culture Collection of Cyanobacteria, Paris, France. The B2666 strain was acquired from University of Texas Algal Culture Collection (UTEX), Austin, TX, USA, and NIES 1099 from the National Institute for Environmental Studies, Tsukuba-City, Japan.

### **2.2.2 Media**

To ensure a supply of cyanobacterial inoculum, cultures were routinely sub-cultured. The medium that cultures were grown in was BG-II (Stanier *et al.* 1971). Stock solutions of the different components that make up the medium were prepared and stored at room temperature (Table 2.1). The medium was prepared by transferring 10 mL of each of the first eight stock solutions into a 1 L volumetric flask. Then 1 mL of the trace element stock was added and the volume made up to 1 L with distilled water. All chemicals were obtained from Fisher Scientific (Leicestershire, UK) and used as received.

**Table 2.1:** Composition of BG-II medium (Stanier *et al.*, 1971).

<b>Component</b>	<b>BG-II (g L<sup>-1</sup>)</b>
Sodium nitrate (NaNO <sub>3</sub> )*	0.75
Dipotassium phosphate (K <sub>2</sub> HPO <sub>4</sub> )	0.040
Magnesium sulphate septahydrate (MgSO <sub>4</sub> .7H <sub>2</sub> O)	0.075
Calcium chloride dihydrate (CaCl <sub>2</sub> .2H <sub>2</sub> O)	0.036
Sodium carboate (Na <sub>2</sub> CO <sub>3</sub> )	0.020
Citric acid (C <sub>6</sub> H <sub>8</sub> O <sub>7</sub> )	0.006
Iron sulphate septahydrate (FeSO <sub>4</sub> .7H <sub>2</sub> O)	0.006
EDTA (di sodium)	0.001
Trace element solution	1 mL L <sup>-1</sup>
<b>Trace element solution:</b>	
Boric acid (H <sub>3</sub> BO <sub>3</sub> )	2.86
Manganese chloride tetrahydrate (MnCl <sub>2</sub> .4H <sub>2</sub> O)	1.81
Zinc sulphate septahydrate (ZnSO <sub>4</sub> .7H <sub>2</sub> O)	0.222
Sodium molybdate dihydrate (Na <sub>2</sub> MoO <sub>4</sub> .2H <sub>2</sub> O)	0.390
Copper sulphate pentahydrate (CuSO <sub>4</sub> .5H <sub>2</sub> O)	0.079
Cobalt nitrate hexahydrate (Co(NO <sub>3</sub> ) <sub>2</sub> .6H <sub>2</sub> O)	0.049

\*Sodium nitrate was replaced with stable isotope labelled nitrate (<sup>15</sup>N) (Cambridge Isotope Laboratories, Inc., Andover, MA, USA) where dictated by the experimental design.

### 2.2.3 Cell enumeration by flow cytometry

Cell counting was performed with a Beckman Coulter *Coulter Epics XI-MCL* (Beckman Coulter, Fullerton, CA, USA) flow cytometer. Samples were diluted with non-sterile BG-II medium before cell counting. The BG-II medium was first vacuum filtered using GF/C (5.5 cm diameter) (Schleicher and Schuell, Maidland, UK), then syringe filtered using a BD Discardit II 20 mL syringe (BD, Franklin Lakes, NJ, USA) with a Spectrum

ME/0.2  $\mu\text{m}$  filter with a surface area of 5.5  $\text{cm}^2$  (Spectrum, Gardena, CA, USA) to ensure the elimination of background particles. Samples were diluted 100-fold and placed in micro-centrifuge tubes (1.5 mL). After dilution, samples were loaded into the flow cytometer (injection volume 15  $\mu\text{L}$ ) and the cell count was recorded.

## **2.2.4 Analysis of microcystins**

### **2.2.4.1 HPLC-PDA analysis of microcystins**

The instrument used was a Waters 2695 Separation Module. High resolution photodiode detection was performed with a Waters 2996 Photodiode Array Detector (PDA) (Waters, Elstree, UK). Separation of analytes was performed with a Sunfire C18 column (2.1 mm x 150 mm; 5  $\mu\text{m}$  particle size) (Waters, Elstree, UK). The mobile phase used was Milli-Q and acetonitrile ( $\text{C}_2\text{H}_3\text{N}$ ), containing 0.05 % trifluoroacetic acid (TFA). The flow rate applied was 0.3  $\text{mL min}^{-1}$ . The PDA resolution was set to 1.2 nm and data was acquired in the range of 200 to 400 nm. Column temperature was maintained at 40  $^\circ\text{C}$ . The method used was based on Lawton *et al.* (1994) (table 2.2).

**Table 2.2:** The solvent gradient used in the method for the analysis of microcystins (Lawton *et al.*, 1994). Solvent A: Milli-Q water with 0.05 % TFA; Solvent B: Acetonitrile with 0.05 % TFA.

<b>Microcystin method (Lawton <i>et al.</i>, 1994)</b>		
<b>Time (min)</b>	<b>A (%)</b>	<b>B (%)</b>
0-24	75	25
25	15	85
27-33	0	100
33-35	75	25

#### **2.2.4.2 HPLC-MS analysis of microcystins**

The instrument used was a Waters 2695 Separation Module coupled to a Micromass ZQ 2000 MS detector (Waters, Elstree, UK). High resolution photodiode detection was performed with a Waters 2996 Photodiode Array Detector (Waters, Elstree, UK). Separation of analytes was performed with a Sunfire C18 (column 2.1 mm x 150 mm; 5  $\mu$ m particle size) (Waters, Elstree, UK). The mobile phase used was Milli-Q and acetonitrile (C<sub>2</sub>H<sub>3</sub>N) (Rathburn, Walkerburn, UK), containing 0.05 % trifluoroacetic acid (TFA) (Fischer Scientific, Leicestershire, UK). The flow rate applied was 0.3 mL min<sup>-1</sup>. Mass spectrometric analysis was performed in positive ion electrospray mode. Mass to charge ratios ( $m/z$ ) from 100 to 1200 were scanned with a scan time of 2 seconds and an inter-scan delay of 0.1 seconds. Sprayer voltage was set at 3.07 kV, the cone voltage at 80 V, and desolvation and source temperatures were 300°C and 100°C respectively. The PDA resolution was set to 1.2 nm and data was acquired in the range of 200 to 400 nm. The wavelength used to analyse microcystins was 238 nm. Column temperature was maintained at 40 °C. The HPLC-MS used an injection volume of 25  $\mu$ L for samples and 10  $\mu$ L for the standards. Microcystins were identified based on their characteristic retention times,

UV spectra and by their mass fragmentation pattern. A set of point standards was analysed along with each batch of samples. The standards consisted of two replicates each of MC-LR ( $100 \mu\text{g mL}^{-1}$ ) and a mix of MC-LY, MC-LW, and MC-LF ( $50 \mu\text{g mL}^{-1}$ ). A 35 minute method was used to analyse various microcystin variants by PDA and MS (table 2.3).

**Table 2.3:** The solvent gradient used for the general analysis of microcystins. Solvent A: Milli-Q water with 0.05 % TFA; Solvent B: Acetonitrile with 0.05 % TFA.

<i>HPLC-MS Method</i>		
<b>Time (min)</b>	<b>A (%)</b>	<b>B (%)</b>
0-24	85	15
25-26	35	65
27-33	0	100
34-35	85	15

#### **2.2.4.3 UPLC-MS analysis of microcystins**

For the final two investigations on the pheromonal effects of microcystin-LR sample analysis was conducted by UPLC-MS. The system used was a ACQUITY UPLC system with an ACQUITY UPLC PDA photodiode array detector coupled with a Xevo TQD tandem quadrupole mass spectrometer in series (Waters, Elstree, UK). The column used was a ACQUITY UPLC BEH C18 column (2.1 mm diameter, 100 mm length,  $1.7 \mu\text{m}$  particle size) (Waters, Elstree, UK). For PDA detection samples were monitored from 200 to 400 nm with a resolution of 1.2 nm. For mass spectrometric analysis, positive ion electro-spray (ES+) ionisation was used, the detector scanned from  $m/z$  50 to  $m/z$  2000 Da with a scan time of 0.25 seconds and an inter-scanner delay time of 0.025 seconds. The capillary voltage applied was 3.0 kV and cone voltage was set to 25 V. The source



and desolvation temperatures were 80 °C and 300 °C respectively. The flow rate for the cone gas was set to 50 L h<sup>-1</sup> and the flow rate of the desolvation gas was set to 40 L h<sup>-1</sup>. "The solvents applied are Milli-Q water and acetonitrile both with 0.1 % formic acid added as ion suppression agent. The solvents are applied in a gradient starting with 20 % acetonitrile, which is increased to 80 % over 10 minutes, followed by a washing step (100 % acetonitrile) and re-equilibration over the next 5 minutes. Total gradient time is 15 minutes. The flow-rate applied is 0.2 mL min<sup>-1</sup>."

## **2.2.5 Elucidation of growth characteristics of four different *M.***

### ***aeruginosa* strains**

Four different strains of *M. aeruginosa* were used: PCC 7820, PCC 7813, B2666, NIES 1099. Four replicates for each strain were prepared, by adding 100 mL of BG-II medium into a 250 mL flask. The media was then autoclaved (20 min, 121 °C). A culture inoculum (10 mL) was added to the flasks under aseptic conditions. Sampling was performed every three to four days (twice weekly). For each sampling 1 mL of culture was aseptically removed from the flasks and placed in a micro-centrifuge tube (1.5 mL). Cell counting was performed on each sample as described in section 2.2.3. HPLC analysis was carried out as described in section 2.2.4, using PDA detection. The duration of the experiment was 45 days.

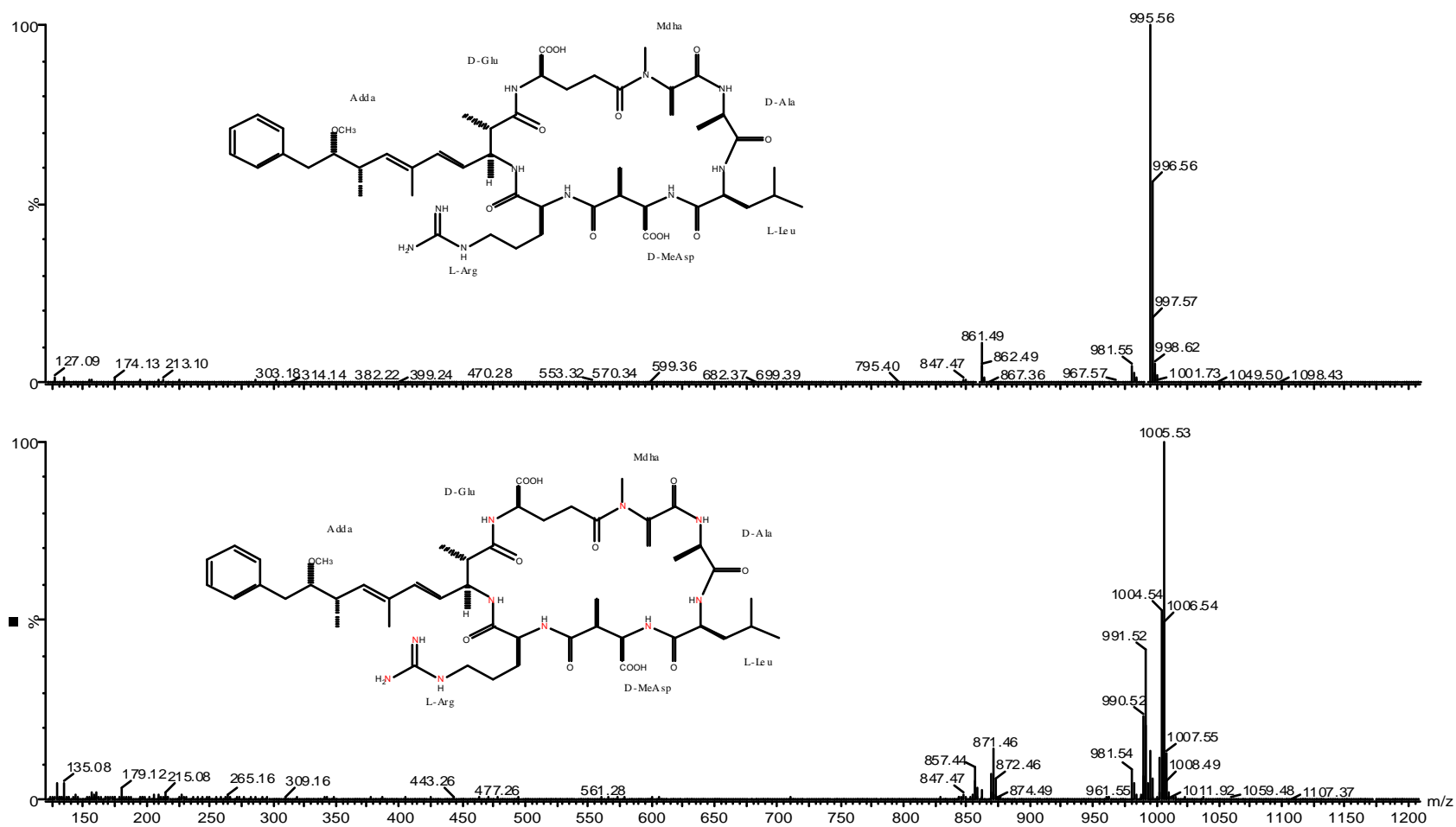
### 2.2.6 Stable isotope labelling microcystins with $^{15}\text{N}$

In order to be able to differentiate between microcystin already present in the cell and *de novo* toxin, stable isotope labelling with  $^{15}\text{N}$  was employed. The stable isotope labelled  $^{15}\text{N}$  was supplied as sole nitrogen source in the BG-II growth medium. This would ensure that any *de novo* toxin synthesised in the cells over the course of the experiment would include labelled MC. The labelled toxin differs in mass from an unlabelled molecule (ten mass units heavier), this difference can be detected mass spectrometrically (figure 2.1). The difference in mass can also be observed in the major fragment ions (figure 2.2; table 2.4).

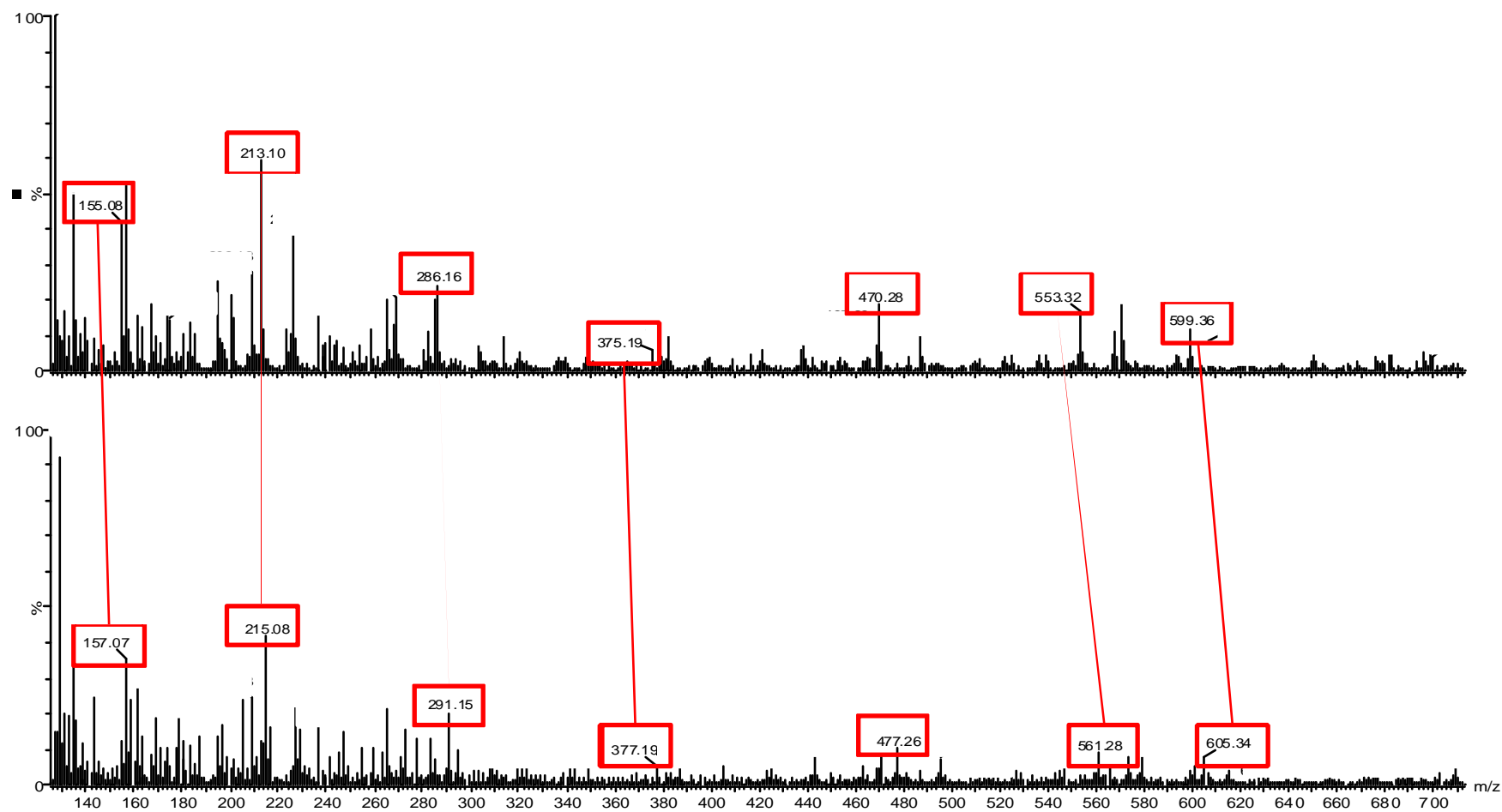
**Table 2.4:** Fragment ions of unlabelled ( $^{14}\text{N}$ ) and labelled ( $^{15}\text{N}$ ) microcystin-LR

<b><i>Ion structure</i></b>	<b><i>m/z</i> <math>^{14}\text{N}</math></b>	<b><i>m/z</i> <math>^{15}\text{N}</math></b>
[Mdha-Ala+H] <sup>+</sup>	155	157
[Glu-Mdha+H] <sup>+</sup>	213	215
[Arg-MeAsp+H] <sup>+</sup>	286	291
[C <sub>11</sub> H <sub>15</sub> O-Glu-Mdha+H] <sup>+</sup>	375	377
[Arg-Adda+H] <sup>+</sup>	470	477
[Mdha-Ala-Leu-MeAsp-Arg+H] <sup>+</sup>	553	561
[MeAsp-Arg-Adda+H] <sup>+</sup>	599	605

The application of the labelled isotopes was performed as described in Pestana (2008). The recipe for BG-II was altered by replacing unlabelled sodium nitrate with labelled sodium nitrate. In all other respects medium preparation remained unchanged.



**Figure 2.1:** MS chromatograms of unlabelled ( $^{14}\text{N}$ ) and labelled ( $^{15}\text{N}$ ) microcystin-LR and their corresponding structures (labelled nitrogen atoms are indicated in red).



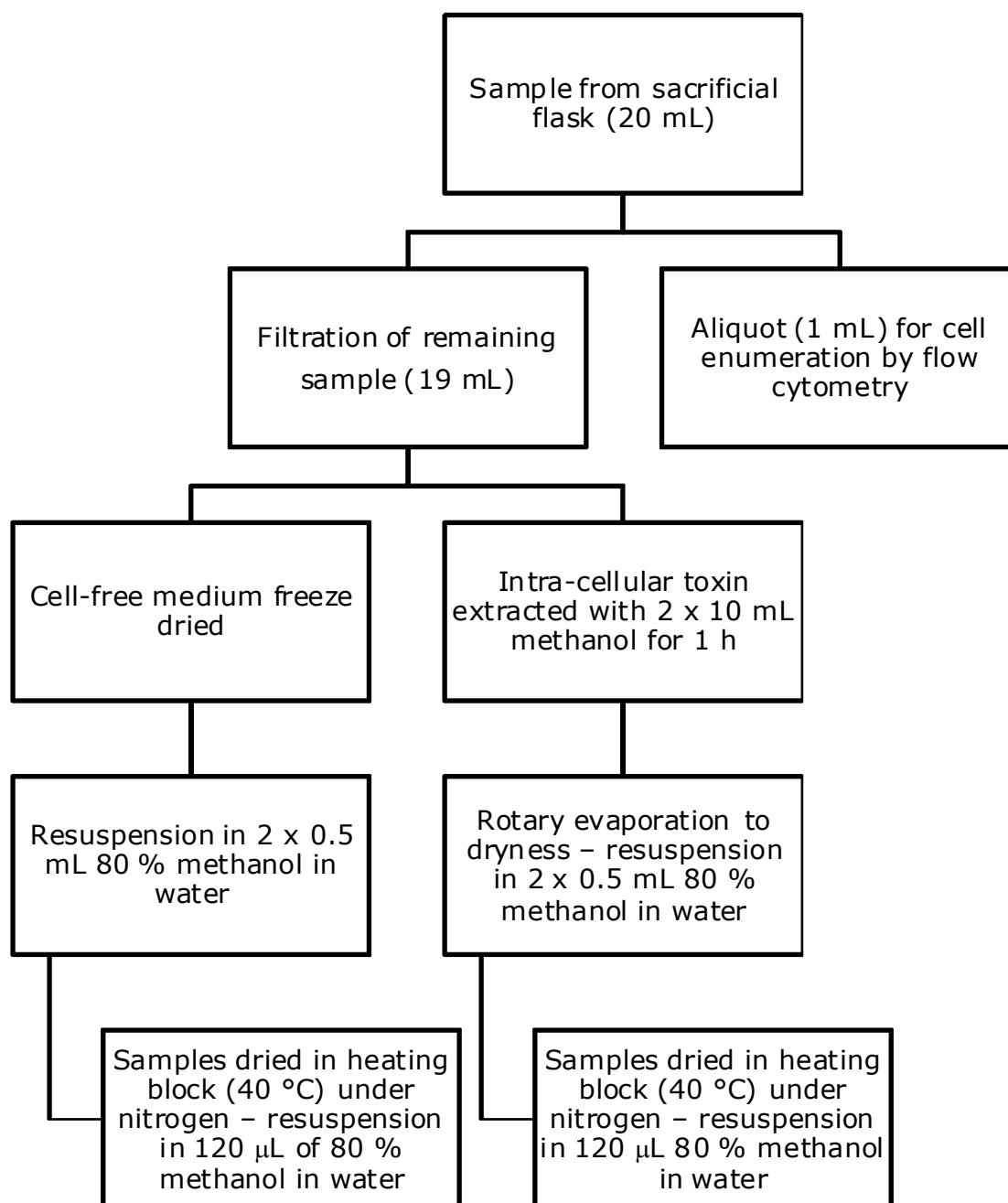
**Figure 2.2:** Chromatogram of labelled ( $^{15}\text{N}$ ) and unlabelled ( $^{14}\text{N}$ ) microcystin-LR (scanned to m/z 700 to include major fragment ions). Major fragment ions with the corresponding labelled analogue are indicated (table 2.4)

### 2.2.7 Assessing the impact of microcystin as a pheromone

To determine the amount of *de novo* microcystin produced under different treatment regimes, cultures were grown in the presence of stable isotope labelled sodium nitrate ( $^{15}\text{N}$ ), which would ultimately be incorporated into all *de novo* toxin molecules altering their molecular mass, thus making them distinguishable from the existing MC. Three different types of media were used: ( $^{14}\text{N}$ ) unlabelled BG-II, ( $^{15}\text{N}$ ) labelled BG-II, and ( $^{15}\text{N}$ ) labelled BG-II with the addition of microcystin ( $10\ \mu\text{g mL}^{-1}$ ). All three treatments were prepared in triplicate. The experiment was conducted for 10 days with sampling and cell counting daily. All cultures were grown in 50 mL sacrificial flasks with a culture volume of 20 mL. To prepare the inoculums, cells grown in  $\text{Na}^{14}\text{NO}_3$  BG-II were centrifuged. Approximately 2000 mL of a 16 day-old (thus ensuring log-phase bacteria) *M. aeruginosa* PCC 7820 culture were transferred to multiple 50 mL centrifugation tubes and were centrifuged at approximately  $2000 \times g$  for 20 minutes at room temperature. After centrifugation the supernatant was discarded and the pellets were resuspended in fresh medium ( $^{14}\text{N}$  or  $^{15}\text{N}$  BG-II medium). For inoculation autoclaved (20 min,  $120\ ^\circ\text{C}$ ) flasks were filled with 10 mL of fresh medium (either  $^{14}\text{N}$  or  $^{15}\text{N}$  BG-II) and then inoculated with 10 mL of cultures from the respective media. The flasks that had the toxin added were filled with 9 mL of  $^{15}\text{N}$  medium and 1 mL of a  $200\ \mu\text{g mL}^{-1}$  microcystin-LR solution (resulting in a final concentration of  $10\ \mu\text{g mL}^{-1}$  per flask), and 10 mL of culture with the appropriate medium. For the duration of the experiment the cultures were incubated at  $22\ ^\circ\text{C} \pm 2\ ^\circ\text{C}$  under continuous illumination of  $6.51 \pm 1.07\ \mu\text{mol m}^{-2} \text{s}^{-1}$  by cool white fluorescent tubes. Cell enumeration was performed for each sample on the

day of sampling as described in section 2.2.3. After sampling, cells were separated from the medium by vacuum filtration (GF/C, 5.5 cm diameter). Both filtrate and the filter disks (containing retained cells) were stored in the freezer at -20°C until processed. For the extraction of the extra-cellular toxin the filtrate was freeze-dried (Modulyo freeze drier; Fischer Scientific, Giessen, Germany), then resuspended in two times 0.5 mL of 80 % methanol in water. Samples were then centrifuged to remove suspended solids. The samples were then placed in a drying block and sparged with nitrogen to complete dryness at 45°C. The samples were then resuspended in 120 µL of 80 % methanol in water and stored in the freezer at -20°C until analysis. In order to extract the toxin from the cells the filter disks were placed in glass universal bottles. The bottles were then filled with methanol (10 mL) (Rathburn, Walkerburn, UK) and extracted for one hour with occasional agitation. The solvent was then transferred to pear-shaped rotary evaporation flasks (Büchi, Flawil, Switzerland). The extraction procedure was repeated to give a total volume of 20 mL. Rotary evaporation was conducted on a Büchi Rotavapor R-200 rotary evaporator, at 200 mbar and water bath temperature of 45 °C for approximately 20 to 25 minutes. The pressure was then lowered to approximately 75 mbar for 10 to 15 minutes to evaporate the sample to dryness by removing residual water. The samples were resuspended in two times 0.5 ml of 80 % methanol in water and placed in microcentrifuge tubes (1.5 mL). Then samples were placed in a heating block at approximately 40°C and sparged with nitrogen to complete dryness. Samples were then resuspended in 120 µL of 80 % methanol in water and stored in microcentrifuge tubes (1.5 mL) in the freezer at -20°C until

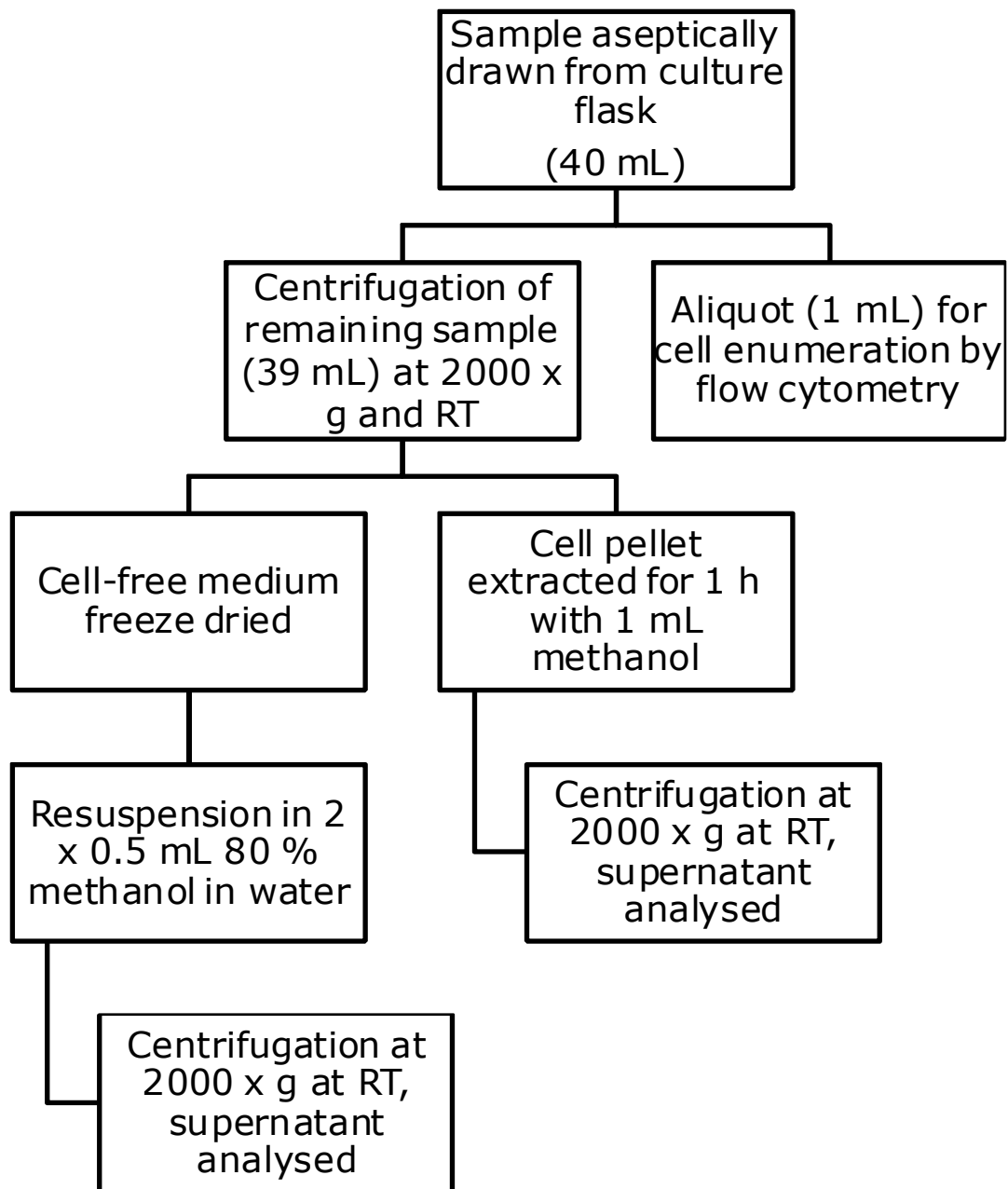
analysis (figure 2.3). HPLC-MS analysis was performed as described in section 2.2.4.2.



**Figure 2.3:** Sampling procedure in the investigation of the putative pheromonal effect of MC-LR in cultures of *M. aeruginosa* PCC 7820

To assess the effect of cell density on toxin production a new investigation was designed. Furthermore, it was decided to simplify the sampling procedure to reduce the impact of random and systematic error. For this investigation an inoculum of *M. aeruginosa* PCC 7820 was grown until a culture age of 18 days. The cultures were transferred to centrifuge tubes (50 mL) and centrifuged for 20 minutes and 2000 x g at room temperature to separate cells and medium. The supernatant was discarded and the cells were aseptically resuspended in <sup>15</sup>N BG-II medium. Sterile <sup>15</sup>N BG-II medium was transferred into sterile 500 mL Erlenmeyer flasks and varying amounts of culture added to achieve different inoculation cell densities (2.5, 5, 10, 20, 30 x 10<sup>6</sup> cells mL<sup>-1</sup>; 2.5 x 10<sup>6</sup> cells mL<sup>-1</sup> + 10 µg mL<sup>-1</sup> MC-LR), in triplicated. Sampling was performed immediately after inoculation, after 3, 7, and 10 days. On each sampling day, 40 mL was aseptically removed from the cultures. Of the samples 1 mL was used for cell enumeration with flow cytometry (2.2.3), the remaining 39 mL were centrifuged (50 mL centrifuge tubes) for 20 minutes at 2000 x g at room temperature. The supernatant was removed, frozen then freeze-dried, the toxin was extracted from the cell pellet with methanol (1 mL) for 1 h with occasional agitation. The freeze-dried supernatant was resuspended with 2 times 0.5 mL of 80 % methanol in water (figure 2.4). Samples were analysed by UPLC (section 2.2.4.3).





**Figure 2.4:** Elucidation of the effect of cell density and the putative pheromonal effect of MC-LR on toxin synthesis in *M. aeruginosa* PCC 7820.

To elucidate the fate of the exogenous toxin, the PCC 7820 strain of *M. aeruginosa* was exposed to labelled ( $^{15}\text{N}$ ), exogenous MC-LR. For this labelled ( $^{15}\text{N}$ ) MC-LR had to be produced. Cultures of *M. aeruginosa* PCC 7820 (100 mL) were grown in  $\text{Na}^{15}\text{NO}_3$  BG-II for 21 days, the cultures

were then used to inoculate a culture volume of 1 L, and subsequently, after another 28 days were used to inoculate a culture volume of 10 L. The cultures were then grown for 42 days and then harvested and the <sup>15</sup>N-MC-LR was purified according to Edwards *et al.* (1996). For the elucidation of the fate of the exogenous toxin, the experimental design was as described in the previous investigation with the difference that only 2.5 x 10<sup>6</sup> cells mL<sup>-1</sup> and 2.5 x 10<sup>6</sup> cells mL<sup>-1</sup> with 1 µg mL<sup>-1</sup> labelled MC-LR were used. The experiment was carried out in triplicate.

Statistical analysis on the samples was performed when determining the statistical significance of medium additives and/or cell densities. In these instances the paired t-test was selected (equation 2.1).

$$= \frac{\Sigma}{\frac{(\Sigma \quad) - (\Sigma \quad)}{-1}}$$

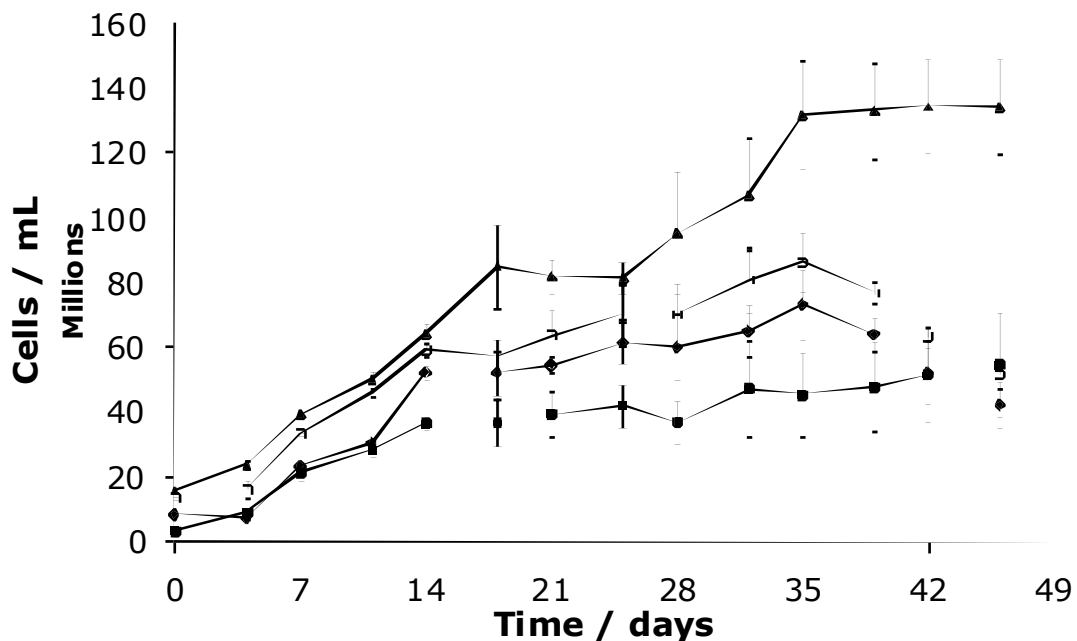
**Equation 2.1:** Paired t-test used to determine statistical significance between sample sets.

The acquired result was crossed referenced with a probability level of 0.05 and 2 degrees of freedom on a critical values table and the result for *p* was reported.

## 2.3 Results

### 2.3.1 Elucidation of growth characteristics of four different *M. aeruginosa* strains

In order to investigate and elucidate the growth dynamics of four different MC-producing strains of *Microcystin aeruginosa*, a growth experiment was performed with bi-weekly cell counting using flow cytometry (figure 2.5). The strains were examined to ensure that cultures used in future experiments were in log-phase growth. In addition the toxin production of these strains was monitored.

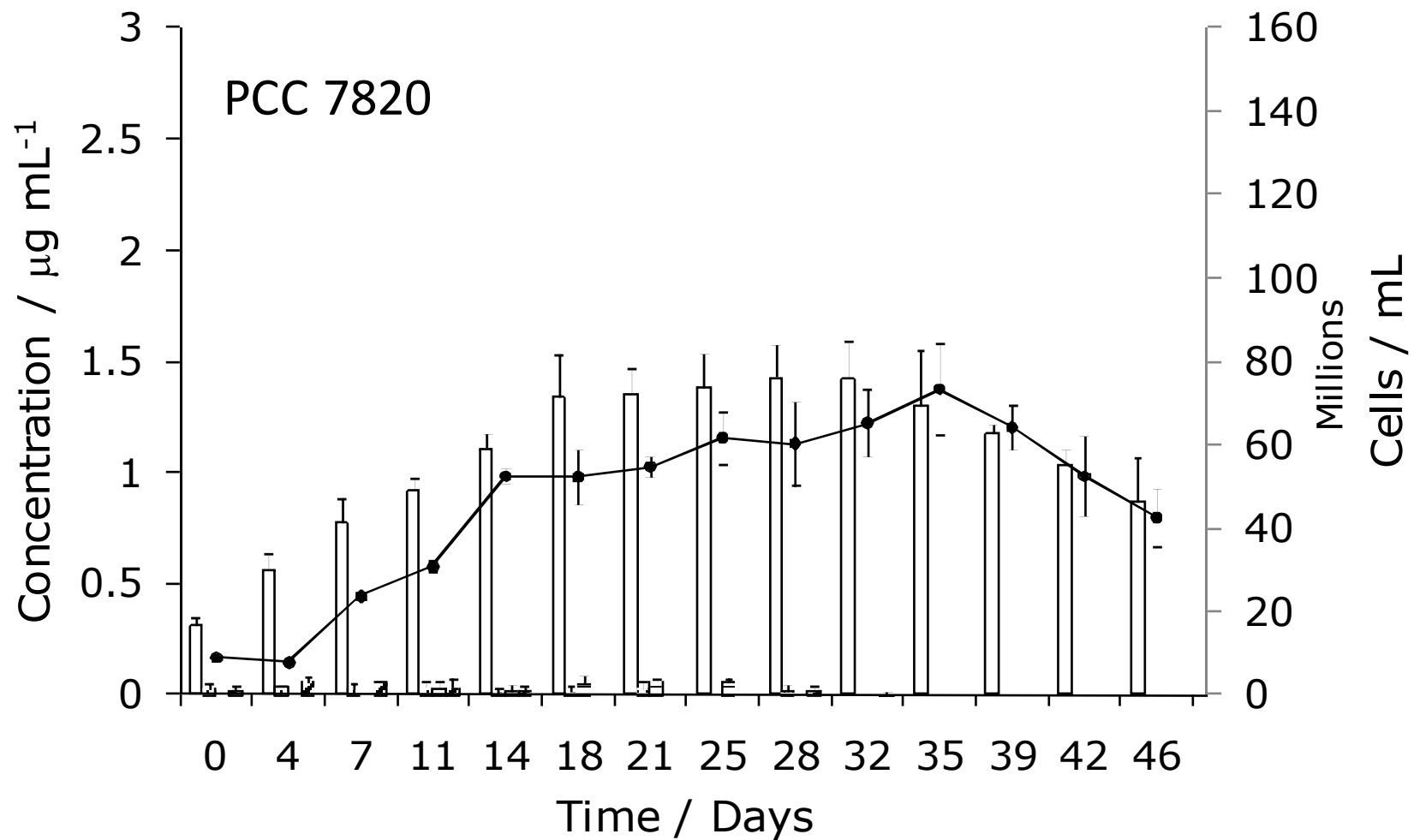


**Figure 2.5:** Growth dynamics of four strains of *M. aeruginosa*, grown for 7 weeks. ■ *M. aeruginosa* PCC 7813; ♦ *M. aeruginosa* PCC 7820; ▲ *M. aeruginosa* B2666; □ *M. aeruginosa* NIES 1099. Error bars=1 SD; n=4

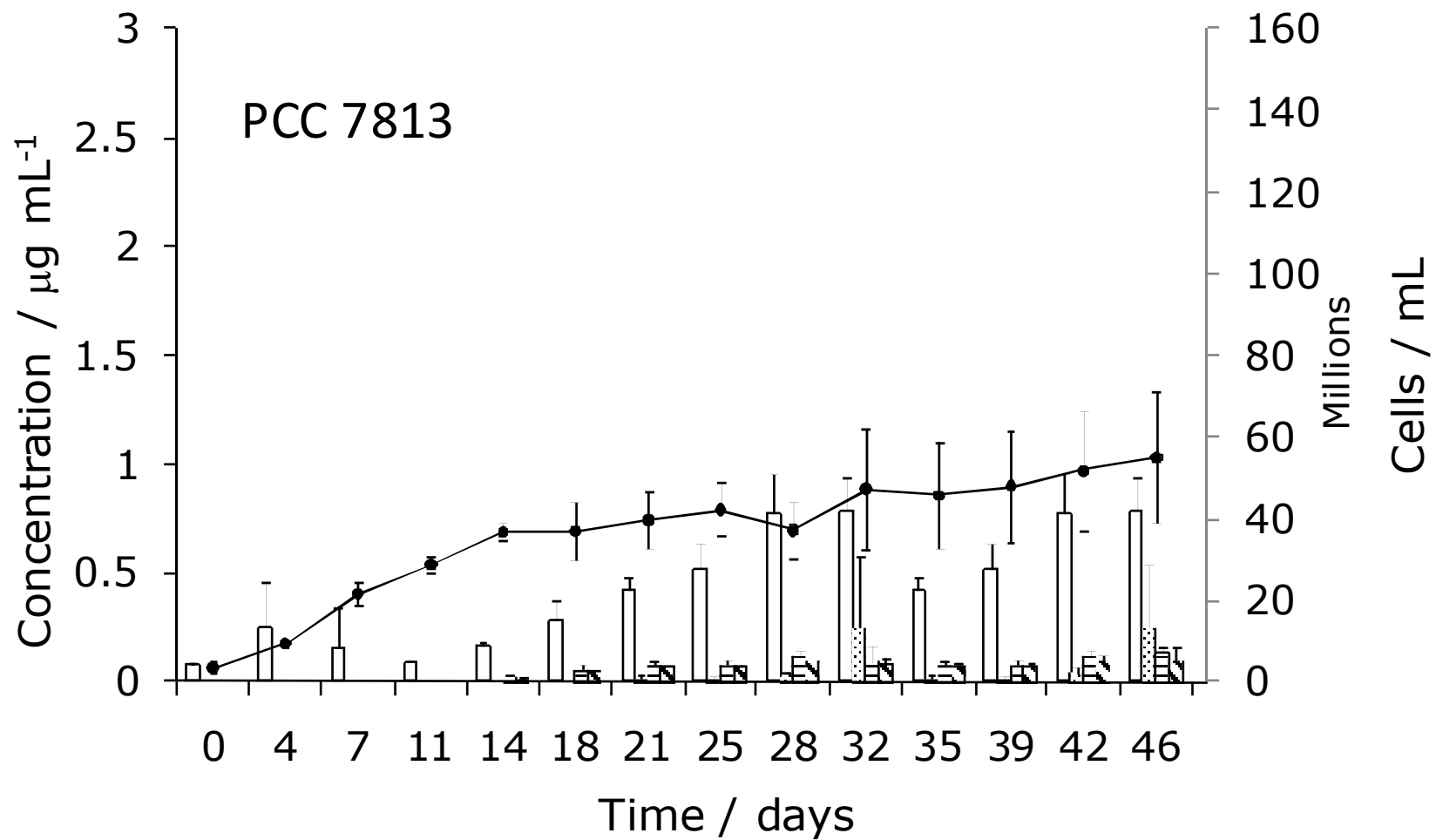
The PCC 7820 and NIES 1099 strains follow a similar growth pattern, with steadily increasing cell numbers until a peak is reached after five weeks, following this cell numbers drop as cells enter the death phase. The B2666

strain doubles its cell numbers in ever increasing intervals. It does not show signs of decreasing cell numbers at the end of the experiment. PCC 7813 doubles its cell numbers approximately every seven days for the first 14 days, after which cell numbers remain steady for the remainder of the experiment. It is known that this strain does not contain gas vesicles and since there was no agitation of the cultures this may have limited growth. The four strains were also monitored for their production of the microcystin variants they produce (figure 2.6).

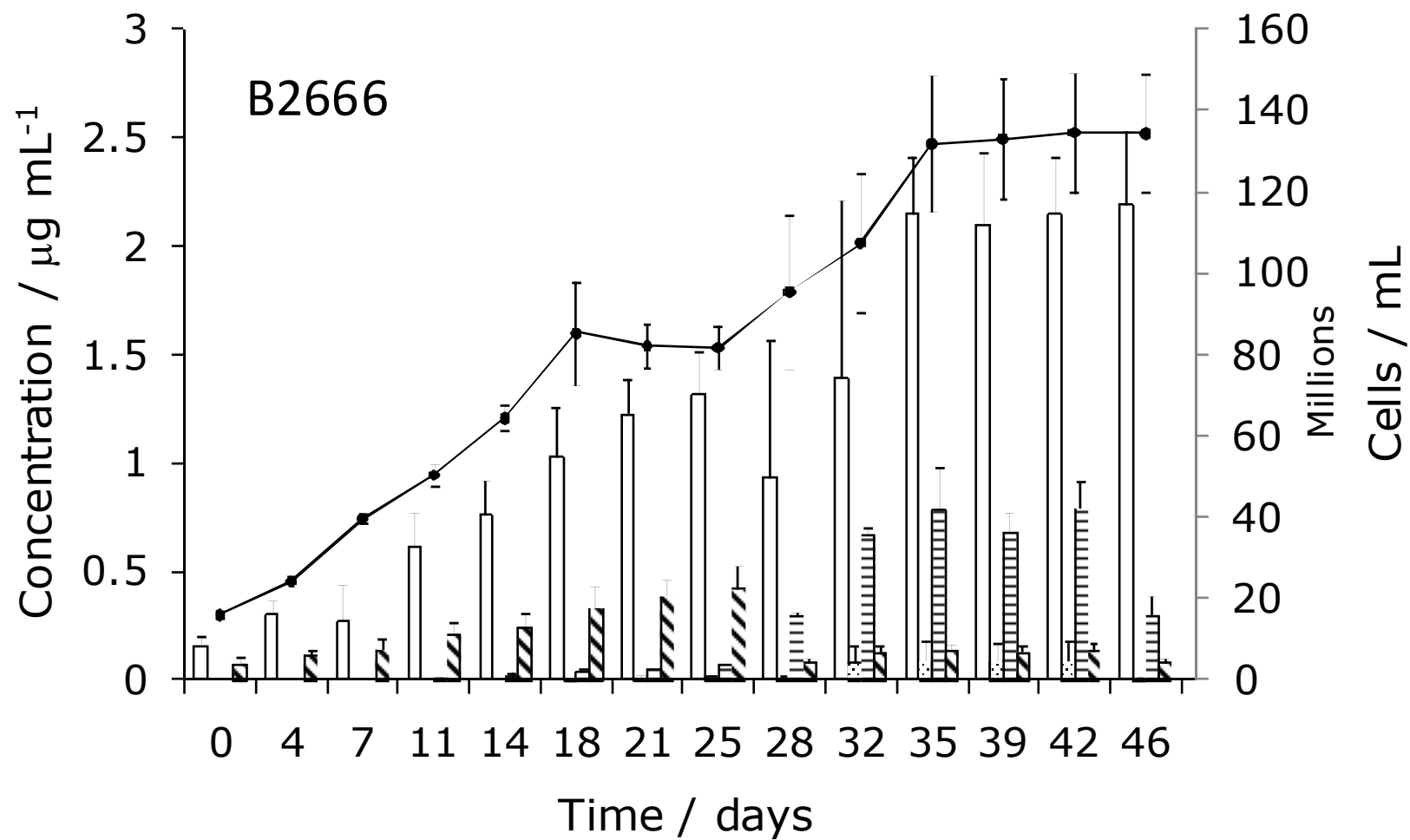
All four strains produced MC-LR. *M. aeruginosa* B2666 produced the highest amount during the time frame of the experiment, with approximately  $2.5 \mu\text{g mL}^{-1}$ . The PCC 7820 strain produced about  $1.5 \mu\text{g mL}^{-1}$ , PCC 7813 produced just less than  $1 \mu\text{g mL}^{-1}$  and the NIES1099 strain produced  $0.18 \mu\text{g mL}^{-1}$ . Neither of the strains of the Pasteur Collection produced a high amount of the other three variants, with PCC 7820 (MC-LY:  $0.24 \mu\text{g mL}^{-1}$ , MC-LW:  $0.11 \mu\text{g mL}^{-1}$  and MC-LF:  $0.11 \mu\text{g mL}^{-1}$ ) producing more than PCC 7813 (MC-LY:  $0.3 \mu\text{g mL}^{-1}$ , MC-LW:  $0.06 \mu\text{g mL}^{-1}$  and MC-LF:  $0.06 \mu\text{g mL}^{-1}$ ).



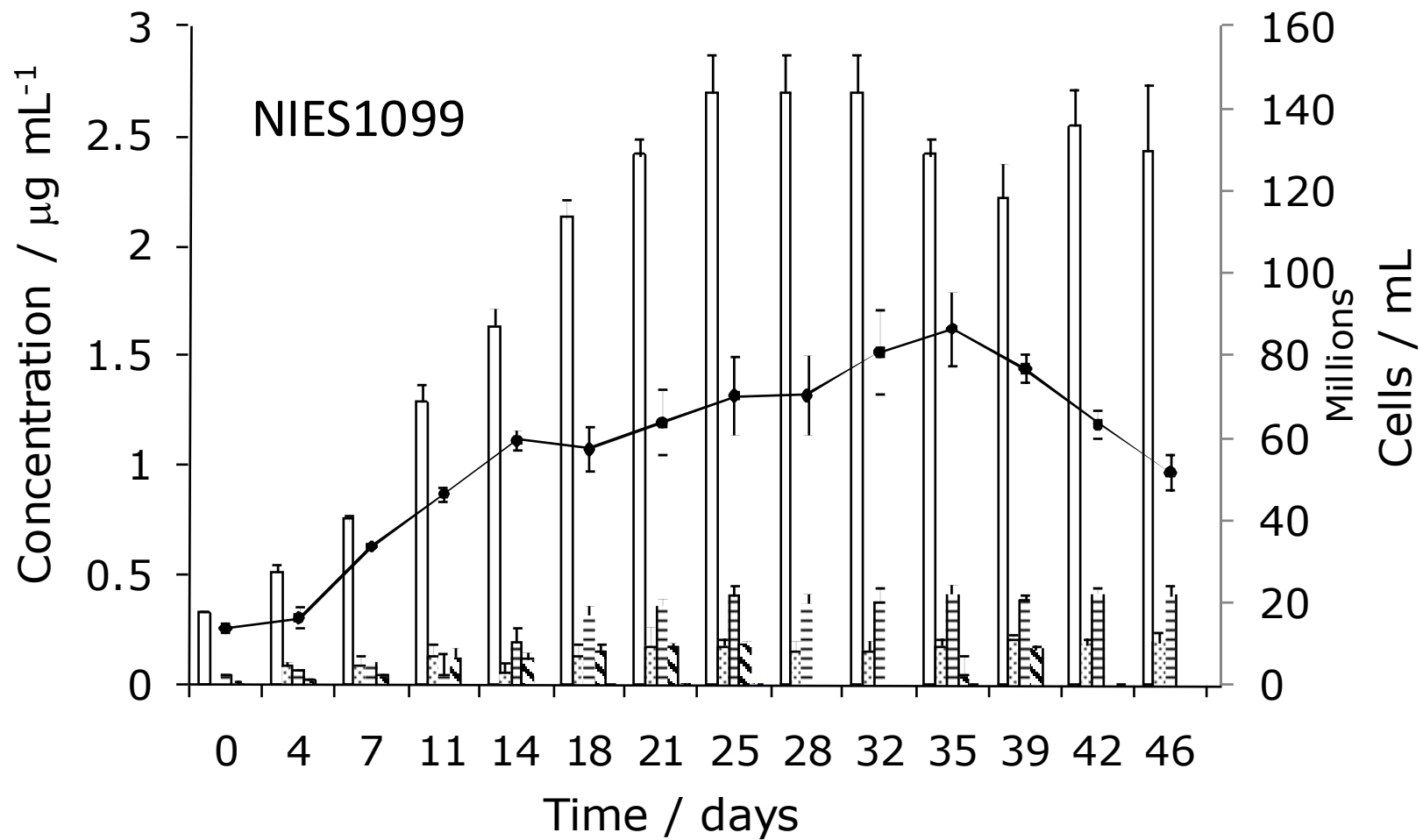
**Figure 2.6a:** Correlation between cell number and toxin production over a 7 week period in *M. aeruginosa* PCC 7820 as determined by HPLC-PDA (extracted at 238 nm) and flow cytometry: — MC-LR, ◻ MC-LY, = MC-LW, ◼ MC-LF. Error bars=1 SD; n=4



**Figure 2.6b:** Correlation between cell number and toxin production over a 7 week period in *M. aeruginosa* PCC 7813 as determined by HPLC-PDA (extracted at 238 nm) and flow cytometry: — MC-LR, ▨ MC-LY, ▩ MC-LW, ▧ MC-LF. Error bars=1 SD; n=4



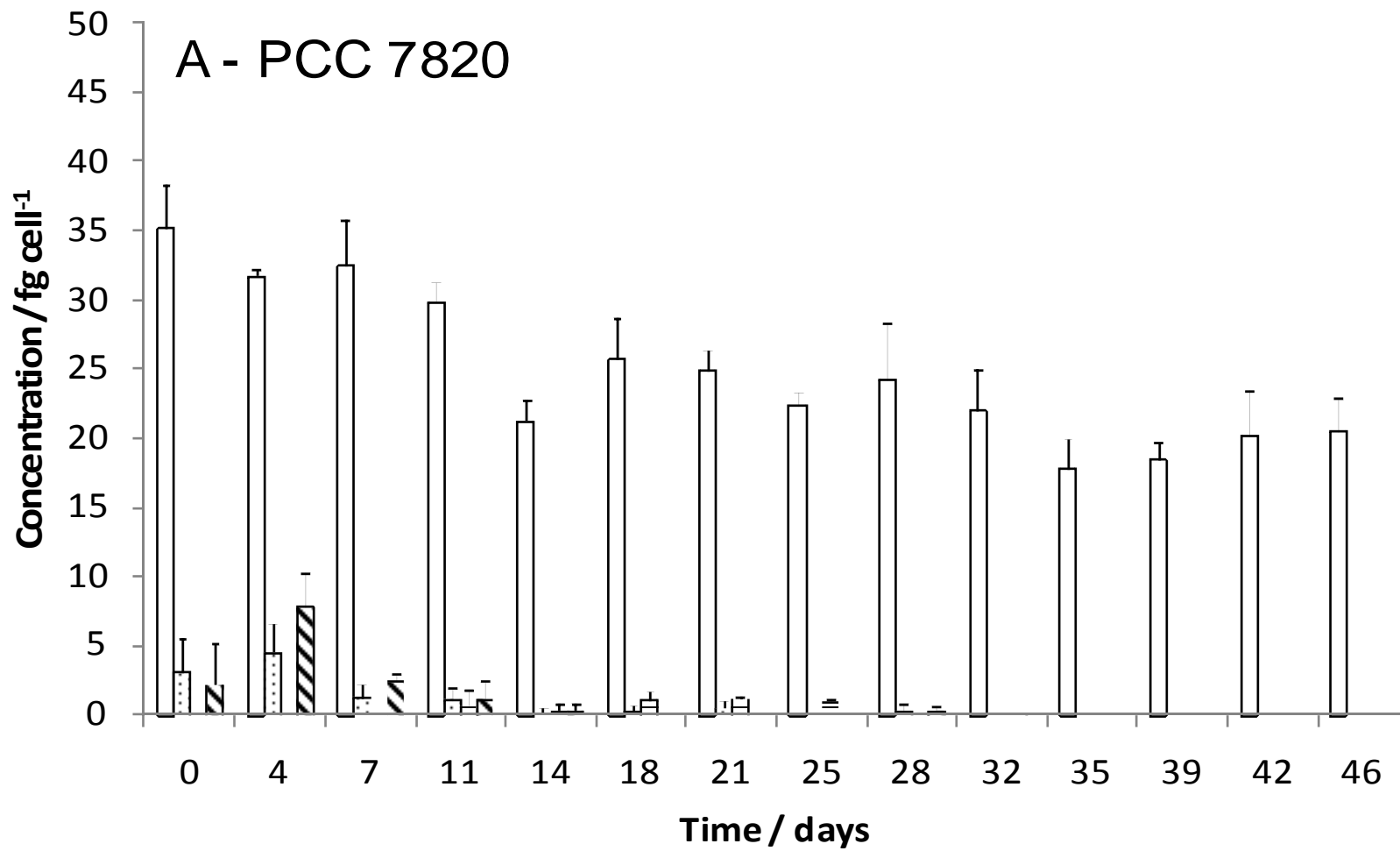
**Figure 2.6c:** Correlation between cell number and toxin production over a 7 week period *M. aeruginosa* B2666 as determined by HPLC-PDA (extracted at 238 nm) and flow cytometry: — MC-LR, ▨ demethylated MC-LA, ▤ unidentified microcystin, ▩ MC-LA. Error bars=1 SD; n=4



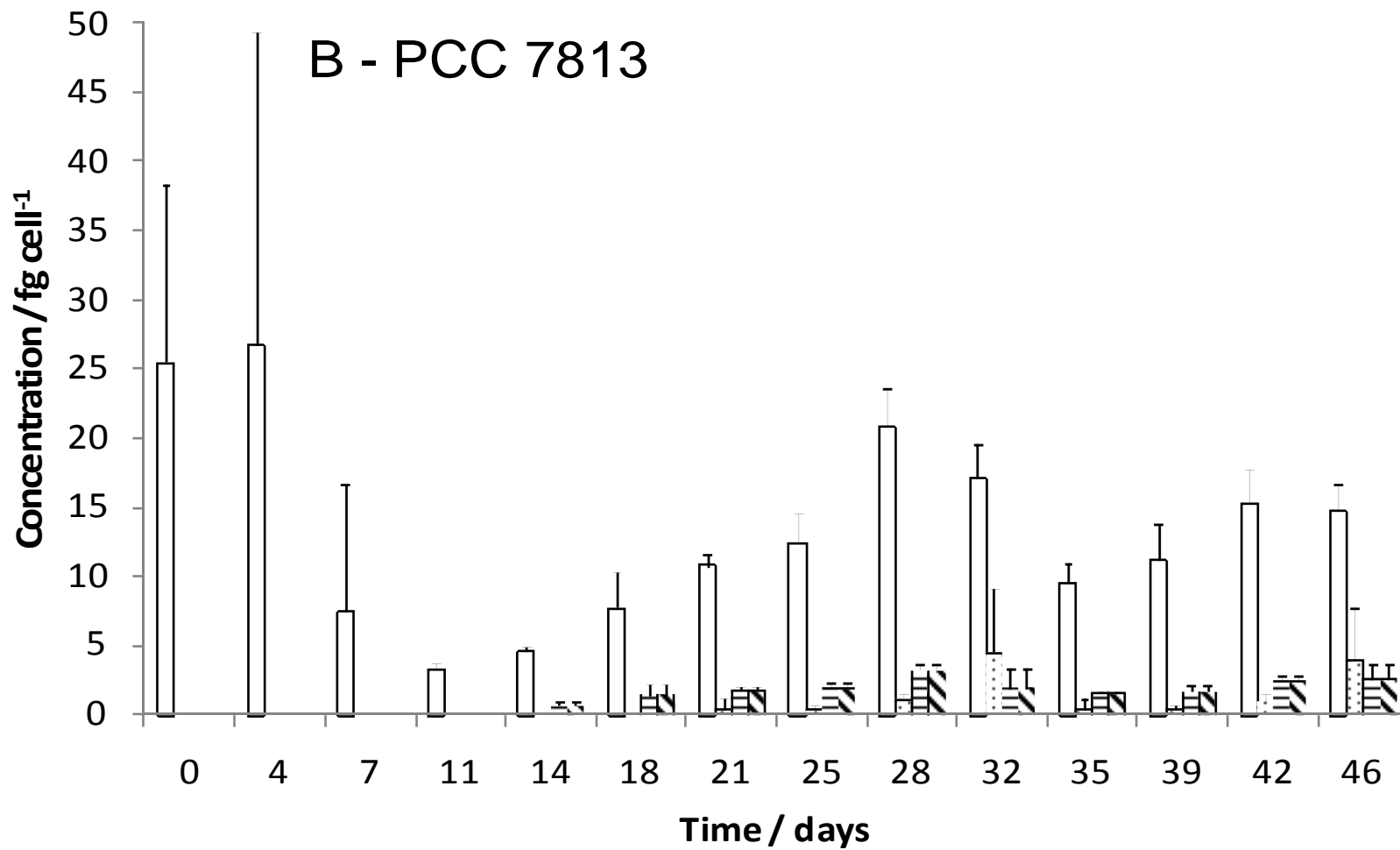
**Figure 2.6d:** Correlation between cell number and toxin production over a 7 week period *M. aeruginosa* NIES 1099 as determined by HPLC-PDA (extracted at 238 nm) and flow cytometry:  $\square$  MC-RR,  $\Gamma$  unidentified microcystin,  $\text{F}$  MC-YR,  $\text{▣}$  MC-LR. Error bars=1 SD; n=4



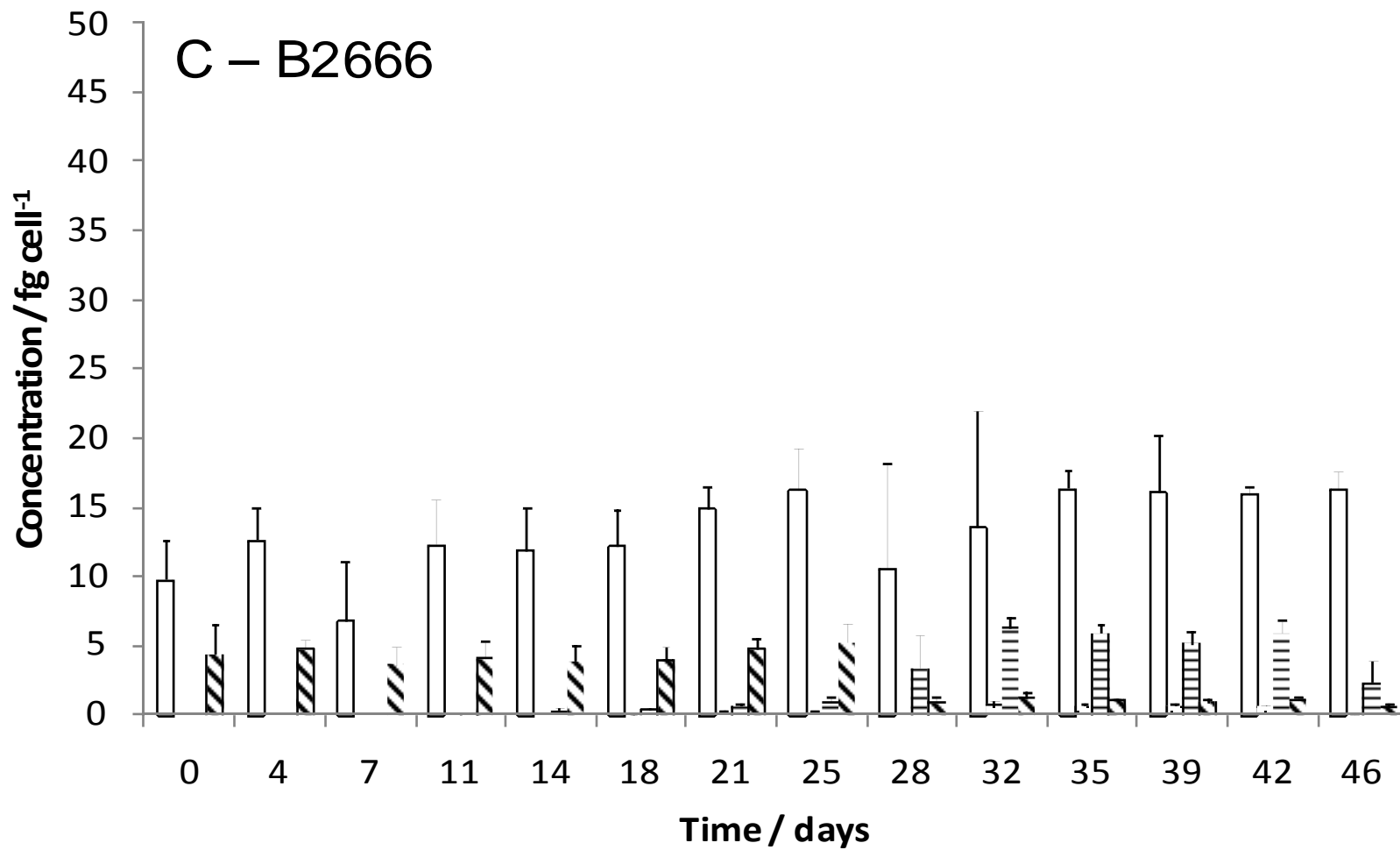
The B2666 strain produced relatively high amounts of an unidentified microcystin (up to  $0.77 \mu\text{g mL}^{-1}$ ). Furthermore MC-LA and methylated MC-LA are synthesised ( $0.44$  and  $0.10 \mu\text{g mL}^{-1}$  respectively) by B2666. Of the variants produced by NIES 1099 MC-RR stood out with high amounts ( $2.7 \mu\text{g mL}^{-1}$ ) produced and with very low amounts of MC-WR ( $0.1 \mu\text{g mL}^{-1}$ ). The NIES 1099 strain also produced an unknown MC ( $0.21 \mu\text{g mL}^{-1}$ ). For the PCC 7820 strain it can be observed that the intra-cellular toxin concentrations slowly increase as the culture is in the log phase, remains stable as the culture enters and remains in the plateau phase and declines as more and more cells die and lyse, thus releasing the intra-cellular toxin into the extra-cellular matrix. None of the other variants appears to follow that pattern in the observed time frame. When directly comparing the cell numbers to the amount of intra-cellular toxin, one can see a dependence relationship. In all of the four strains the amount of the main MC analogue produced correlates to the number of cells, i.e. when the cell number is high the amounts of the main analogue are high. This is not the case for the other analogues produced (figure 2.7). When investigating the amount of toxin  $\text{cell}^{-1}$ , it can be seen that, even though PCC 7820 and PCC 7813 only differ in their ability of producing gas vacuoles, the amount of MC-LR produced  $\text{cell}^{-1}$  is different. Furthermore both cultures appear to be producing the same MC analogues at different times. Whereas PCC 7820 produces small amounts of MC-LY and LF from the start, and MC-LW after approximately 11 days, it stops producing the variants and after 35 days (5 weeks) only MC-LR can be detected intra-cellularly.



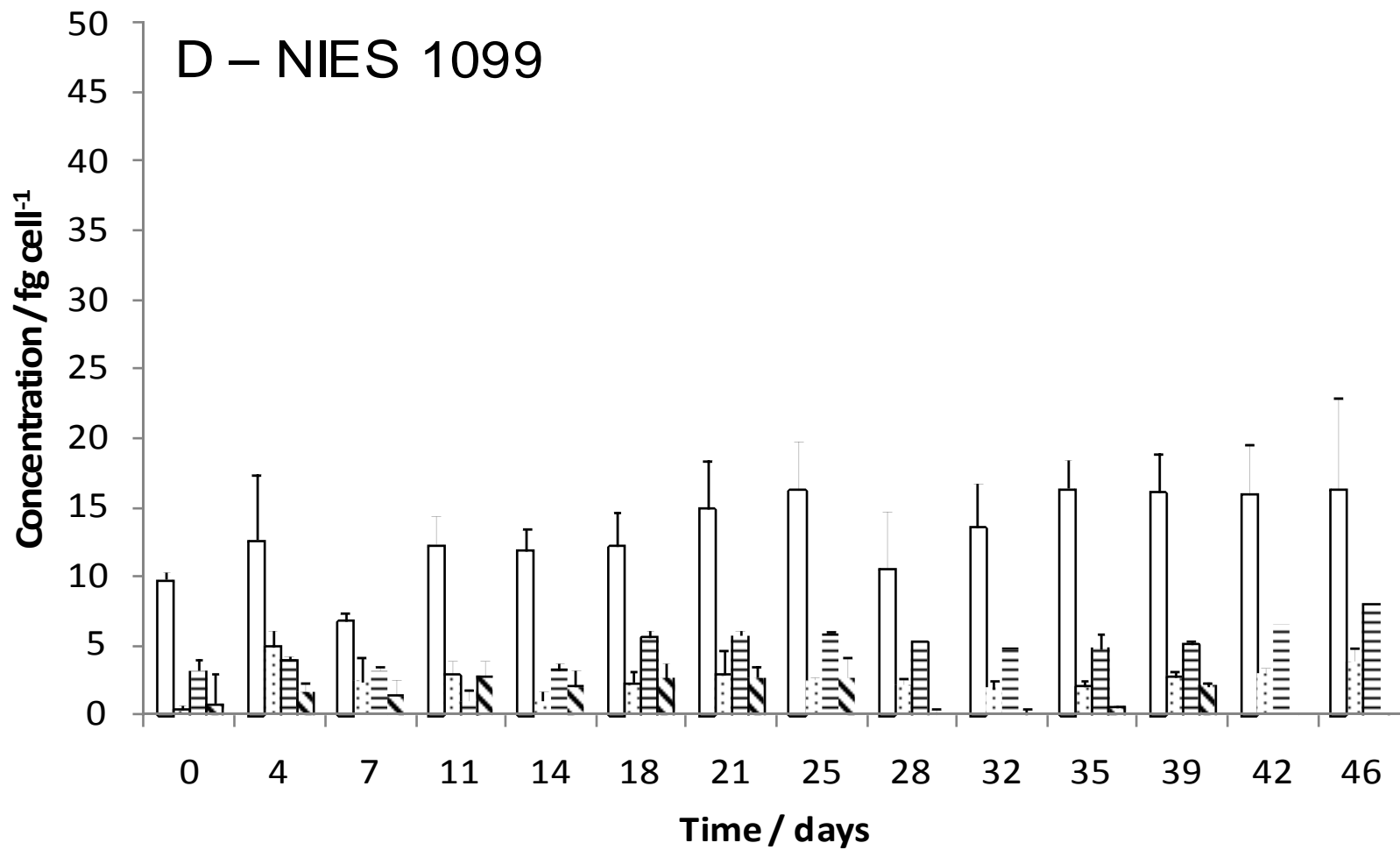
**Figure 2.7a:** Amount of toxin cell<sup>-1</sup> in *M. aeruginosa* PCC 7820 over seven weeks as determined by HPLC-PDA (extracted at 238 nm) and flow cytometry:  $\square$  MC-LR,  $\square$  MC-LY,  $\square$  MC-LW,  $\square$  MC-LF. Error bars=1 SD; n=4



**Figure 2.7b:** Amount of toxin  $\text{cell}^{-1}$  in *M. aeruginosa* PCC 7813 over seven weeks as determined by HPLC-PDA (extracted at 238 nm) and flow cytometry:  $\square$  MC-LR,  $\square$  MC-LY,  $\blacksquare$  MC-LW,  $\square$  MC-LF. Error bars=1 SD; n=4



**Figure 2.7c:** Amount of toxin  $\text{cell}^{-1}$  in *M. aeruginosa* B2666 over seven weeks as determined by HPLC-PDA (extracted at 238 nm) and flow cytometry:  $\square$  MC-LR,  $\text{▨}$  demethylated MC-LA,  $\text{▤}$  unidentified microcystin,  $\blacksquare$  MC-LA. Error bars=1 SD; n=4

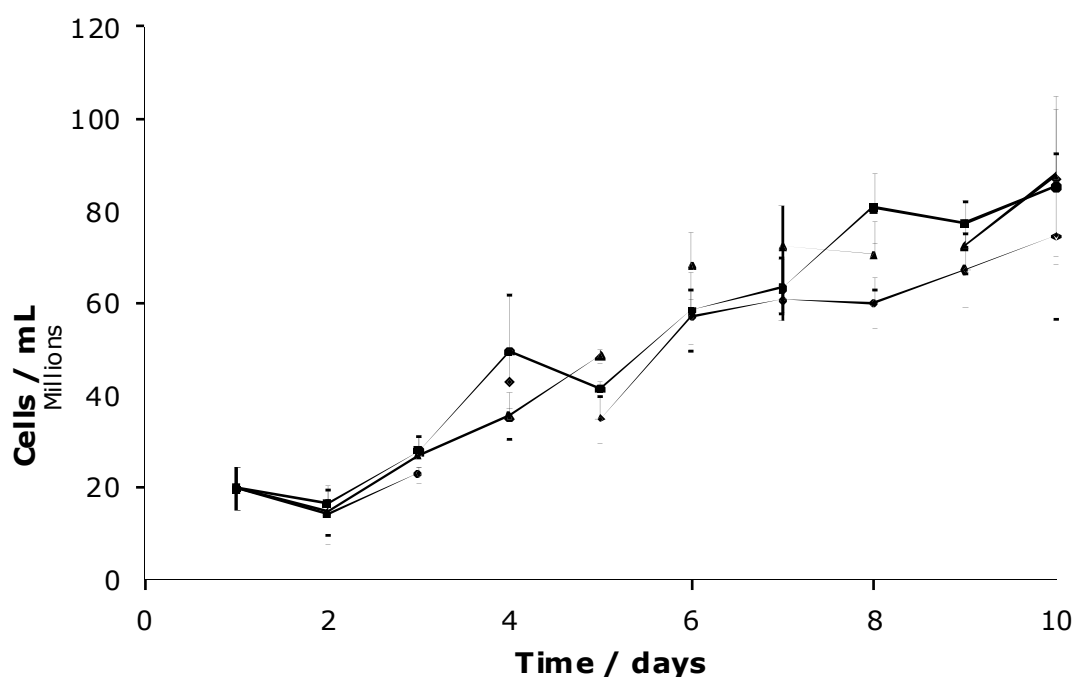


**Figure 2.7d:** Amount of toxin cell<sup>-1</sup> *M. aeruginosa* NIES 1099 over seven weeks as determined by HPLC-PDA (extracted at 238 nm) and flow cytometry: □ MC-RR, ▨ unidentified microcystin, ▤ MC-YR, ▩ MC-LR. Error bars=1 SD; n=4

Whereas PCC 7813 does not start producing other MC analogues until day 14 (MC-LW and MC-LF, followed by MC-LY from day 21), however, it continues producing them until the end of the experiment (day 46). A similar pattern to this can be observed in B2666, it produces MC-LR and MC-LA from the start of the experiment with MC-LR clearly the main analogue produced. It is on day 11 that the unknown MC produced by B2666 can be detected and on day 18 that demethylated MC-LA was detected. Noticeable is the fact that the synthesised amounts of the unknown MC overtakes that of MC-LA by day 28 and appears to be produced in similar amounts as MC-LA had been before the change. The NIES 1099 strain produces all four of its analogues from start, with MC-RR being the main analogue. Furthermore all of its analogues are produced over the entire time frame of the experiment. The amounts of MC-LR cell<sup>-1</sup> are very low towards the end of the experiment. What can also be seen is the fact that of the strains that produce MC-LR as their main analogue PCC 7820 clearly produces the most amount of toxin cell<sup>-1</sup>. The data in figure 2.6 might have suggested that B2666 would be the better strain to use, considering the total amount of toxin produced by it. However, the total amount of MC-LR in the B2666 cultures is higher than that in the PCC 7820 cultures solely due to the fact that there are more cells of B2666 than of PCC 7820. Therefore it was decided to use the PCC 7820 strain of *M. aeruginosa* for future investigations.

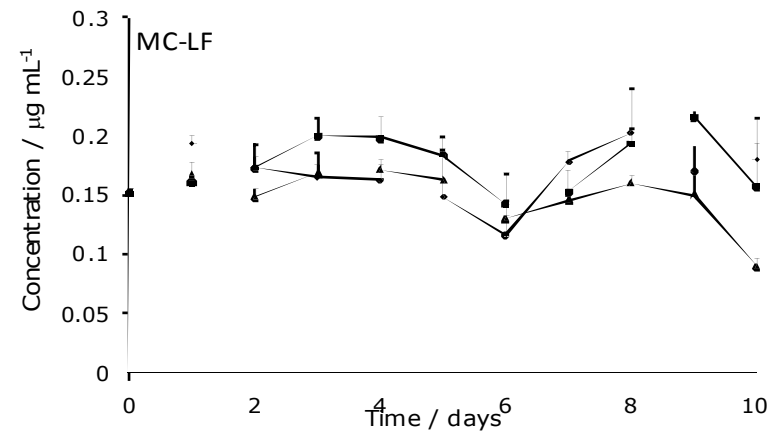
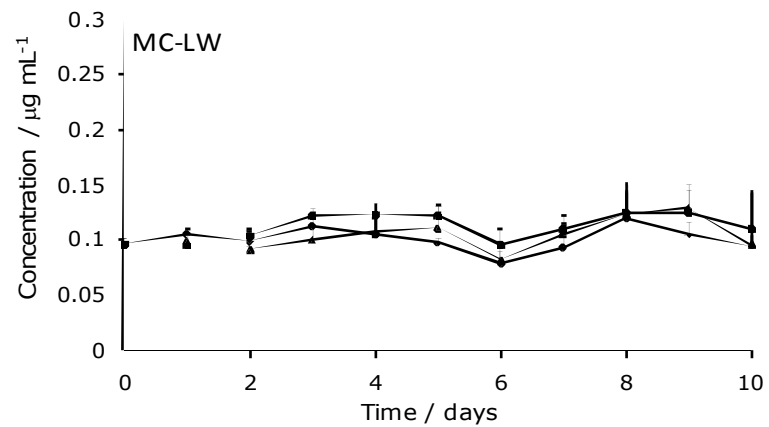
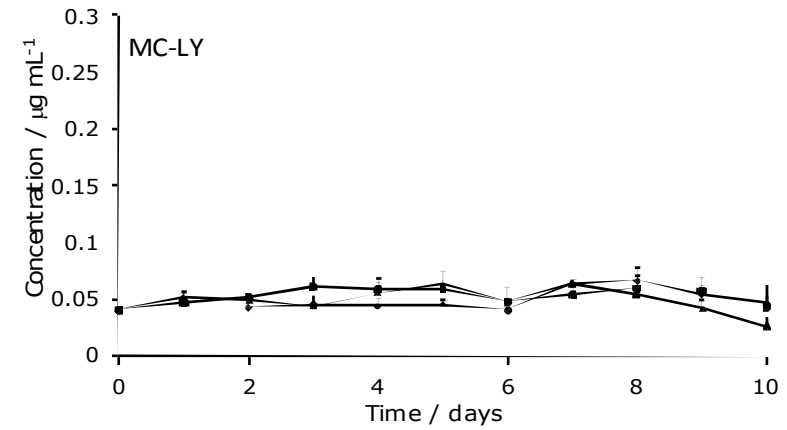
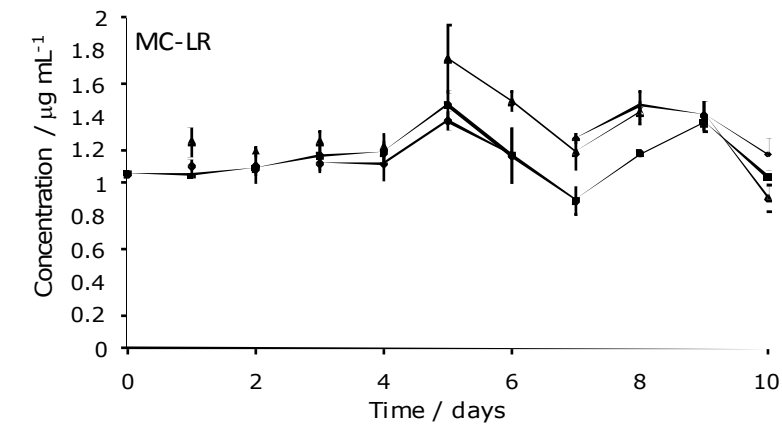
### 2.3.2 Assessing the impact of microcystin as a pheromone

To assess the impact of microcystin on toxin production in *M. aeruginosa* three cultures of *M. aeruginosa* PCC 7820 were grown in different media ( $^{14}\text{N}$ ,  $^{15}\text{N}$ , and  $^{15}\text{N}$  + MC-LR), with daily sampling and cell enumeration (figure 2.8). The cultures displayed healthy growth, with cell numbers approximately doubling every two to three days.



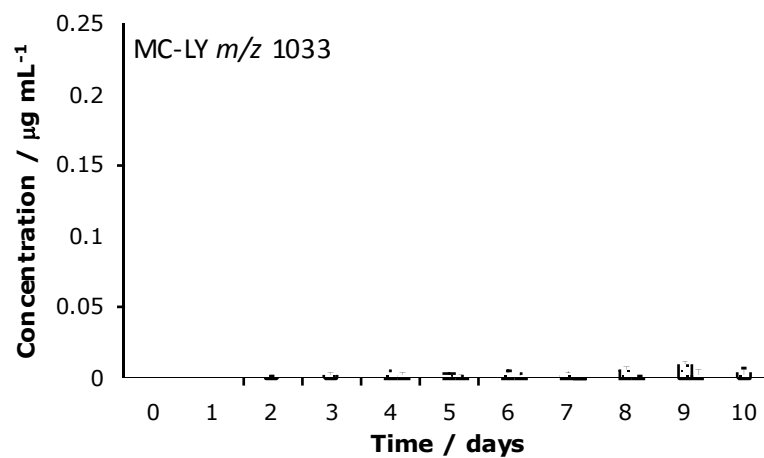
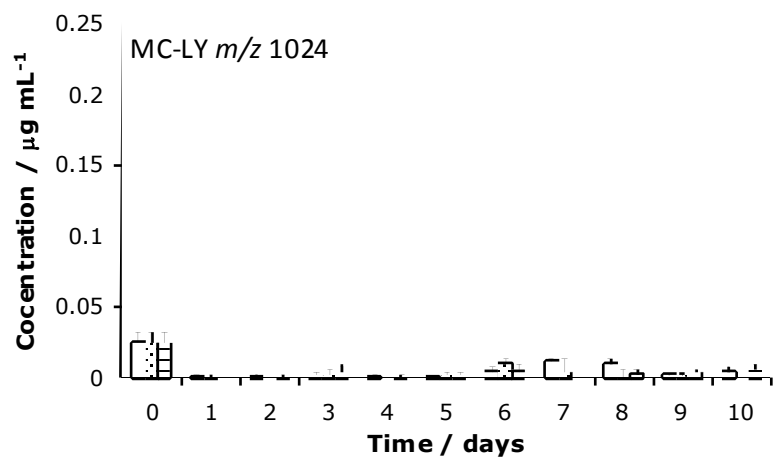
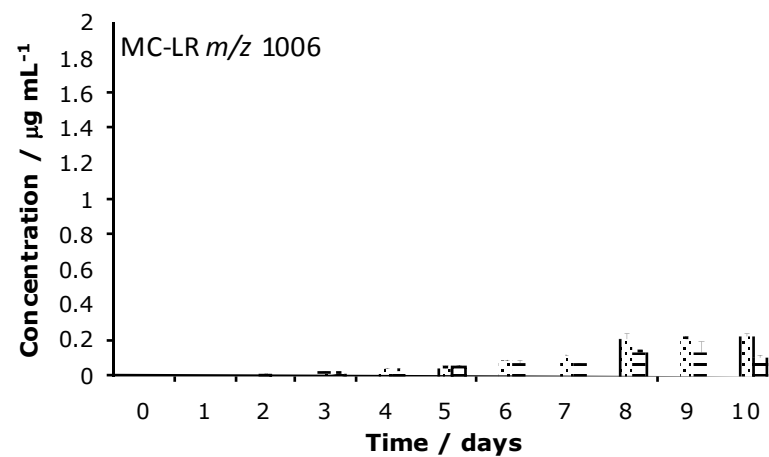
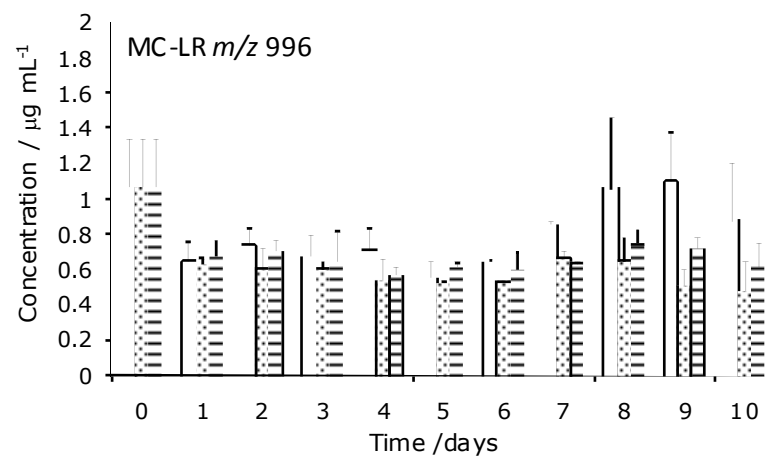
**Figure 2.8:** Flow cytometric cell enumeration of *M. aeruginosa* in different media over ten days. ♦  $^{14}\text{N}$  BG-II medium; ■  $^{15}\text{N}$  BG-II medium; ▲  $^{15}\text{N}$  BG-II medium with microcystin-LR ( $10\ \mu\text{g mL}^{-1}$ ). Error bars=1 SD; n=3

The analysis of intra-cellular toxin was performed using HPLC-MS analysis, samples were detected with PDA at 238 nm (figure 2.9). The extra-cellular concentration of MC in the spiked samples is in general lower than expected. In addition to the PDA analysis, mass spectrometric analysis was also carried out (figure 2.10 and 2.11), in order to be able to distinguish between: different analogues, labelled and unlabelled toxin.

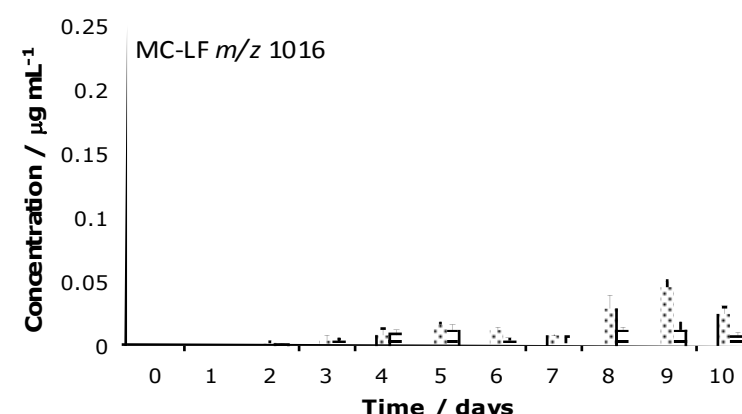
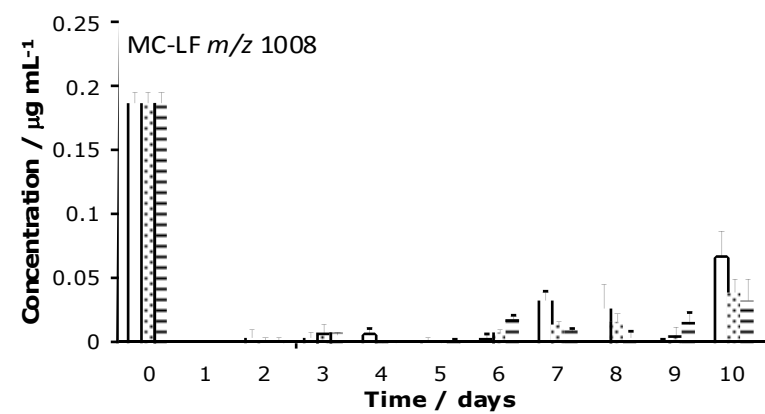
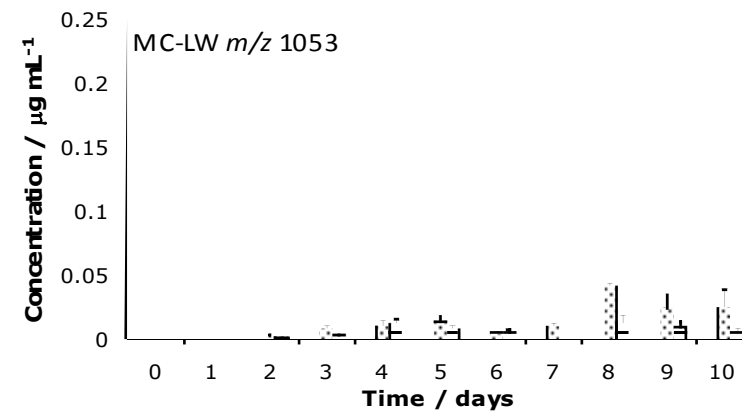
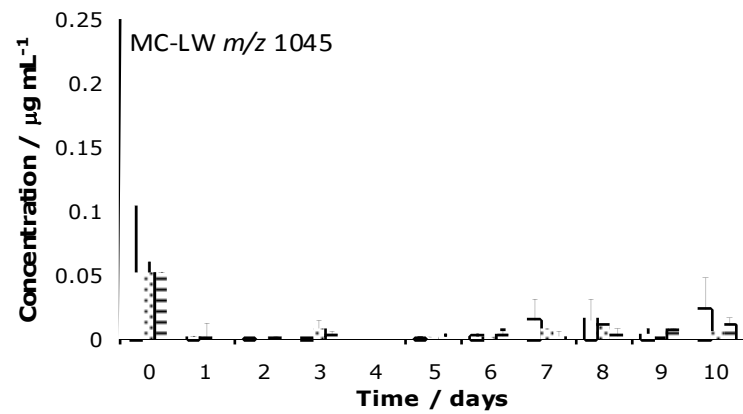


**Figure 2.9:** HPLC-PDA analysis (extracted at 238 nm) of intra-cellular microcystin analogues in PCC 7820. ♦  $^{14}\text{N}$  BG-II medium; ■  $^{15}\text{N}$  BG-II medium; ▲  $^{15}\text{N}$  BG-II medium with microcystin-LR ( $10 \mu\text{g mL}^{-1}$ ). Error bars=1 SD; n=3



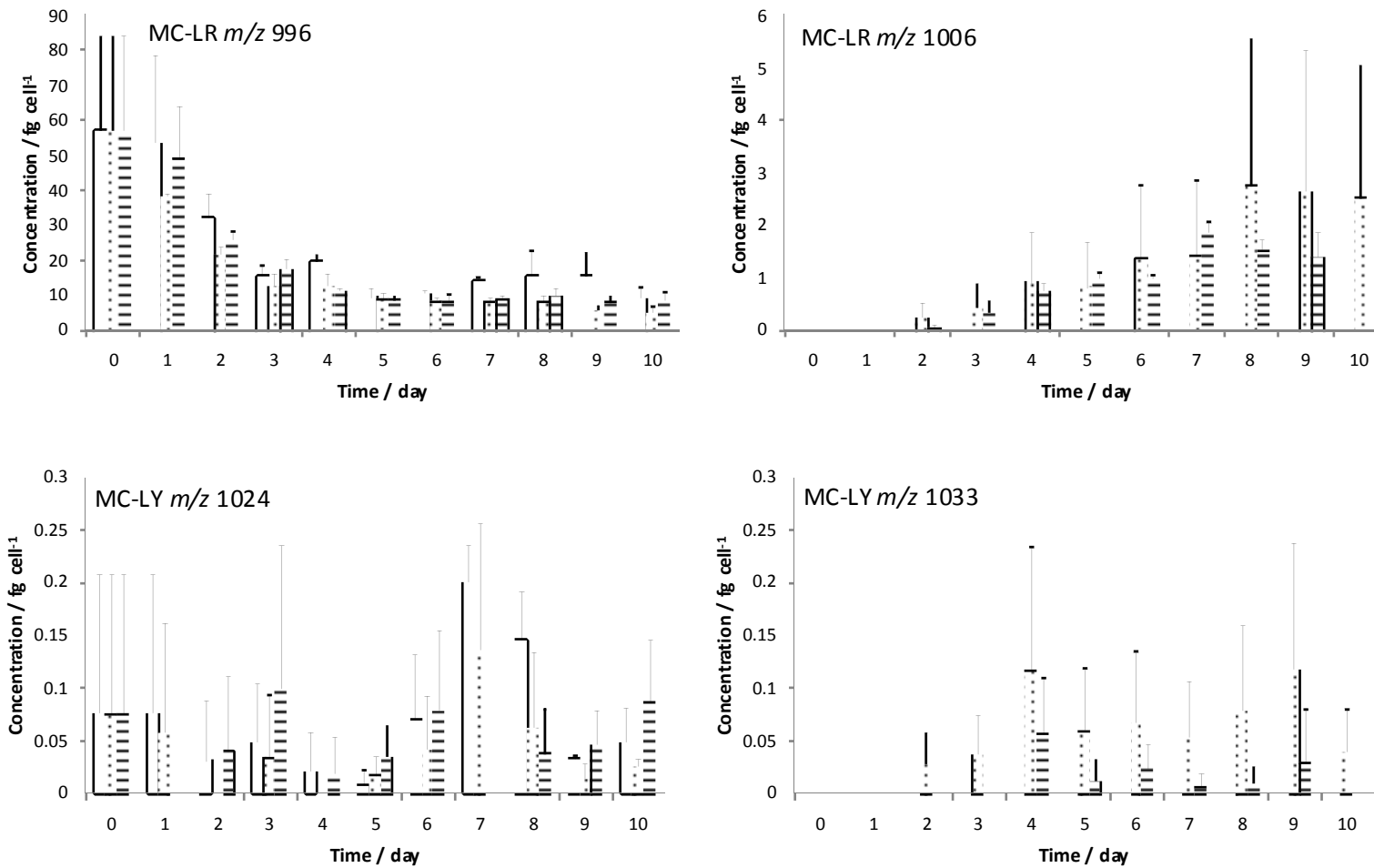


**Figure 2.10:** Mass spectrometric analysis ( $m/z$   $[\text{M}+\text{H}]^+$ ) of intra-cellular microcystin analogues in PCC7820:  $^{-}$   $^{14}\text{N}$  BG-II medium;  $\nabla$   $^{15}\text{N}$  BG-II medium;  $=$   $^{15}\text{N}$  BG-II medium with microcystin-LR ( $10 \mu\text{g mL}^{-1}$ ). Error bars=1 SD;  $n=3$

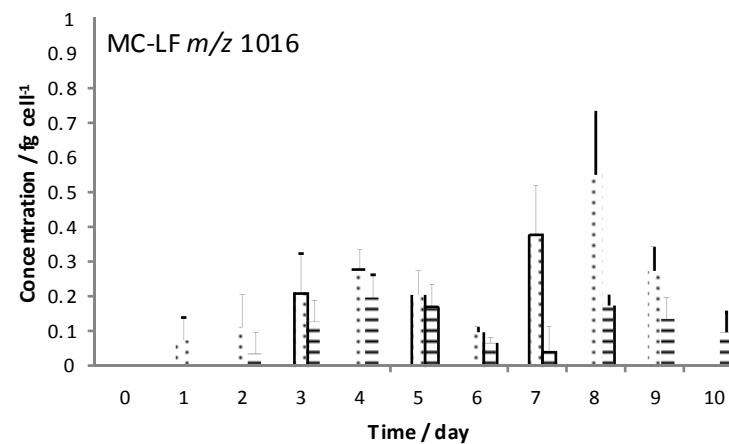
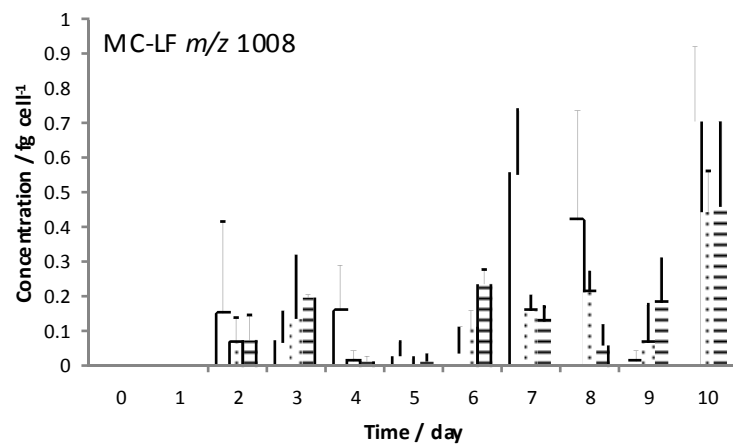
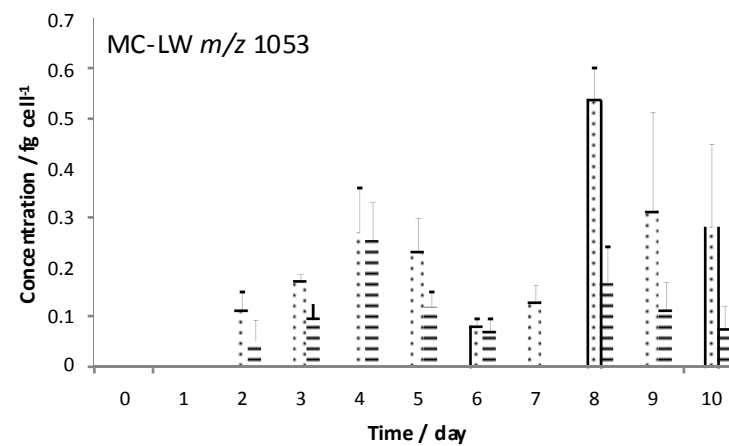
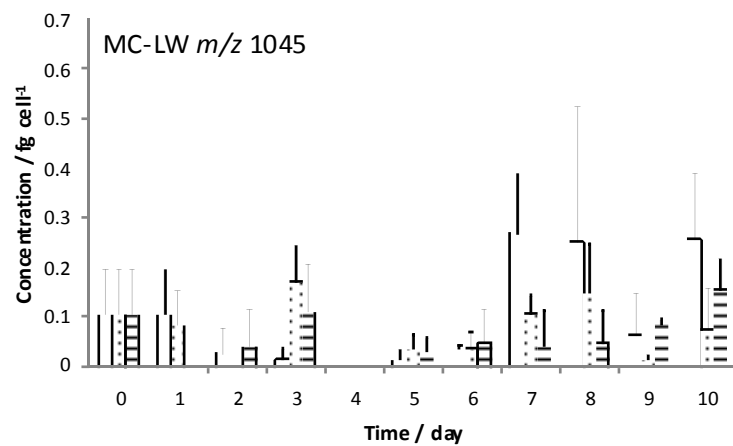


**Figure 2.11:** Mass spectrometric analysis ( $m/z$   $[M+H]^+$ ) of intra-cellular microcystin analogues in PCC7820:  $^{-14}\text{N}$  BG-II medium;  $^{-15}\text{N}$  BG-II medium;  $^{-15}\text{N}$  BG-II medium with microcystin-LR ( $10 \mu\text{g mL}^{-1}$ ). Error bars=1 SD;  $n=3$

After the MS analysis, it was observed that the sample where exogenous microcystin was added, appeared to produce less microcystin-LR (figure 2.9; MC-LR  $m/z$  1006). This is seen as a consistent trend across the four microcystins produced by PCC 7820. Intra-cellular concentrations of the spiked cultures do not mirror the amount of toxin that was added to the growth medium ( $10 \mu\text{g mL}^{-1}$ ). When considering the amount of MC  $\text{cell}^{-1}$  it can be observed that, as expected, the amount of unlabelled MC-LR ( $m/z$  996) decreases as approximately the same amount of toxin is spread over an increasing number of cells as the culture increases in size (figure 2.12). The same is not true for the other MC analogues produced by PCC 7820 (figure 2.13), as observed previously (figure 2.6), the other MC analogues are not produced from the start of the experiment but only later in the growth of the culture. The amounts  $\text{cell}^{-1}$  remain relatively unchanged for the cultures in the  $^{14}\text{N-BG-II}$ . And it can be observed that in the later phase of the experiment the culture in the  $^{15}\text{N-BG-II} + \text{MC-LR}$  produces slightly less  $\text{cell}^{-1}$  than the cultures in  $^{15}\text{N-BG-II}$  medium. This is reflected in the total toxin amounts (figure 2.10; figure 2.11).



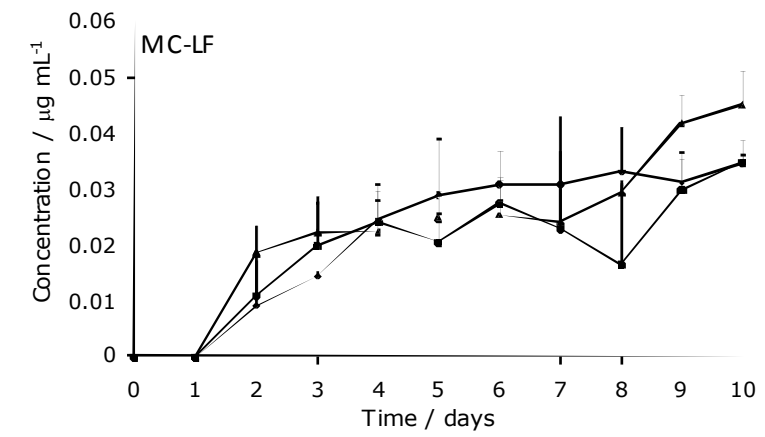
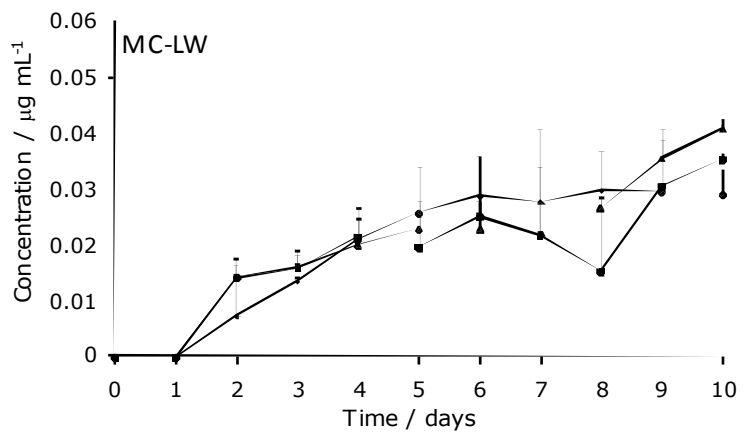
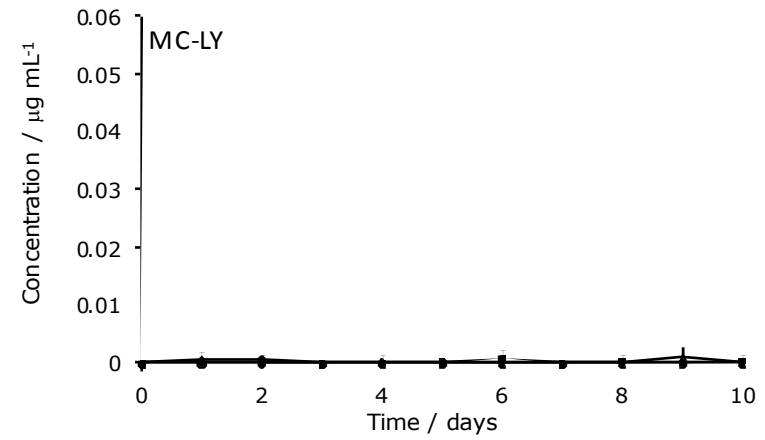
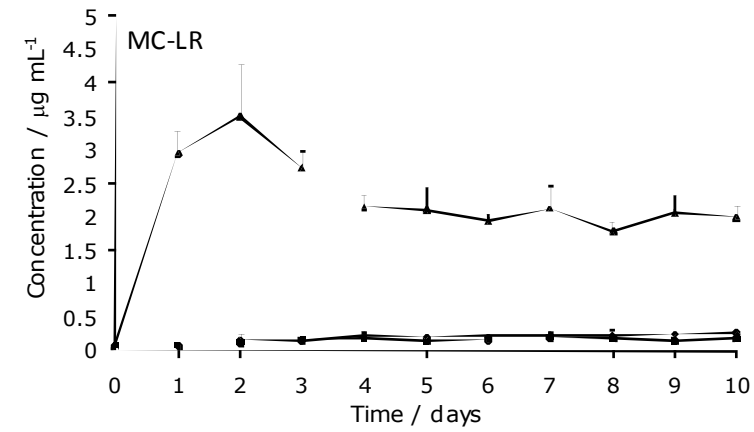
**Figure 2.12:** Mass spectrometric analysis ( $m/z$   $[M+H]^+$ ) of intra-cellular microcystin analogues in PCC7820  $\text{cell}^{-1}$ :  $\square$   $^{14}\text{N}$  BG-II medium;  $\dots$   $^{15}\text{N}$  BG-II medium;  $\text{▨}$   $^{15}\text{N}$  BG-II medium with microcystin-LR (10  $\mu\text{g mL}^{-1}$ ). Error bars=1 SD; n=3



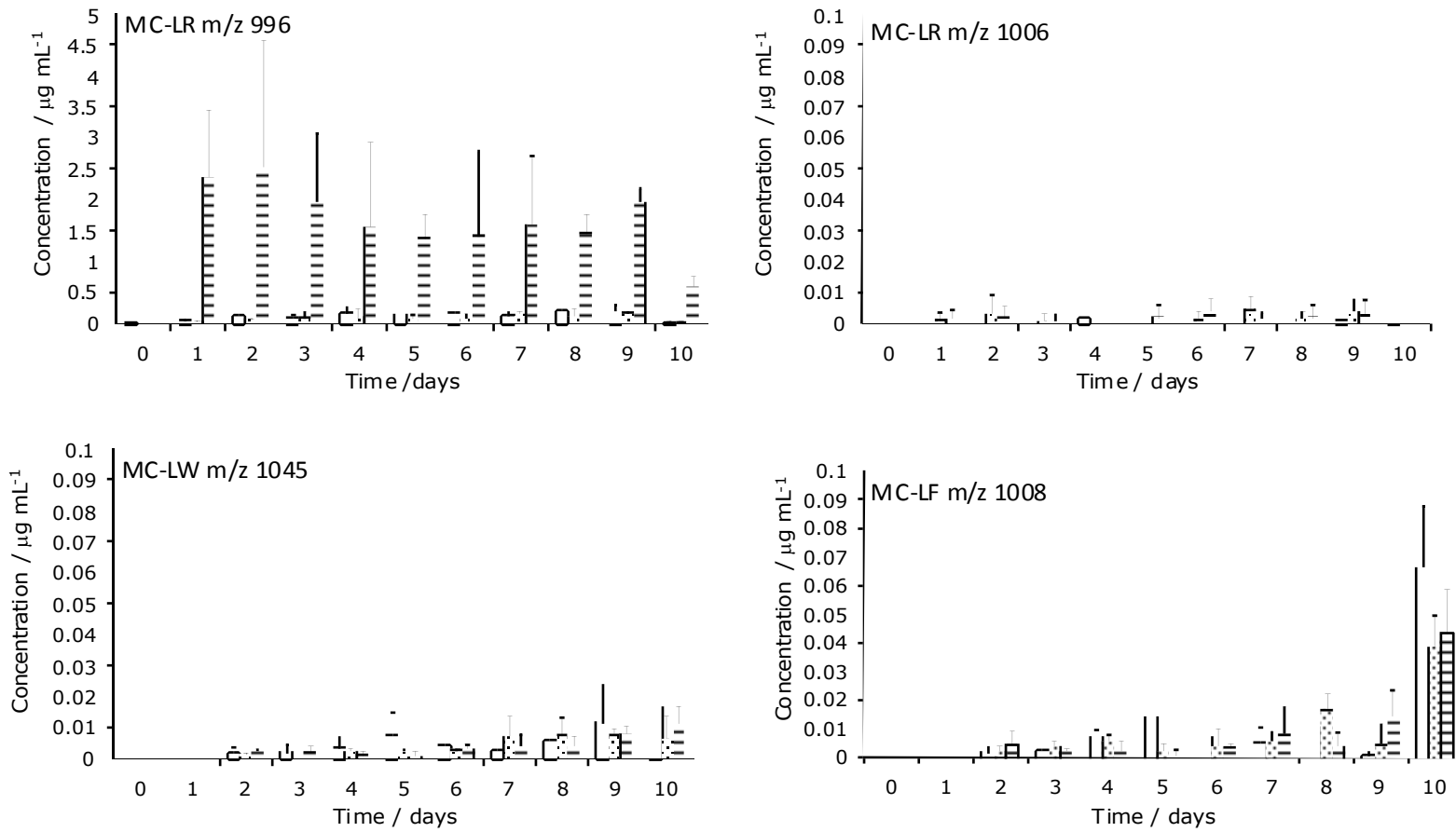
**Figure 2.13:** Mass spectrometric analysis ( $m/z$   $[M+H]^+$ ) of intra-cellular microcystin analogues in PCC7820 cell<sup>-1</sup>: □ <sup>14</sup>N BG-II medium; ▨ <sup>15</sup>N BG-II medium; ▩ <sup>15</sup>N BG-II medium with microcystin-LR (10 μg mL<sup>-1</sup>). Error bars=1 SD; n=3

The extra-cellular toxin was analysed by HPLC-PDA (extracted at 238 nm) (figure 2.14) followed by mass spectrometric analysis (figure 2.15).

PDA analysis at 238 nm revealed an increase in extra-cellular microcystin over the time frame of the experiment for MC-LR, MC-LW, and MC-LF. Hardly any MC-LY was detected by the HPLC-PDA analysis. MS analysis revealed that there were negligible amounts of MC-LY, and no *de novo* -LW and -LF in the extra-cellular matrix. The cultures spiked with MC show elevated levels of extra-cellular MC-LR, which was to be expected. However, none of the amounts detected were close to the initial spike of  $10 \mu\text{g mL}^{-1}$ , the highest measurement suggests a concentration of  $4.5 \mu\text{g mL}^{-1}$ , whereas the highest mean is approximately  $2.5 \mu\text{g mL}^{-1}$ .



**Figure 2.14:** HPLC-PDA analysis of extra-cellular MC analogues of PCC 7820: ♦  $^{14}\text{N}$  BG-II medium; ▪ in  $^{15}\text{N}$  BG-II medium; ▲  $^{15}\text{N}$  BG-II medium with MC-LR ( $10 \mu\text{g mL}^{-1}$ ). Error bars=1 SD; n=3



**Figure 2.15:** Mass spectrometric analysis of extra-cellular MC analogues of PCC7820. Note MC-LY (unlabelled or labelled), labelled MC-LW and LF could not be detected. |  $^{14}\text{N}$  BG-II medium; I:  $^{15}\text{N}$  BG-II medium; =  $^{15}\text{N}$  BG-II medium with MC-LR ( $10 \mu\text{g mL}^{-1}$ ). Error bars=1 SD; n=3



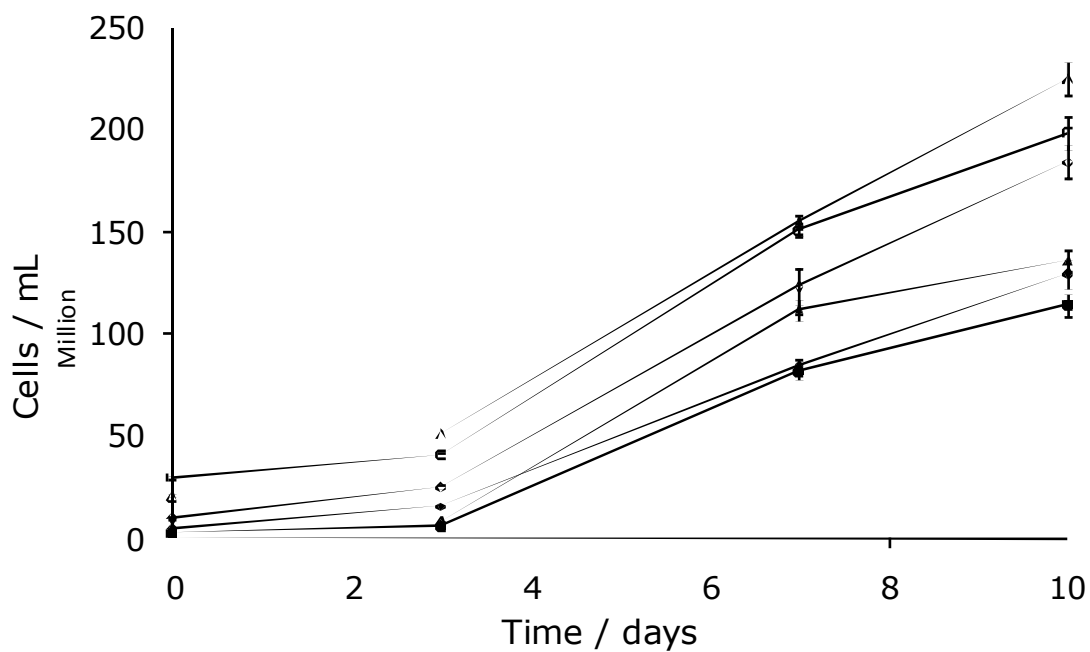
No MC-LY was detected by the mass spectrometer in the extra-cellular samples, nor were labelled MC-LW or LF. The results suggest that exogenous MC-LR may have a pheromonal inhibitory effect on the toxin production in *M. aeruginosa* for all four toxin variants produced by the PCC 7820 strain. However, the high cell numbers used in this experiment, to achieve improved quantification of the MCs by HPLC-MS, might have had a detrimental effect on toxin production. High cell counts may result in metabolic changes due to self shading.

The use of the stable isotope labelling enables the determination of MC production (i.e. amount of toxin  $\text{day}^{-1} \text{cell}^{-1}$ ) (table 2.5).

**Table 2.5:** Mean amount of microcystins analogues produced  $\text{cell}^{-1} \text{day}^{-1}$  by PCC 7820 over ten days.

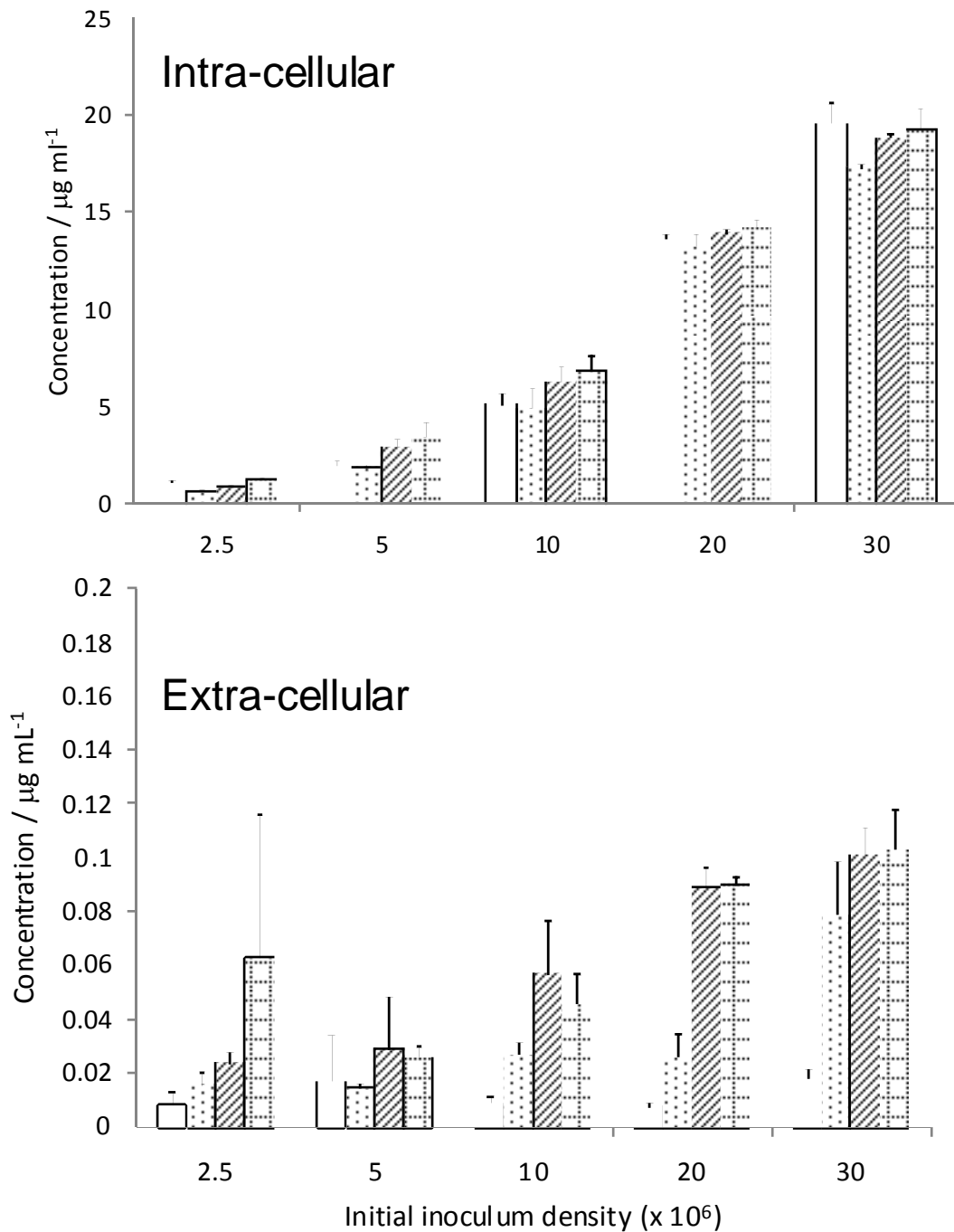
<b>MC analogue</b>	<b>Mean toxin <math>\text{day}^{-1} \text{cell}^{-1} \text{}^{15}\text{N BG-II}</math> (fg)</b>	<b>Mean toxin <math>\text{day}^{-1} \text{cell}^{-1} \text{}^{15}\text{N BG-II} + \text{MC-LR}</math> (fg)</b>
MC-LR	$1.48 \pm 0.49$	$0.98 \pm 0.43$
MC-LY	$0.06 \pm 0.04$	$0.01 \pm 0.02$
MC-LW	$0.21 \pm 0.15$	$0.09 \pm 0.07$
MC-LF	$0.24 \pm 0.15$	$0.11 \pm 0.06$

To ascertain whether cell density has an impact on toxin synthesis, different starting inocula were used with simplified sample protocol. The number of cells present in the samples was enumerated by flow cytometry (figure 2. 16).



**Figure 2.16:** Flow cytometric cell enumeration of *M. aeruginosa* with different starting inocula. ▲  $2.5 \times 10^6$  cells with MC-LR ( $10 \mu\text{g mL}^{-1}$ ); ■  $2.5 \times 10^6$  cells; ◆  $5 \times 10^6$  cells, ◇  $10 \times 10^6$  cells; Δ  $20 \times 10^6$  cells, □  $30 \times 10^6$  cells. Error bars=1 SD; n=3

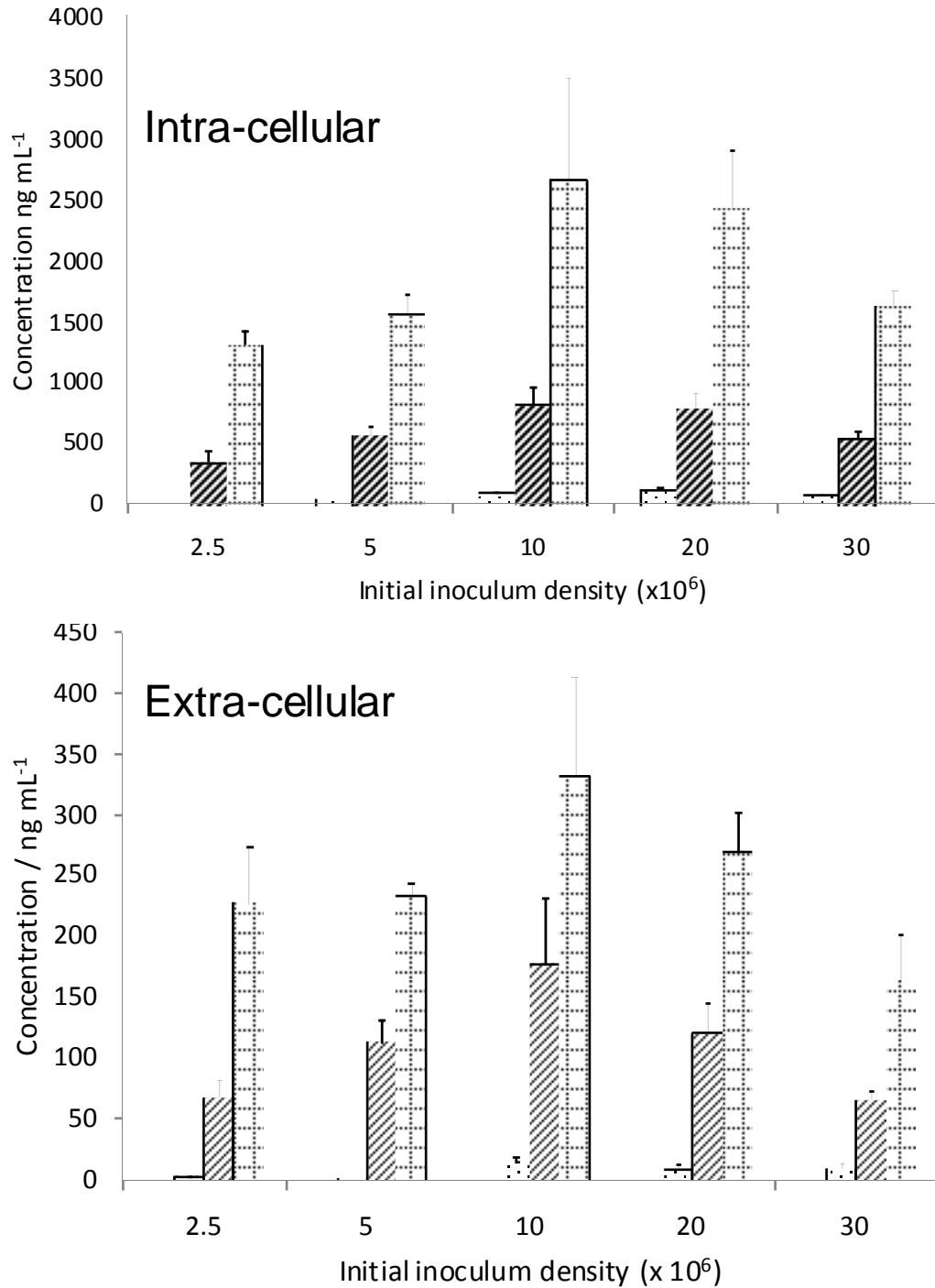
Since MC-LR is the main toxin produced by PCC 7820, it was decided to focus on the assessment of the effect of cell numbers on *de novo* MC-LR synthesis. Extra- and intra-cellular samples were analysed by UPLC-MS (figure 2.17).



**Figure 2.17:** UPLC determination of intra- and extra-cellular concentrations of unlabelled microcystin-LR ( $m/z$  996) in PCC 7820. — T<sub>0</sub>; ▨ day 3; ▩ day 7; ▤ day 10. Error bars=1 SD; n=3

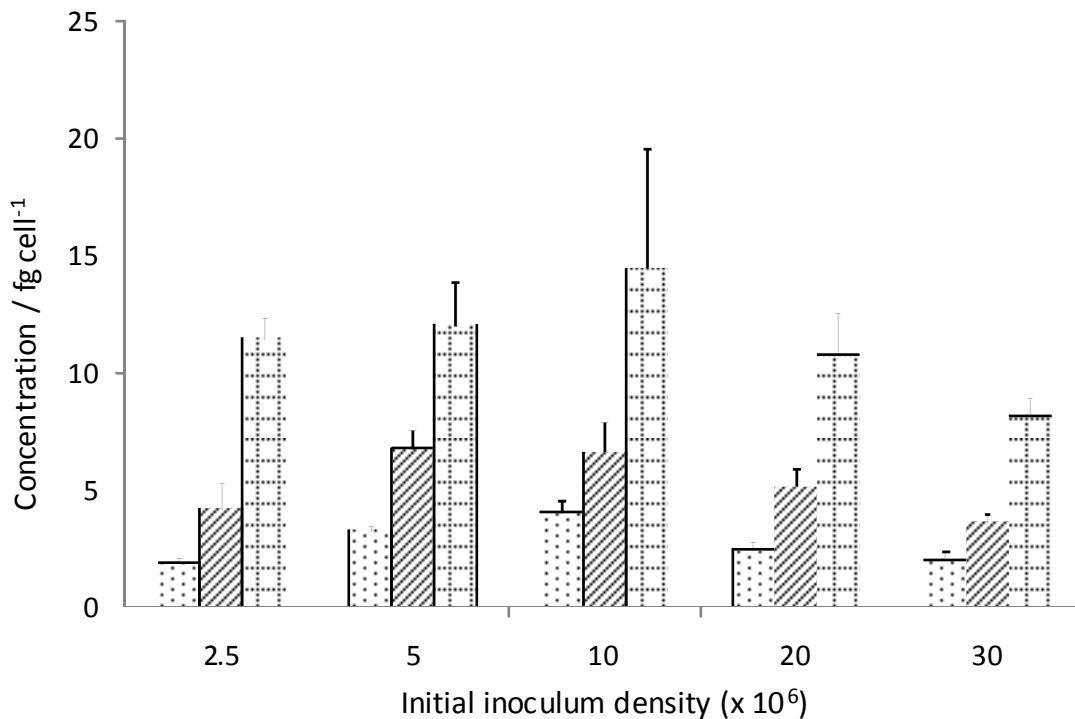
The intra-cellular levels of the unlabelled toxin remain stable over the course of the experiment as would be expected. The concentration reflects the

inoculation volume well, the more cells are present, the more toxin was observed. The intra- and extra-cellular *de novo* toxin levels were also monitored by UPLC-MS (figure 2.18).



**Figure 2.18:** UPLC-MS determination of intra- and extra-cellular concentrations of labelled microcystin-LR ( $m/z$  1006) in PCC7820. — T<sub>0</sub>; ▨ day 3; ▩ day 7; ▤ day 10. Error bars=1 SD; n=3

As expected there is no labelled toxin detectable at the time of inoculation ( $T_0$ ). More labelled toxin is detectable in the cultures with higher starting inocula from day 3 onward. It was observed that the amount of cells present in a culture may have an impact on *de novo* toxin synthesis (figure 2.19).



**Figure 2.19:** UPLC-MS determination of *de novo* microcystin-LR ( $m/z$  1006) combined with flow-cytometric cell enumeration to determine the amount of toxin produced  $\text{cell}^{-1}$  on each sampling day. □ day 3; ▨ day 7; ▩ day 10. Error bars=1 SD;  $n=3$

Furthermore the production rate of *de novo* MC-LR was determined (table 2.6). It can be seen that cell density has a significant impact on MC-LR synthesis. The highest production rate was observed in the cultures with 2.5 and 10 x 10<sup>6</sup> cells mL<sup>-1</sup> initial inocula. The lowest production rates were observed in the cultures with 30 x 10<sup>6</sup> cells mL<sup>-1</sup> starting inoculum.

**Table 2.6:** *De novo* MC-LR (*m/z* 1006) synthesis  $\text{cell}^{-1} \text{day}^{-1}$  in cultures with different initial inoculation densities.

Time / d	<b><i>De novo</i> MC-LR (<i>m/z</i> 1006) / fg cell<sup>-1</sup> day<sup>-1</sup></b>				
	2.5 x 10 <sup>6</sup> cells	5 x 10 <sup>6</sup> cells	10 x 10 <sup>6</sup> cells	20 x 10 <sup>6</sup> cells	30 x 10 <sup>6</sup> cells
0-3	0.61	1.09	1.35	0.81	0.67
3-7	0.59	0.51	0.64	0.68	0.40
7-10	2.42	1.74	2.59	1.88	1.5

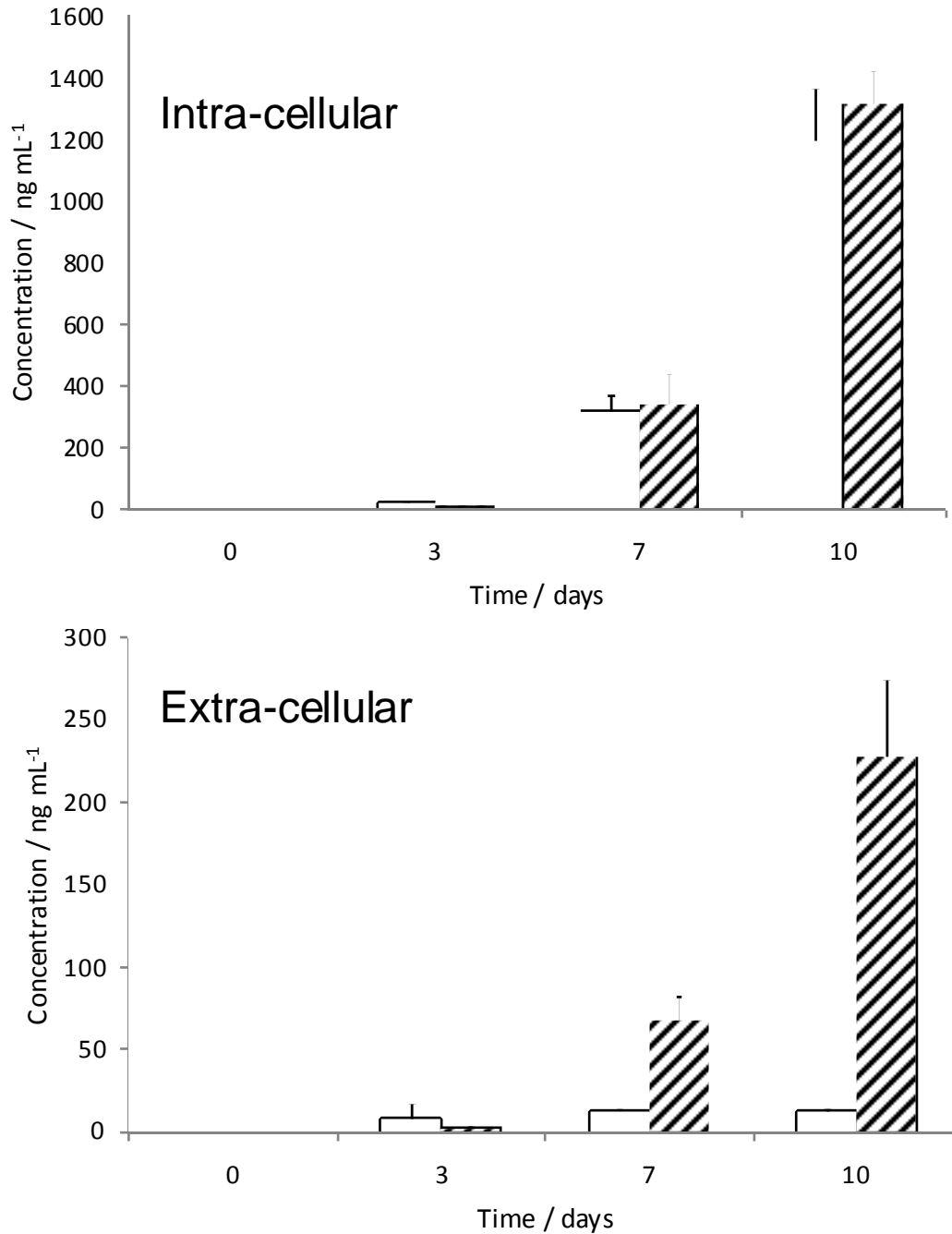
The effect of exogenously added MC-LR on MC-LR synthesis required further elucidation. Cultures with a relatively low initial inoculation density ( $2.5 \times 10^6$  cells mL<sup>-1</sup>) were spiked with exogenous MC-LR and analysed by UPLC-MS and enumerated by flow cytometry. Exogenous MC-LR appears to have an effect on the synthesis of MC-LR. It can be observed that even though the presence of exogenous MC-LR in the medium appears to stimulate growth (figure 2.16), it appears to have an inhibitory effect on the synthesis of MC-LR in PCC 7820, this is also reflected in the amount of *de novo* toxin produced  $\text{cell}^{-1} \text{day}^{-1}$  (table. 2.7).

**Table 2.7:** *De novo* MC-LR (*m/z* 1006) synthesis  $\text{cell}^{-1} \text{day}^{-1}$  in cultures with different medium additives.

Time / d	<b><i>De novo</i> MC-LR (<i>m/z</i> 1006) / fg cell<sup>-1</sup> day<sup>-1</sup></b>	
	2.5 x 10 <sup>6</sup> cells + MC-LR	2.5 x 10 <sup>6</sup> cells
0-3	0.88	0.61
3-7	0.04	0.59
7-10	1.97	2.42

Furthermore, it was observed that the distribution of intra- and extra-cellular MC-LR was altered in the cultures that were inoculated into the medium with the exogenous MC-LR (figure 2.20). A ten-fold decrease of extra-cellular labelled MC-LR (*m/z* 1006) was observed in the samples that were cultured

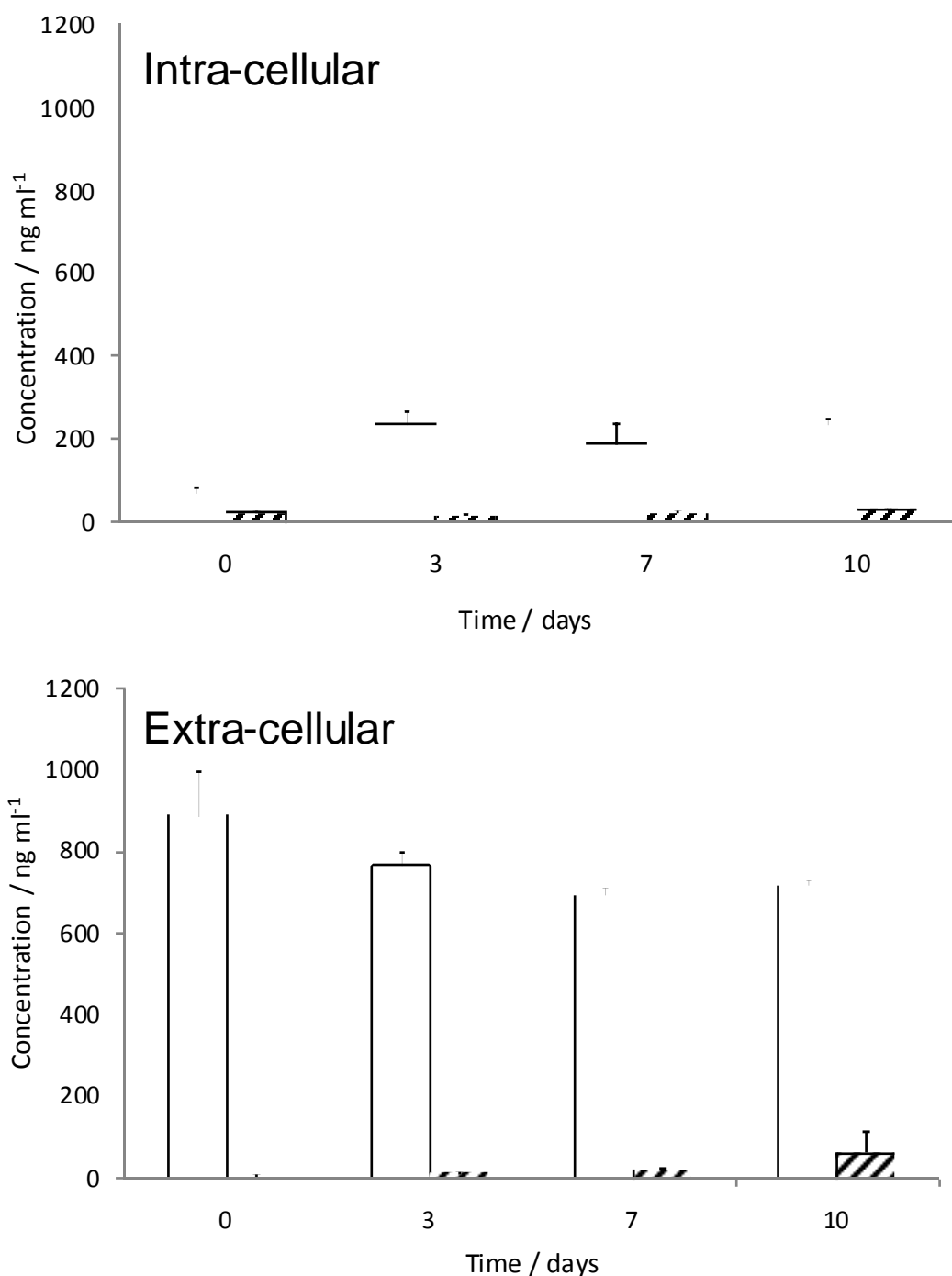
with exogenous MC-LR. The intra-cellular levels of the labelled toxin are comparable to each other.



**Figure 2.20:** UPLC-MS determination of intra- and extra-cellular labelled MC-LR ( $m/z$  1006) in PCC 7820 cultured with exogenous MC-LR. L  $2.5 \times 10^6$  cells mL<sup>-1</sup> + MC-LR ( $10 \mu\text{g L}^{-1}$ );  $\blacksquare$   $2.5 \times 10^6$  cells mL<sup>-1</sup>. Error bars=1 SD, n=3

The exogenous MC-LR ( $m/z$  996) was, to some degree, taken up by the cells in the cultures, as over time the amount of exogenous toxin decreases in the extra-cellular matrix. However, the amount of unlabelled MC-LR does not increase with the exogenous toxin present (figure 2.21). Noticeable is the fact that as described above, the actual spiked concentration of  $10 \mu\text{g mL}^{-1}$  of MC-LR could not be detected.

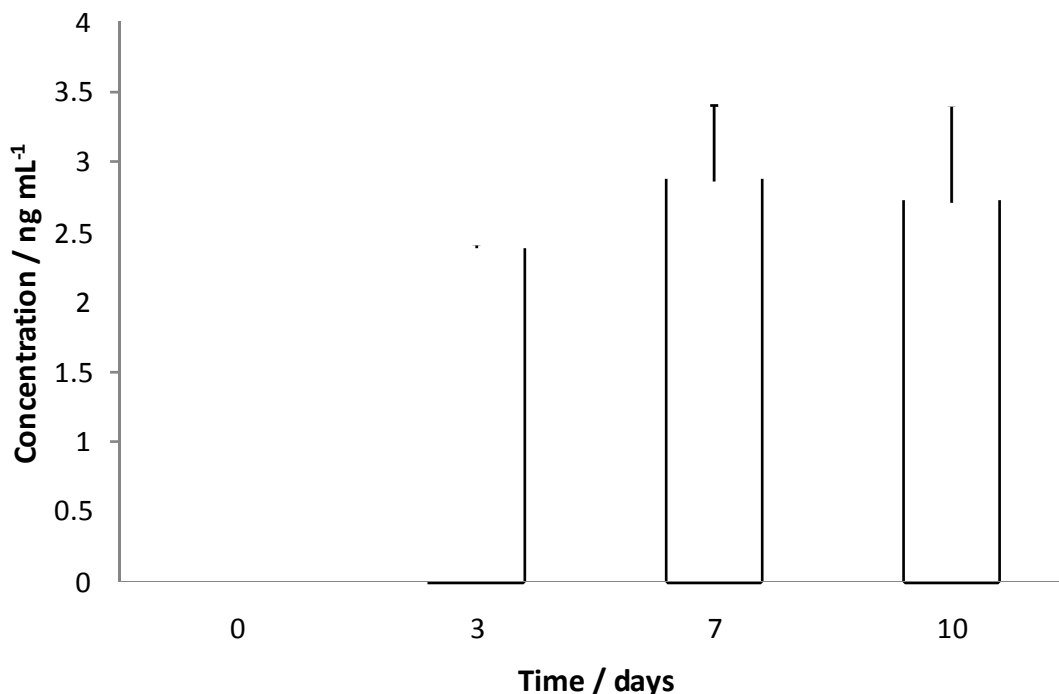




**Figure 2.21:** UPLC-MS determination of intra- and extra-cellular unlabelled MC-LR ( $m/z$  996) in PCC 7820 cultured with exogenous MC-LR.  $2.5 \times 10^6$  cells mL<sup>-1</sup>+ MC-LR ( $10 \mu\text{g mL}^{-1}$ );  $\blacksquare$   $2.5 \times 10^6$  cells mL<sup>-1</sup>. Error bars=1 SD, n=3

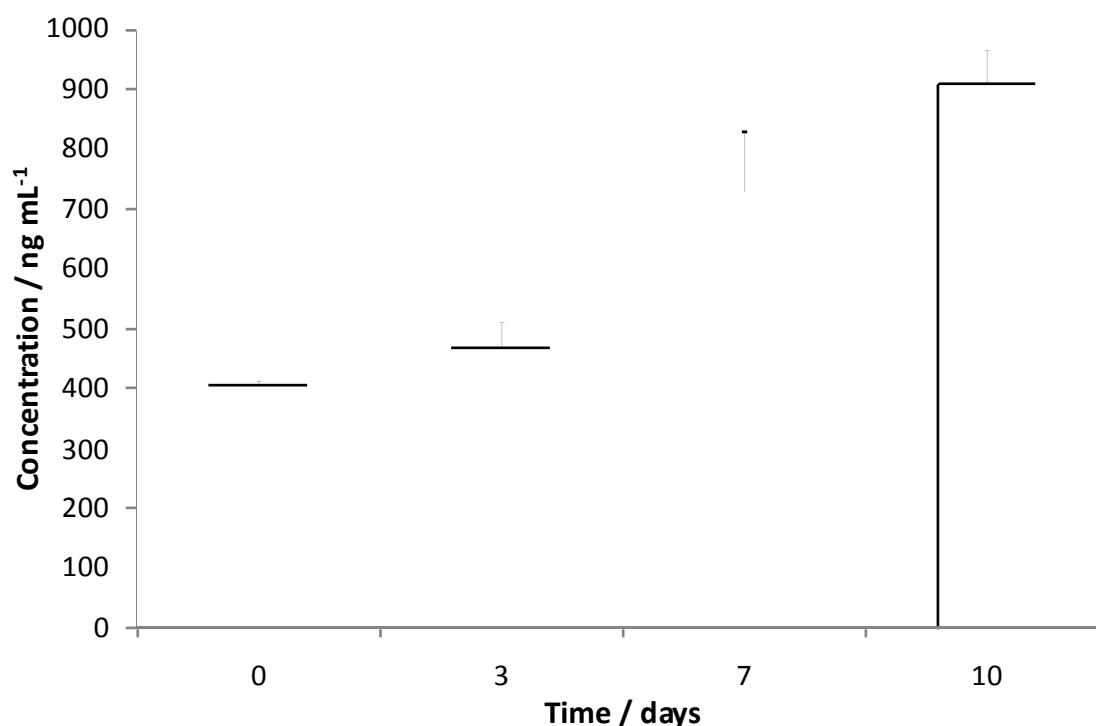
To ascertain the fate of the exogenous MC-LR another investigation was designed, where labelled MC-LR ( $m/z$  1006) was added to the extra-cellular matrix only containing an unlabelled nitrogen source ( $^{14}\text{N}$ ). It can be seen that

very small amounts of labelled toxin appear to be associated with the cells (figure 2.22).



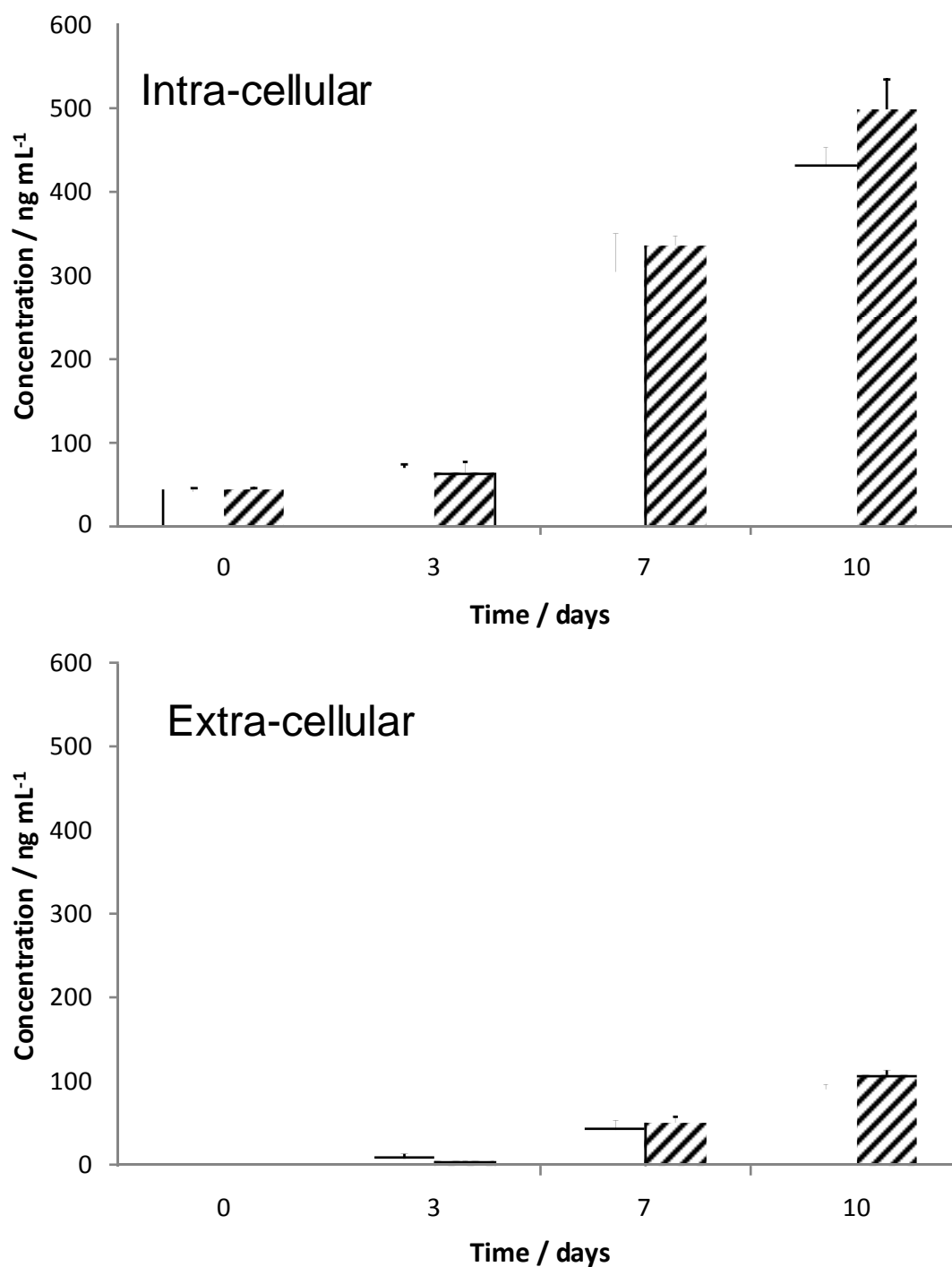
**Figure 2.22:** Amount of intra-cellular, labelled MC-LR ( $m/z$  1006) in cultures of *M. aeruginosa* PCC 7820 exposed to  $1 \mu\text{g mL}^{-1}$  exogenous labelled  $^{15}\text{N}$ -MC-LR. Error bars=1 SD;  $n=2$

The amount of labelled MC-LR detected in the extra-cellular matrix is considerably lower than expected (figure 2.23). A similar observation was made in the first investigation attempting to elucidate the effect of exogenously added MC-LR.



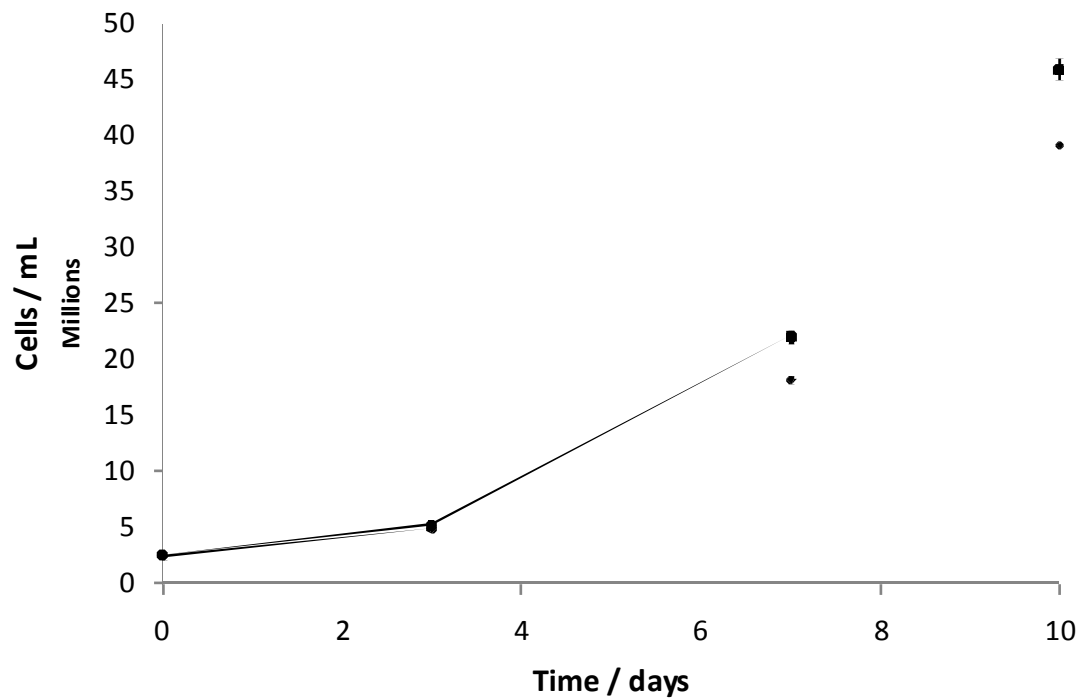
**Figure 2.23:** Amounts of exogenous, labelled MC-LR ( $m/z$  1006) in the extra-cellular matrix in cultures of *M. aeruginosa* PCC 7820. Amount of the originally added exogenous was  $1 \mu\text{g mL}^{-1}$ . Error bars=1 SD;  $n=2$

The apparent increase in the amounts of labelled MC-LR over the course of the experiment is an artefact due to evaporation. Assessing the intra-cellular amounts of unlabelled MC-LR it can be observed that the cultures with the exogenous labelled MC-LR produce similar amounts compared to the cultures grown in the untreated medium, a significant difference (paired t-test;  $p$ -value=0.0404) can only be observed at the last sampling point (day 10) (figure 2.24). When comparing the amounts of extra-cellular unlabelled MC-LR it can be observed that the exogenously added labelled MC-LR had an effect on the amount of unlabelled MC-LR that was released into the extra-cellular matrix, however, it is not as pronounced as it was in the previous investigation (figure 2.20). However, the effect is still statistically significant (paired t-test;  $p$ -value=0.0471).



**Figure 2.24:** UPLC-MS determination of intra- and extra-cellular unlabelled MC-LR ( $m/z$  996) in *M. aeruginosa* PCC 7820 cultured with exogenous labelled MC-LR ( $m/z$  1006). ▭  $^{14}\text{N}$  BG-II +  $^{15}\text{N}$ -MC-LR ( $1 \mu\text{g mL}^{-1}$ ); ▨  $^{14}\text{N}$  BG-II. Error bars=1 SD,  $n=3$

As could be observed previously the exogenously added MC-LR again affected the number of cells (figure 2.25).



**Figure 2.25:** Flow cytometric cell enumeration of *M. aeruginosa* PCC 7820 ♦ without exogenous MC-LR and ■ with exogenous, labelled MC-LR ( $m/z$  1006). Error bars=1 SD;  $n=3$

The cultures with the exogenous MC-LR display a 17 % growth increase at the end of the experiment.

## 2.4 Discussion

Cyanobacteria, and especially the secondary metabolites they produce can cause severe harm to humans and animals alike. Due to their tendency to appear in mass occurrences (blooms) the presence and potentially harmful effects of their secondary metabolites is increased as many individual compounds can contribute to the general pool of harmful substances. One group of cyanobacterial secondary metabolites especially gives rise to concerns in potable water: microcystins. These hepatotoxic compounds are potentially harmful to humans acutely, when exposed in high doses, and chronically with low dose exposure over a period of time. It is therefore important that the factors affecting toxin synthesis and possible means of toxin synthesis inhibition are explored. To date the biological function of microcystins has not been satisfactorily explained, though a number of functions have been proposed, such as intra-cellular iron scavengers, as components in light adaptation processes, as extra-cellular allelomone and/or pheromone (Kaebernick and Neilan, 2001). The proposition that microcystins serve no biological function seems unlikely considering the relative chemical complexity of the molecule and the comparably high energy cost involved in their production (Young *at al.*, 2005). Pearson *at al.* (2004) have characterised a transporter protein within the microcystin synthetase gene cluster which is suspected to be involved in the export of microcystin molecules from the cell. Considering this, it appears likely that microcystins serve a signalling function, either allelomonal, pheromonal, or both. Furthermore due to the fact that cyanobacteria tend to occur in blooms, the effects of cell density were considered as a factor that might affect microcystin synthesis. This investigation attempted to elucidate a possible pheromonal role of

microcystin-LR, the most commonly occurring microcystin analogue, by monitoring cell density by flow cytometry and the use of stable isotope labelling employing <sup>15</sup>N.

It had to be determined which culture to use for the pheromonal investigations. Four strains of *Microcystis aeruginosa* were cultured over a period of seven weeks with bi-weekly sampling, which consisted of cell enumeration by flow cytometry and intra-cellular toxin analysis by HPLC-PDA. The four cultures chosen were *M. aeruginosa* PCC 7820, PCC 7813, B2666, and NIES 1099. The cyanobacteria exhibited characteristic growth patterns for *M. aeruginosa* (figure 2.5) in laboratory conditions with doubling rates of approximately 48-96 h (Moisander *at al.* 2009). The four strains that were selected for this investigation produced a variety of microcystin analogues (table 2.8). Microcystin-LR is the most commonly produced analogue by the four test strains (figure 2.6).

**Table 2.8:** Microcystin analogues produced by four strains of *M. aeruginosa*.

<b><i>M. aeruginosa</i> strain</b>	<b><i>Microcystin analogues produced</i></b>
PCC 7820	MC-LR, MC-LY, MC-LW, MC-LF
PCC 7813	MC-LR, MC-LY, MC-LW, MC-LF
B2666	MC-LR, demethylated MC-LA, MC-LA, unidentified MC
NIES 1099	MC-RR, MC-YR, MC-LR, unidentified MC

As can be seen the cell numbers correspond well with the amount of toxin. Only intra-cellular toxin was determined, which explains the concentration

decrease in toxin levels towards the end of the experimental time frame. This is due to cells dying and lysing and spilling their contents into the extra-cellular matrix. PCC 7820 mainly produced microcystin-LR and in much reduced amounts microcystin-LY, LW, and LF. The *M. aeruginosa* strain PCC 7813, which only differs from PCC 7820 by the lack of gas vacuoles, produces the same microcystin analogues. B2666 was the strain that produced most MC-LR of all the strains, it is also the main analogue produced by that strain. Other microcystin analogues produced by B2666 include MC-LA and demethylated MC-LA. In addition to these another as of yet unidentified microcystin is also produced by B2666. The NIES 1099 strain also produces a different unidentified MC analogue, in addition to MC-RR, LR, and YR. For NIES 1099 MC-LR is not the main variant, but MC-RR is. When comparing the amount of toxin cell<sup>-1</sup> (figure 2.7) it becomes obvious why flow cytometry is a useful tool for cell enumeration, by being able to accurately correlate the amount of toxin to the amount of cells, elucidates the fact that, even though it appears that B2666 produces significantly more MC-LR than PCC 7820, the amount of MC-LR cell<sup>-1</sup> is greater in the PCC 7820 strain. The strain chosen for further experiments was PCC 7820, because all of the variants it produces are characterised and it displayed the highest amounts of MC-LR cell<sup>-1</sup>, the most studied microcystin analogue. Furthermore it is not hindered by the lack of gas vacuoles and its growth dynamics are characteristic for most cyanobacteria with a doubling rate of approximately 72 h (Moisander *at al.*, 2009).

The use of stable isotope labelling using <sup>15</sup>N was explored after the selection of the appropriate *M. aeruginosa* strain to carry out the pheromonal and cell density investigations. *M. aeruginosa* PCC 7820 was grown in either <sup>14</sup>N-BG-II, <sup>15</sup>N-BG-II, or <sup>15</sup>N-BG-II medium with exogenous MC-LR added. Sampling



was performed daily and included cell enumeration by flow cytometry and HPLC-MS determination of intra- and extra-cellular toxin concentrations. The flow cytometric cell enumeration showed that cultures under all treatment regimes displayed similar growth behaviour, confirming that neither the exogenously added MC-LR, nor the labelling had a detrimental effect on the cultures (figure 2.8).

The *de novo* microcystin levels are relatively low in all cultures, including the control, this might be due to the high cell density at inoculation and subsequently during the experiment (figure 2.10; figure 2.11). The increased cell numbers could lead to self-shading of the culture thus decreasing the amount of available light to individuals deeper in the culture and/or in the water column. This could be one explanation for the decreased amount of toxin detected, since it has previously been shown that the availability of light has a direct impact on the total amount of toxin produced by a culture (Kaebernick *et al.*, 2000; Wiedner *et al.*, 2003; Jiang *et al.* 2008). Another possible explanation for the low toxin amounts detected, which can also be linked to the increased number of cells in the inoculum, could be signalling between individual cells. The physical vicinity of one cell to the next could trigger inhibitory reactions that reduce toxin production. Comparing the amounts of toxin cell<sup>-1</sup>, it can be seen that the concentration cell<sup>-1</sup> of unlabelled MC-LR (m/z 996) decreases over the course of the investigation, as very little new <sup>14</sup>N-MC-LR is produced and the remaining <sup>14</sup>N-MC-LR is spread over increasing number of cells. The development of the amount of <sup>15</sup>N-MC-LR over time is a mirror image of the amount of <sup>14</sup>N-MC-LR. As the amount cell<sup>-1</sup> of the <sup>14</sup>N-MC-LR decreases over time, the amounts of <sup>15</sup>N-MC-LR increase.

The amount of the MC analogue  $\text{cell}^{-1}$  is very variable over the observed time, all labelled ( $^{15}\text{N}$ ) analogues are only synthesised from day 2 onwards, representing a lack of *de novo* synthesis as the newly inoculated culture recovers from the inoculation, and the remaining  $^{14}\text{N}$  in the cells is used up, before any molecules containing the  $^{15}\text{N}$  are synthesised. The amount of unlabelled MC-LR detected in spiked samples was lower than expected (figure 2.14; figure 2.15). Originally  $10 \mu\text{g mL}^{-1}$  was added to the cultures, however, no more than  $2.5 \mu\text{g mL}^{-1}$  was detected. The observed decrease in concentration may be due to cells taking up the toxin into the intra-cellular matrix or the MC physically attaching to the outside of the cell. Both of the latter explanations could indicate a pheromonal role of microcystin. The effect that the exogenous MC-LR has on the MC synthesis (table 2.5) is remarkable. The distinct lag of one or two days that can be noticed in the intra-cellular labelled MC-LR concentration (figure 2.10; figure 2.12) is due to the fact that complete integration of the labelled nitrogen ( $^{15}\text{N}$ ) is not immediately achieved. Rather isotopomers are created that include any number of labelled nitrogen atoms. Any of these isotopomers can be considered *de novo* synthesised toxin. For the present investigations, however, only fully labelled MC-LR ( $m/z$  1006) will be the focus as this is sufficient to identify trends. Sano *et al.* (2011) who have investigated the use of labelled nitrogen ( $^{15}\text{N}$ ) to create analytical standards of MC-LR had pre-cultured MC-LR producing strains for six months in labelled nitrogen medium in order to ensure full incorporation of the labelled nitrogen. This demonstrates how long it may take before complete integration of the labelled nitrogen is achieved.

The effect of adding exogenous MC-LR to the cultures has a pronounced effect on the toxin synthesis in *M. aeruginosa* PCC 7820. The cultures grown in medium with exogenous toxin added produced significantly less MC-LR than those cultures without the toxin present (table 2.9). Labelled versions of the other microcystin analogues produced by *M. aeruginosa* PCC 7820 could be detected in low concentrations in the intra-cellular matrix, however, could not be detected in the extra-cellular matrix (figure 2.12; figure 2.15). The cultures that were grown with the exogenous MC-LR present in the medium appear to be synthesising less of the other variants as well (table 2.9), which is an indication that MC-LR not only affects MC-LR *de novo* synthesis but also the synthesis of other MC analogues (figure 2.12; figure 2.15). The exogenous toxin had (statistically) the most significant effect on MC-LY and LF.

**Table 2.9:** Statistical significance of *de novo* microcystin synthesis inhibition by exogenous microcystin-LR in *M. aeruginosa* PCC7 820.

<b><i>Microcystin analogue</i></b>	<b><i>Statistical significance of inhibited de novo MC synthesis (paired t-test; p-value)</i></b>
Microcystin-LR	0.0410
Microcystin-LY	0.0087
Microcystin-LW	0.0454
Microcystin-LF	0.0166

To date there are few studies investigating the effect of MC-LR on MC production, i.e. a putative pheromonal role of MC-LR. Schatz *et al.* (2007) have been able to correlate increased MC-LR concentration and an up-regulation of McyB gene (part of the MC synthesis McyA-J gene cluster) with the presence of cell extracts as well as MC-LR in the medium. This is disparate to what has been found in this study. It was shown that the addition of exogenous MC-LR decreased toxin production in *M. aeruginosa* PCC 7820. In

the past proposed role of microcystin as signalling compound had been mostly disregarded because a degree of uncertainty exists in regards to the intra- or extra-cellular movement of microcystins (Kaebernick and Neilan, 2001). However, a number of studies have investigated the localisation of microcystin-LR within the cell (*M. aeruginosa*) either by radioactive labelling or immunolabelling (Shi *et al.*, 1995; Young *et al.*, 2005; Rohrlack and Heyenstrand, 2007; Young *et al.*, 2008). The general consensus between the studies is that within the cell microcystin-LR is located around the nucleoplasmic region and the thylakoids. However Shi *et al.* (1995) also found MC-LR associated to the cell wall. This might indicate an active transport to the outside or from the outside in. Pearson *et al.* (2004) have been able to identify a transporter gene in toxigenic *M. aeruginosa* that is linked to the active transport of the toxin into the extra-cellular matrix. In their study they found that a mutant that had this gene disabled resulted in the loss of toxigenicity. In most studies the presence of microcystin in the extra-cellular medium has been associated with cell lysis due to detrimental growth factors or the age of the culture (Kaebernick and Neilan, 2001). The presence of an active transport supports the theory of microcystins as semiochemical.

To further explore the effects of exogenous MC-LR and to elucidate the role of cell density in regards to MC-LR synthesis, a study was designed. In this new study the sampling procedure was simplified, in an attempt to achieve better precision in the analysis. Furthermore the analysis was carried out with the more sensitive UPLC-MS. Different inoculation densities were chosen to assess the impact of cell density on MC synthesis and exogenous MC-LR (10  $\mu\text{g ml}^{-1}$ ) was added to some cultures. At sampling cells were enumerated (figure 2.16). The cell enumeration shows that the cultures with the highest

starting inoculum ( $30 \times 10^6$  cells  $\text{mL}^{-1}$ ) produce lower cell numbers than the culture with  $20 \times 10^6$  cells  $\text{mL}^{-1}$  over the course of the experiment. This can be explained with the fact that the higher cell numbers cause a self shading effect that inhibits extensive culture growth, the dependency of light availability and cell density has been demonstrated by Martinez *et al.* (2012) who have shown that irradiance in a dense cyanobacterial culture (*Synechocystis* sp.) is attenuated by cell adsorption and self-shading effects. The highest growth is achieved by the cultures inoculated with  $20 \times 10^6$  cells  $\text{mL}^{-1}$ . Least growth was observed by the cultures with a starting inoculum of  $2.5 \times 10^6$  cells  $\text{mL}^{-1}$ . The cultures, however, that had exogenous MC-LR present in their growth medium achieved a higher final cell density ( $135 \times 10^6$  cells  $\text{mL}^{-1}$ ) than the  $5 \times 10^6$  cells  $\text{mL}^{-1}$  starting inoculums ( $115 \times 10^6$  cells  $\text{mL}^{-1}$ ). And compared to the control cultures ( $2.5 \times 10^6$  cells  $\text{mL}^{-1}$ ) achieved 18 % higher growth. Based on this observation it has been shown that exogenous MC-LR has a growth stimulating effect that is statistically very significant (paired t-test,  $p$ -value=0.0087). Gan *et al.* (2011) have shown that the addition of MC-RR and MC-LR at environmentally relevant concentrations ( $0.25$ - $10 \mu\text{g L}^{-1}$ ) increases the colony size (diameter) significantly. While not directly comparable, this illustrates that MCs may have a pheromonal effect that affects culture development. The observations in this investigation and the Gan *et al.* (2011) investigation contradict the observations made in Schatz *et al.* (2007) who found that exogenous MC-LR and/or the addition of *M. aeruginosa* cell extract lead to a decreased cell count in their cultures (*M. aeruginosa* PCC 7806). It is possible that different strains are affected differently by exogenous MCs. The potential strain-specificity is supported by the work of Zilliges *et al.* (2008) who have identified an extra-cellular glycoprotein (designated microcystin-related

protein C; MrpC) which is located on the cell wall and may function as a receptor for MCs. However, MrpC is only associated with toxigenic cyanobacteria and was only identified in 30 % of tested toxigenic *M. aeruginosa* strains. Gan *et al.* (2011) used different toxigenic and non-toxigenic strains, three of which were isolated from a bloom in a Chinese lake and two were acquired from the FACHB collection in China (it is not clarified which strains were isolates and which were laboratory cultures). The strains reacted differently to the two MC analogues (MC-RR, MC-LR) used in their investigation. The intra- and extra-cellular toxin concentrations were monitored by UPLC-MS. The unlabelled MC-LR ( $m/z$  996) stayed relatively stable over the course of the experiment especially for the higher inoculation densities ( $10, 20, \text{ and } 30 \times 10^6 \text{ cells mL}^{-1}$ ) (figure 2.14). A marginal increase in unlabelled toxin concentration in the  $5 \times 10^6 \text{ cells mL}^{-1}$  cultures was noted between days three and seven. This is most likely due to remaining unlabelled nitrogen in the cells being used to synthesise MC-LR. The MC-LR concentrations in the extra-cellular matrix remain comparatively stable for the cultures with lower inoculation densities ( $2.5, 5, \text{ and } 10 \times 10^6 \text{ cells mL}^{-1}$ ), in the cultures with  $20 \text{ and } 30 \times 10^6 \text{ cells mL}^{-1}$  starting inocula more extra-cellular toxin can be detected during the later sampling days. The  $20 \times 10^6 \text{ cells mL}^{-1}$  cultures display more extra-cellular toxin from day seven onward, while the  $30 \times 10^6 \text{ mL}^{-1}$  cultures display increased amounts of extra-cellular toxin from day three onwards. One possible explanation would be the excretion of MC-LR as a signalling compound linked to the cell density. This would explain why the increased extra-cellular concentrations are first observed in the cultures with the higher starting inoculum. Considering that the presence of exogenous MC-LR stimulated culture growth in the spiked

cultures, the controlled release MC-LR into the extra-cellular matrix could indicate favourable growth conditions. A high cell density could be interpreted as favourable growth conditions thus the release of MC-LR could be a signal to focus on growth. Comparing the *de novo* production across the different inoculation densities it can be observed that the relative amounts of labelled toxin ( $m/z$  1006) at day ten is almost the same across the different inoculation volumes (figure 2.18). During the other sampling points the cultures with higher inoculation densities ( $10$  to  $30 \times 10^6$  cells  $\text{mL}^{-1}$ ) present slightly more toxin than the two lower starting densities. Comparing the extra-cellular concentrations of the *de novo* MC-LR it can be observed that the concentrations in the extra-cellular matrix are approximately equivalent across the inoculation densities. The amount of *de novo* MC-LR produced  $\text{cell}^{-1} \text{day}^{-1}$  is lower in the  $30 \times 10^6$  cells  $\text{mL}^{-1}$  starting density culture than it is for any of the others (figure 2.19). This might be due to only a fraction of the cells in that culture actively producing *de novo* toxin due to light availability, i.e. cells deeper within the culture that receive less light than those on the periphery limit their MC-LR synthesis and thus conserve energy. This is reflected in the production rates predicted from the cell enumeration and the UPLC-MS toxin determination (table 2.6). The  $30 \times 10^6$  cell  $\text{mL}^{-1}$  starting inoculation culture displays the lowest production rate. The low production rate may be connected to the light availability, as the light dependency of microcystin-LR synthesis is well documented (Jähnichen *et al.*, 2011; Zilliges *et al.*, 2011; Briand *et al.*, 2012). Alternatively the synthesis of MC-LR is limited by the presence of MC-LR in the medium which functions as semiochemical. As stated earlier, exogenous MC-LR appears to have a growth stimulating effect, considering the UPLC-MS determination of *de novo* toxin concentrations in the cultures treated

with exogenous MC-LR it can be observed that MC-LR also has a limiting effect of MC-LR synthesis (table 2.7). The treated cultures produced approximately 25 % less *de novo* MC-LR than the untreated culture (significant difference, paired t-test;  $p$ -value=0.0328). The mean amount of *de novo* toxin  $\text{cell}^{-1} \text{day}^{-1}$  is reduced by approximately 22 % (table 2.6). The distribution of the *de novo* toxin in the treated cultures was different as well compared to the untreated one (figure 2.20). The cultures with exogenous MC-LR added display a ten-fold decrease in the amount of *de novo* toxin present in the extra-cellular matrix at day 10. The trend, however, can already be observed at day seven. Comparing the amounts of unlabelled toxin in the treated and untreated cultures (figure 2.21), it can be seen that the extra-cellular exogenous toxin present at  $T_0$  is slowly decreasing in concentration which could be linked to the low increase of intra-cellular unlabelled MC-LR. A small percentage of that increase is due to unlabelled nitrogen in the cells that is utilised in the synthesis of MC-LR. Remarkable is the fact that again the actual spiked amount of  $10 \text{ mg mL}^{-1}$  MC-LR could not be detected in the extra-cellular matrix. The repetition of this phenomenon makes it likely that it may be linked to MC-LR as a semiochemical. It may be that that exogenous MC-LR is taken up by the cells or associated with the outside of the cell wall, to putative receptors (as proposed in Zilliges *et al.* 2008) and subsequently structurally changed, which may result in non-detection with the applied methods.

To elucidate the fate of the exogenous MC-LR, *M. aeruginosa* PCC 7820 grown in unlabelled BG-II ( $^{14}\text{N}$ ) was exposed to exogenous labelled ( $^{15}\text{N}$ ) MC-LR. It can be seen that only a very small ( $3\text{-}4 \text{ ng mL}^{-1}$ ) amount of the originally



added exogenous labelled MC-LR is taken up by the cells and that the intra-cellular concentrations of the exogenous MC-LR remain stable (figure 2.22). Examining the extra-cellular concentrations it can be observed that the original spike of  $^{15}\text{N}$ -MC-LR cannot be detected in the  $T_0$  sample, only  $450 \text{ ng mL}^{-1}$  of the originally added  $1000 \text{ ng mL}^{-1}$  (figure 2.23). This continues the trend that was observed in the two previous investigations where the original added amount could also not be detected. This may point at an uptake with subsequent modification of the MC molecule thus leading to non-detection in the analysis. The addition of the  $^{15}\text{N}$ -MC-LR to the growth medium has also stimulated growth in the treated cultures compared to the control cultures (figure 2.25) as was described previously (figure 2.16). The cell numbers are increased by 17 % in the treated cultures compared to the control cultures, which is almost equal to the increase of cell numbers induced by the addition of  $10 \mu\text{g mL}^{-1}$  of exogenous MC-LR. The effect on the toxin synthesis was also comparable to the investigation described previously (figure 2.20). Although the monitoring of the *de novo* MC-LR is not as precise as before where the *de novo* toxin was labelled, an approximation can still be made by subtracting the amount of intra-cellular MC-LR at  $T_0$  from any results obtained at later sampling dates (figure 2.24). *De novo* toxin production was decreased by 14 % in the cultures treated with exogenous MC-LR. Compared to the previously obtained results that represents a higher limiting effect (14 % compared to 9 %). This might indicate a dose-dependency, which would be supported by Schatz *et al.* (2004) who, although achieving results that contradict the present study, i.e. exogenous toxin increased toxin synthesis, also found a dose-dependency. Increasing the dose of exogenous MC-LR led to increasing amounts of MC-LR synthesised. The potential dose-dependency of MCs as

semiochemicals was also observed by Gan *et al.* (2011) who noticed an increased culture diameter with increased doses of exogenous MC-LR and MC-RR respectively. The distribution between the intra- and extra-cellular matrix was affected as well (figure 2.24). The effect was not as pronounced as it had been previously where the amount of extra-cellular toxin was decreased by 80 %, however, the amount of MC-LR in the extra-cellular matrix was reduced by 20 %. Considering a ten-fold decrease in the exogenous MC-LR concentration still affected this decrease.

In the past, MCs were not thought to be semiochemicals though increasing evidence has been presented in recent times that a reconsideration of their roles as putative semiochemicals is necessary. The presented work indicates that MC-LR may have a pheromonal effect on *M. aeruginosa*. It has been shown to induce increased cell numbers, independent of dose, limit *de novo* toxin synthesis, which may be dose dependant, and alter the distribution of intra- and extra-cellular toxin. It has furthermore been demonstrated that a ten-fold decrease in the amount of exogenously added MC-LR still showed significant growth stimulating- and toxin synthesis limiting effects.

**Photocatalytic water  
treatment**

### **3 Photocatalytic Water Treatment**

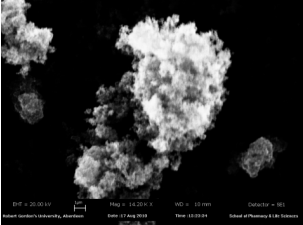
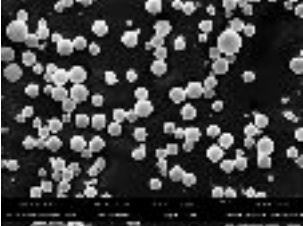
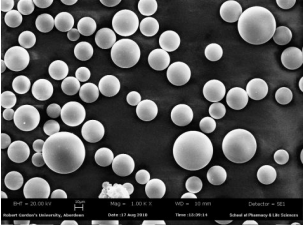
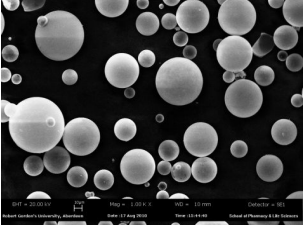
#### **3.1 Introduction**

Cyanobacteria and their secondary metabolites, especially their toxins, pose a serious health hazard. The management of cyanotoxins is important when considering potable water safety. Failing to control the propagation of cyanobacteria and the production of their toxic secondary metabolites in drinking water systems, means of removal have to be explored. Titania assisted photocatalytic destruction of cyanotoxins, especially microcystin-LR is well studied (Robertson *et al.*, 1999; Lawton *et al.*, 1999; Cornish *et al.*, 2000; Liu *et al.*, 2002, Shephard *et al.*, 2002; Fieng *et al.*, 2006). However, high operating costs of UV radiation and the physico-chemical properties of the photocatalyst have to date hindered the wide application of advance oxidation process with photocatalysts (Liu *et al.*, 2009).

To date there are generally three ways of applying TiO<sub>2</sub> as a semi-conductor photocatalyst: (nanoparticulate) powder, pellets, or fixing of some form to a surface, e.g. as film, sol gel, or nano tubes (Meyer *et al.*, 2003, Sonawane *et al.*, 2002; Imai *et al.*, 1999). All three different ways have specific applications and inherent advantages and disadvantages. Powders generally perform well in the photodecomposition of organic compounds, due to their large surface area and ready distribution in the suspension. Challenges faced when using powders are relatively complicated and the ways of removal from suspension (Meyer *et al.*, 2003) are often impractical. Pellets alleviate the issue of removal, but tend to perform less efficiently in comparison to the powders (Liu *et al.*, 2009). Another disadvantage of pellets is the fact that vigorous mixing can break the pellets, which results in the same issue of removal that one is

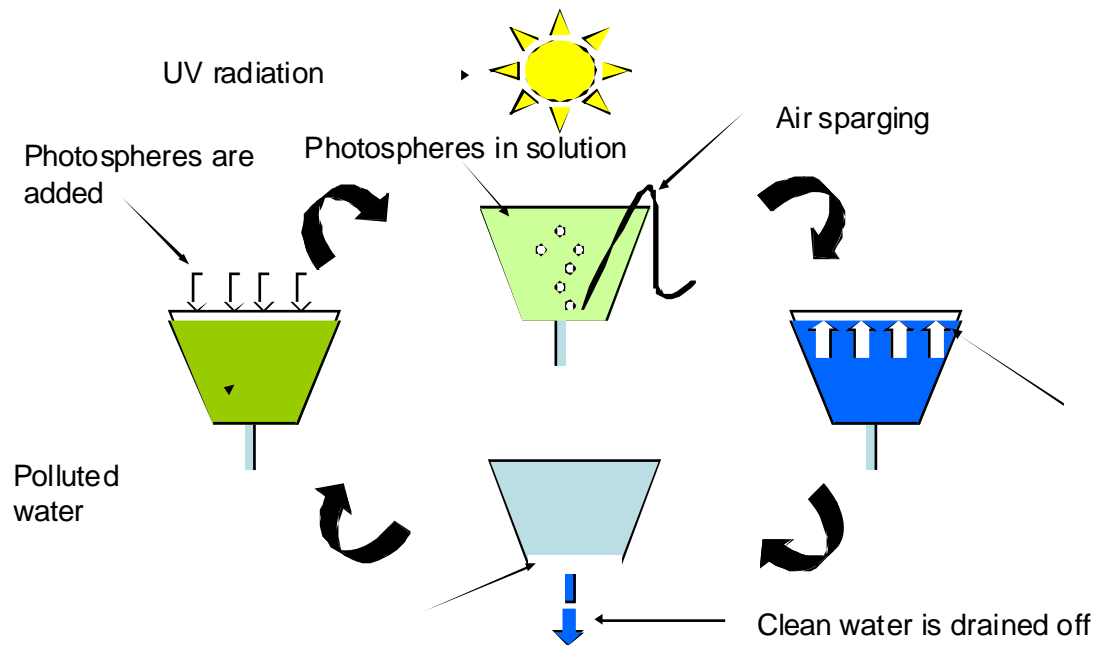
presented with when using powders (Liu *et al.*, 2009). The third presentation of TiO<sub>2</sub> can be as a fixed matrix, usually as a film, a sol gel, or in the form of nano tubes/rods. The inherent issues with this approach are the high production cost for relatively small yields of finished product and often convoluted and cost intensive manufacturing processes that require specialist equipment (Kobayashi *et al.*, 2000; Meyer *et al.*, 2003). A novel approach to the presentation of TiO<sub>2</sub> is the annealing of the catalyst to hollow, buoyant glass spheres, or magnetic pellets. The size of these products ranges from micro to millimetre range. One of these novel products was used in this series of investigations: Photospheres™. Photospheres™ are available in a range of conformations (table 3.1).

**Table 3.1:** Properties of four titania based photocatalysts. All images at X 1000. (Liu *et al.*, 2009; personal communication NSA Ltd.)

<b>Material</b>	<b>Properties</b>	<b>Image</b>
<b>Degussa P25</b>	Nanoparticulate powder, BET surface area: 50 m <sup>2</sup> g <sup>-1</sup> , average particle size 20 nm	
<b>Photospheres™ 15µm</b>	Coated silica beads, BET surface area: 38 m <sup>2</sup> g <sup>-1</sup> , average particle size 15 µm	
<b>Photospheres™ MTO/0131</b>	Coated silica beads, no surface area information available, average particle size 15 µm	
<b>Photospheres™ 40µm</b>	Coated silica beads, BET surface area: 48 m <sup>2</sup> g <sup>-1</sup> , particle size 40 µm (range from 10 to 60 µm)	

Photospheres™ were recently developed by the company Nanoparticulate Surface Adhesion Ltd. (NSA Ltd.). The hollow, buoyant silica beads coated with TiO<sub>2</sub> allow for easy removal, due to the buoyancy, while still providing a high surface area. As can be seen Photospheres™ come in a variety of sizes and are coated with 100 % anatase TiO<sub>2</sub>. NSA Ltd. envisage a mode of operation where contaminated water and Photospheres™ are brought together in a reactor that is radiated with UV light and sparged with air. After the treatment process the Photospheres™ are allowed to settle on the surface and the water is siphoned off (figure 3.1). The tank can then be refilled as the Photospheres™ are capable of repeated usage. This would suggest that the

Photospheres™ may be suitable for the removal of microcystins and other trace organic pollutants from drinking water.



**Figure 3.1:** Process of water treatment using Photospheres™.

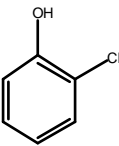

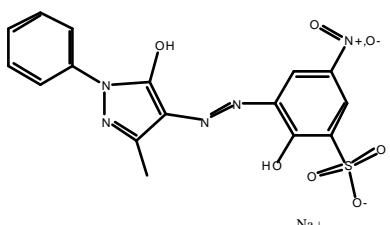
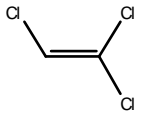
A number of researchers have conducted work with titania covered spheres or formed spheres from titania. Li *et al.* (2008, 2010) successfully degraded methylene blue and orange II with titanium dioxide covered hollow silica spheres. Zhao *et al.* (2011) successfully degraded rhodamine B under visible light with hollow spheres (Si/Ti hybrid) of Ag doped titania. And Ren *et al.* (2003) produced hollow Ti spheres, however, did not test their photocatalytic efficiency.

The aim of this series of investigations is to assess the suitability of a novel titania based photocatalyst called Photospheres™ in the destruction of the cyanotoxin microcystin-LR. This particular microcystin analogue was chosen due to the fact that it is the most commonly reported toxin of the microcystin family. Furthermore the efficacy of the novel catalyst will be assessed with ten other microcystin analogues and the sister compound nodularin because cyanotoxins are usually presented as a mixture when appearing in water. Due to the fact that in a water treatment scenario other organic compounds will be present, the photocatalytic destruction of four model compounds (table 3.2) will also be attempted.

The widely investigated Degussa P25 will serve as a benchmark catalyst, it is a mixture of the anatase and rutile types (74 % anatase and 25 % rutile types) (Liu *et al.* 2009). To make the photocatalytic destruction of the cyanotoxins and organic pollutants more cost and energy effective the efficacy of the Photospheres™ and P25 will also be tested in a reactor utilising light emitting diodes (LEDs) as the source of irradiation.



**Table 3.2:** Organic pollutants used in investigation (Wamer, 1985; WHO, 2003, 2008; Kasarskis, 2008; Gash, 2008; Engel, 2008, ATSDR, 2010; Problete *et al.*, 2011)

<b>Compound</b>	<b>Source</b>	<b>Health Implications</b>	<b>Regulation</b>
<p><b>2-chlorophenol</b></p> 	<p>Disinfectants Pesticides</p>	<p>Attacks central nervous system and heart, dysrhythmia, seizures, coma</p>	<p>WHO guide line: 1 mg L<sup>-1</sup></p>
<p><b>p-cresol</b></p> 	<p>Land fill leachate Disinfectants Deodorisers Pesticides Wood-preservatives Text markers</p>	<p>Irritant Abdominal pain Vomiting Heart damage Anaemia Damage to liver, nervous system, and kidneys</p>	<p>ATSDR minimal risk level for oral exposure: 0.1 mg kg<sup>-1</sup> 0.2 d<sup>-1</sup></p>
<p><b>Acid orange 74</b></p> 	<p>Textile dye Run-off from textile industry</p>	<p>Carcinogen</p>	<p>Not regulated</p>
<p><b>Trichloroethylene</b></p> 	<p>Industrial solvent Anaesthetic (use stopped in developed countries after 1980, still used in development countries)</p>	<p>Carcinogen Amyotrophic lateral sclerosis Parkinson-like disease</p>	<p>ATSDR minimal risk level for oral exposure: 0.2 mg kg<sup>-1</sup> d<sup>-1</sup></p>

ATSDR = American Agency for Toxic Substances and Disease Registry

## **3.2 Materials and methods**

### **3.2.1 Reagents**

Degussa P25 was obtained from Evonik, Degussa (UK), and used as received. All microspheres (15 micron Photospheres™, 40 micron Photospheres™, and MTO/0131) were test samples provided by Microsphere Technology Ltd., Adare, Co. Limerick, Ireland. Microcystins were taken from laboratory stocks, which were obtained from laboratory cultures using the method described in Edwards *et al.* (1996). Cresol (C<sub>7</sub>H<sub>8</sub>O; molecular weight: 108.14), Acid Orange 74 (AO) (C<sub>16</sub>H<sub>12</sub>N<sub>5</sub>NaO<sub>7</sub>S; molecular weight: 441.36), Trichloroethylene (TCE) (C<sub>2</sub>HCl<sub>3</sub>; molecular weight; 131.39), and 2-chlorophenol (CP) (C<sub>6</sub>H<sub>5</sub>ClO; molecular weight: 128.56) were supplied by Sigma Aldrich and were used as received. HPLC solvents were acetonitrile (Rathburn, Walkerburn, UK) and Milli-Q water, to which each trifluoroacetic acid (Fischer Scientific, Leicestershire, UK) was added as an ion-pairing agent. All aqueous solutions were prepared with Milli-Q water (Millipore, Watford, UK).

### **3.2.2 HPLC-PDA detection of analytes (pollutants and microcystins)**

The instrument used was a Waters 2695 Separation Module. High resolution photodiode detection was performed with a Waters 2996 Photodiode Array Detector (PDA) (both Waters, Elstree, UK). Separation of analytes was performed with a Sunfire C18 column 2.1 mm (inner diameter) x 150 mm, with a 5 μm particle size (Waters, Elstree, UK). The mobile phases used were Milli-Q and acetonitrile (C<sub>2</sub>H<sub>3</sub>N), both contained 0.05 % trifluoroacetic acid (TFA). The flow rate applied was 0.3 mL min<sup>-1</sup>. The PDA resolution was set to

1.2 nm and data was acquired in the range of 200 to 400 nm. Column temperature was set to 40°C.

The method used for the assessment of microcystin-LR was the same HPLC method that was used in the cell signalling investigation (chapter 2), based on Lawton *et al.* (1994) (table 3.3).

**Table 3.3:** The solvent gradient used in the method for the analysis of microcystins (Lawton *et al.*, 1994). Solvent A: Milli-Q water with 0.05 % TFA; Solvent B: Acetonitrile with 0.05 % TFA.

<b><i>Microcystin method (Lawton et al., 1994)</i></b>		
<b><i>Time (min)</i></b>	<b><i>A (%)</i></b>	<b><i>B (%)</i></b>
0-24	75	25
25	15	85
26	35	65
27-33	0	100
33-35	75	25

In the investigation of the eleven microcystin analogues, a more rapid analysis method was needed, a new method was developed that reduced analysis time by more than half (table 3.4).

**Table 3.4:** The solvent gradient for a fast method for the analysis of microcystins. Solvent A: Milli-Q water with 0.05 % TFA; Solvent B: Acetonitrile with 0.05 % TFA.

<b><i>Rapid microcystin method</i></b>		
<b><i>Time (min)</i></b>	<b><i>A (%)</i></b>	<b><i>B (%)</i></b>
0-9	85	15
10	35	65
11	0	100
12	0	100
13-15	85	15

A different method was required when the waste water pollutants were assessed. The new method was rapid and was successfully applied to the analysis of all four pollutants (table 3.5).

**Table 3.5:** The solvent gradients used in the analysis of the water pollutants. Solvent A: Milli-Q water with 0.05 % TFA; Solvent B: Acetonitrile with 0.05 % TFA.

<b>water pollutant method</b>		
<b>Time (min)</b>	<b>A (%)</b>	<b>B (%)</b>
0-9	75	25
10	35	65
11	0	100
12-14	75	25

Different wavelengths were used to detect the varied analytes (table 3.6). Analytes were identified based on their characteristic retention times and UV spectra. A set of appropriate point standards was analysed along with each batch of samples.

**Table 3.6:** The different wavelengths that were applied in the analysis of the different analytes in PDA analysis.

<b>Analyte</b>	<b>Wavelength (nm)</b>
2-chlorophenol	265
<i>p</i> -cresol	265
Acid Orange 74	238
trichloroethylene	204
microcystins (and nodularin)	238

### **3.2.3 Photocatalytic destruction of microcystin-LR with Degussa P25**

This experiment was derived from the methods used in Robertson *et al.* (1997). A 20 mm, 20 mL glass sample vial (Kinesis, Beds, UK) was filled with an aqueous microcystin solution (10 mL) with a concentration of 20 µg mL<sup>-1</sup>. This

was located on a stirring block in front of a Xenon lamp (480 W UVASpot 400 lamp, Uvalight Technologies Ltd., spectral output 330-450 nm, photonic efficiency:  $1230 \mu\text{mol s}^{-1} \text{m}^{-2}$  at 20 cm distance) at a distance of 20 cm. Samples of 120  $\mu\text{L}$  were taken at the beginning of the experiment ( $T_{01}$ ) prior to the addition of the catalyst. Added to this was 1 % (w/v) Degussa P25 and the vial was kept in the dark for two minutes, after which another sample was taken ( $T_{02}$ ). The vial was then exposed to the UV light and samples were taken at the following time points: 1, 2, 3, 4, 5, 6, 8, 10, 12, 14, 16, 20, 30, 40 minutes. The samples were placed in micro-centrifuge tubes (1.5 mL) and centrifuged for 5 minutes at approximately  $2000 \times g$  at room temperature to remove the  $\text{TiO}_2$ , then analysed with HPLC-PDA (section 3.2.2). In addition two controls were performed: one in the dark to confirm that any decrease in concentration was due to photocatalytic activity and one without the catalyst present to assess the possible effect of UV irradiation on the target analytes, all samples were tested in triplicate.

.

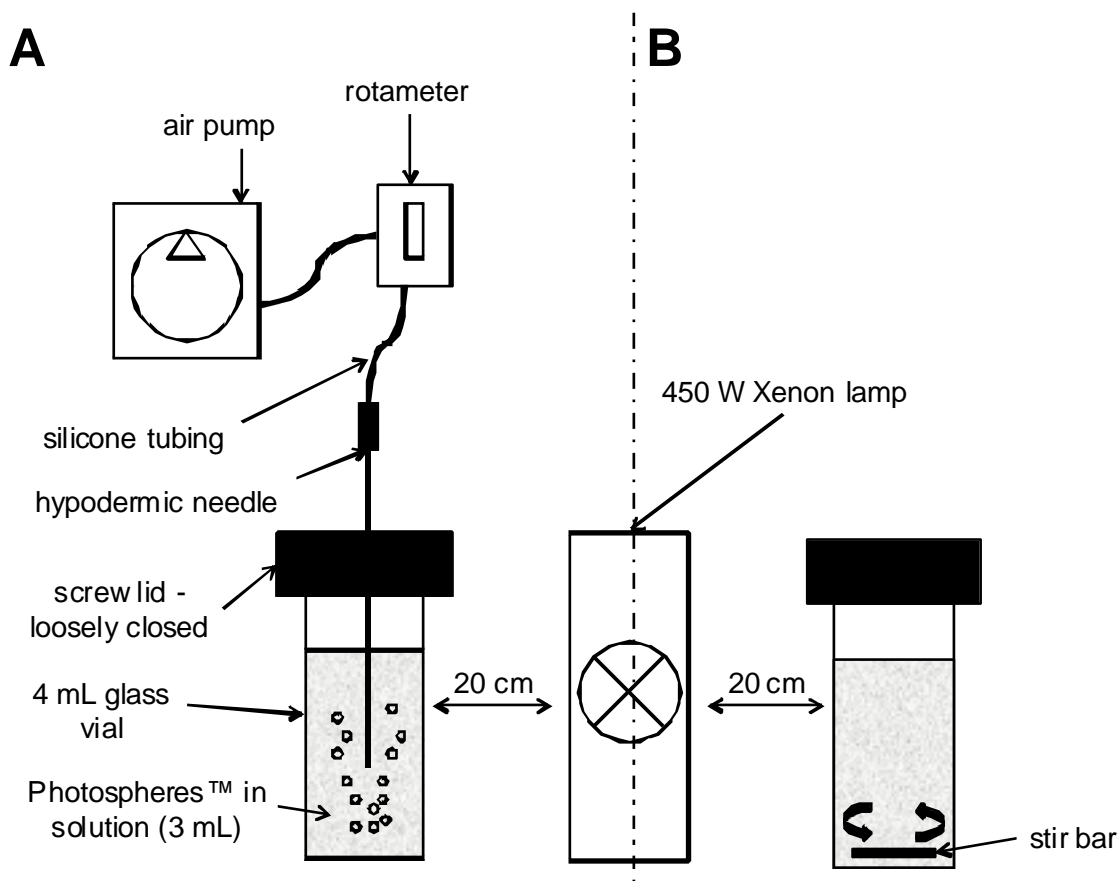
### **3.2.4 Photocatalytic destruction of microcystin-LR with $\text{TiO}_2$ Photospheres™15 $\mu\text{m}$**

The experiment with the Photospheres™15 $\mu\text{m}$  was conducted (section 3.2.3) with 1 % (w/v) Photospheres™15 $\mu\text{m}$  instead of Degussa P25 powder, in addition the number of sampling points was reduced, and the experiment was stopped after 10 minutes. Furthermore, the sample volume was decreased to achieve a more economic usage of the cyanotoxins, to this end an aqueous solution of microcystin-LR (3 mL) with a concentration of  $10 \mu\text{g mL}^{-1}$  was placed into a 13 mm, 4 mL screw top vial (Kinesis, Beds, UK) with a plastic lid with a self-healing rubber septum with silicon facing.

The catalyst could not be removed by standard centrifugation due to the buoyancy of the Photospheres™, therefore a centrifugation filtration device was used (Spin-X filter tubes, 2 mL, Corning incorporated, Corning, NY, USA). This permitted sample and catalyst separation with minimum loss of sample. This experiment was performed in duplicate and analysed by HPLC (section 3.2.2).

### **3.2.5 Photocatalytic destruction of microcystin-LR with Degussa P25, Photospheres™15µm, and Photospheres™MTO/0131**

While carrying out photocatalysis in the presence of Photospheres™15µm (3.2.4), it was noted that good mixing of the Photospheres™ was not achieved by stirring. At low stirring speed accumulation on the surface was noticed which is due to the photosphere's inherent buoyancy, with increased stirring speeds a grinding effect was noticed by the formation of a layer at the bottom of the vial, suggesting damage to the Photospheres™. To achieve better mixing, a new system was designed that utilised sparging for mixing instead of stirring. To achieve this, a hypodermic needle was inserted through the rubber septum of the vial into the solution. This was connected via silicon tubing to a rotameter (Influx Measurements, Alresford, UK), which, in turn, was connected to an air pump (JUN-AIR, Nørresundby, Denmark) (figure 3.2)



**Figure 3.2:** Experimental design for the photodegradation of microcystin in sparged system (A) and a stirred system (B).

The distance between the glass vial and the UV lamp (same as in previous experiments) was 20 cm. The airflow was set to  $0.2 \text{ cm}^3 \text{ min}^{-1}$ . A sample ( $120 \text{ }\mu\text{L}$ ) was taken at the beginning ( $T_{01}$ ), which established the initial microcystin concentration. Then the Photospheres™ were added (1 % (w/v)). After 2 minutes in darkness, another sample was taken ( $T_{02}$ ), which established the amount of dark adsorption. The light was then switched on and samples were taken after 1, 2, 3, 4, 5, 6, 8, and 10 minutes respectively; all samples were placed in Spin-X filter tubes for Photosphere™ products and microcentrifuge tubes (1.5 mL) for P25. Samples were then centrifuged at approximately 2000 g for 5 minutes at room temperature, then analysed with HPLC-PDA (section 3.2.2). This experiment was performed in duplicate.

### **3.2.6 Light and scanning electron microscopic investigation of Photospheres™ samples**

A microscopic investigation of both, the Photospheres™15µm and the Photospheres™MTO/0131 was conducted by adding a small amount (5-10 mg) of catalyst to 250 µL of water in a microcentrifuge tube (1.5 mL). After vortexing a wet slide was prepared and examined under a light microscope. This revealed a significant amount of debris that could be glass and/or loose TiO<sub>2</sub>. A Scanning electron microscopic investigation of the Photospheres™15µm, 40µm, MTO/0131 and P25 was performed by mounting a small amount of sample on a double sided carbon pad which in turn was placed on an aluminium stub. The samples were scanned with a Leo S430 Scanning Electron Microscope (Leo Electron Microscopy, Cambridge, UK) coupled with an energy dispersive x-ray analyser PentaFET Precision IncaX-act (Oxford Instrumetns, Abingdon, UK).

### **3.2.7 Evaluation of the removal of fines from Photospheres™ preparations and weight adjustment**

A step to remove loose fines from the Photospheres™ was included in order to determine whether the debris observed was contributing to the destruction of the microcystin. This consisted of adding 300 mg of Photospheres™15µm to approximately 25 mL of Milli-Q water in a 40 mL centrifugation tube. The tube was vortexed vigorously, then centrifuged at approximately 2000 x g for 15 minutes at room temperature. The supernatant (containing the washed Photospheres™) was then vacuum filtered with Whatman GFC filterpaper (5.5 cm diameter). The filter disk was placed in a plastic petri dish and dried in an



oven at 60°C overnight. The photocatalytic performance of the fines-free Photospheres™ 15µm was determined as before (section 3.2.2).

### **3.2.8 Photocatalytic destruction of microcystin-LR with three different Photospheres™ preparations and influence of catalyst load**

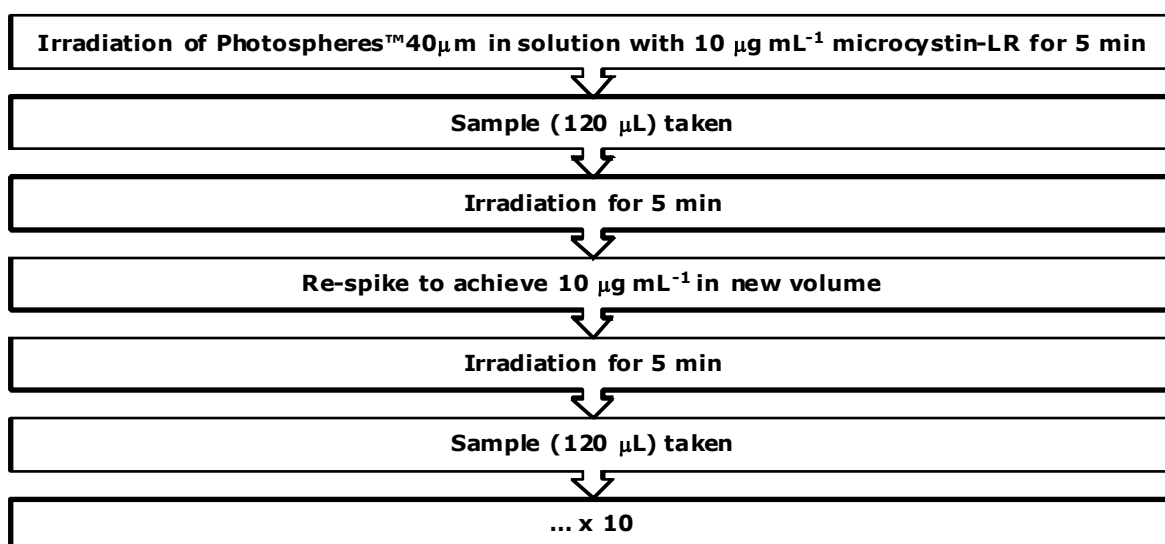
It was found that only 17 % of the mass of the Photospheres™ consists of TiO<sub>2</sub> (personal communication, Dr Tom Johnston, Operations Manager, Nanoparticulate Surface Adhesion Ltd). In order to allow a direct comparison between active catalyst load, the amount was increased to 5.88 % (w/v) of photosphere™ material to achieve 1 % (w/v) of TiO<sub>2</sub>. In all other respects this experiment was performed as section 3.2.5. The Photospheres™ 40µm, introduced by the producer as a higher grade product were tested not only at the recommended level of 1 % (w/v) TiO<sub>2</sub>, but also at lower concentrations. The catalyst load was tested from 0.2 % (w/v) TiO<sub>2</sub> to 1 % (w/v) TiO<sub>2</sub> in 0.2 % steps. Samples were analysed by HPLC-PDA (section 3.2.2)

### **3.2.9 Photocatalytic destruction of different microcystin variants and nodularin with Photospheres™ 40µm**

This experiment was carried out as section 3.2.5 with a catalyst load of 1 % (w/v) TiO<sub>2</sub>, a toxin concentration of 10 µg mL<sup>-1</sup> and the following different microcystin variants (in the place of microcystin-LR): demethylated microcystin-RR, microcystin-RR, demethylated microcystin-YR, microcystin-YR, demethylated microcystin-LR, methylated microcystin-LR, microcystin-LA, microcystin-LY, microcystin-LW, microcystin-LF, and nodularin. All experiments were performed in duplicate.

### 3.2.10 Investigation of photosphere™40µm reuse

This experiment was performed in order to assess the re-usability of Photospheres™40µm. It was performed as section 3.2.5 with the following alterations: After the initial sample ( $T_{01}$ ) and the time allowed for equilibrium to be reached ( $T_{02}$ ), a sample (120 µL) was taken after 5 minutes of UV radiation. Following this the solution was irradiated for 5 min to remove any remaining microcystin-LR, then the solution was spiked with an appropriate amount of microcystin-LR to reach the initial concentration of 10 µg mL<sup>-1</sup> in the solution. This was repeated ten times (figure 3.3).

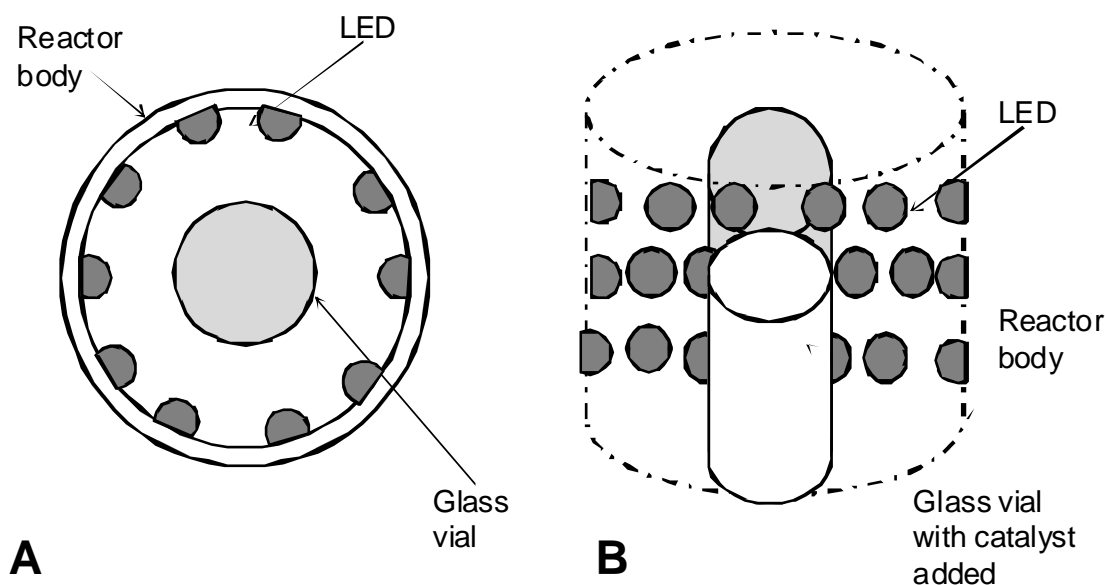


**Figure 3.3:** Schematic workflow for the investigation of Photosphere™40µm reuse

Samples were analysed with HPLC-PDA (section 3.2.2)

### 3.2.11 Evaluation of the use of light emitting diodes (LEDs) in the photocatalytic destruction of microcystin-LR

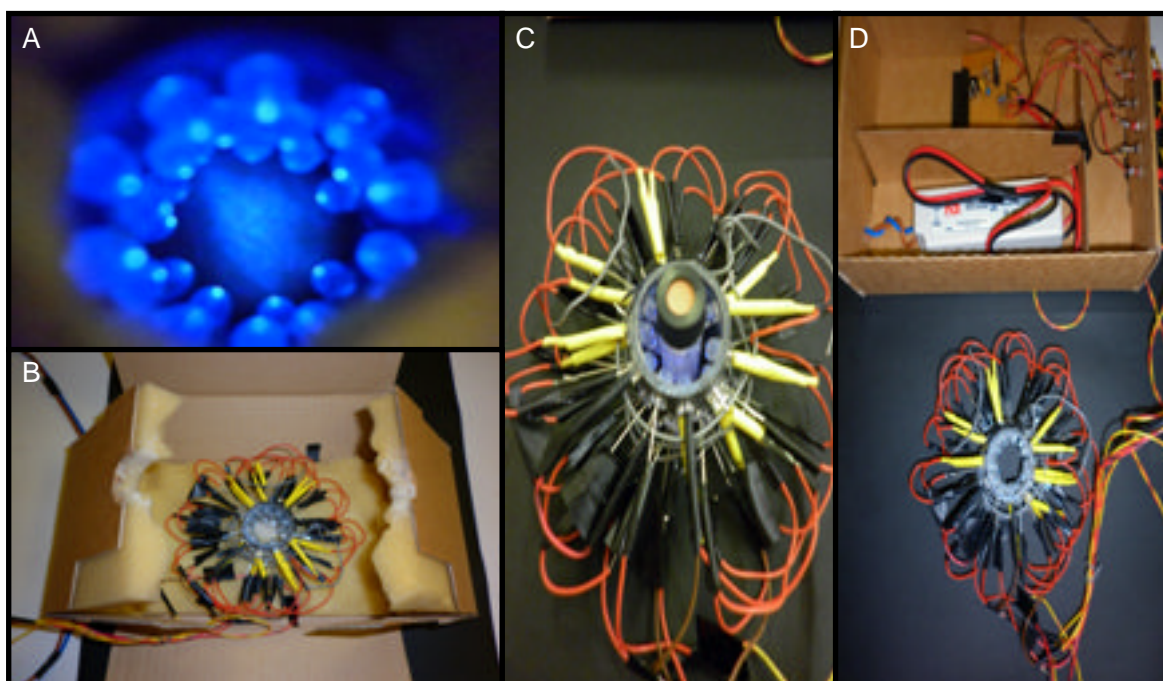
To evaluate a lower energy light source, a small scale reactor was designed to take a 13 mm, 4 mL screw top vial centred in a ring of 30 LEDs in three rows (10 LEDs per row) (figure 3.4). The reactor was constructed by drilling holes for the LEDs into an appropriately sized PVC tube (47 mm inner diameter, 51 mm outer diameter, 45 mm height). The LEDs (AT Technologies, Bath, UK) have a diameter of 5 mm, a 15° aperture,  $\lambda$  360 nm, and a power output of 750  $\mu$ W at 20 mA DC/3.8 V. Each chain of 10 LEDs was connected in series by soldering. The three LED chains were in turn connected in parallel to the control unit (figure 3.5).



**Figure 3.4:** Schematic of the small scale LED reactor. A) top view B) side view.

The control unit included the appropriate resistors to protect the rig from power fluctuations. The control unit was connected to a conventional wall plug. The distance between the wall of the screw-top vial and the LEDs was 1.5 mm.

A comparison study with Degussa P25 and Photospheres™40µm was performed for a duration of 10 minutes. The investigation was executed as 3.2.2.4 with the exception of applying LEDs as the source of irradiation. The samples were analysed by HPLC-PDA (section 3.2.2). All experiments were conducted in triplicate.



**Figure 3.5:** Photographs of the custom built LED reactor for use with small volume vials (4 mL). A) UV LEDs in operation; B) Opened reactor; C) Reactor with small volume vial (4mL) in operation (no agitation); D) reactor with control unit.

### 3.2.12 Evaluation of Photospheres™40µm for the removal of waste water pollutants

Aqueous solutions (3 mL, 10 µM) of the relevant pollutant (AO, CP, *p*-cresol, or TCE) were prepared and were transferred into a 13 mm, 4 mL screw top vial with plastic lid and a self-healing rubber septum with silicon facing. Mixing was initially provided by stirring, however, the investigation of TCE made it clear that sparging was not an appropriate means of agitation for that

compound due to volatisation. For this reason, small glass magnetic stirrer bars were manufactured and agitation of the compounds was provided by stirring (figure 3.6 – B). The distance between the glass vial and the Xenon lamp was 20 cm. Sampling was performed by switching off the stirrer and allowing the catalysts to settle, then a 100  $\mu$ L HPLC/GC injection syringe was used to penetrate the layer of catalyst and to draw an 100  $\mu$ L sample from under that layer. The sample was placed immediately into a low volume glass insert that was embedded into a microcentrifuge tube (1.5 mL) (Eppendorf, Hamburg, Germany) with BlueTac<sup>®</sup>. For P25 the supernatant was transferred into a low volume glass insert for analysis, for the Photospheres<sup>™</sup>40 $\mu$ m the HPLC injection needle was used again to penetrate the layer of spheres and draw approximately 80  $\mu$ L of sample which was then placed into a low volume glass insert for analysis. A sample (100  $\mu$ L) was taken at the start of the experiment ( $T_{01}$ ), then the catalyst was added (30 mg of P25, 176.5 mg of Photospheres<sup>™</sup>40 $\mu$ m, equal to 1% (w/v) of TiO<sub>2</sub>, respectively). After 20 minutes in darkness, another sample was taken ( $T_{02}$ ). The light was then switched on and samples were taken every half hour for CP, *p*-cresol, and TCE, it was found that AO degrade so rapidly that a different sampling regime was employed (samples taken every 5 minutes). Samples were then centrifuged at approximately 2000 x g for 5 minutes at room temperature and analysed with HPLC-PDA (section 3.2.2). All experiments were performed in duplicate. Furthermore, two negative controls were included in the experimentation, the UV negative control to assess UV degradation without catalyst and the dark negative control which was conducted in the presence of catalyst but in the absence of irradiation. For both negative controls, samples were treated exactly the same as above, but no catalyst was added to the

solutions for the UV negative control; for the dark negative control catalyst was added but the samples were kept in the dark. In all other respects the negative controls were treated the same as the actual samples.

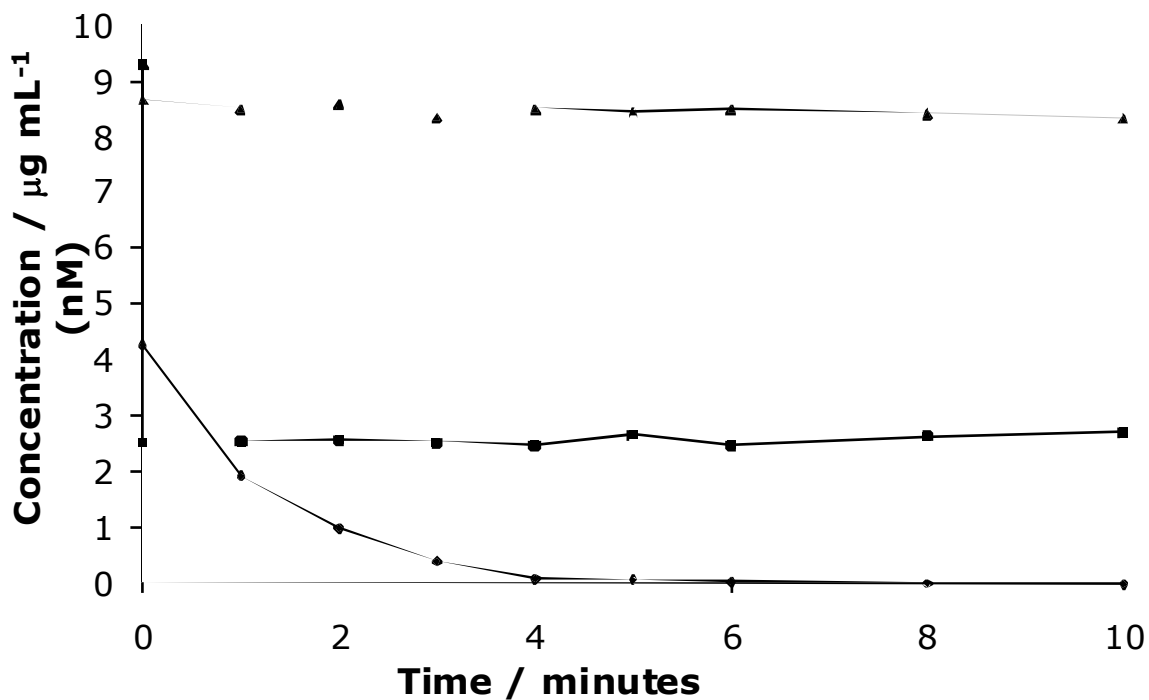
### **3.3 Results**

The aim of these investigations was twofold. The first series of investigations focuses on the potential of applying Photospheres™ to the control of harmful secondary cyanobacterial metabolites. A series of different configurations of Photospheres™ were used in the photocatalytic decomposition of different types of the harmful hepatotoxin microcystin. In order to assess the suitability of the Photospheres™ a comparison with the widely used TiO<sub>2</sub> based catalyst Degussa P25 was carried out.

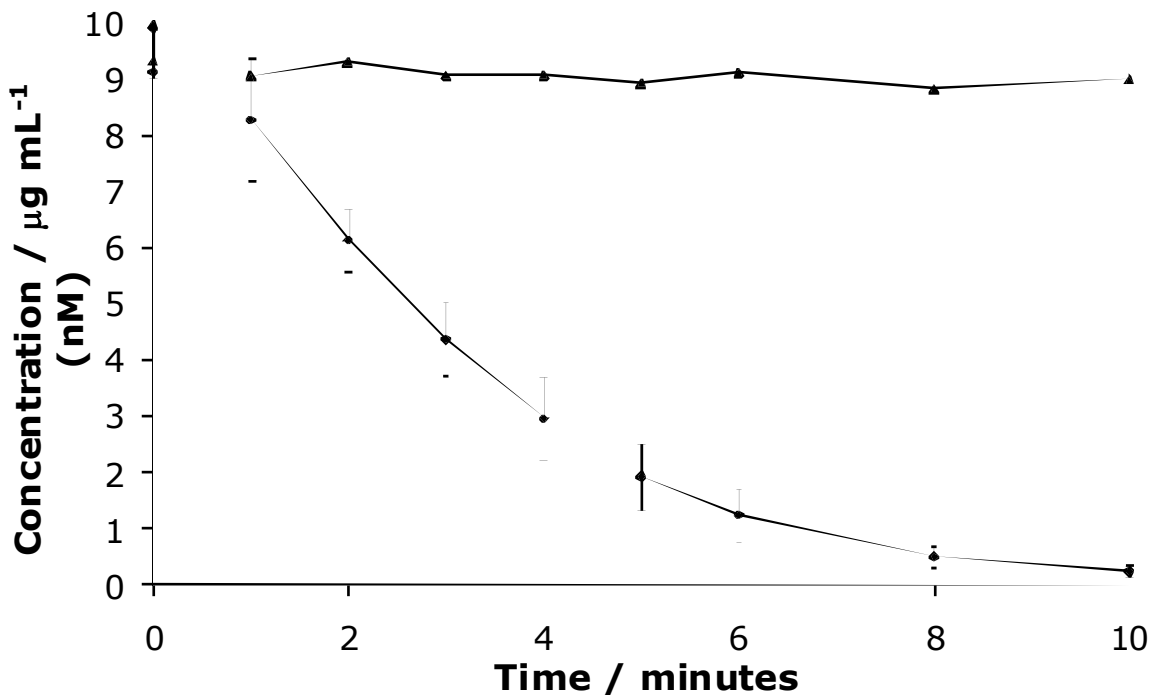
In the second series of investigations the photocatalytic efficiency of the novel Photospheres™ was compared to that of the well studied catalyst P25 in the photocatalytic destruction of four common waste water pollutants. The four pollutants (the azo-dye Acid Orange 74, 2-chlorophenol, *p*-cresol, and trichloroethylene) were chosen due to their common appearance in mostly industrial waste waters and due to their inherently detrimental effects on human health and well-being.

#### **3.3.1 Photocatalytic destruction of microcystin-LR with Photospheres™ and Degussa P25**

Degussa P25 is a thoroughly investigated photocatalyst with a documented ability to successfully decompose microcystins (Robertson *et al.* 1997). In order to set a bench mark to compare the results obtained in later experiments with Photospheres™ the performance of TiO<sub>2</sub> in the form of Degussa P25 (powder) was investigated in a stirred system (figure 3.6).



**Figure 3.6:** Photocatalytic decomposition of microcystin-LR by Degussa P25 in a stirred system (◆); dark control (■); UV control (▲). Error bars= 1 SD; n=3



**Figure 3.7:** Photocatalytic decomposition of microcystin-LR with Photospheres™ 15μm in a stirred system (◆); dark control (▲). Error bars= 1 SD; n=2



Degussa P25 displayed a very high dark adsorption (approximately 54 %). Total decomposition of microcystin is achieved between minutes 8 and 10 after the beginning of radiation. The two controls applied reacted as expected: the dark control, without UV radiation, only displayed dark adsorption, after which toxin concentration remains stable. As there is no input of energy, no other reaction takes place. The other control that excluded the catalyst, also acted as was expected, with no degradation. Having performed this experiment it was deemed that experimental time could be considerably shortened and the time frame for future experiments was set to 10 minutes.

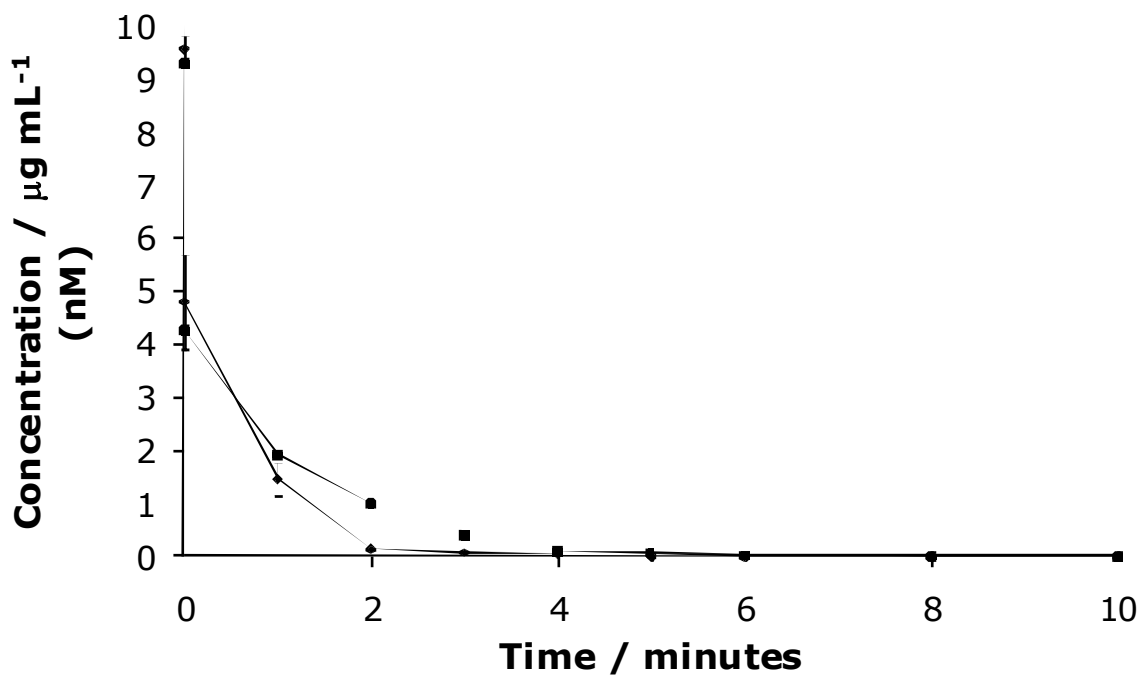
After having established the performance of P25, the experiment was repeated using Photospheres™ 15µm instead of P25. These experiments were performed using the same protocol as for Degussa P25, however, with a shortened experimental time frame (10 min) (figure 3.7).

The Photospheres™ 15µm display a decreased amount of dark adsorption compared to Degussa P25 (approximately 9 %). Total decomposition of microcystin is not achieved within the observed time, however, approximately 97 % of microcystin had been decomposed. Two things were noticed during this investigation, conducting the experiment in a stirred system did not achieve sufficient distribution of the Photospheres™. Due to the inherent buoyancy the Photospheres™ accumulated at the surface, forming a thick layer there, with very few spheres actually dispersed in the solution. When the stirring speed was increased it was noticed that the stirrer ground the Photospheres™, which lead to them breaking and a noticeable layer of debris

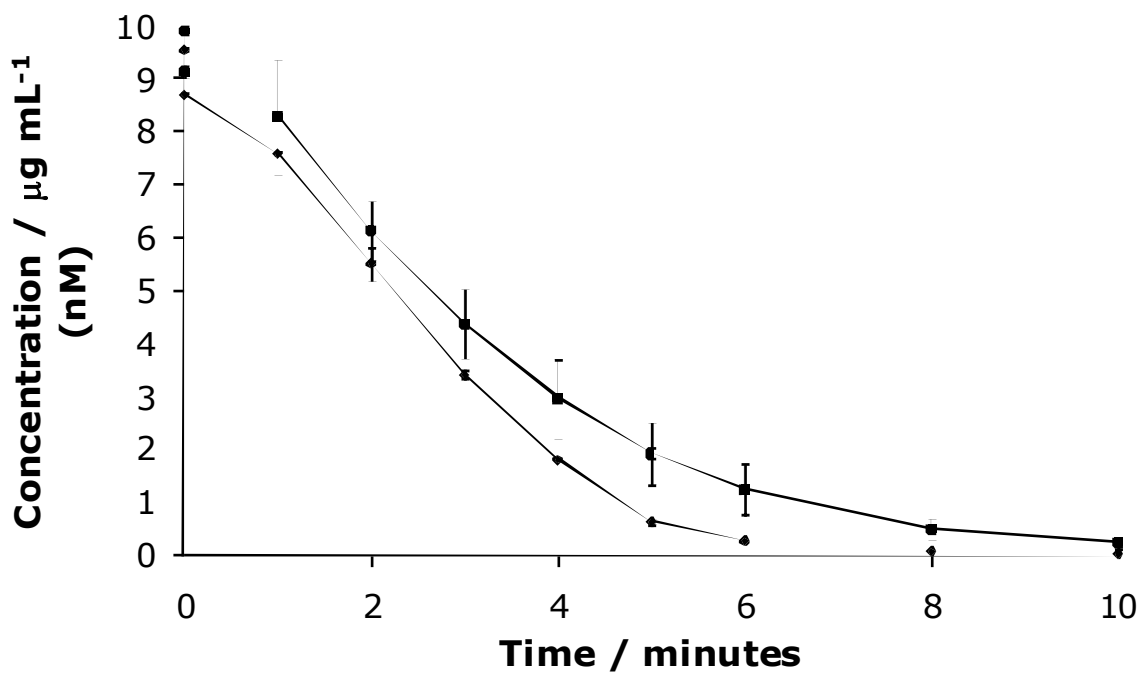
formed at the bottom of the vial. This prompted a modification in the experimental design.

### **3.3.2 Photocatalytic destruction of microcystin-LR with Photospheres™ 15µm, Photospheres™ MTO/0131 and P25**

The first, more fundamental, change made was a newly designed system. The advantages of this new system were two-fold, firstly it allowed for sparging of the test solution rather than stirring and secondly, it allowed the use of less toxin per experiment in order to decrease toxin consumption. The benefits of using a sparged system included an improved mass transport and also ensuring good availability of O<sub>2</sub> as this is essential for degradation. The other parameters remained the same. P25 was tested again in the new system to set a bench mark with which to compare the performance of the Photospheres™. When the degradation of microcystin-LR by P25 was compared in the two systems, it was found that an enhanced rate of degradation occurred in the sparged system (figure 3.8). The same was found to be true for the Photospheres™ 15µm (figure 3.9).



**Figure 3.8:** Performance of P25 in the photocatalysis of microcystin-LR in two different systems: sparged (♦); and stirred (■). Error bars=1SD; n=2

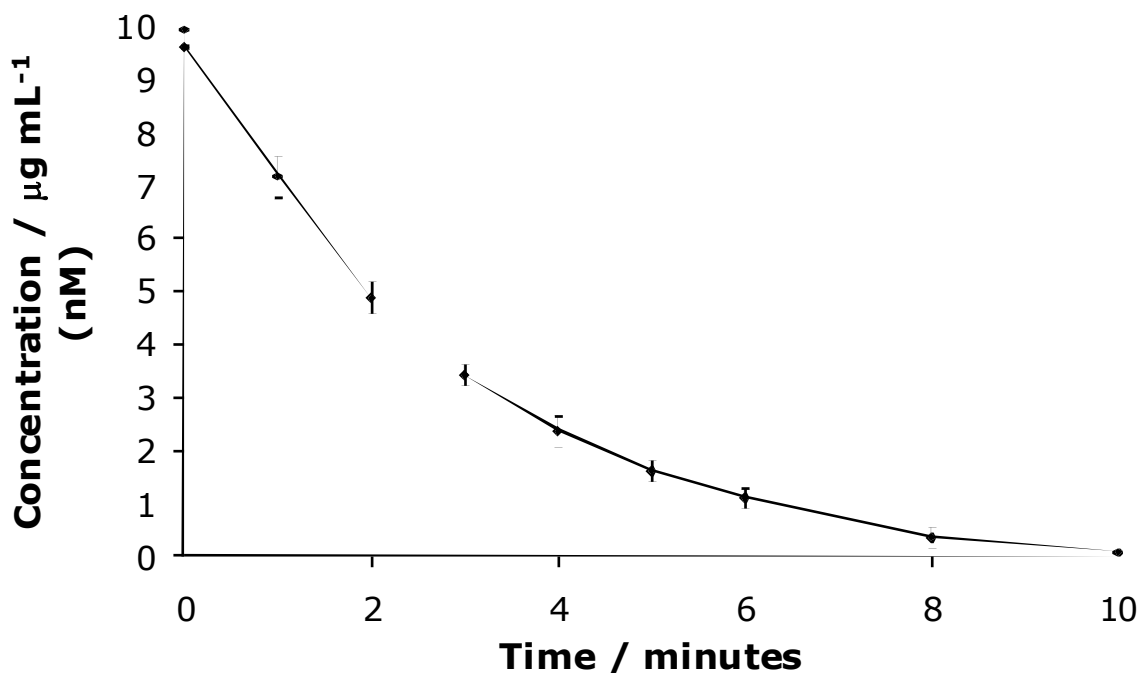


**Figure 3.9:** The performance of Photospheres™15µm in the photocatalysis of microcystin-LR in two different systems: sparged (♦); and stirred (■). Error bars=1SD; n=2

The type of agitation of the system, sparged or stirred does not seem to affect the dark adsorption of microcystin-LR to either catalyst, it is slightly higher in the stirred system (54 %) compared to 50 % in the sparged system for P25. Total decomposition is achieved earlier in the sparged system (6 min), whereas total decomposition in the stirred system occurs between minutes 8 and 10.

For the Photospheres™15µm, neither mode of agitation achieves total decomposition, the catalyst in the sparged system decomposes approximately 98 % of the initial microcystin-LR concentration, whilst the catalyst in the stirred system approximately 97 %. Reproducibility is also greatly enhanced in the sparged system for both catalysts (figure 3.9).

A different version of the Photospheres™, Photospheres™MTO/0131, which was provided by the manufacturer as a higher quality product compared to the Photospheres™15µm, was used in the same sparged system (Figure 3.10).



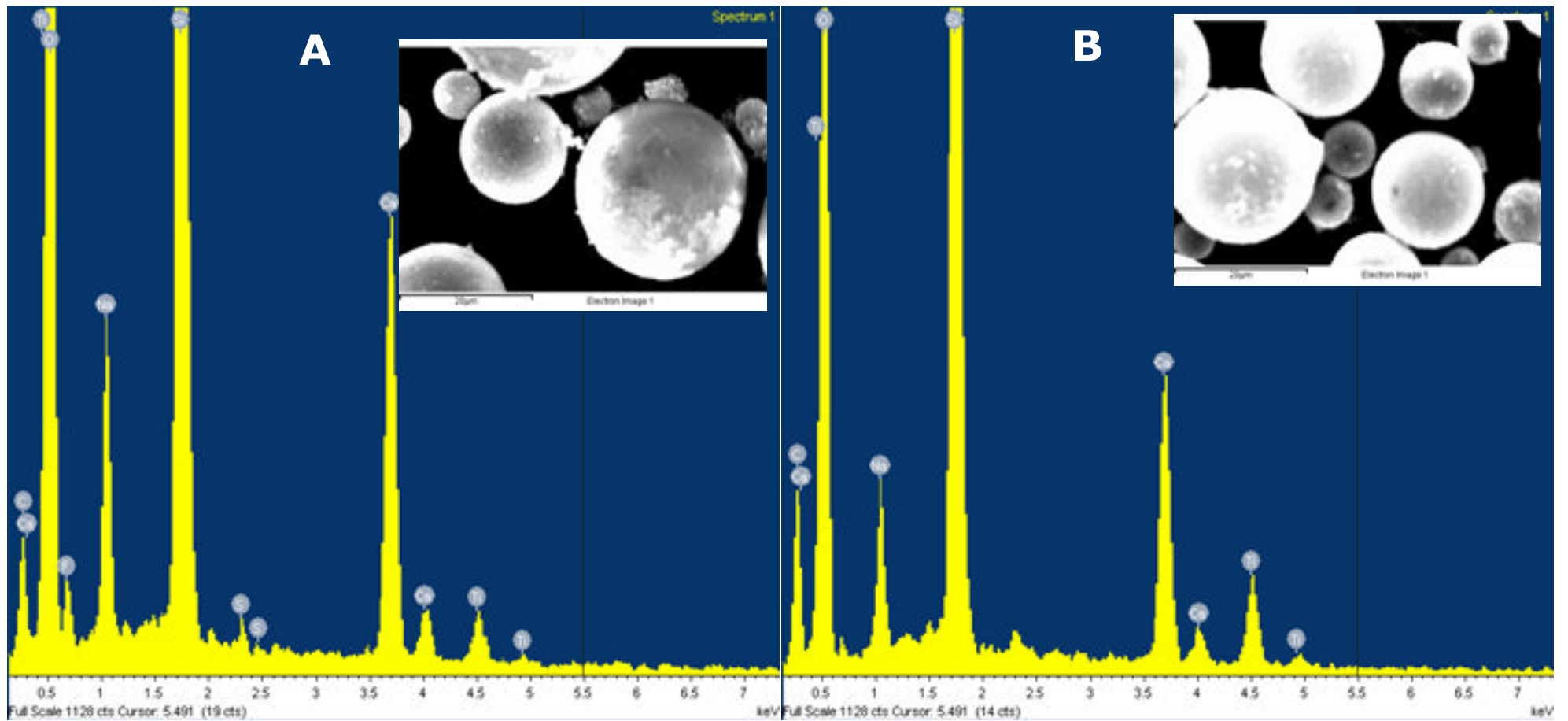
**Figure 3.10:** The performance of Photospheres™ MTO/0131 in the photocatalysis of microcystin-LR in a sparged system. Error bars=1SD; n=2

The Photospheres™ MTO/0131 have a lower dark adsorption with approximately 3 % compared with the Photospheres™ 15 $\mu\text{m}$ . Total decomposition of microcystin-LR is not achieved in the experimental time frame, however, approximately 99 % are decomposed. As was the case for the Photospheres™ 15 $\mu\text{m}$ , the  $\text{TiO}_2$  content only accounts for 17 % of the total weight of the sample, thus the weight needs to be adjusted to allow a direct comparison between the Photospheres™ and P25.

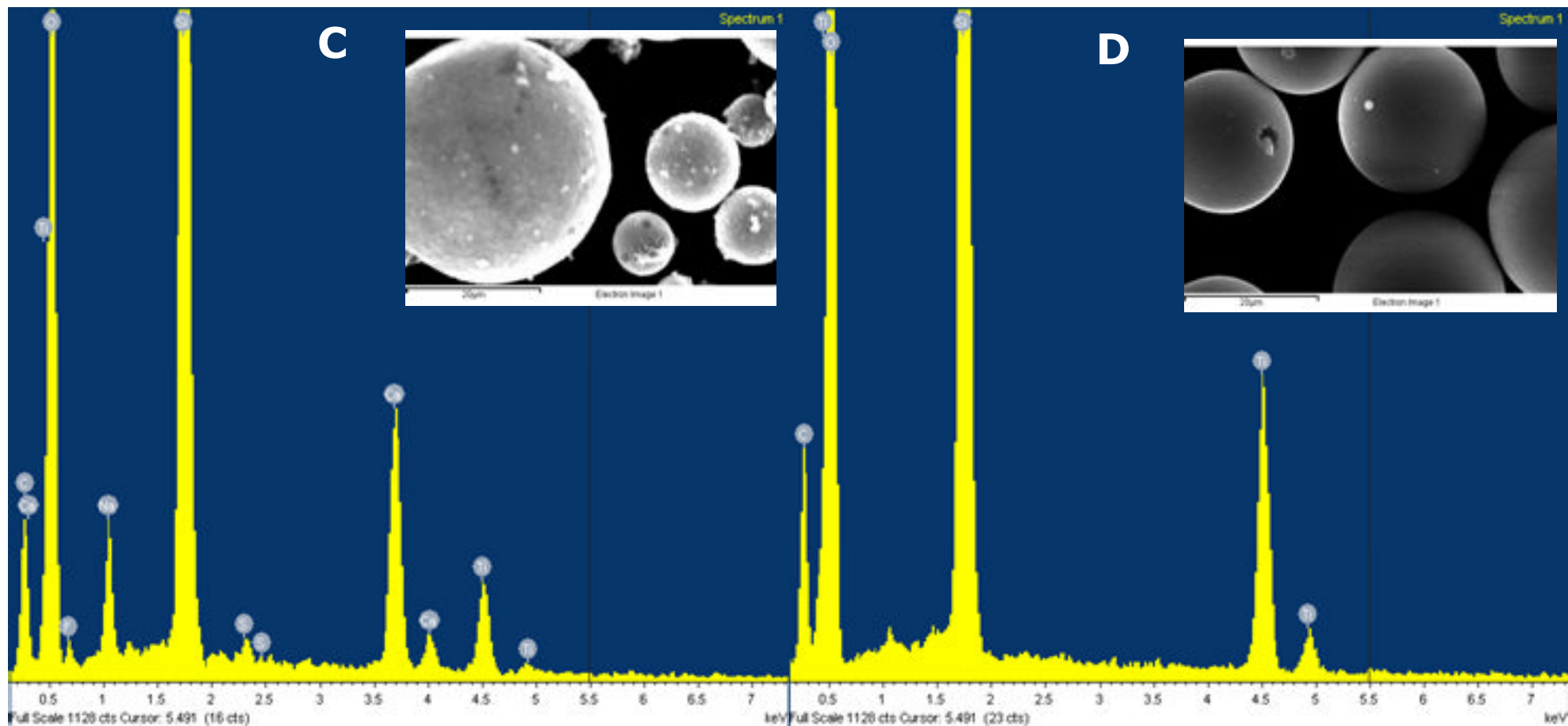
### 3.3.3 Light and scanning electron microscopic investigation of Photosphere™ samples

The microscopic investigation revealed that the Photospheres™ 15 $\mu\text{m}$  sample contained a lot of debris that was broken Photospheres™ and other undefined debris that could be free  $\text{TiO}_2$ . Furthermore a scanning electron microscopic

(SEM) and energy dispersive x-ray spectroscopy (EDX) was carried out (figure 3.11a, b, c). It shows, as would be expected, that the major elements present are silica, titanium, and oxygen. This is true for all the Photosphere™ products. The EDX analysis of the Photosphere™15µm, as received, and the Photospheres™15µm that were washed, shows a higher titanium content. The MTO/0131 Photospheres™, which were reputed to be higher quality products by the manufacturer, did not contain such free TiO<sub>2</sub> and the debris in form of broken Photospheres™ was considerably lower, which was also confirmed by the SEM-EDX analysis. The SEM-EDX analysis also shows what appears to be a smoother coating of the silica beads that the Photosphere™15µm product, furthermore sphere size appears to be more uniform.

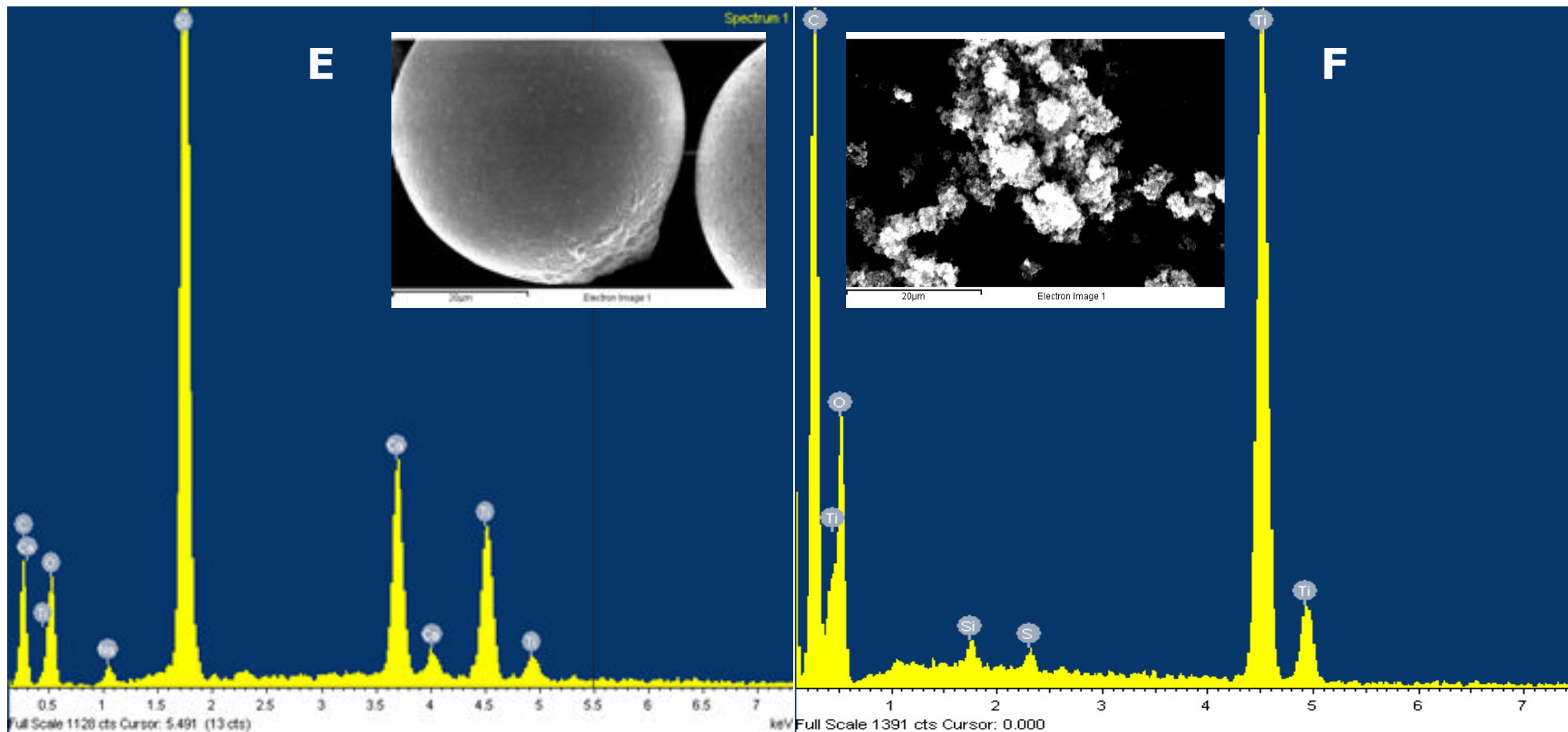


**Figure 3.11a:** SEM-EDX chromatograms of different photocatalytic materials based on titanium dioxide. A) Photospheres™ 15µm, as received; B) Photosphere™ 15µm fines-free



**Figure 3.11b:** SEM-EDX chromatograms of different photocatalytic materials based on titanium dioxide. C) Photospheres™ 15µm after one photocatalytic cycle; D) MTO/0131 Photospheres™, as received;





**Figure 3.11c:** SEM-EDX chromatograms of different photocatalytic materials based on titanium dioxide. E) Photospheres™40µm, as received; F) Degussa P25, as received

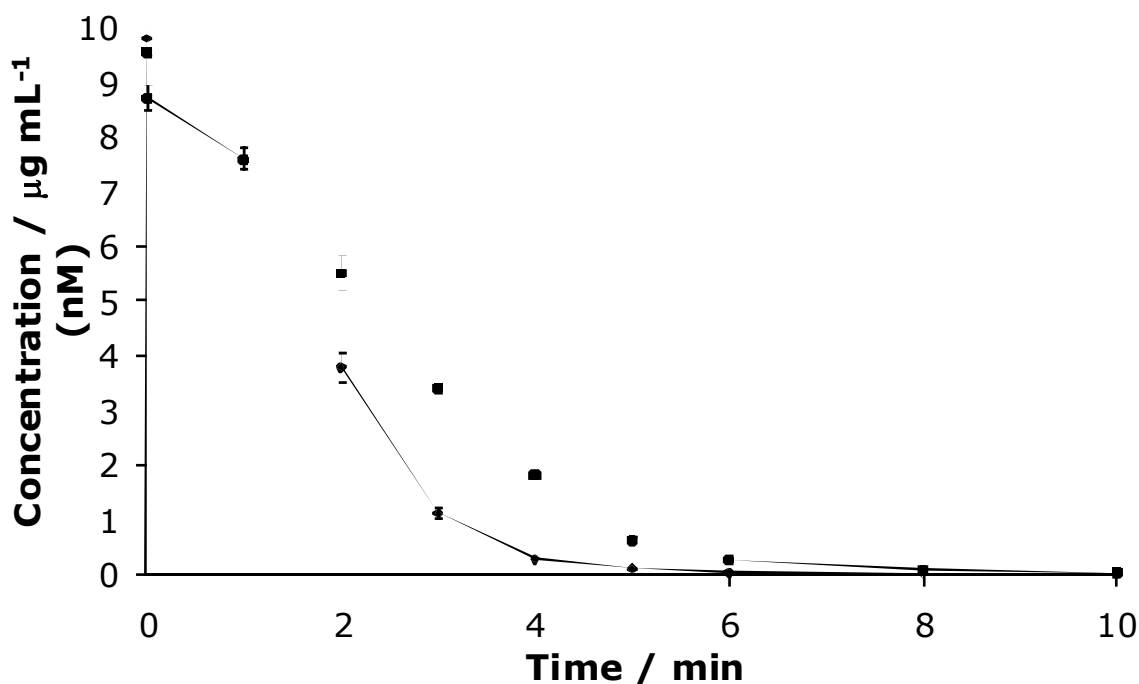
The Photospheres™40µm were provided as another higher grade product with a sphere size of 40 µm on average but a range of 10 µm to 60 µm (personal correspondence, NSA Ltd.).

It was decided to include a washing step with Milli-Q water with the Photospheres™15µm and compare their performance with an unwashed sample of Photospheres™15µm. The higher titanium content observed in the washed sample of Photospheres™15µm by SEM-EDX supports the results, showing a more effective decomposition of microcystin-LR in the washed sample, suggesting that some inert material from the manufacturing process was packaged with the spheres.

#### **3.3.4 Effects of a fines-removal step and weight adjustment of different types of Photospheres™ and the effect of catalyst load**

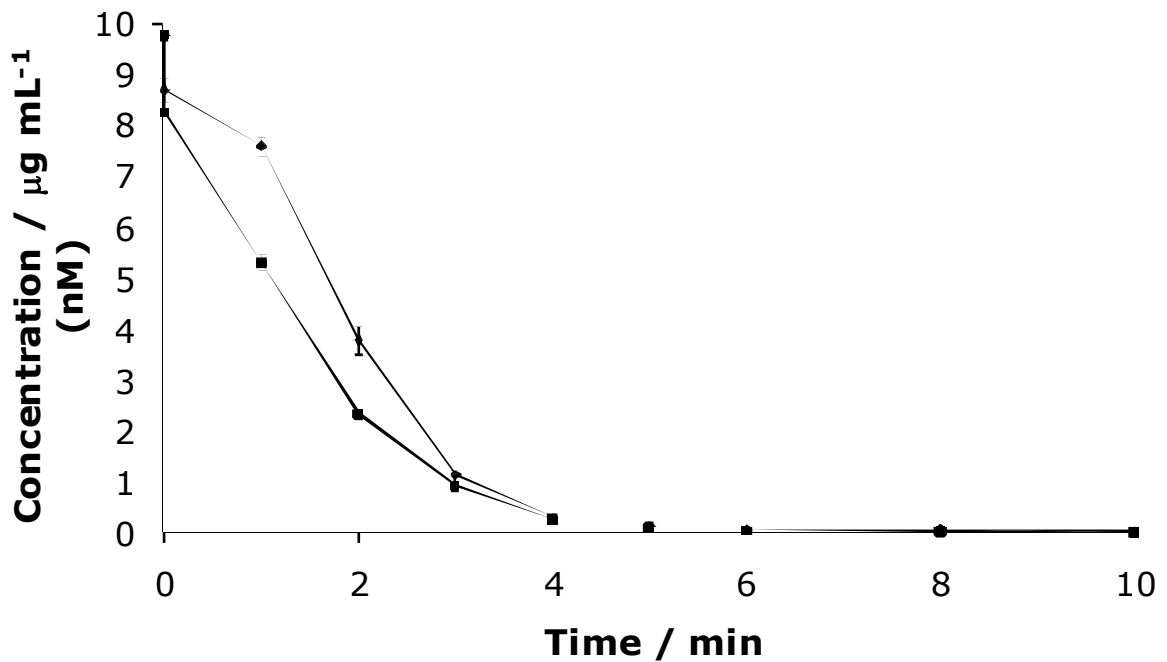
The results from the test that investigated the effect of fines removal clearly show that the Photospheres™15µm degrade microcystin-LR more rapidly after the fines removal (figure 3.12). The dark adsorption is similar in both treatments (6 % compared to 9 %), although slightly higher in the washed sample, which was to be expected since more active Photospheres™ are present than in the unwashed sample, since its weight is partially made up of inactive debris. Decomposition is more rapid with the washed sample, although neither sample achieves total decomposition within the time frame of the experiment (washed approximately 98 % decomposition of microcystin-LR, unwashed approximately 95 % decomposition of microcystin-LR). This proves that the debris is effectively “dead weight” as it is inactive. It was not, as

previously suspected, free  $\text{TiO}_2$  that contributes to the photocatalytic reaction and biases the results.



**Figure 3.12:** The performance of fines-free (♦) and non fines-free (▪) Photospheres™ 15 $\mu\text{m}$ . Error bars=1 SD; n=2

Having tested the fines-free Photospheres™ 15 $\mu\text{m}$ , the weight was now adjusted to ensure that actually 1 % (w/v)  $\text{TiO}_2$  was applied to the test solution. Of the Photospheres™ total mass, just 17 % consisted of  $\text{TiO}_2$ ; the remainder was accounted for by the mass of the silica beads (personal correspondence with NSA Ltd.). To achieve 1 % (w/v)  $\text{TiO}_2$  in the test amount of Photospheres™ added to the test solution was 5.88 % (w/v). The performance of the fines-free and weight adjusted Photospheres™ 15 $\mu\text{m}$  was compared to the untreated version (figure 3.13), as might be expected the increased mass of Photospheres™ resulted in a more rapid decomposition rate.

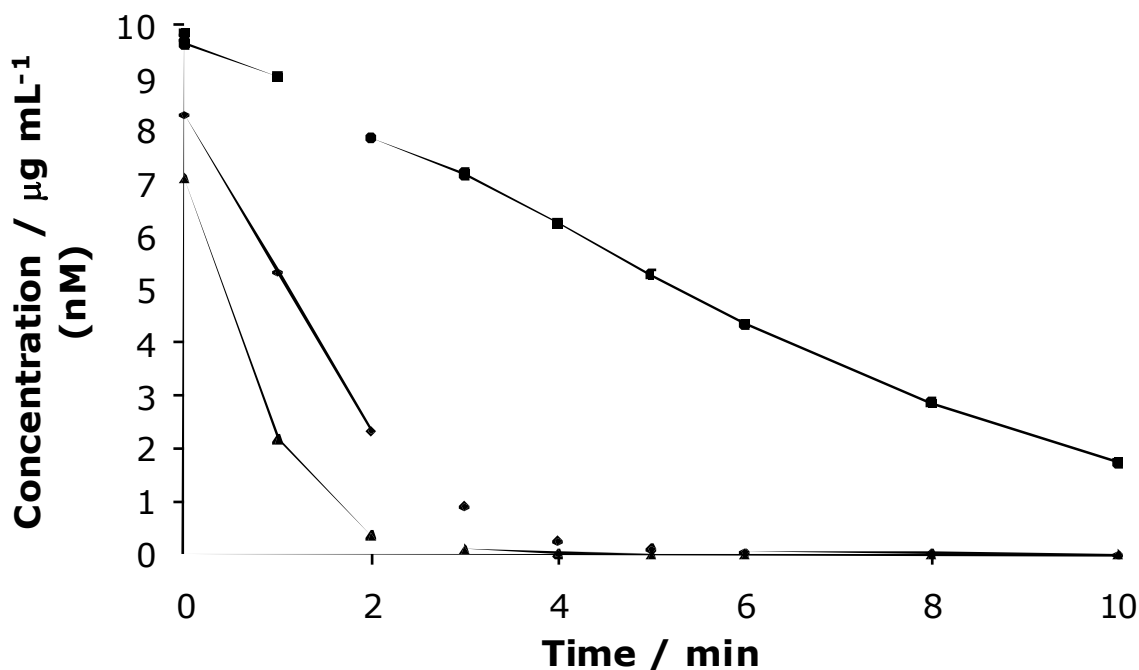


**Figure 3.13:** The performance of fines-free and weight adjusted Photospheres™15µm (■) compared to non weight adjusted, non fines-free Photospheres™15µm (◆) in the photocatalytic decomposition of microcystin-LR in a sparged system. Error bars=1 SD; n=2

For the fines-free and weight adjusted Photospheres™15µm the dark adsorption is higher (15 %), than it is for the untreated spheres (8 %), which was to be expected because of more available sites for microcystin to bind to in the washed and weight adjusted sample compared to the untreated Photospheres™15µm. The fines-free and weight adjusted Photospheres™ achieve total decomposition between minutes 8 and 10, whereas the untreated Photospheres™ do not achieve total decomposition within the experimental time (approximately 98 % decomposition).

After having removed the fines and adjusted the weight of the Photospheres™15µm, the other two photosphere™ samples were investigated with their weight adjusted and compared to the Photospheres™15µm with

adjusted weight (figure 3.14). A fines removal step for the MTO/0131 sample and the Photospheres™40µm was not deemed necessary after microscopic investigation.

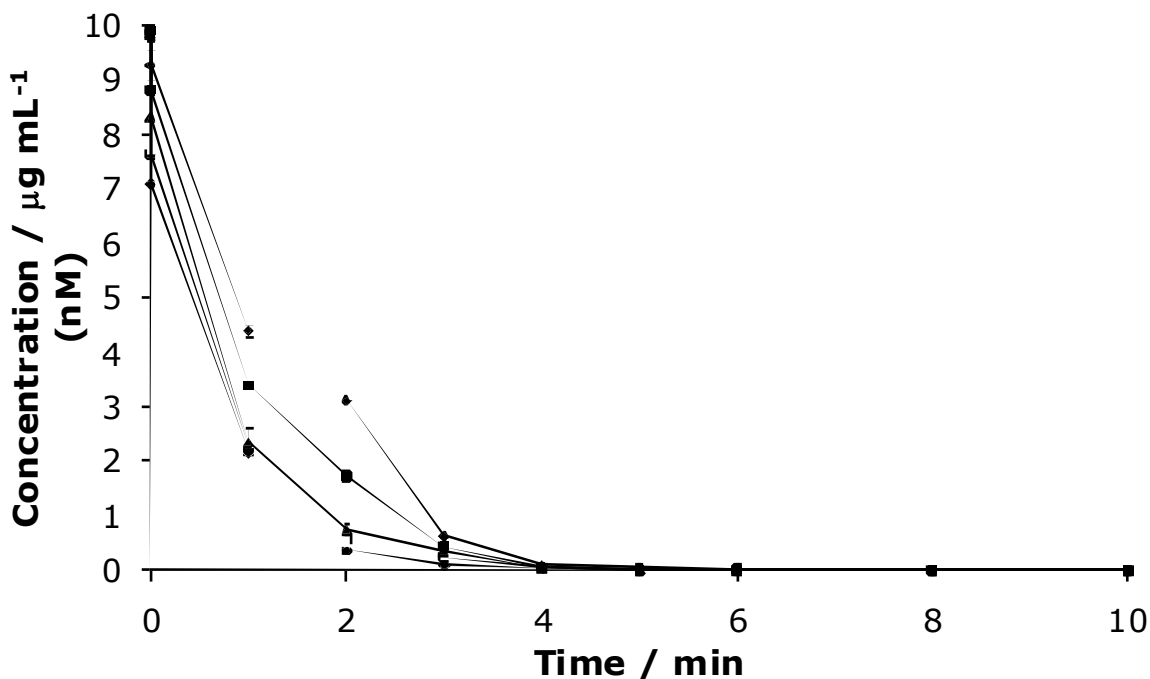


**Figure 3.14:** The performance of fines-free and weight adjusted Photospheres™15µm (♦) compared to weight adjusted Photospheres™MTO/0131 (▪) and weight adjusted Photospheres™40µm (▲) in the photocatalytic decomposition of microcystin-LR in a sparged system. Error bars=1 SD; n=2

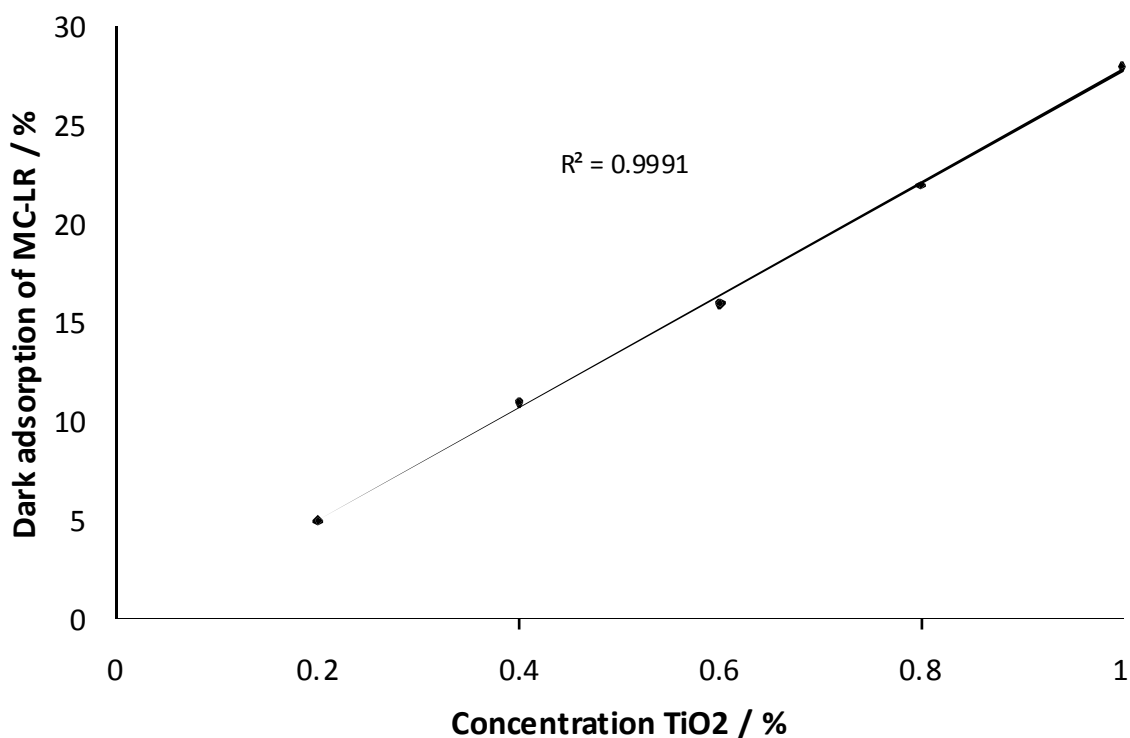
Out of the three samples of Photospheres™ tested, the Photospheres™40µm performed best with total degradation achieved after 5 minutes. Dark adsorption is approximately 27 %, which is higher than the dark adsorption values of Photospheres™MTO/0131 (2 %) and the Photospheres™15µm (15 %). Photospheres™15µm achieved total degradation between minutes 8 and 10, while Photospheres™MTO/0131 did not perform as well with total degradation not achieved within the experimental time frame (82 % decomposition). The dark adsorption of the Photospheres™MTO/0131 sample

is comparable to the previous experiment with 3 %, a higher dark adsorption was expected as, physically, more Photospheres™ are available to have toxin bound to them.

After having established that the weight adjusted concentration of the Photospheres™MTO/0131 seems to inhibit photocatalysis, it was decided to perform a study of different catalyst loads of the 40 micron Photospheres™ to determine whether lower concentrations would perform better, i.e. improved mixing and improved light infiltration due to a reduced catalyst load. A number of concentrations (0.2, 0.4, 0.6, 0.8, and 1.0 % TiO<sub>2</sub>) were tested (figure 3.15). It was found that while photocatalytic decomposition greatly improved from the 0.2 to 0.4, and 0.4 to 0.6 % (w/v) TiO<sub>2</sub>, a marked increase in the concentrations from 0.6 % (w/v) TiO<sub>2</sub> was not observed. The dark adsorption increases linearly with the TiO<sub>2</sub> concentration (figure. 3.16). Adjusting the weight to 1 % TiO<sub>2</sub> did not have the same inhibiting reaction as it had for the Photospheres™MTO/0131 sample. This could be due to the size of the Photospheres™40µm compared to the sphere size of the Photospheres™MTO/0131 sample (approximately 15 micron diameter on average). At the same concentration of TiO<sub>2</sub> there are physically fewer Photospheres™ present in the test solution allowing for sufficient mixing with sparging.



**Figure 3.15:** The effect of different catalyst load of Photospheres™40µm in the photocatalytic decomposition of microcystin-LR in a sparged system. (♦) 0.2 % TiO<sub>2</sub>; (▪) 0.4 % TiO<sub>2</sub>; (▲) 0.6 % TiO<sub>2</sub>; (□) 0.8 % TiO<sub>2</sub>; (•) 1.0 % TiO<sub>2</sub>. Error bars=1 SD; n=2



**Figure 3.16:** Dark adsorption of microcystin-LR to Photospheres™40µm in a sparged system under UV radiation at different catalyst loads.

### 3.3.5 Photocatalytic destruction of 11 different microcystin variants with Photospheres™40µm

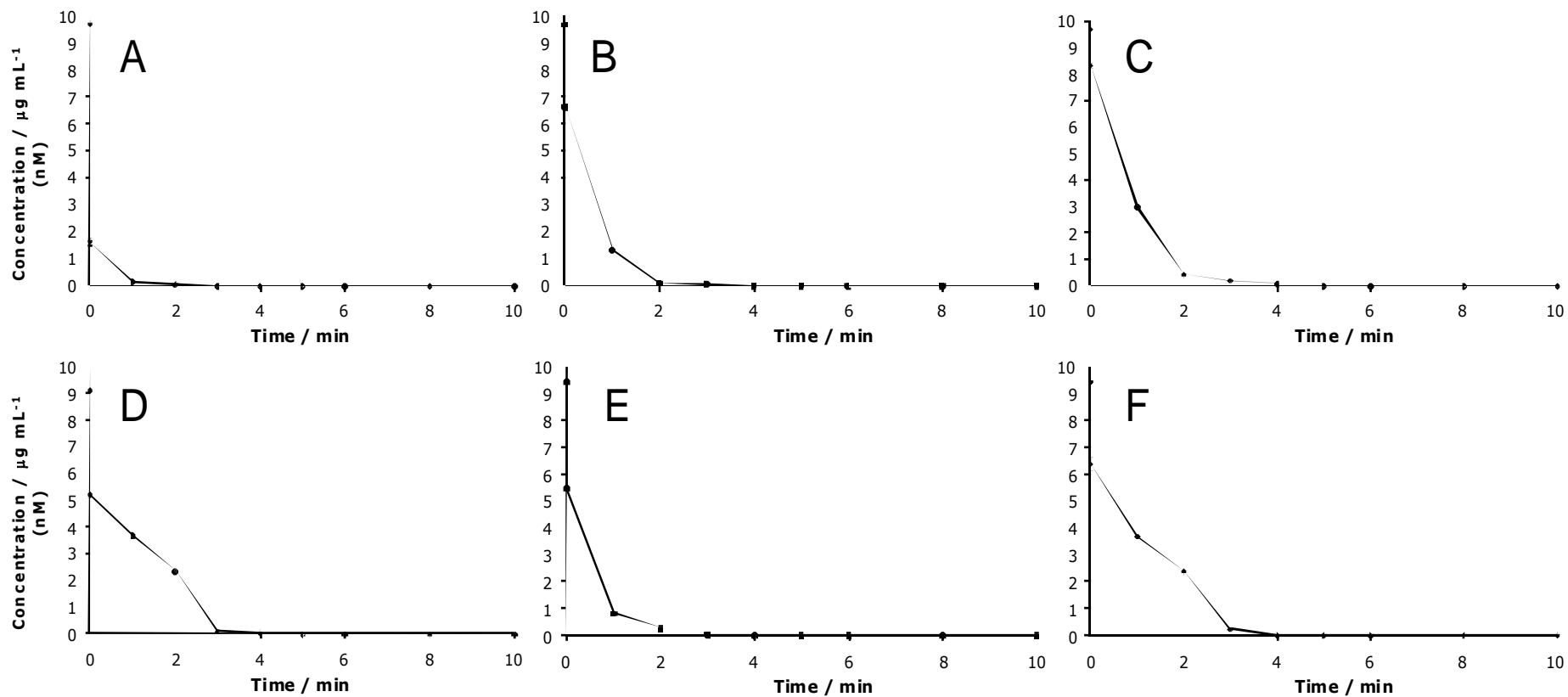
The photocatalytic effect of Photospheres™40µm on 10 different microcystin variants and nodularin was investigated in a sparged system. The results of the investigation revealed that the Photospheres™40µm were capable of degrading all tested variants in 5 minutes or less (table 3.7).

**Table 3.7:** Summary of the degradation and dark adsorption of 11 different microcystin variants with 40 micron Photospheres™ in a sparged system.

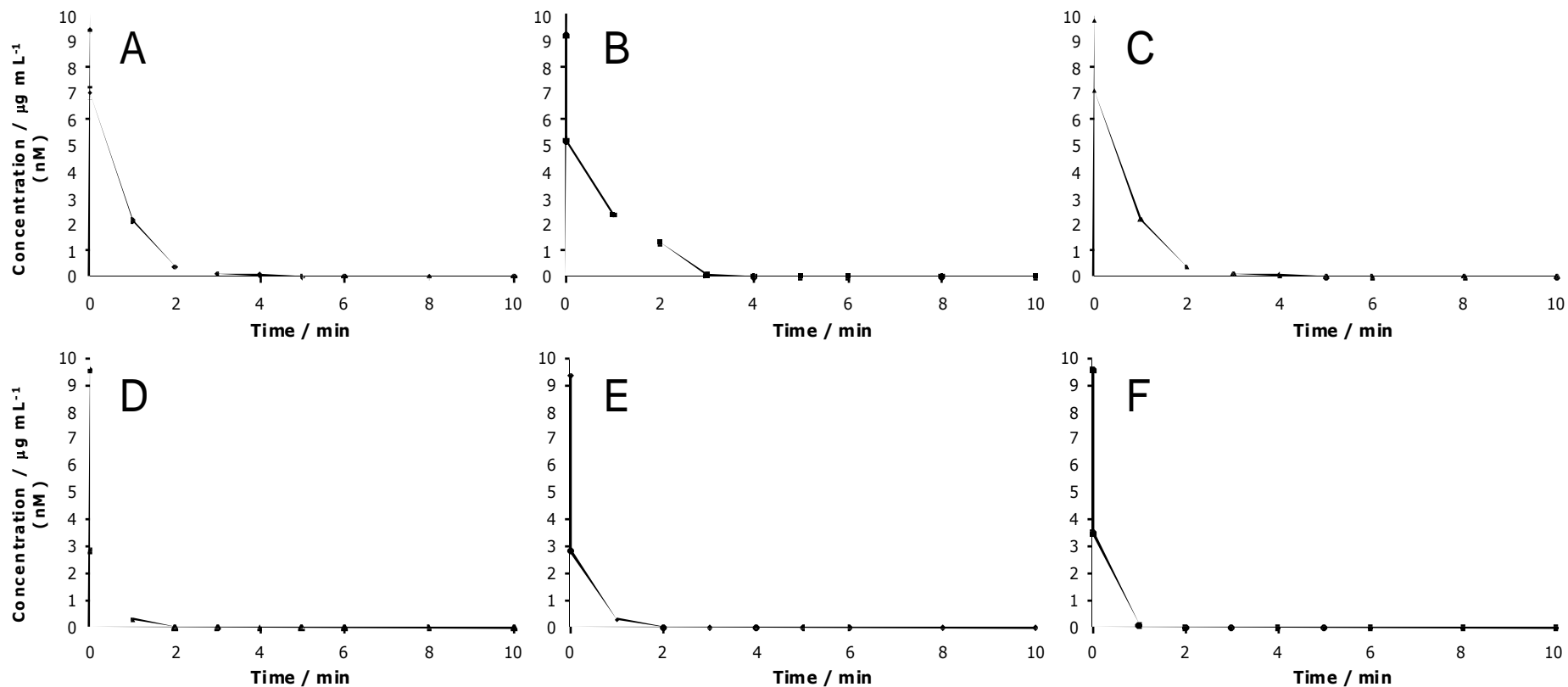
<i>Microcystin Variant</i>	<i>Dark adsorption (%)</i>	<i>Complete degradation (min)</i>
Nodularin	14	4
Microcystin-RR	21	3
Microcystin-LR	27	5
Demethylated Microcystin-RR	32	4
Microcystin-LA	34	4
Homotyrosine	43	5
Demethylated Microcystin-LR	44	5
Methylated Microcystin-LR	45	4
Microcystin-YR	46	4
Microcystin-LY	48	2
Microcystin-LW	64	2
Microcystin-LF	70	2

Microcystin-LW, -LF, and -LY were degraded the fastest, with no detectable amounts remaining after two minutes (figure 3.17, 3.18).





**Figure 3.17:** Decay curves of the photocatalytic destruction of different microcystin analogues over photosphere™40 $\mu\text{m}$ . A) microcystin-RR; B) demethylated microcystin-RR; C) nodularin; D) homotyrosine (methylated microcystin-YR); E) microcystin-YR; F) microcystin-LA



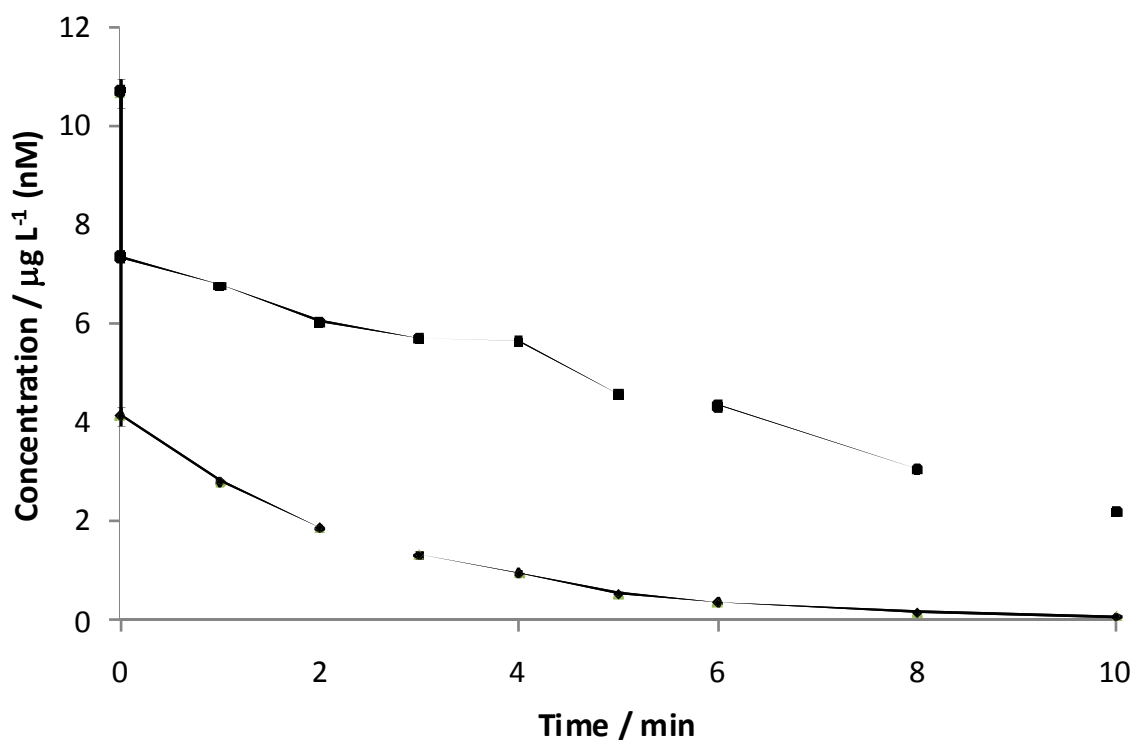
**Figure 3.18:** Decay curves of the photocatalytic destruction of different microcystin analogues over photosphere™40 $\mu\text{m}$ . A) demethylated microcystin-LR; B) methylated microcystin-LR; C) microcystin-LR; D) microcystin-LF); E) microcystin-LY; F) microcystin-LW

Nodularin and Homotyrosine (methylated microcystin-YR) were more slowly degraded with no detectable amounts remaining after 4 and 5 minutes respectively. This is a similar speed to the decomposition of microcystin-LR, which was used in previous investigations.

### **3.3.6 Evaluation of the use of light emitting diodes (LEDs) in the photocatalytic destruction of microcystin-LR**

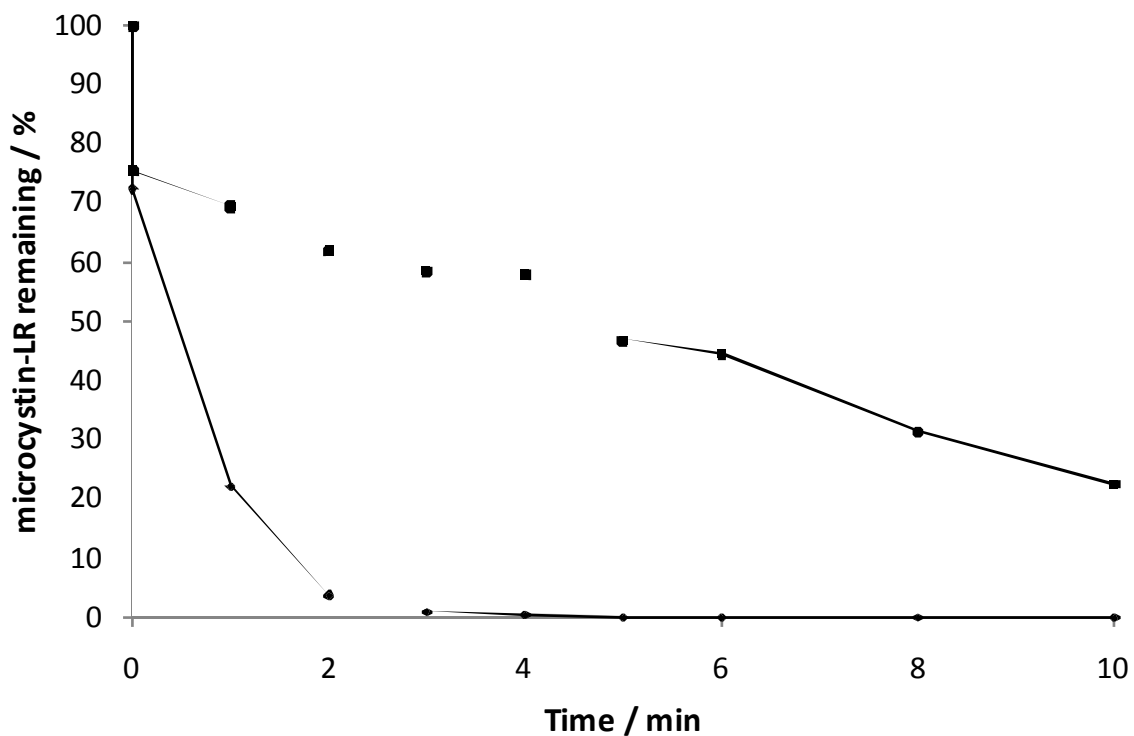
The aim of this investigation was to assess the efficacy of UV light emitting diodes (LED) in the photocatalytic decomposition of microcystin-LR. LEDs offer a number of advantages over other sources of UV radiation, the most pertinent being cost- and energy efficiency.

A purpose built reactor was used in this series of investigations. The initial experiment which was set out as the previous degradation studies of microcystin-LR with the exception of the different light source yielded no complete degradation of the cyanobacterial toxin for either catalyst used in the experiment (figure 3.19).

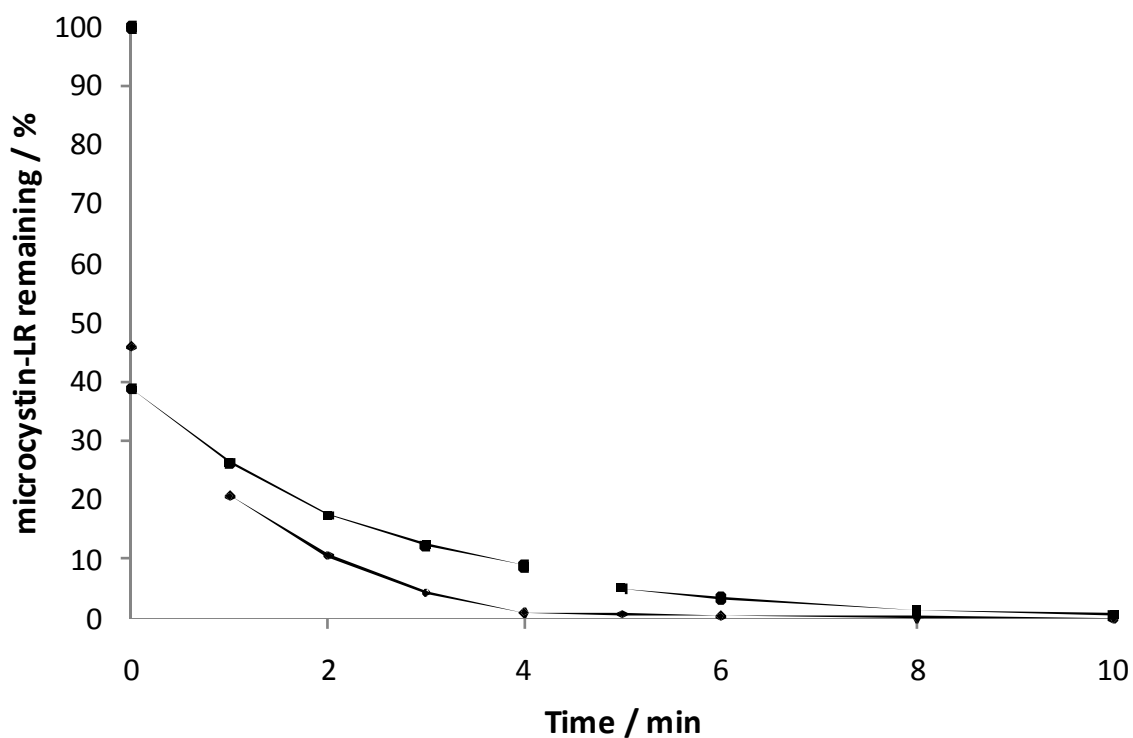


**Figure 3.19:** Degradation study of microcystin-LR using UV LEDs as source of radiation. (▪) Photospheres™40 $\mu\text{m}$ ; (♦) Degussa P25. Error bars=1 SD; n=2

When comparing the performance of P25 regarding the photocatalytic decomposition of microcystin-LR in the two different reactor types, it is apparent that it performs slightly better in the reactor that utilises the Xenon lamp (figure 3.21). This is easily explained by the immense energetic output of that type of lamp compared to the LEDs. The Photospheres™40 $\mu\text{m}$  performed less efficiently in the LED reactor (figure 3.20).



**Figure 3.20:** A comparison of the efficiency of Photospheres™40µm in the photocatalytic decomposition of microcystin-LR with different sources of radiation. (♦) 450 W Xenon lamp; (■) 22.5 x 10<sup>-3</sup> W LEDs (30 LEDs). Error bars=1 SD; n=2



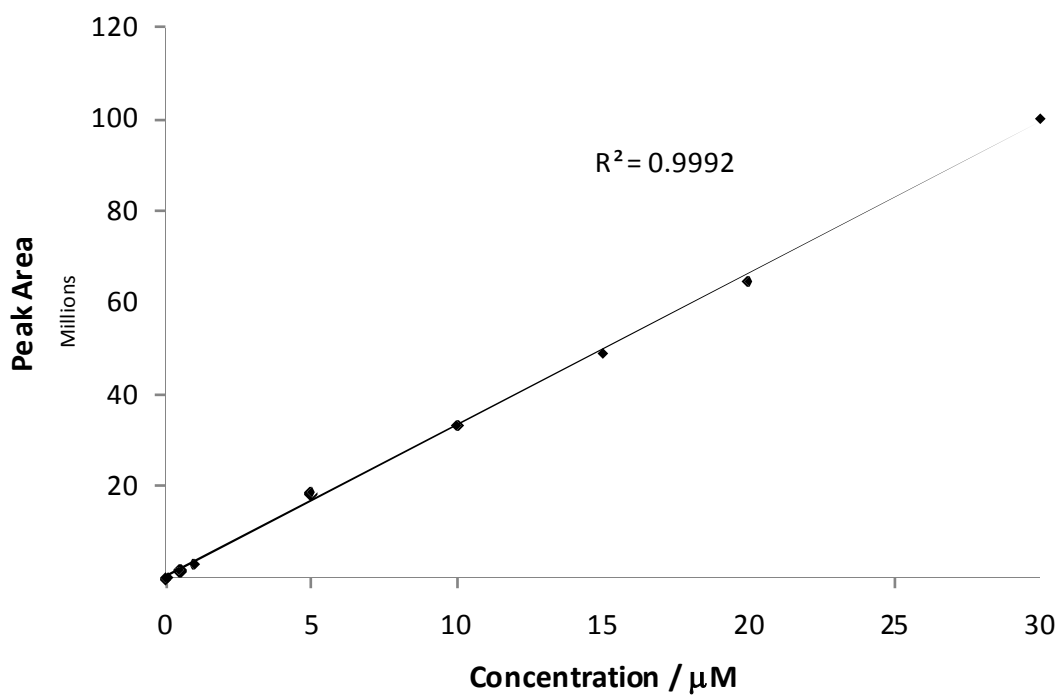
**Figure 3.21:** A comparison of the efficiency of Degussa P25 in the photocatalytic decomposition of microcystin-LR with different sources of radiation. (♦) 450 W Xenon lamp; (■) 22.5 x 10<sup>-3</sup> W LEDs (30 LEDs). Error bars=1 SD; n=2

### **3.3.7 Photocatalysis of waste water pollutants**

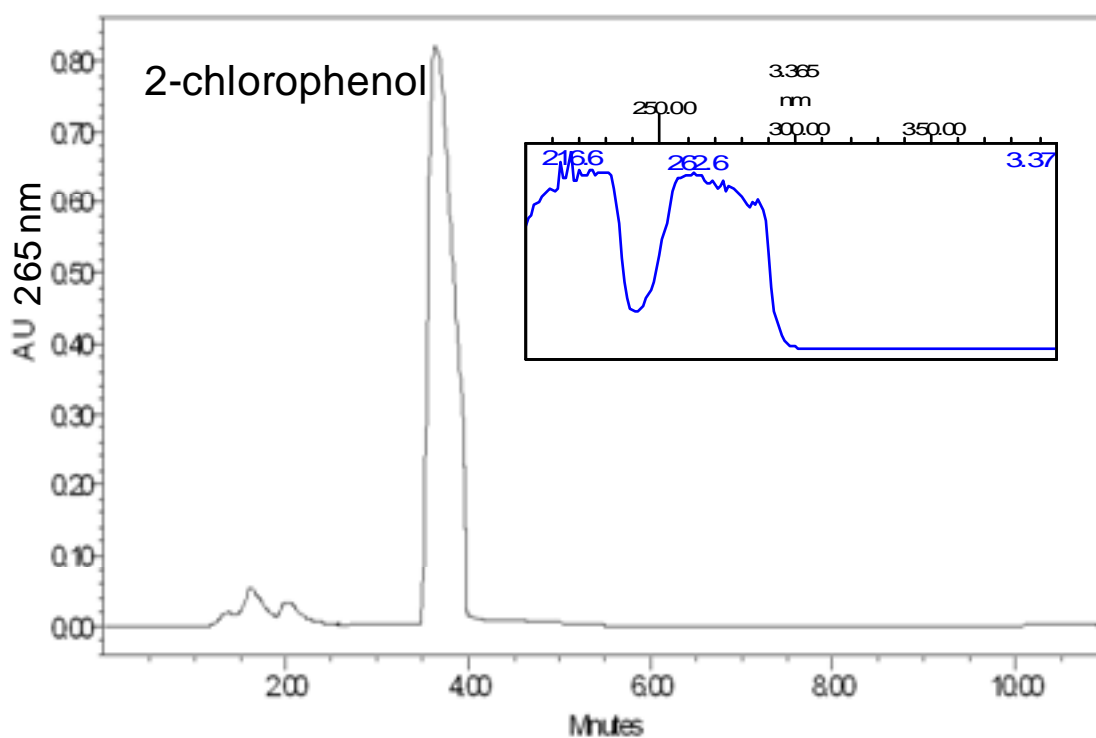
This investigation was carried out to assess the photocatalytic efficiency of Photospheres™40µm compared to the widely used P25, using four common waste water pollutants, 2-chlorophenol, *p*-cresol, Acid Orange 74, and trichloroethylene.

The hydrocarbon 2-chlorophenol (CP) was investigated first. The starting concentration for all CP solutions was 10 µM, this concentration is about fifty times higher than the normal occurrence levels according to the World Health Organisation's Drinking Water Guidelines (WHO, 2008) and it is five times the level at which action should be taken in recreational waters, as stipulated in the WHO's Recreational Water Guidelines (WHO, 2003). All of the pollutants were tested at the same molar concentration (10 µM) to ensure that the photocatalytic efficiency was evaluated using the same number of molecules of the target compound.

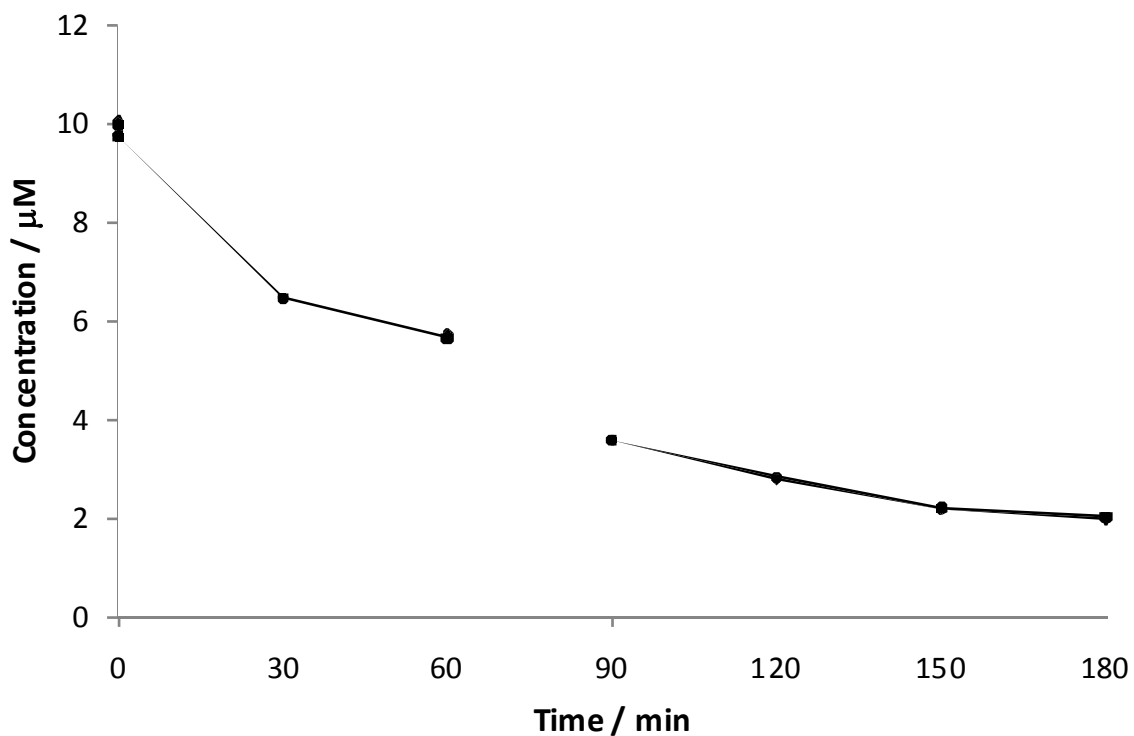
To facilitate the monitoring of the depletion a series of standards was produced. The concentration of 2-chlorophenol was found to be linear in the range from 0 to 30 µM (figure 3.22), samples were analysed at 265 nm (figure 3.23).



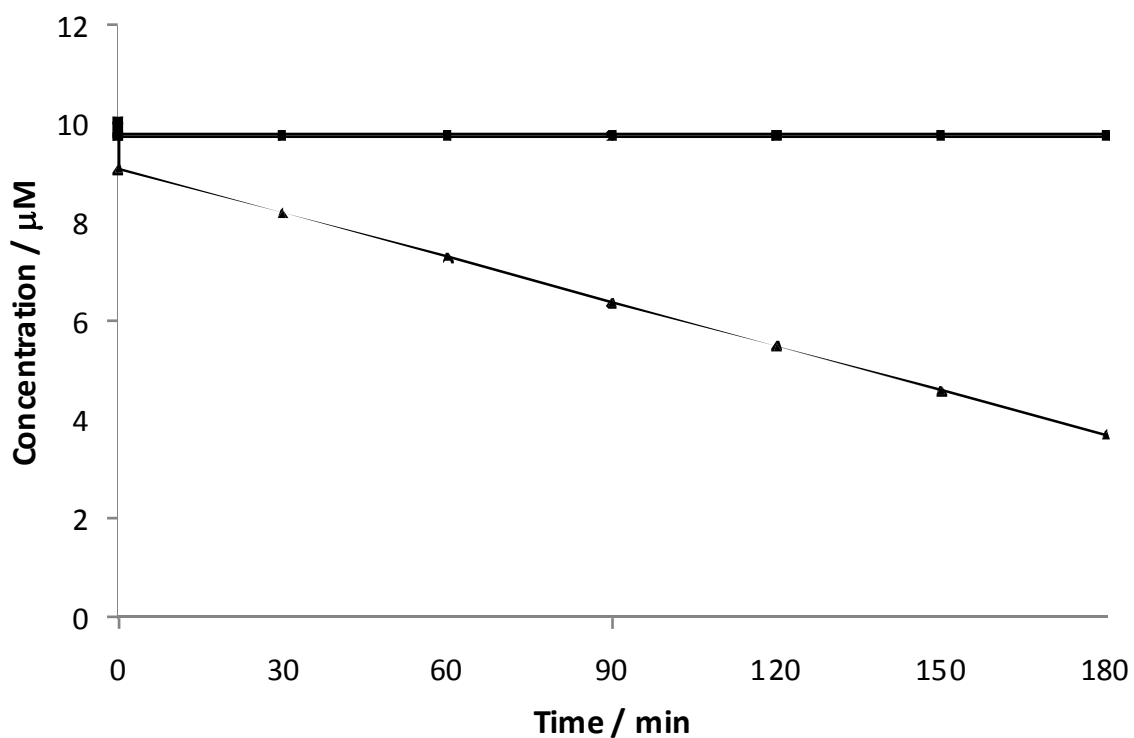
**Figure 3.22:** HPLC-PDA calibration for 2-chlorophenol in the range from 0 to 30  $\mu\text{M}$ . Error bars=1 SD; n=3



**Figure 3.23:** HPLC chromatogram and UV spectrogram of 2-chlorophenol. The photocatalytic decomposition of 2-chlorophenol was successful by both Photospheres™ and P25 (figure 3.24).



**Figure 3.24:** The photocatalytic decomposition of 2-chlorophenol by P25 ( $\blacksquare$ ) and Photospheres™40 $\mu\text{m}$  ( $\blacklozenge$ ). Error bars=1 SD; n=2



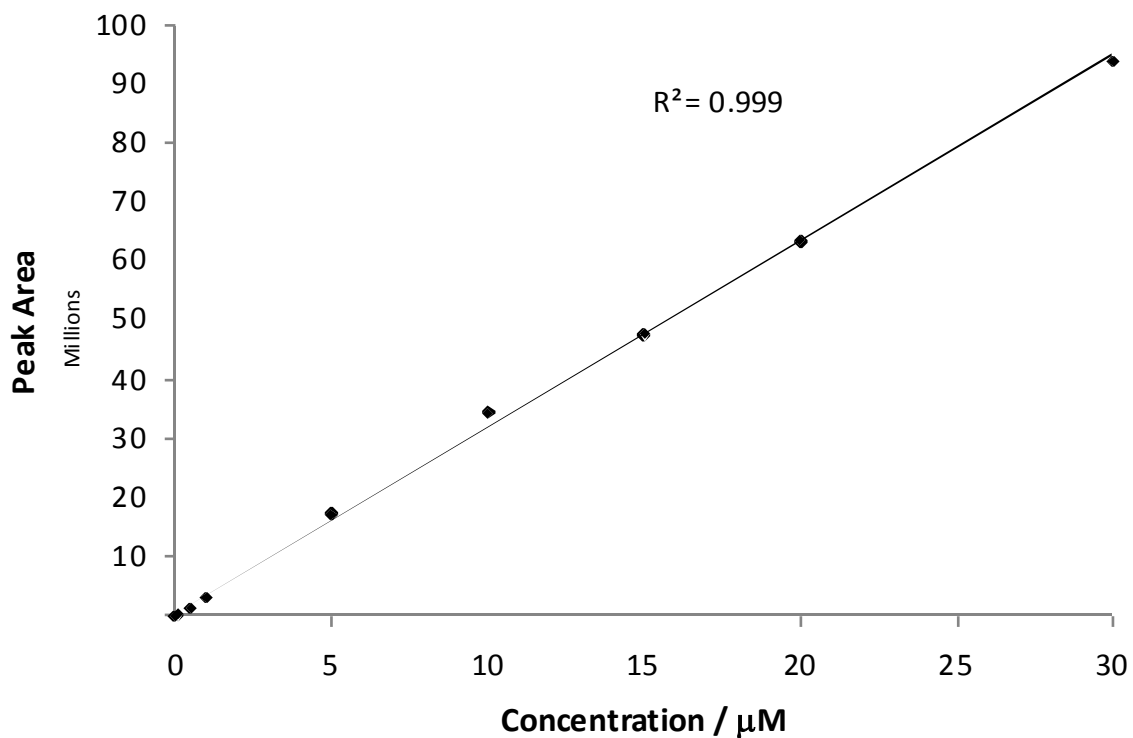
**Figure 3.25:** UV control ( $\blacktriangle$ ), dark control for Photospheres™40 $\mu\text{m}$  ( $\blacksquare$ ), dark control for P25 ( $\blacklozenge$ ) for the photocatalytic decomposition of 2-chlorophenol over Photospheres™40 $\mu\text{m}$  and P25. Error bars=1 SD; n=2



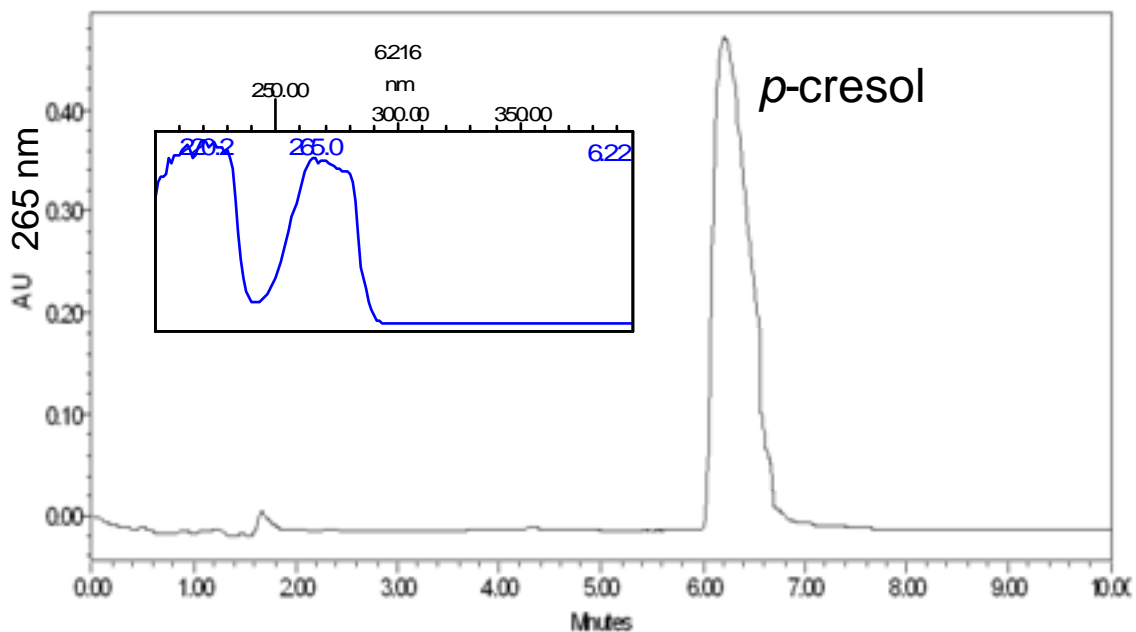
Low dark adsorption for both Photospheres™ 40µm and P25 was observed. The amount of dark adsorption for both catalysts is almost identical. The negative control experiments show that UV light alone also shows a high amount of degradation (figure 3.25).

The next waste water pollutant investigated was the aromatic methylphenol *p*-cresol which was used in this series of investigations to compare the photocatalytic efficiency of Photospheres™ and P25.

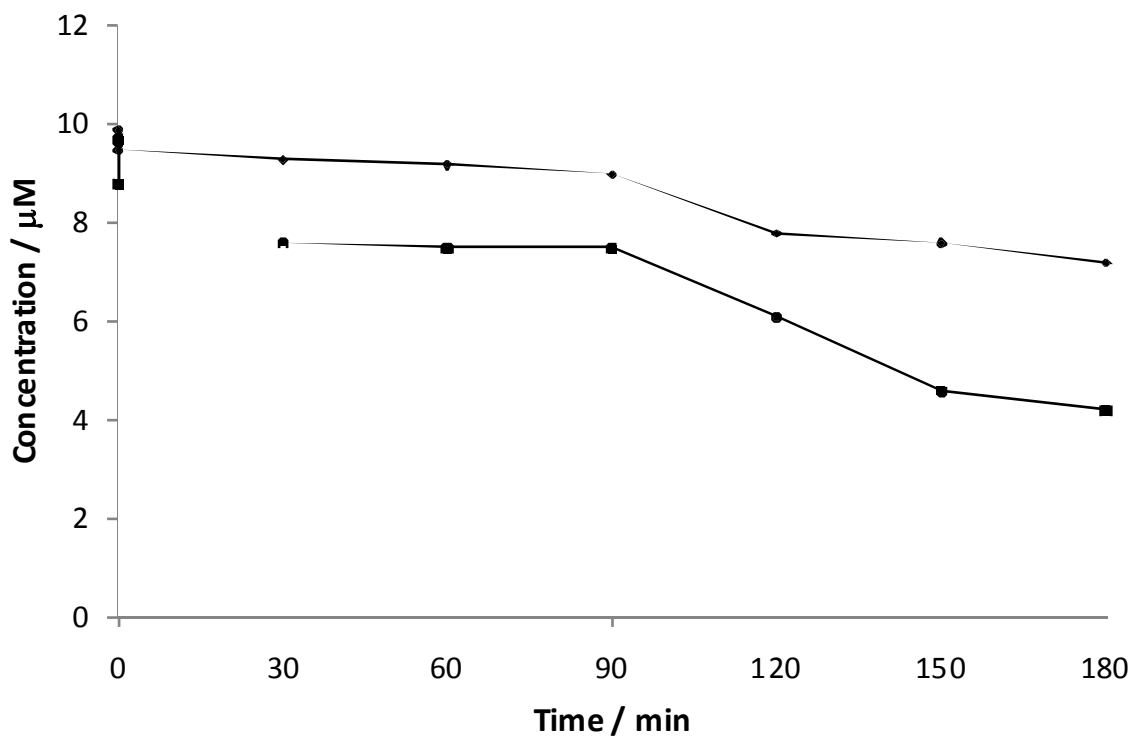
The concentration for all solutions in this experiment was 10 µM. It was determined by HPLC that the concentration of *p*-cresol is linear over a range from 0 to 30 µM (figure 3.26). All samples of *p*-cresol were analysed at 265 nm (figure 3.27). Both Photospheres™ and P25 have displayed degradation of *p*-cresol over the experimental time frame of 3 h (figure 3.28).



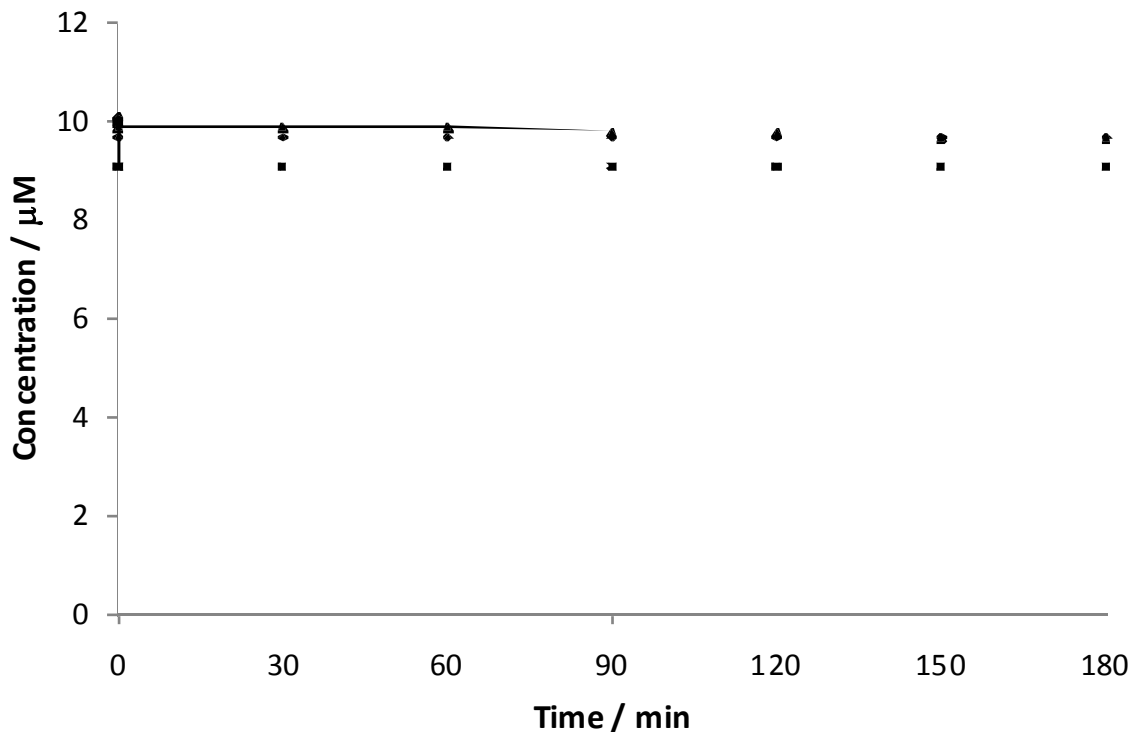
**Figure 3.26:** HPLC-PDA calibration for *p*-cresol in the range from 0 to 30  $\mu\text{M}$ . Error bars=1 SD; n=3



**Figure 3.27:** HPLC chromatogram and UV spectrogram of *p*-cresol.



**Figure 3.28:** The photocatalytic decomposition of *p*-cresol by Photospheres™40µm (♦) and P25 (■). Error bars=1 SD; n=2

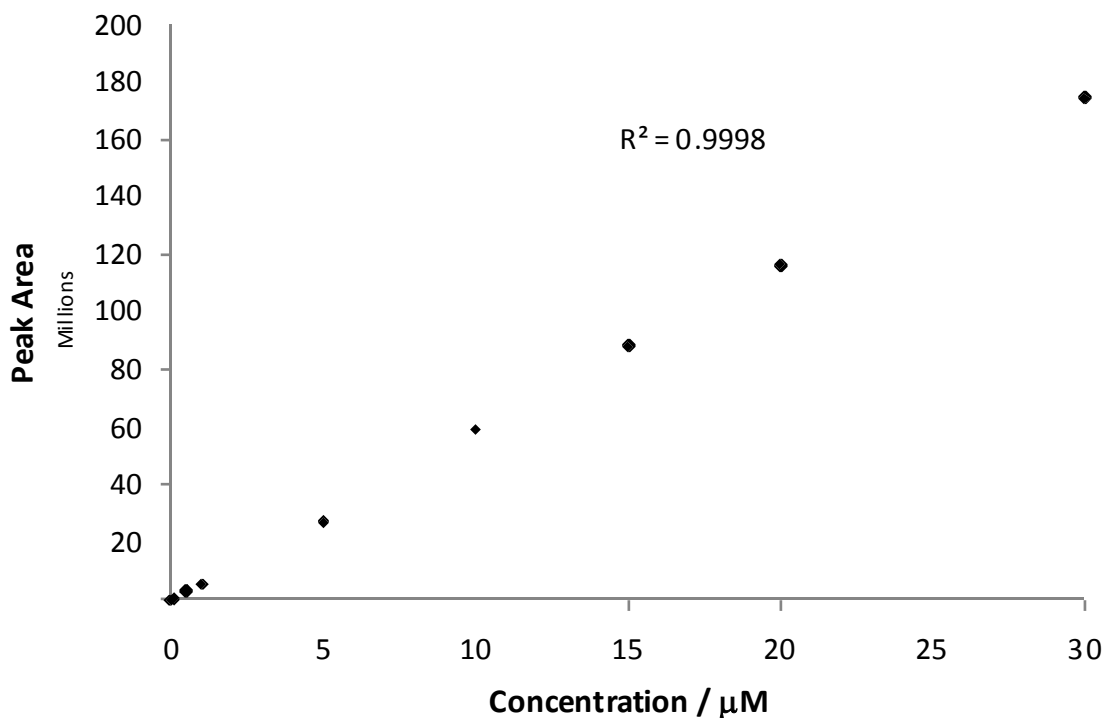


**Figure 3.29:** UV control (▲), dark control for Photospheres™40µm (♦), dark control for P25 (■) for the photocatalytic decomposition of *p*-cresol over Photospheres™40µm and P25. Error bars=1 SD; n=2

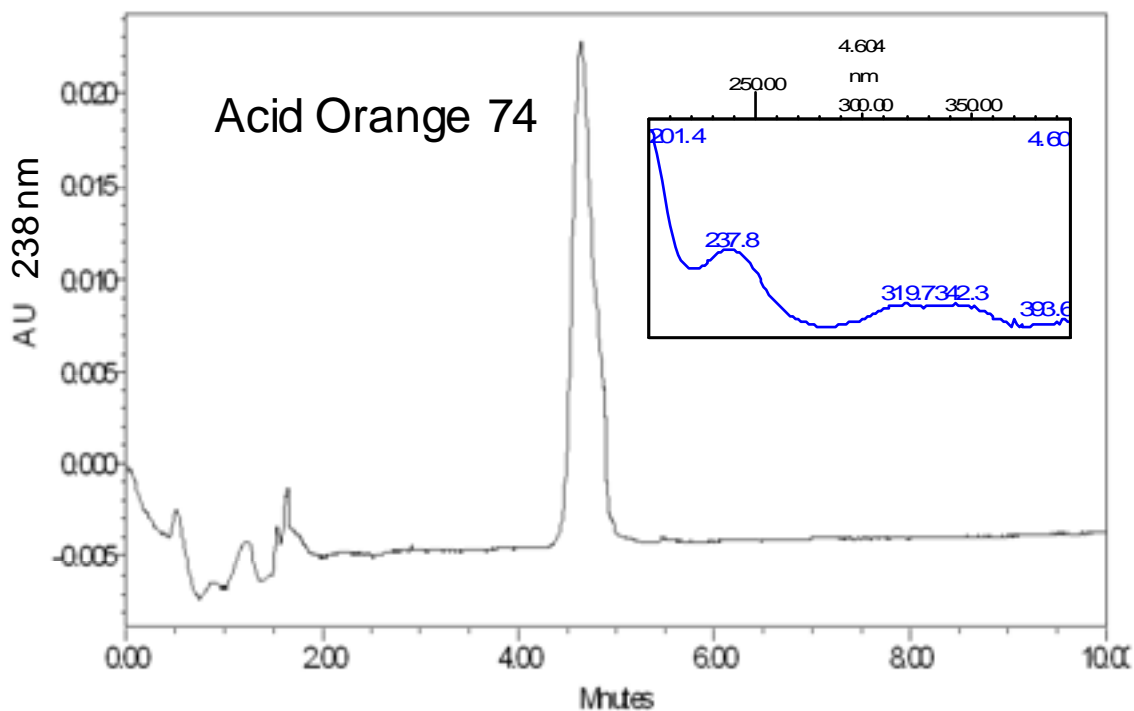
The difference in the performance of the Photospheres™40µm and P25 may be explained by the higher dark adsorption of P25 (9 % compared to 4 %), which is a recurrent observation between these catalysts. In total the Photospheres™40µm achieve a degradation of 24 % and P25 achieves 52 %, once dark adsorption is taken into account. The UV control shows that very little *p*-cresol is degraded by UV radiation. The controls for the dark adsorption show that dark adsorption for P25 is twice as high as it is for Photospheres™40µm (figure 3.29).

The third compound investigated was the azo-dye Acid Orange 74, used to assess the photocatalytic efficiency of Photospheres™ and P25. The starting concentration of AO for all test solutions was 10 µM. The concentration of AO was found to be linear in the range of 0 to 30 µM (figure 3.30), all samples were integrated at 238 nm (figure 3.31).

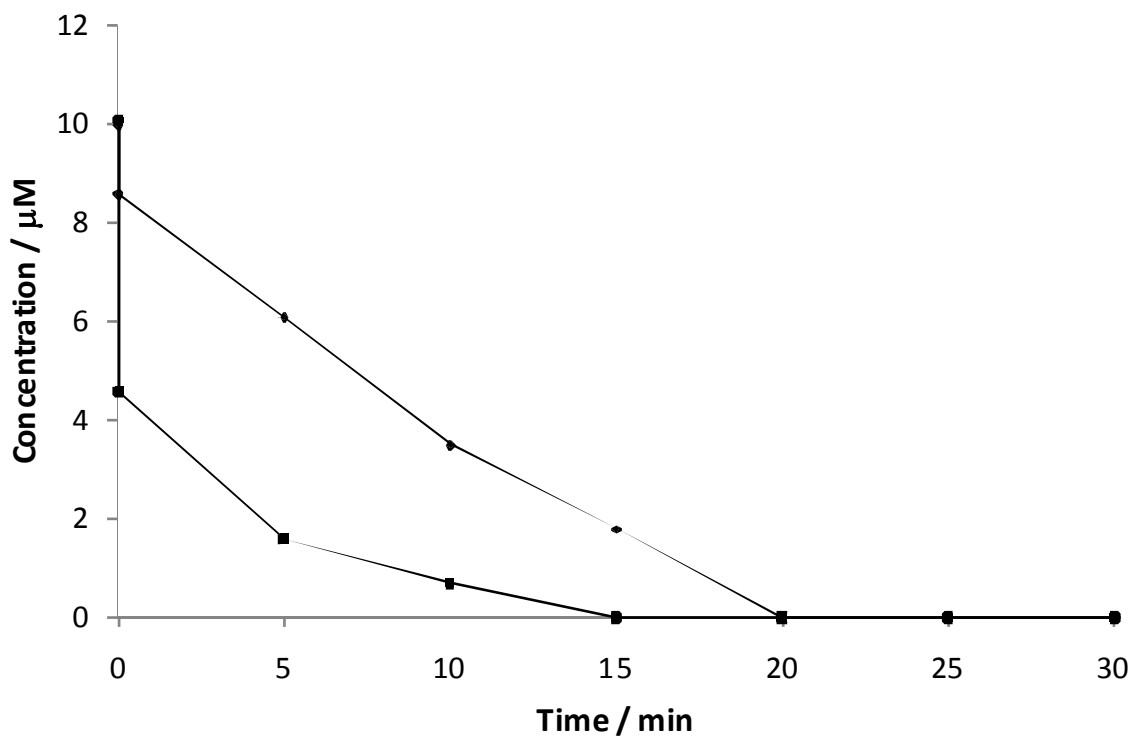
The photocatalytic decomposition of AO was extremely successful with both Photospheres™ and P25 achieving complete removal within the first 30 minutes (figure 3.32).



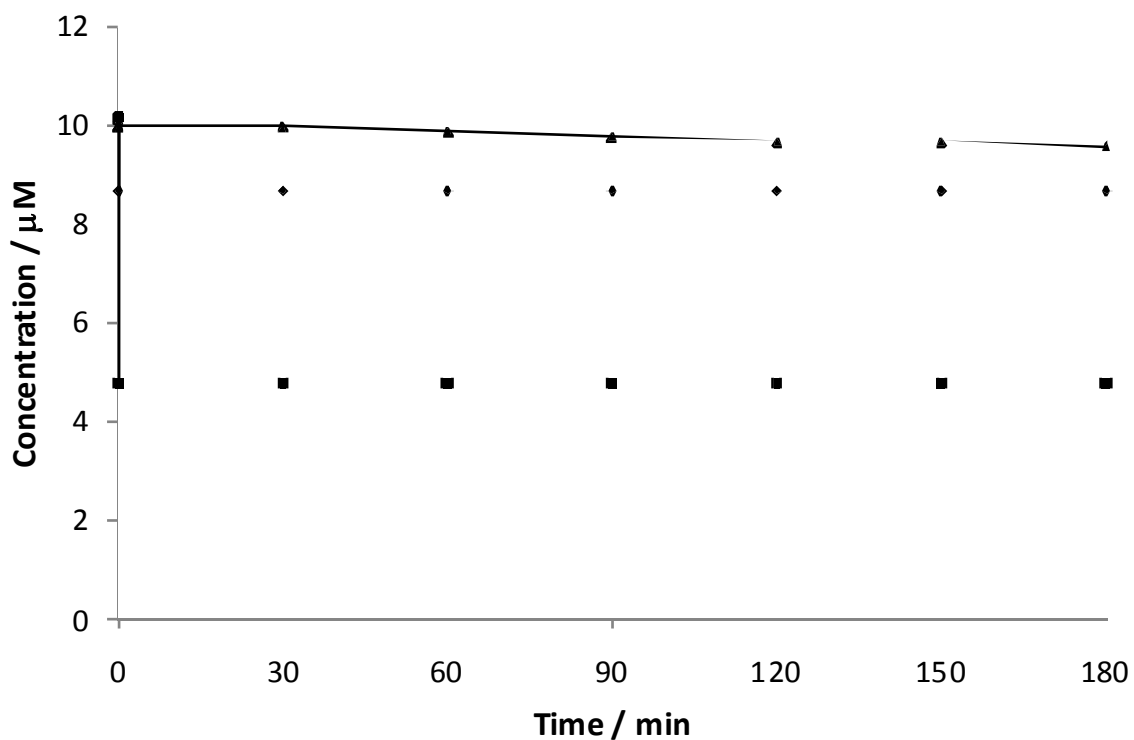
**Figure 3.30:** HPLC-PDA calibration of Acid Orange 74 over a range of 0 to 30  $\mu\text{M}$ . Error bars=1 SD; n=3



**Figure 3.31:** HPLC chromatogram and UV spectrogram of Acid Orange 74.



**Figure 3.32:** The photocatalytic decomposition of Acid Orange 74 by Photospheres™ 40µm (♦) and P25 (■). Error bars=1 SD; n=2

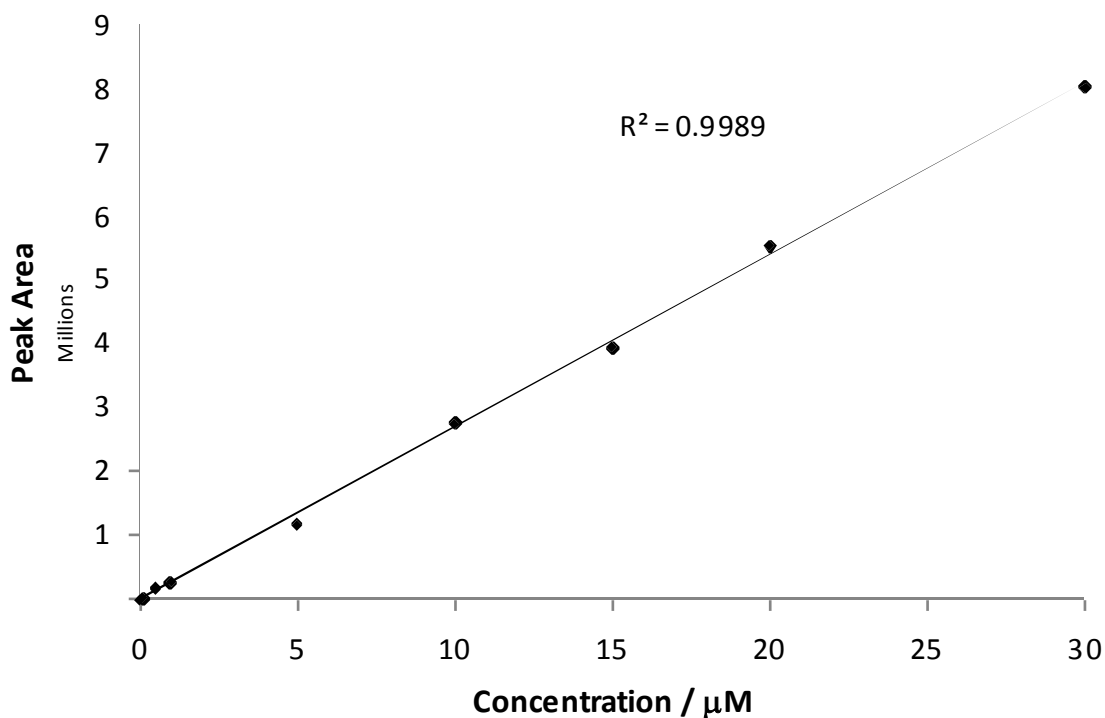


**Figure 3.33:** UV control (▲), dark control for Photospheres™ 40µm (♦), dark control for P25 (■) for the photocatalytic decomposition of Acid Orange 74 over Photospheres™ 40µm and P25. Error bars=1 SD; n=2

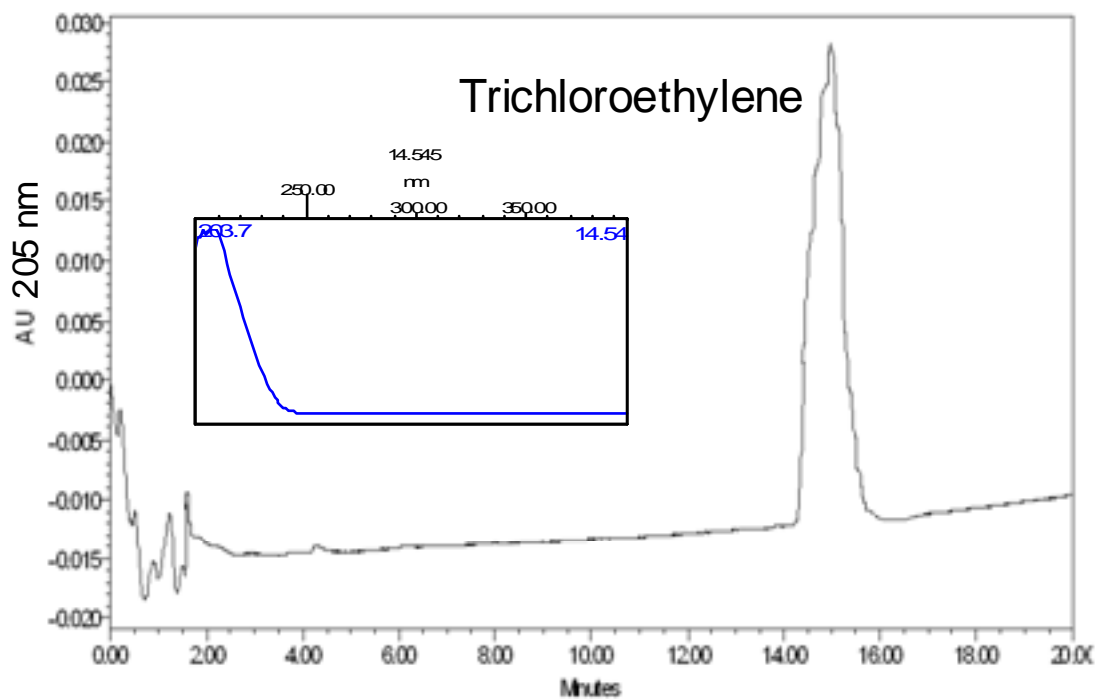
Very little degradation (4%) occurred under ultra violet (UV) light only (figure 3.33). The nanoparticulate P25 displays a higher dark adsorption (54 %) than the Photospheres™ (14 %) do, this is a trend that has been observed for the pollutants tested, but is very pronounced for AO.

The last of the waste water pollutants studied in this series of investigations was the hydrocarbon trichloroethylene (TCE). It was used in this investigation to determine the photocatalytic efficiency of Photospheres™40µm and P25. The concentration for all solutions of TCE in this series of experiments was 10 µM. TCE was determined to be linear over a range of 0 to 30 µM (figure 3.34). All solutions of TCE were analysed at 205 nm (figure 3.35).

There is a steady decomposition of TCE by UV light. The controls for the dark adsorption show a steady decrease of the TCE concentration as it continues to equilibrate over time (figure 3.36).



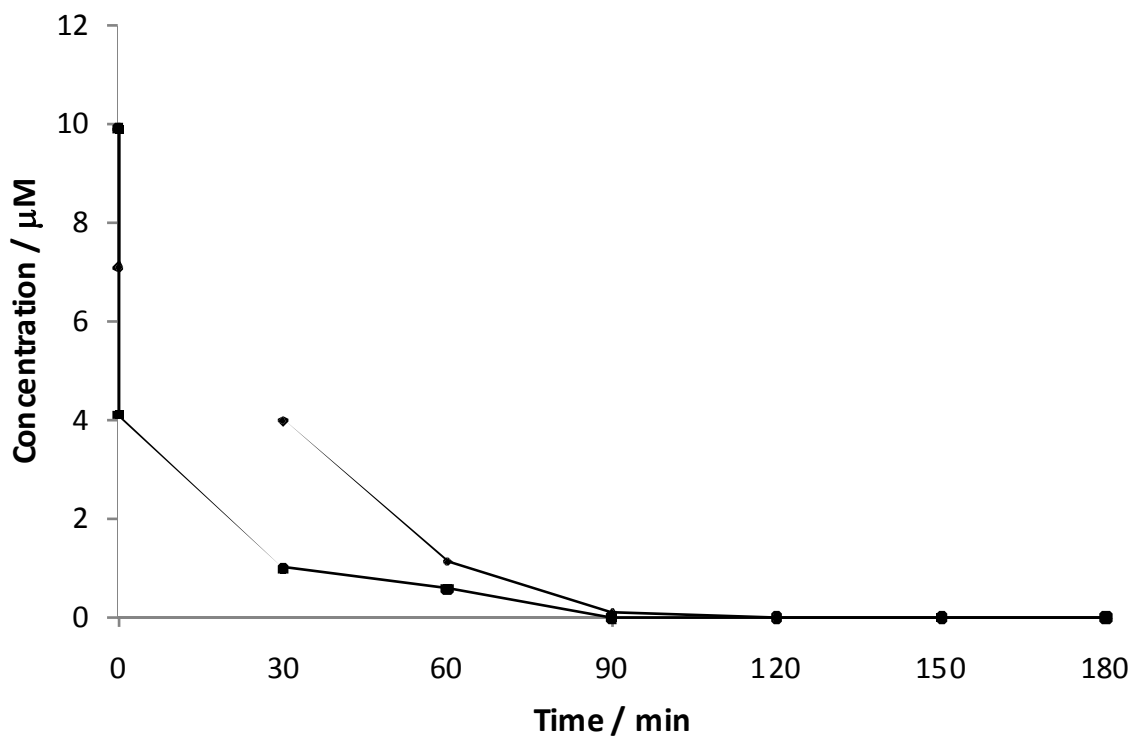
**Figure 3.34:** HPLC-PDA calibration for trichloroethylene in the range from 0 to 30  $\mu\text{M}$ . Error bars=1 SD; n=3



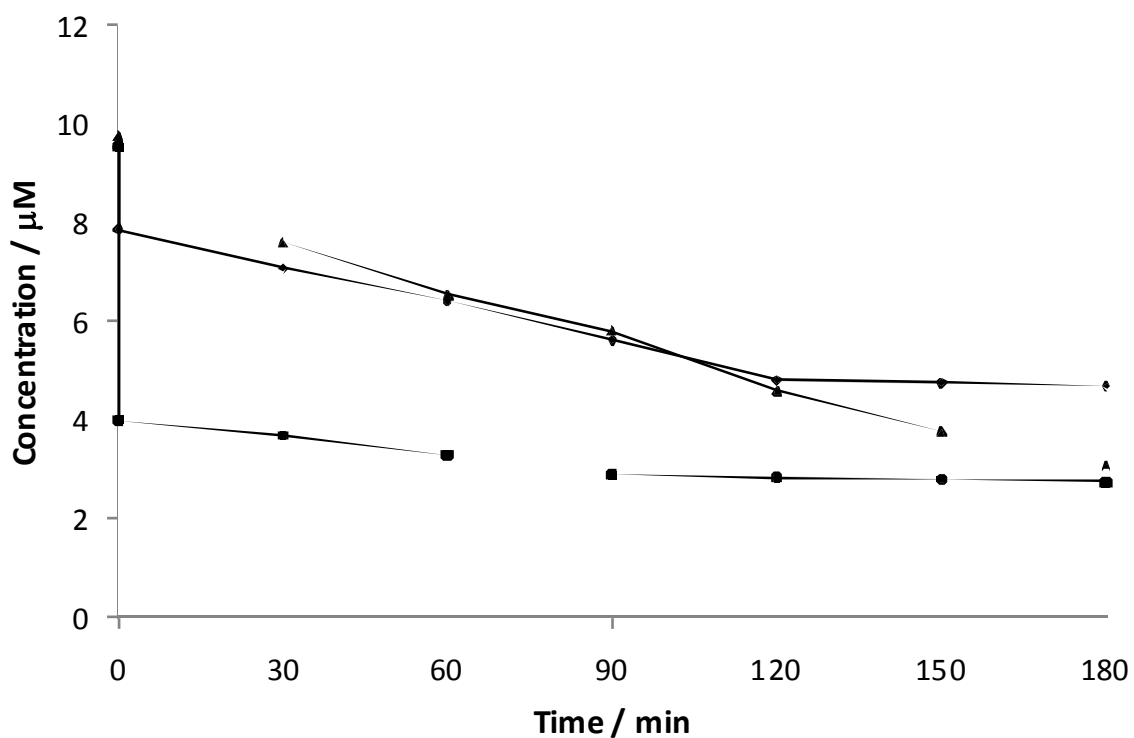
**Figure 3.35:** HPLC chromatogram and UV spectrogram of trichloroethylene.

TCE was successfully degraded by the Photospheres™ between 90 and 120 minutes and between 60 and 90 minutes for P25 (figure 3.37).





**Figure 3.36:** The photocatalytic decomposition of TCE by Photospheres™ (◆) and P25 (■). Error bars=1 SD; n=2



**Figure 3.37:** UV control (▲), dark control for Photospheres™40 $\mu\text{m}$  (◆), dark control for P25 (■) for the photocatalytic decomposition of TCE over Photospheres™40 $\mu\text{m}$  and P25. Error bars=1 SD; n=2

### 3.4 Discussion

Semiconductor photocatalysis could be a useful tool in the management of cyanobacterial toxins, especially microcystins in potable water treatment. A number of studies have shown the efficacy of semiconductor photocatalysis of microcystin-LR (and some analogues) over titanium dioxide (TiO<sub>2</sub>) in aqueous solutions (Lawton *et al.*, 1999; Robertson *et al.*, 1999; Lawton *et al.*, 2003). These studies all applied Degussa P25 as catalyst, while P25 is very successful in the photocatalytic degradation of microcystins it has inherent drawbacks. These drawbacks are due to its nature as a nanoparticulate powder, which is difficult to remove from suspension after treatment (Liu *et al.*, 2009). Nanoparticulate Surface Adhesion Ltd. (NSA) have introduced a novel product that promises to alleviate this issue. Their Photosphere™ products are a presentation of TiO<sub>2</sub> coated on hollow (and thus buoyant) silica microspheres (diameters in micrometer range). In this series of investigations, the efficiency of Photosphere™ products was tested in the photocatalytic destruction of microcystins and nodularin. The efficiency was assessed in comparison to the widely used Degussa P25.

Firstly, the efficiency of P25 in the photocatalytic destruction of microcystin-LR was established to confirm the findings of Robertson *et al.* (1997) and to define parameters for testing and comparing the efficiency of the Photospheres™ (figure 3.6). As reported in Robertson *et al.* (1997) microcystin-LR was rapidly degraded by P25 with no detectable amounts remaining after 5 min irradiation with UV light. Dark adsorption of the microcystin to the nanoparticulate powder was high (54 %), which may be due

to the high surface area of P25, which is reported to be  $52.3 \text{ m}^2 \text{ g}^{-1}$  (Swetha *et al.*, 2010). With increasing time the relative amount of toxin degraded decreases slightly which is expected as with a decreasing number of toxin molecules fewer catalyst molecules come into contact, thus the rate decreases. The next investigation focussed on the photocatalytic destruction of microcystin-LR with Photospheres™ $15\mu\text{m}$ . The novel catalyst performed well, almost completely degrading the microcystin present (figure 3.7). Although it took longer for the Photospheres™ than it did for P25, there are a number of reasons that may explain this. The dark adsorption of microcystin-LR to the Photospheres™ is six times lower (9 % compared to 54 %) which means that more toxin is still unbound at the beginning of irradiation. This may account for the slower degradation, the difference in the amount of dark adsorption may be in part explained by the BET surface area of the Photospheres™ which, with  $42 \text{ m}^2 \text{ g}^{-1}$  (personal correspondence with NSA Ltd.), is lower than that of P25, but not six times. Furthermore, it was noticed that the mixing achieved with stirring was problematic in that too slow a speed causes insufficient mixing and an accumulation of the Photospheres™ on the top of the water inside the reaction vessel. If the mixing speed was increased to achieve sufficient mixing, it was found that a layer of what could only be broken spheres accumulated at the bottom of the reaction vessel; the stir bar appeared to destroy the spheres by physically grinding them. It was decided to change the mode of agitation to sparging in order to avoid breaking the Photospheres™ while still achieving sufficient mixing. In the following series of investigations, Photospheres™ $15\mu\text{m}$ , Photospheres™MTO/0131 and P25 were evaluated in a sparged system. It was found that P25 degraded microcystin-LR

faster in the sparged than in the stirred system (figure 3.8). This is most likely due to increased mass transport and an increase in the availability of O<sub>2</sub> which is crucial, even rate determining, for the oxidation processes involved in TiO<sub>2</sub> photocatalysis (Li *et al.*, 2012). The same trend was observed with the Photospheres™ 15µm, when comparing degradation in the sparged against the stirred system (figure 3.9). Interestingly the improved mass transport did not affect the amount of dark adsorption of microcystin-LR to either compound. The Photospheres™ 15µm now achieved complete degradation at 10 minutes. Another effect of the sparging on the Photospheres™ 15µm is an increase in precision, which may be attributed to the better mixing of the catalyst within the suspension. A second sample of Photospheres™ that was provided by the manufacturer were Photospheres™ MTO/0131. These Photospheres™ also were 15 µm in diameter, but were said to have a more uniform coating thickness and were more uniform in diameter. The production cost of this type of Photospheres™ was said to be higher than that of the Photospheres™ 15µm due to an additional solvent washing step included in that product's manufacture (personal communication with NSA Ltd.). The Photospheres™ MTO/0131 showed degradation of microcystin-LR at a much reduced rate compared to P25 and relatively similar to the supposed lower quality Photospheres™ 15µm (figure 3.10). No total degradation was achieved within the time frame of the experiment. Noticeable is the decreased dark adsorption of only 3 %. This low dark adsorption may in part suggest a reason for the lower degradation achieved. After further communication with NSA Ltd., a further sample of Photospheres™ was received, Photospheres™ with an average 40 µm diameter (range from 10 to 60 µm). Before these were tested,

however, a light and scanning electron magnetic microscope investigation of the received samples and P25 was carried out. In the light microscopic investigation, loose particles were found to be present in the samples of the Photospheres™15µm, it was unclear whether these were silica or loose TiO<sub>2</sub>. If it was loose TiO<sub>2</sub>, it could be contributing to the photocatalytic efficiency of the Photospheres™? Based on the visual inspection of the Photospheres™15µm it was decided to include a fines-removal step in future experiments. No such debris was found in either the Photospheres™MTO/0131, which would correlate to that type being of a higher quality than the Photospheres™15µm, nor in the Photospheres™40µm. The SEM-EDX analysis revealed the elemental composition of the Photospheres™ products to be consisting mostly of silica, carbon, titanium and oxygen with small amounts of calcium and sodium in some of the samples (figure 3.11a, b, c). The presence of sodium and calcium in the Photospheres™15µm was noteworthy as these elements are known to interfere with photocatalysis over titanium dioxide (Paz *et al.*, 1995; Paz and Heller, 1997) (figure 3.11a – A). The amounts of both elements were decreased in samples of the Photospheres™15µm that had been already used in an experiment (figure 3.11a – B). This was further corroborating the need for a fines-removal step before the use of Photospheres™15µm, as the SEM-EDX examination hinted at the fact that the fines present in the received samples might be glass dust which if it contained calcium and sodium might be detrimental to the photocatalysis. After performing the fines-removal step further SEM-EDX analysis revealed similar calcium and sodium levels as were found in the Photospheres™15µm sample that had been previously used in a photocatalytic investigation (figure 3.11b – C). The SEM-EDX further revealed

that the Photospheres™MTO/0131 did not contain either element in measurable amounts which correlates to the mentioned additional solvent washing step included in that product's manufacture (figure 3.11b – D). The latest Photosphere™ product, the Photospheres™40µm did contain only a very low amount of sodium and a decreased amount of calcium (figure 3.11c – E). All these findings correlate to the light microscopic investigation that did not reveal any fines in the Photospheres™MTO/0131 or 40µm samples. When a fines-removal step was introduced for the Photospheres™15µm, an increase in the degradation is observed (figure 3.12). The dark adsorption increased slightly from 6 to 9 %, however, complete degradation was still not achieved. One of the potential reasons why the Photosphere™ products performed less efficiently than P25, was the possible interference of fines with the photocatalytic process, had been addressed. However, there was another obvious difference between the photosphere™ products and P25, in both cases 1 % (w/v) of the respective catalyst was used, however, P25 is > 98 % TiO<sub>2</sub>, whereas a substantial part of the mass of the Photospheres™ was accounted for by the silica sphere. Thus 1 % (w/v) of P25 did not equal 1 % (w/v) of Photospheres™ in terms of the actual amount of TiO<sub>2</sub>. The actual amount of TiO<sub>2</sub> in the Photospheres™ was found to be 17 % (personal communication with NSA Ltd.). Thus when comparing a fines-free and weight adjusted sample of the Photospheres™15µm with a sample that was neither fines-free nor weight adjusted, it is obvious that the treated catalyst performs more efficiently than the untreated one (figure 3.13). The amount of dark adsorption was increased almost two-fold and total degradation is achieved by 10 minutes. To compare how the other two Photosphere™ preparations

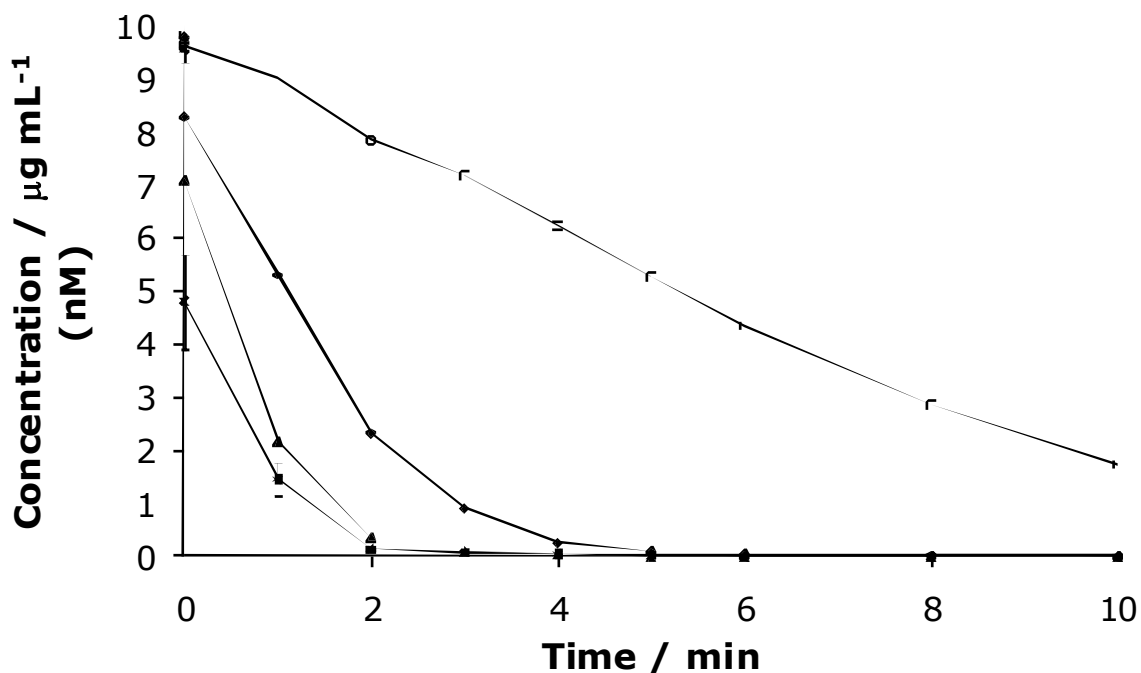
compared against this the Photospheres™40µm and MTO/0131 were tested in a weight adjusted experiment (figure 3.14). When comparing the photocatalytic efficiency of the weight adjusted Photospheres™40µm with the 15µm type it is obvious that the larger diameter spheres perform more efficiently, with complete degradation achieved by 5 minutes. This may be correlated back to their larger dark adsorption of 27 % which originates from their slightly larger BET surface area of 48 m<sup>2</sup> g<sup>-1</sup> (personal communication with NSA, Ltd.). Photospheres™MTO/0131 perform least efficient, the increased amount of the spheres created a slurry rather than a suspension which appears to have inhibited its photocatalytic efficiency. Oxygen deficiency might be one of the reasons for the decrease in photocatalytic efficiency, as the state of the slurry would have made it hard for the sparged air to be dispersed evenly throughout the slurry. Furthermore, it would have been difficult for the UV irradiation to penetrate far into the slurry, so self-shading may further impact negatively on the photocatalytic efficiency (Pinho *et al.*, 2012).

The results of the previous investigation suggest that the Photospheres™40µm is the most efficient of the Photosphere™ product family. The next step was to evaluate the effect of catalyst load on the photocatalytic efficiency of the Photospheres™40µm (figure 3.15). Here it can be seen that the catalyst load is a limiting factor when it comes to the photocatalytic efficiency. There is relatively little difference in the performance of the 1, 0.8, and 0.6 % TiO<sub>2</sub> test samples suggesting that in an application less than 1 % could still be achieving the desired degree of toxin removal, which would impact positively

on the cost. A noticeable decrease of photocatalytic efficiency was observed with the samples containing 0.4 and 0.2 % TiO<sub>2</sub> respectively. The relationship between catalyst load and photocatalytic efficiency is well established (Andreozzi *et al.*, 2000; Pekakis *et al.*, 2006). This investigation also demonstrates the existence of a linear relationship between catalyst load and amount of dark adsorption (figure 3.20), which corroborates the fact that the dark adsorption of the Photospheres™ 15µm increased when that product was weight adjusted (figure 3.13).

In summary, it can be seen that of the different catalysts tested P25 and the 40 micron Photospheres™ are the most effective, the 40 micron Photospheres™ are slightly faster in the decomposition of the toxin than P25. MTO/0131 performed least efficient (figure 3.38). The 15 micron Photospheres™ performed better than MTO/0131 but could not perform as well as the 40 micron Photospheres™. The 40 micron Photospheres™ have a much lower dark adsorption (28 %) than P25 (50 %), which accounts for the initial faster rate of decomposition of P25. The higher dark adsorption can partially be explained by the fact that the powder has a slightly higher surface area than the Photospheres™ (approximately 4 m<sup>2</sup> g<sup>-1</sup> more), so initially more microcystin is bound in the dark adsorption phase. Total decomposition is achieved earlier for the 40 micron Photospheres™, at 5 minutes, whereas total decomposition is only achieved after six minutes for P25.





**Figure 3.38:** Efficiency of microcystin-LR photocatalytic destruction over (■) P25; (▲) Photospheres™ 40µm; (◆) Photospheres™ 15µm; (□) Photospheres™ MTO/0131 in a sparged system. Error bars=1 SD; n=2

The Photospheres™ 40µm appeared to be the most efficient Photosphere™ product in the destruction of microcystin-LR. But because there are more than 80 analogues of microcystin it is important that a photocatalyst employed to remove these toxins from potable water is able to remove a wide variety of these analogues successfully. For this purpose, an investigation into the photocatalytic efficiency of Photospheres™ 40µm in the removal of ten microcystin analogues and the structurally very similar nodularin, was launched. The novel catalyst was able to degrade all eleven tested toxins in 5 minutes or less (figure 3.17; 3.18; table 3.7).

Different effects have had an influence on the rapidity of the degradation and the amounts of dark adsorption. Methylation and demethylation of microcystin variants appears to be increasing the dark adsorption to TiO<sub>2</sub>, as can be

observed for microcystin-LR and -RR. Only Homotyrosine does not accord to that trend with a slightly reduced dark adsorption. The results clearly show that the amount of dark adsorption of microcystin to TiO<sub>2</sub> is dependent on the variable amino acid in the microcystin structure. This is confirmed by similar findings by Lawton *et al.* (2003), where it was shown that different microcystin variants adhered in differing degrees to P25. A follow up study by the same group investigating mainly the effect of pH on the surface interaction and photocatalytic destruction of four different microcystins (Lawton *et al.*, 2003) concluded that the hydrophobicity of the target analyte also plays a role. They found that the more hydrophobic microcystin variants (microcystin-LW and microcystin-LF) had a higher amount of dark adsorption (at pH 4) than the less hydrophobic variant microcystin-RR. While the amount of dark adsorption differs in direct comparison, the general relationship remains the same with microcystin-RR having the lowest dark adsorption and microcystin-LW the highest. The difference in the amount of dark adsorption is most likely due to the different catalysts used, as previously shown Degussa P25 tends to have a higher dark adsorption than the microsphere products. Feitz *et al.* (1999) and Lawton *et al.* (2003) have shown a clear correlation between the amount of dark adsorption and removal rate, for effective removal, good dark adsorption is required. This observation conflicts with a number of the microcystin analogues, microcystin-YR and methylated microcystin-LR display a very similar amount of dark adsorption (45 and 46 % respectively) when compared to microcystin-LY (48 %), total degradation, however, takes twice as long for microcystin-YR and more than twice as long for methylated microcystin-LR when compared to microcystin-LY. Also the fact that microcystin-RR degrades

almost twice as fast as Homotyrosine, while having about half that analogue's dark adsorption. Other factors that influence the rate of degradation are the pH of the solution as well as the temperature (Lawton *et al.*, 2003). Another factor that may be influencing dark adsorption might be steric hindrance posed by one, both, or the combination of the variable amino acids. In their 2005 study Liu *et al.* showed that the successful photocatalytic decomposition of nodularin with TiO<sub>2</sub> (Degussa P25). Dark adsorption differs greatly between that study and the present investigation (44 % compared to 14 %) and complete degradation was achieved in the present study, however, this can be explained by the various differences between the two studies (glass vessel thickness, mode of agitation, distance to light, toxin concentration, and catalyst concentration).

It has been shown that the Photospheres™ can facilitate the photocatalytic destruction of microcystin-LR as rapid, if not more rapid than the widely used P25. Not only was it successful in the destruction of microcystin-LR but also in the destruction of ten microcystin analogues and nodularin. However, there remain drawbacks inherent to the photocatalytic destruction of the cyanotoxins. The need for UV irradiation at the appropriate wavelength is one, if not the cost determining factor in photocatalysis. To alleviate the cost UV irradiation light emitting diodes (LEDs) offer a viable alternative. LEDs are low power devices that emit at almost monochromatic levels (spectral line half width of < 20 nm) (Gorges *et al.*, 2004) of light. This is remarkable as almost all of the energetic output of a UVLED (360 nm) can be directed at facilitating the activation of a photocatalyst whereas the spectral output of the 450 W

Xenon lamp, used in these investigations, is 330 to 450 nm, which means a large portion of the output is wasted. LEDs have further inherent advantages, such as a long life of at least 100,000 h compared to the 1000 h of gas discharge sources (Natarajan *et al.*, 2011a; Natarajan *et al.*, 2011b). Furthermore LEDs hardly heat up during use, which means that they are able to convert almost all the electric energy into spectral output because none is wasted as heat (Natarajan 2011a). In addition LEDs can be designed for periodic illumination, which decreases electron-hole recombination and thus increases photonic efficiency (Natarajan *et al.*, 2011c). The size of LEDs allow for purpose-built designs in many shapes and forms. Another advantage is the fact that in an array of a multitude of LEDs, the breakage of one single, or even a number of LEDs does not compromise the efficiency of the rig (Natarajan *et al.*, 2011c).

With these inherent advantages it was a logical step to attempt the photocatalytic degradation of microcystin-LR in a reactor with UVLED irradiation. P25 was, again, used as benchmark against which the Photospheres™ (Photospheres™40µm) were tested. The Photospheres™40µm could not achieve complete degradation, however, 77 % of microcystin-LR is degraded within 10 minutes of UVLED irradiation (figure 3.19). Considering that the energy output of the LEDs is several orders of magnitude lower than that of the Xenon lamp used in previous degradation studies ( $22.5 \times 10^{-3}$  W opposed to 450 W), but yet is able to achieve 77 % destruction of the cyanotoxin. This means that with an energetic output decrease of 20,000-fold a destruction of 77 % can still be achieved. The standard catalyst P25

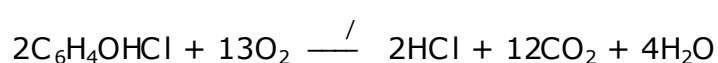
achieved almost complete degradation (> 99 %). Comparing the degradation of microcystin-LR for the Photospheres™40µm for both types of irradiation a difference in performance is obvious (figure 3.20), it has to be remembered however, that more than two thirds of the toxin originally present was degraded with 2000 times less energy used. Further optimisation, such as increasing the number of LEDs and periodic illumination might further enhance the toxin degradation to be on par with what P25 can achieve at a fraction of the energetic cost. P25 performs almost as efficient in the UVLED reactor as it does with the high power Xenon lamp proving again the point that high photocatalytic efficiency can be achieved at severely reduced energetic cost (figure 3.21). The overall efficiency is very similar, with almost complete degradation achieved by 10 minutes, this concurs with the findings of Levine *et al.* (2011), who have shown that UV light emitting diodes performed on par with conventional UV radiation sources in the removal of dyes. Similarly in two comparisons of UVA, UVC light sources and UV LEDs in the photocatalytic decomposition of formaldehyde and toluene, respectively, by silver doped titanium dioxide by Shie *et al.* (2007) and Shie and Pai (2010), the UV LEDs performed on par with the other two light sources tested.

It has been shown that the Photosphere™ products can successfully assist in the destruction of ten microcystin analogues and nodularin, as well as achieve a high rate of degradation in a low power radiation system, making the photocatalytic destruction of these compounds not only energetically more efficient but also more cost effective. However, water that undergoes treatment is a complex matrix with a variety of organic pollutants present. An advanced oxidative process needs to be able to remove a variety of organic

pollutants to be a viable option in water treatment. To this end the Photospheres™40µm were tested in the destruction of four common water pollutants: 2-chlorophenol (CP), *p*-cresol, Acid Orange 74 (AO), and trichloroethylene (TCE). P25 was again employed as a comparison compound to measure the efficiency of the Photospheres™ against.

It can be seen that the Photospheres™40µm are able to degrade 2-chlorophenol successfully with no measurable difference between the performance of the spheres and P25 (figure 3.24). The performances of the Photospheres™40µm and P25 are virtually identical. No complete degradation was achieved in the experimental time frame of 180 minutes. This may be due to the chemically relatively stable ring structure. Another reason for the slow degradation might lie in the degradation pathway of chlorophenol as stipulated by Peiró *et al.* (2000) when they investigated the titania assisted photodegradation of 2-chlorophenol. In this study it was found that the first step in the breakdown of 2-chlorophenol is the dechlorination of the molecule. In their study they found increased concentrations of chloride ions in the solution detected by GC-MS. They found that after 5 h of radiation 86 % of the chloride ions initially found in the 2-chlorophenol molecule were loose in solution. A similar observation was made by Minero *et al.* (1991), who have studied the titania assisted photodegradation of 2-fluorophenol, and have found that the first step in the decomposition of 2-fluorophenol is defluorination of the 2-fluorophenol molecule. Furthermore they found that the liberated fluorine hindered the photocatalysis due to the fact that it bound to the titania. Considering the similarities of chlorine and fluorine (both halogens)

it can be assumed that the loose chloride ions also hinder the photocatalysis by binding to the titania, which might account for the fact that complete removal could not be achieved over the course of the experiment. The formation of aromatic intermediates and chloride ions in the photocatalytic decomposition of CP has also been demonstrated and documented by Ilisz *et al.* (2002). Rideh *et al.* (1997) have proposed that CP is degraded in an illuminated suspension of titanium dioxide thus:



This suggests that the liberated chloride ions eventually form hydrochloric acid with hydrogen. This is further supported by Suryaman and Hasegawa (2010) who have shown that P25 can be reused after the decomposition of CP without any pretreatment. It is safe to assume the same would be true for the Photospheres™, considering that both catalysts are made from mostly the same material (anatase). Also remarkable is the fact that the dark adsorption for both types of catalyst is almost identical, which, with regard to the microcystins, had never been the case. It can be seen that UV radiation alone has a strong effect on CP with a steady rate of degradation over the experimental time frame (figure 3.25). This concurs with the findings of Pouloupoulos *et al.* (2007), Karunakaran and Dhanalakshmi (2008), and Oyama *et al.* (2011). Ku *et al.* (1996) have shown successful degradation of CP with titanium dioxide, where they found a strong correlation between the intensity of radiation and the rate of removal. A similar observation was made by Peiró

*et al.* (2000) when they investigated the titania assisted photodegradation of 2-chlorophenol. No degradation occurs in the dark control for either catalyst. Ways to improve the reaction are numerous: the effect of the pH on the photocatalytic destruction of CP has been illustrated by Ku *et al.* (1996) and Rideh *et al.* (1997), who show that an acidic solution is more effective than an alkaline one, the addition of hydrogen peroxide (H<sub>2</sub>O<sub>2</sub>) and sparging with ozone (O<sub>3</sub>) have shown to improve the rate of reaction (Bertelli and Selli, 2006; and Oyama *et al.*, 2011, respectively), and also the addition of certain dissolved metallic ions such as Ag<sup>+</sup>, Cr<sub>2</sub>O<sub>7</sub><sup>2-</sup>, Cu<sup>2+</sup>, and Fe<sup>2+</sup> have shown to have a beneficial effect on the photocatalysis (Rideh *et al.*, 1997).

*P*-cresol is another aromatic hydrocarbon that is commonly found in waste water. The degradation of *p*-cresol with the Photospheres™40µm is slow and not as successful as that of CP with only 27 % removed after 180 minutes of irradiation (figure 3.28). P25 was able to destroy more than double the amount, with 56 % in the same time frame. The dark adsorption of P25 was more than twice as high compared to the dark adsorption of the Photospheres™, with 9 % compared to 4 %. Remembering the statement of Feitz *et al.* (1999) that a high amount of dark adsorption translates into a good initial photocatalytic efficiency, it can be proposed that the slow initial rate of destruction of the Photospheres™ compared to P25 is due to the lower amount of dark adsorption. Considering the graph it appears as if the destruction undergoes phases of adsorption followed by destruction followed by adsorption. P25 shows degradation over the first thirty minutes of irradiation, followed by 60 minutes of adsorption with little degradation,



followed by 60 minutes of degradation, followed by a period of slow degradation. The same pattern can be observed with the Photospheres™, although the periods of little to no degradation are longer for the spheres. The decreased amount of dark adsorption and elongated periods with little photocatalytic activity may be attributed to the mode of agitation. The microcystin studies have illustrated that sparging is the more efficient mode of agitation for the Photospheres™. The relatively slow degradation of the pollutant may be attributed to the comparatively stable aromatic ring. The UV and dark controls show no measurable degradation of *p*-cresol which concurs with Karetnikova *et al.* (2008), Karunakaran and Dhanalakshmi (2008), and Poblete *et al.* (2011) (a slightly modified version of TiO<sub>2</sub> was used in this investigation, WTiO<sub>2</sub>) (figure 3.29).

Another organic pollutant was the azo dye AO. It is the largest of the organic pollutants and the most complex molecule. The photocatalytic destruction of AO was extremely successful with the Photospheres™ with total degradation achieved in 20 minutes (figure 3.32). P25 achieves total degradation in 15 minutes, however, the dark adsorption of P25 is almost four times higher than that of the Photospheres™40μm, 54 % compared to 14 %. The rate of the degradation of AO by the Photospheres™ is, however, not four times slower but in fact comparable, considering the time point at which half of the remaining pollutant is destroyed is approximate 8.3 minutes for the Photospheres™ and 4.5 for P25. From that point on, both catalysts require another 10 minutes approximately to remove the remaining amounts thus showing that the Photospheres™ are as effective as the P25 if not more

effective, considering that more material was left and was removed in the same amount of time it took P25 to remove the remaining AO. There is only one previous study that has investigated the photocatalytic degradation of AO, Song *et al.* (2010) managed to remove approximately 48 % of AO in 24 h of solar radiation over TiO<sub>2</sub>. In their study they found that 24 h of solar radiation alone (without catalyst present) only removed 27 % of the dye. This is mirrored in the UV control that showed 4 % degradation over 180 minutes which equates to 28 % over 24 h assuming a linear relationship of degradation over time (figure 3.33). These studies have all found that the pH (2-6) of the test solution can beneficially affect the rate of reaction and amount of initial binding (dark adsorption) to the catalyst. Catalyst load can have a small effect on the rate of reaction (Velegraki *et al.*, 2006). There was no observable degradation in the dark controls.

Trichloroethylene was the last of the four pollutants studied and the most troublesome. All initial experiments were conducted in a sparged system after it had been established in the photocatalytic destruction of microcystin-LR that sparging as mode of agitation was more beneficial to the Photospheres™. When the photocatalytic destruction of TCE was attempted in a sparged system, no measurable amounts of TCE could be detected even in the T<sub>02</sub> samples. This suggested that sparging led to volatisation of the compound. It was decided to revert to stirring as mode of agitation. Both the Photospheres™40µm and P25 were successful in degrading TCE (figure 3.36). P25 displays dark adsorption that is twice as high as that of the Photospheres™ (58 % compared to 28 %). And again appears to degrade the

pollutant more rapidly with total degradation achieved in 90 minutes, whereas the Photospheres™ need 120 minutes to achieve complete removal. This impression, however, is deceptive as again, investigating the time it takes each catalyst to remove the remaining 50 % after dark adsorption, it can be seen that the Photospheres™ remove the remainder of the pollutant in the same time as it takes P25. Showing again that once the issue of low dark adsorption is overcome, the Photospheres™40µm are capable of removing organic pollutants with the same efficiency as the standard catalyst P25. There has only been a limited amount of research conducted into the titania assisted photodegradation of TCE in aqueous solutions. As TCE is considered a volatile compound most research on the photocatalysis is centred on TCE in the gaseous phase rather than in aqueous solution. This approach is somewhat limited because TCE can and does appear in the aqueous solution in drinking water and warrants further investigation. The fact that TCE poses challenges when conducting experiments could be an attributing factor to the dearth of published investigations. The negative controls display a steady decrease of TCE concentration under UV radiation (figure 3.37). Furthermore the dark adsorption for P25 is higher than that for the Photospheres™. A remarkable fact is that for both catalysts the concentration only levels out after 120 minutes. For the Photospheres™ the initial dark adsorption is 17 % and a further 38 % of the remaining TCE binds to the catalyst; for P25 the initial dark adsorption is 59 % and a further 29 % of the remaining TCE binds to the P25 present. This percentage is drastically lower for the other pollutants (table 3.8).

**Table 3.8:** Additional dark adsorption in dark control after T<sub>02</sub> sample.

	<b>Compound</b>			
	<b>CP</b>	<b>p-cresol</b>	<b>AO</b>	<b>TCE</b>
Photospheres™40µm (%)	<1	<1	0	38
P25 (%)	<1	1	0	29

In summary it can be said that the Photospheres™ performed at a level similar to that of P25 (table 3.9).

**Table 3.9:** Degradation of four common water pollutants by P25 and Photospheres™40µm.

	<b>Compound</b>			
	<b>CP</b>	<b>p-cresol</b>	<b>AO74</b>	<b>TCE</b>
PS™ degradation (%)	80	27	100	100
P25 degradation (%)	80	57	100	100
PS™ dark adsorption (%)	3	4	14	28
P25 dark adsorption (%)	2	9	54	58
PS™ complete degradation (min)	>180	>>180	25	90
P25 complete degradation (min)	>180	>>180	20	120

The Photospheres™40µm can thus be considered a more practical alternative to P25 in the application of water treatment combining the advantages of a high surface area with a high photocatalytic efficiency. Their applicability has not only been shown to successfully degrade the most common microcystin, but also 10 analogues and the sister compound nodularin. Above and beyond the successful degradation of the cyanotoxins it has been shown that the Photospheres™40µm are well capable of removing other organic compounds from aqueous solution, including two little studied compounds (AO and TCE). The cost efficiency could be enhanced by applying LEDs as source of irradiation. It has been shown that, even at a very rudimentary level, 77 % of the efficiency of a high power UV lamp can be achieved at a fraction of the

monetary and energy cost. Making the combination of Photospheres™ in a UVLED driven reactor a viable alternative to other advanced oxidation processes in water treatment.

**Monitoring and controlling  
of the cyanobacterial  
metabolites 2-MIB and GSM**

## **4 Monitoring and controlling the cyanobacterial metabolites 2-MIB and GSM**

### **4.1 Introduction**

Cyanobacteria have been shown to produce potentially harmful metabolites (cyanotoxins). In addition to these compounds cyanobacteria are also capable of producing secondary metabolites that are not directly harmful, but constitute problems in potable water supply and in aquaculture. This group of compounds that impart an unpleasant taste and smell to water have been shown to be produced by cyanobacteria (and other biota). The two most prominent members of this group of taste and odour compounds are 2-methylisoborneol (2-MIB) and geosmin (GSM). Both compounds can have a significant financial impact on drinking water providers as well as fish farmers (Izaguirre *et al.*, 1982; Hanson, 2003). They confer a musty-earthy flavour and smell to water and any produce grown in contaminated water, such as farmed fish (Howgate, 2003; Robertson *et al.*, 2006). Significant financial losses are incurred by drinking water companies due to rejection of the product by customers (Sklenar and Horne, 1999). Similar issues are present in aquaculture as well, where conventional recirculation systems fail to remove these compounds successfully. In fact, conventional recirculation systems can exacerbate the presence of both 2-MIB and GSM as there are a number of species of actinomyces, often found in recirculation system biofilters that are capable of producing 2-MIB and GSM. The severity of contamination with 2-MIB and GSM in aquacultures arises from the fact that even a relatively short contact time of a few hours is enough for measurable amounts to bioaccumulate in the fatty tissue (due to their lipophilic nature) of the fish

(Howgate, 2004). It has also been shown that the depuration, or the removal of 2-MIB and GSM from the fish tissue can take up to several days, provided uncontaminated water can be supplied to the fish in that period (Howgate, 2004). A large volume of literature focuses on farmed fresh water fish, especially channel catfish (*Ictalurus punctatus*) in the United States of America (Lorio *et al.*, 1992; Conte *et al.*, 1996; Schrader *et al.*, 2011). Farmed rainbow trout (*Onchorhynchus mykiss* and *Cyprinus carpio*) and carp rearing in the UK and France have also been under investigation (Robertson and Lawton, 2003; Robin *et al.*, 2006; Vallod *et al.*, 2007), as well as tilapia (*Oreochromis niloticus*) (Yamprayoon and Noomhorm, 2000) and salmon (*Salmo salar*) (Farmer *et al.*, 1995). The financial impact caused by the taste and odour compounds including 2-MIB and GSM cost the channel catfish rearing industry \$ 15 to \$ 23 million annually (Hanson, 2003). The issue of off-flavour in aquaculture is compounded by the fact that the concentration of 2-MIB and GSM in water is not representative of the concentration in the fish (Howgate, 2004). The concentration of 2-MIB and GSM in the fish greatly depends on the fat content of the meat and thus can vary considerably between individuals and species respectively. Lovell *et al.* (1986) report a sensory detection threshold of 8.5 mg kg<sup>-1</sup> for GSM in channel catfish and Yurkowski and Tabachek (1974) report a threshold in trout (species not stated) of 6 mg kg<sup>-1</sup>. However, controlling the amount of 2-MIB and GSM in the water also controls the amount in the fish tissue. Therefore it is important for the potable water and aquaculture industries to monitor and control the presence of both 2-MIB and GSM. Treatment strategies are manifold and dependant on the application. In aquaculture, recirculation systems, employing activate carbon



filters (Tucker, 2000), and purging (Guttman and van Rijn, 2008) (keeping the produce in clean water for a number of days) are employed. In water treatment applications, it has been found that conventional treatment methods are ineffective in removing 2-MIB and GSM from water (Nerenberg *et al.*, 2000). Oxidation of the compounds with chlorine or ozone does not always completely remove them (Glaze *et al.*, 1990). Treatment with activated carbon has been tried with success (Cook, 2000). The drawback of the activated carbon method is the fact that the carbon eventually saturates and either needs to be destroyed by incineration, regenerated by heating in a non-reactive atmosphere at 800 °C, or deposited in a landfill (San Miguel *et al.*, 2001; Chestnutt *et al.*, 2007). A promising alternative, or indeed supplementary treatment, could be the implementation of titanium dioxide assisted photodegradation of 2-MIB and GSM. Promising results in a lab scale study have been achieved by Lawton *et al.* (2003) where it was shown that titanium dioxide (nanoparticulate powder) successfully decomposed both 2-MIB and GSM within 60 minutes. Further studies by this group demonstrated that the pellet form of the photocatalyst also successfully degraded geosmin (Bellu *et al.*, 2008; Robertson *et al.*, 2011). While a number of studies (Lawton *et al.*, 2003; Yoon *et al.*, 2007; Bellu *et al.*, 2008; Robertson *et al.*, 2011) have demonstrated the potential application of TiO<sub>2</sub> photocatalysis in batch reactors, it is desirable to develop and evaluate a continuous flow reactor, which is more practical because it may reduce the need for aeration, a major cost factor due to energy consumption, and allows a large volume through-put, both are desirable in a commercial setting where cost-efficiency and the processing of large volumes are the prime objectives.

The need to monitor 2-MIB and GSM both in potable water and in aquaculture is significant. However, the analysis of 2-MIB and GSM presents a number of challenges due to the fact that the human taste and odour threshold, i.e. the lowest concentration at which humans can still taste and smell these compounds, is very low (nano gram range) (table 4.1). Traditionally sensory panels, i.e. humans tasting and smelling samples, have been employed to test for the 2-MIB and GSM in both aquaculture (van der Ploeg, 1991; Bett and Diogini, 1997) and the potable water industry (Schweitzer *et al.*, 2004; Wiesenthal *et al.*, 2004). However, this approach has inherent problems. Humans are unable to discriminate between specific smells in the presence of a stronger one, precision and reproducibility can vary widely, and furthermore well trained sensory evaluation staff are costly to maintain (Bett and Diogini, 1997).

**Table 4.1:** Sensory thresholds for 2-MIB and GSM reported in the literature

<b>2-MIB (ng L<sup>-1</sup>)</b>	<b>GSM (ng L<sup>-1</sup>)</b>	<b>Reference</b>
2-10	2-10	Wnorowski, 1992
1.3	-	Young <i>et al.</i> , 1996
4-10	4-10	Suffet, 1996
4-10	4-10	Rashash, 1997
15	35	Howgate, 2004
4-20	-	Davies <i>et al.</i> , 2004
5-10	5-10	Ho <i>et al.</i> , 2007

Due to the low sensory thresholds of both 2-MIB and GSM (low nano gram range) very sensitive methods are required in order to satisfactorily sense these compounds at the levels required. Owing to the physicochemical characteristics of 2-MIB and GSM (volatility) the only analytical method that is

fit for purpose to deliver a reliable response at the concentrations required is gas chromatography (GC), most commonly coupled with mass spectroscopy (MS) (Conte *et al.*, 1996, Lloyd *et al.*, 1998). The requirement of having an increased sensitivity in analysis for the detection of both 2-MIB and GSM at low concentrations makes it essential to include an enrichment or pre-concentration step. Different techniques have been proposed with differing levels of detection (LOD) (table 4.2). The majority of the methods utilise solid phase micro extraction (SPME) as a pre-concentration step prior to GC-MS analysis.

**Table 4.2:** Published limit of detection values for 2-MIB and GSM reported in the literature.

<b>2-MIB LOD (ng L<sup>-1</sup>)</b>	<b>GSM LOD (ng L<sup>-1</sup>)</b>	<b>Method</b>	<b>Reference</b>
-	5	SPE/GC-MS	Dzialowski <i>et al.</i> , 2009
0.5	0.5	SPME/GC-MS	Westerhoff <i>et al.</i> , 2009
0.2	0.2	SPME/GC-MS	Klausen <i>et al.</i> , 2005
1.2	3.3	SPME/GC-MS	Watson <i>et al.</i> , 2000
2	2	USADLLME/ GC-MS	Cortada <i>et al.</i> , 2010
0.6	0.9	SPME/GC-MS	Saito <i>et al.</i> , 2008
10	10	SPME/GC-MS	Lloyd <i>et al.</i> , 1998
0.03	0.05	CLLE/LVI-GC-MS	Zhang <i>et al.</i> , 2006
1*	0.5*	SBSE/GC-MS	Bennanou <i>et al.</i> , 2003

LOD – limit of detection; SPE – Solid phase extraction; SPME – Solid phase micro extraction; USADLLME – Ultra sound assisted dispersive liquid liquid micro extraction; CLLE – Continuous liquid liquid extraction; LVI Large volume injection; SBSE – Stir bar sorptive extraction. \* Limit of quantification value only

While SPME allows the analysis of trace concentration at sub nano gram levels it has two major drawbacks. SPME is difficult to automate and can therefore be labour intensive, allowing only a relatively small sample through-put per

day, due to the need of manually injecting the samples into the gas chromatograph. The drawback of liquid-liquid extraction lies in the large sample volume and therefore considerable sample pre-concentration is required (Johnson *et al.*, 1987). The use of ultra sound assisted dispersive liquid-liquid microextraction requires the use of environmentally harmful solvents (bromoform and tetrachloroethylene) (Cortada *et al.*, 2010). Continuous liquid-liquid extraction requires specialist equipment, the use of environmentally harmful solvents (dichloromethane) and requires an additional pre-concentration step by solid phase extraction (Zhang *et al.*, 2006). Stir bar sorptive extraction also suffers from limitations, including low sample through-put ( $\sim 20 \text{ day}^{-1}$ ) and the need for specialist GC-MS equipment (thermal diffusion capillaries) (Bennanou *et al.*, 2003). Thus the need for a high-sample-through-put method that achieves the required sensitivity without the need for specialist equipment and/or training is apparent. Solid phase extraction has been applied to the analysis of GSM before (Dzialowski *et al.*, 2009), however, the full potential of the technique has not been developed. SPE is financially economical, does not require specialist equipment or training, and allows a high sample through-put  $\text{day}^{-1}$  (50-60 samples  $\text{day}^{-1}$ ) (Conte *et al.*, 1996; Dzialowski *et al.*, 2009).

Some analytical methods require a large volume of sample to be able to detect 2-MIB and GSM at the required concentrations. This presents a host of problems when attempting to acquire environmental samples. Due to the nature of 2-MIB and GSM the samples have to be stored in glass or PTFE bottles to avoid non-specific binding to the sampling container (Elhadi *et al.*,

2004), which makes sampling large volumes and/or sampling in many locations difficult due to the bulk of the containers. Ideally samples in this type of container need to be refrigerated to avoid sample loss by volatilisation and degradation. In instances where the sampling and analysis of the samples is carried out by different persons, shipping of the samples can be involved which adds significant financial cost. A possible means of circumventing the described problems may be the use of certain passive samplers that can be deployed, recovered and transported/shipped easily for subsequent investigation in the laboratory. There is a great deal of choice when it comes to passive samplers, but the selection depends on the target analyte (table 4.3). Polar organic chemical integrative samplers (POCIS) (Alvarez *et al.*, 2004), Chemcatcher (Vrana *et al.*, 2006), and solvent-based cellulose membranes (Hyne and Aistrope, 2008) are used to sample polar organic compounds. Semi-permeable membrane devices (SPMD) (Huckins *et al.*, 1990) and solid phase micro extraction fibres (Nilsson *et al.*, 1997) developed for hydrophobic organic compounds.

**Table 4.3:** Passive sampling devices, their respective target compounds and inherent drawbacks (Hudkins *et al.*, 1990; Koziel *et al.*, 2001; Booij *et al.*, 2002; Alvarez *et al.*, 2004; Vrana *et al.*, 2006; Sakamoto *et al.*, 2006; Hyne and Aistrope, 2008; Liu *et al.*, 2011)

<b>Passive Sampler</b>	<b>Target analyte</b>	<b>Drawbacks</b>
Polar organic chemical integrative samplers (POCIS)	Polar organic compounds	requires cooling after sampling, very bulky
Chemcatcher		requires cooling after sampling, very bulky
Solvent based cellulose membranes		requires cooling after sampling
Semi-permeable membrane device (SPMD)	Hydrophobic organic compounds	Easy volatisation of analytes, requires cooling after sampling
Solid phase micro extraction (SPME) fibres		Easy volatisation of analytes, requires cooling after sampling
Silicone rubber membranes (SRM)	Poly aromatic hydrocarbons	Pre-extraction before use required
Polypropylene glycol coated silicone		Preparation (coating) required before use

The relatively high volatility of both 2-MIB and GSM requires a sampler that is small enough to be stored either at a low temperature or within a solvent (ideally no special storage conditions at all). This rules out SPMDs because of easy volatisation from the fibres, even though SPME fibres have been used before to successfully catch volatiles (Koziel *et al.*, 2001; Sakamoto *et al.*, 2006), but required immersion in liquid nitrogen or alternative refrigeration to contain the volatiles on the fibres during transport to the laboratory. Furthermore POCIS can be ruled out because of their bulk (POCIS generally consist of two flat metal rings with a diameter of 10 to 15 cm, between which

a membrane is sandwiched) (Alvarez *et al.*, 2004). The only report of passive samplers being applied for the determination of 2-MIB and GSM is the use of polypropylene glycol coated hollow fibre membranes (Liu *et al.*, 2011), which delivered reliable results (of spiked environmental samples) but still required SPME as a pre-concentration step prior to GC-MS analysis. Liu *et al.* (2011) achieved detection limits of 4 ng L<sup>-1</sup> for GSM and 9 ng L<sup>-1</sup> for 2-MIB. Furthermore, even though environmental samples were tested, the investigation was still carried out in the laboratory with a finite amount of sample, which cannot guarantee equilibrium between the sampler and the sample. More promising is the approach of Booij *et al.* (2001) that uses silicone rubber membranes (SRMs) for the sampling of polyaromatic hydrocarbons and polychlorinated biphenyls. Low-cost SRMs are pre-extracted and deployed in the field for a finite amount of time and achieved reproducible results after desorption and analysis.

The need for monitoring and controlling the concentrations of 2-MIB and GSM in potable water and aquaculture has been demonstrated. The aim of this work is to develop and optimise a pre-concentration and analysis method (SPE-GC-MS) that is capable of determining 2-MIB and GSM concentration below the human taste and odour threshold. Ideally this proposed method will not require specialist equipment or training, will be cost effective, and allow a high sample through-put, SPE has long been used in water analysis as a robust analyte concentration method. The investigated method will include sample extraction (and pre-concentration) by solid phase extraction and analysis by gas chromatography coupled with mass spectrometry in single ion monitoring

(SIM) mode. With this method the 2-MIB and GSM levels in various sources of water will be determined. Additionally, the use of a continuous flow-reactor for the photocatalytic decomposition of 2-MIB and GSM over titanium dioxide that could be applied in a potable water treatment and aquaculture environment will be explored. The efficiency of the proposed reactor will be corroborated by the proposed analysis method. Laboratory and field tests will be executed in order to assess the feasibility of such a reactor. Furthermore, the possibility of employing silicone rubber membranes (SRMs) as a passive sampling device to monitor levels of 2-MIB and GSM *in vitro* and *in vivo* will be explored.



## **4.2 Materials and methods**

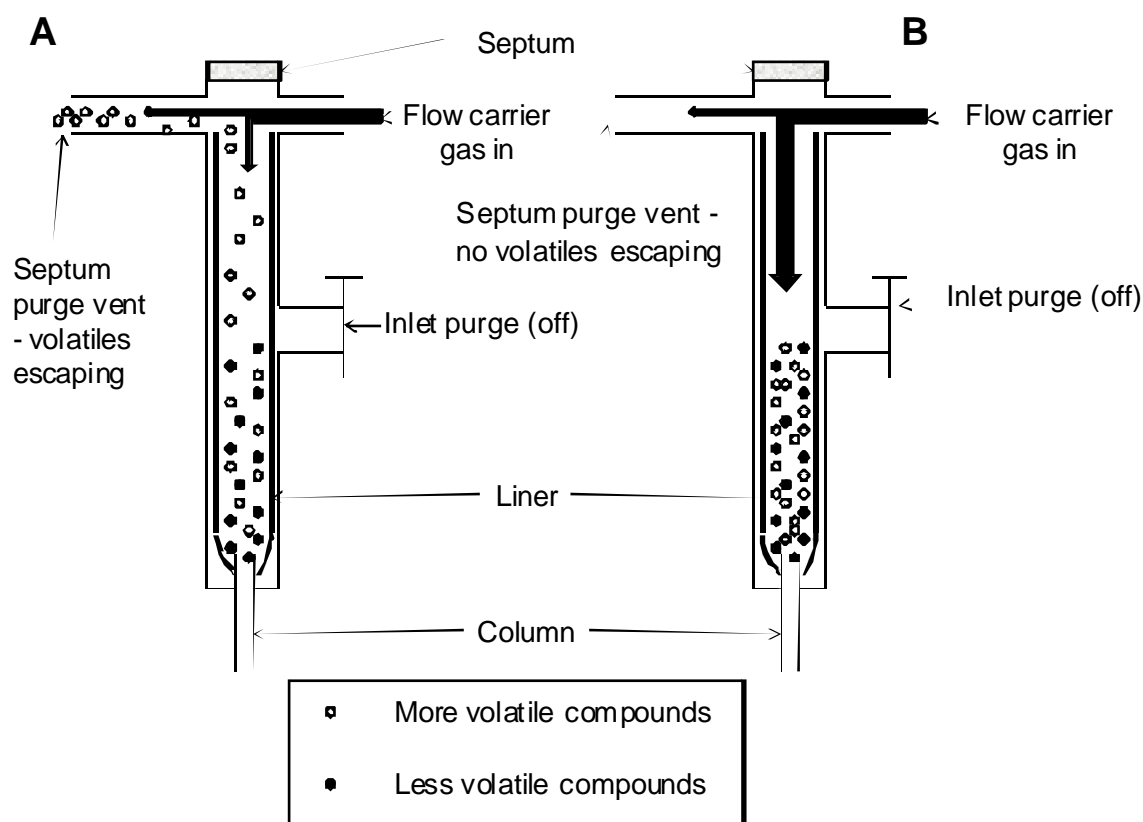
### **4.2.1 Reagents**

The 2-MIB and GSM mixed standard used in all experiments was supplied by Sigma Aldrich (Dorset, UK) and used as received. The internal standard decane was supplied by Fisher Scientific (Leicestershire, UK), as were the solvents 2,2,4-trimethylpentane (isooctane), ethyl acetate, hexane, and acetone, all were HPLC-grade and used as received. Methanol was supplied by Rathburn (Walkerburn, Scotland). Milli-Q water (purified to 18.2 mΩ) was provided by the Milli-Q system (Millipore Watford, UK), distilled water was provided by the laboratory still.

### **4.2.2 Optimised method for GC-MS analysis**

One potential approach to increase the sensitivity (i.e. detection limit) of the analysis by GC is the use of a larger than typical injection volume (3 to 5 μL instead of 1 μL) utilising the pulsed splitless injection mode offered by most gas chromatographs (figure 4.1). This requires no additional, specialist equipment; it is simply a change in settings. Increasing the injection volume allows for more of the analyte to reach the column thus increasing sensitivity. During pulsed splitless injection a high initial column flow rate during the injection of the sample matrix sweeps it out of the inlet rapidly, thereby reducing the loss of analytes caused by adsorption, thermal degradation, and/or volatilisation (Wylie and Uchiyama, 1996). To further decrease the opportunities for sample loss, a high injection temperature (250 - 280 °C) that flash volatilises the sample, reduces the residence time of the analyte in the

injection port, thus minimising sample loss. Following the injection of the sample, the flow rate of the column is automatically reduced to normal gas chromatographic parameters and the lower temperature analytical thermal program starts. Especially when using semi-volatile compounds like 2-MIB and GSM this method greatly improves sensitivity opposed to standard injection methods (Doherty, 2003).



**Figure 4.1:** Different injection modes for gas chromatography. A) standard injection with low inlet pressure and low initial column flow rate; B) pulsed splitless injection mode with high inlet pressure and high initial column flow rate. (adapted from Doherty, 2003).

When using the pulsed splitless injection mode with a high injection temperature, special consideration must be given to the injection solvent.

Most published methods for the analysis of GSM utilise methanol as the injection solvent (Bellu *et al.*, 2008; Działowski *et al.*, 2009). This can

compromise injection precision when attempting larger volume injections, due to the relatively high expansion volume of methanol compared to other solvents, which results in higher back-flash. Expansion volume is usually described as the ratio of the volume of a given solvent at 250 °C and its volume at room temperature (table 4.4).

**Table 4.4:** Vapour volume expansion volume ratios of four common gas chromatography injection solvents at injection conditions for pulsed splitless injection mode, with water as a comparison (adapted from Agilent Technologies, 2012).

<b><i>Solvent</i></b>	<b><i>Polarity index (P')</i></b>	<b><i>Molecular weight</i></b>	<b><i>Expansion ratio</i></b>
Isooctane	0.1	114	138:1
Ethyl acetate	4.4	88	233:1
Acetone	5.1	58	375:1
Methanol	5.1	32	563:1
Water	10.2	18	1261:1

Injection temperature: 250 °C; column head pressure: 13 psi (90 kPa)

If the expansion volume is greater than the volume of the liner (the sample receptacle), the sample vapour will expand (back-flash) against the rubber septum that seals the injection liner. This will result in loss of sample through split vents and the septum purge lines of the injector, which in turn affects reproducibility. In addition to this the introduction of phthalates from the rubber septum into the sample is also possible. If applied prudently with the appropriate type of solvent pulsed splitless injection of (semi-)volatile compounds such as 2-MIB and GSM can greatly enhance sensitivity of analysis and when combined with a pre-concentration step such as solid phase extraction, detection of sub nano gram levels can be achieved.

The proposed method (table 4.5) used in the evaluation of environmental samples was able to detect 2-MIB and GSM concentrations in the low nano gram range.

**Table 4.5:** Parameters of the optimised GC-MS method.

<i>Parameter</i>	<i>Optimised method</i>
Front inlet parameters	
Injection mode	Pulsed splitless
Injection temperature	250 °C
Inlet pressure	10 psi
Injection (pulsed) pressure	25 psi
Pulse time	0.5 min
Injection volume	3 µL
Gas type	Helium
Column	
Column type	Capillary column
Column length	30 m
Column diameter	250 µm
Film thickness	25 µm
Pressure	10 psi
Mass spectrometer – quantification ions (SIM)	
2-methylisoborneol	95, 107, 135
Trichloroanisole (Internal Standard)	167, 195, 210
Geosmin	112, 125, 182
Temperature program	
Initial temperature	60 °C
0 - 1 min	60 °C
2 - 3 min	20 °C min <sup>-1</sup> (to reach 100 °C)
4 - 10 min	7.5 °C min <sup>-1</sup> (to reach 152 °C)
10 - 12 min	Hold temperature (152 °C)

### **4.2.3 SPE method development for the recovery of 2-MIB and GSM from water**

For the pre-concentration step a solid phase extraction protocol had to be developed in order to achieve a good concentration of the samples prior to the GC-MS analysis. To this end several parameters were investigated, including: sorbent type and load, sample drying time, elution solvent, and sample load.

#### **4.2.3.1 Sorbent and elution solvent selection**

Firstly, the sorbent type was investigated. Two different types of cartridges were tested, Isolute C8 25 mg packing material and Isolute C18 end-capped (EC) 25 mg packing material, cartridge volume for both was 1 mL (both Biotage, Upsala, Sweden). Each cartridge was conditioned with 2 mL of the following solvents in the order shown: hexane, acetone, methanol, and 10 mL Milli-Q. The 2-MIB and GSM spiked water (10 mL at a concentration of  $5 \mu\text{g L}^{-1}$  of each analyte) was loaded onto the conditioned cartridges in triplicate for each cartridge type. Experimental blanks (two) were prepared by passing 10 mL of Milli-Q through pre-conditioned cartridges. The cartridges were allowed to dry under the vacuum overnight (16 h). The cartridges were eluted with isooctane in six 250  $\mu\text{L}$  aliquots, with the eluent of each fraction collected separately into pre-weighted GC-vials. The volume in each vial was made up to 1 mL with isooctane by weight. The samples were then analysed by GC-MS (section 4.2.2) and the data was recorded.

As anticipated from previous findings (Bellu, 2007) the recovery from the C18 cartridges was poor and it was decided to select the C8 sorbent for further

evaluation. To further enhance the recoveries of 2-MIB and GSM, increasing the sorbent mass was investigated. The only alteration to the experimental procedure above was the use of C8 100 mg (EC) cartridge 1 mL reservoir, to compare it to the previously used C8 cartridge with 25 mg packing material. Samples were analysed by GC-MS (section 4.2.2). This was performed in triplicate.

After it had been established that the increased sorbent load improved the recovery of 2-MIB and GSM, the effects of drying time and elution solvent were evaluated. The cartridges (C8 100 mg (EC), 1 mL) were conditioned as described previously and spiked water samples (10 mL, 5  $\mu\text{g L}^{-1}$  of 2-MIB and GSM each) were loaded onto the cartridges. Three different drying times were evaluated 5 min, 15 min, and 30 min. The cartridges were eluted with 1 mL of isooctane or with 1 mL of isooctane with 20 % acetone. The samples were then analysed by GC-MS (section 4.2.2). Triplicate samples for each drying time and elution solvent combination were performed.

The increased polarity that was achieved by the addition of acetone ( $P'=5.1$ , table 4.4) compared to the polarity of isooctane ( $P'=0.1$ ) improved the recoveries of both 2-MIB and GSM, which means that a decreased volume of solvent could be used to elute the samples. The less solvent used for elution the higher the pre-concentration achieved by the SPE. Therefore it was decided that a more polar solvent was needed for the elution of 2-MIB and GSM from the SPE cartridges. The new elution solvent also needed to be suitable for pulsed split-less injection in GC analysis. Ethyl acetate appeared to be an ideal candidate for this with a relatively low expansion volume (1:238)

and an increased polarity ( $P'=4.4$ ) compared to isooctane ( $P'=0.1$ ) (table 4.4). The cartridges were conditioned as described previously and loaded with a spiked water sample (1 mL,  $50 \mu\text{g L}^{-1}$  of each analyte). After drying for 30 minutes the samples were eluted with 1 mL of ethyl acetate. The samples were then analysed by GC-MS (section 4.2.2).

Ethyl acetate appeared promising as a potential elution solvent, however, further evaluation was required in regards to the drying time. This investigation was performed by loading a 10 mL spiked solution ( $5 \mu\text{g L}^{-1}$ ) onto the pre-conditioned cartridges (2 mL: isooctane, acetone, methanol; 10 mL: Milli-Q) in triplicate. The cartridges were dried for 5 minutes and then eluted in four sequential elution steps ( $250 \mu\text{L}$ ). The samples were then analysed by GC-MS (section 4.2.2).

Ethyl acetate delivered good reproducibility and recoveries of both 2-MIB and GSM. However, its suitability as GC-MS injection solvent still needed to be confirmed. For this a set of calibration standards of the 2-MIB and GSM combined standard was produced in ethyl acetate ( $0.5$  to  $100 \mu\text{g L}^{-1}$ ) with  $35 \mu\text{g L}^{-1}$  decane as internal standard. The standards were analysed in triplicate by GC-MS (section 4.2.2).

Following the establishment of ethyl acetate as elution solvent for the SPE step, further investigations of the cartridges were conducted. In this investigation the effect of end-capping (EC) was evaluated. Two different Isolute C8 cartridges were investigated, however, the non-EC cartridge had a

larger cartridge volume (5 mL) with the same sorbent load, which meant that the sorbent bed was much thinner than in the cartridges with 1 mL cartridge volume. All cartridges were conditioned by applying 2 mL of isooctane, 2 mL of acetone, 2 mL of methanol, and 10 mL of distilled water. After SPE had been performed all cartridges were dried for five minutes under vacuum. All vials for elution were pre-weighted and had 100  $\mu\text{L}$  of decane ( $35 \mu\text{g L}^{-1}$ ) in ethyl acetate, as internal standard, added before elution. Elution was performed in eight 250  $\mu\text{L}$  fractions. The combined volumes of the internal standard and the eluent were made up to 1 mL by weight prior to analysis (section 4.2.2). This experiment was performed in triplicate. The volume of the test solution was 10 mL; the concentration of 2-MIB and GSM in the spiked solution was  $5 \mu\text{g L}^{-1}$ .

#### **4.2.3.2 Evaluation of sample loading volume**

So far samples had been loaded manually on the SPE cartridges, which was feasible considering the low volumes used so far (10 mL). However, to achieve sufficient pre-concentration during the solid phase extraction, larger volumes of samples had to be loaded onto the cartridges. Manual loading would be inconvenient and increase the amount of time needed per sample. To this end the effect of polytetrafluoroethylene (PTFE) tubing (used to allow automated loading) on the recoveries of 2-MIB and GSM had to be evaluated. The cartridges were conditioned as described previously (2 mL: isooctane, acetone, methanol; 10 mL: Milli-Q). The spiked water samples were loaded onto the cartridges (100 mL,  $0.5 \mu\text{g L}^{-1}$  2-MIB and GSM). One set of spiked water samples was loaded onto the cartridges manually (with a Pasteur pipette) and one set was introduced into the cartridges via PTFE tubing



(Biotage, Uppsala, Sweden). This experiment was performed in duplicate. The samples were eluted in five sequential aliquots which were analysed individually by GC-MS (section 4.2.2).

After it had been established that loading the sample via PTFE tubing had no detrimental effects on the recoveries of 2-MIB and GSM, the volume of the test solution could be increased further to achieve a higher degree of pre-concentration. To test for break-through, a sample volume of 250 mL was evaluated. The cartridges (C8, 25 mg, 100 mg, 1 mL) were conditioned as described previously and loaded with the spiked water samples ( $0.5 \mu\text{g L}^{-1}$  2-MIB and GSM) in triplicate. After 5 minutes of drying time the samples were eluted in three sequential aliquots which were analysed individually by GC-MS (section 4.2.2).

It was established that a test solution volume of 250 mL could not be passed through the cartridges without sample loss occurring. To determine whether actual break-through occurred or whether the sample loss occurred elsewhere, a new investigation was designed. Two separately conditioned cartridges (2 mL: hexane, acetone, methanol; 10 mL; Milli-Q) were placed on top of each other and an amount of spiked water (250 mL,  $0.5 \mu\text{g L}^{-1}$  2-MIB and GSM) was passed through both cartridges. Both cartridges were dried and eluted separately using three elution steps and analysed by GC-MS (section 4.2.2).

A test solution volume of 200 mL was evaluated. Spiked water samples (200 mL,  $0.1 \mu\text{g L}^{-1}$ ) were passed through pre-conditioned cartridges (conditioned

as described previously) in triplicate. After drying for 5 minutes the samples were eluted with 0.5 mL of ethyl acetate and analysed by GC-MS.

Glass fibre filtration was evaluated as an additional sample processing step since suspended particles in environmental samples can cause blocking or slow loading times in SPE. For the evaluation of the effect of glass fibre filtration on the recoveries of 2-MIB and GSM, samples (200 mL, 0.1  $\mu\text{g L}^{-1}$ ) were filtered through GF/C (Whatman, 5.5 cm diameter) and loaded onto pre-conditioned cartridges in triplicate. In parallel an unfiltered spiked water was processed. Samples were eluted with 0.5 mL of ethyl acetate and analysed by GC-MS (section 4.2.2).

#### **4.2.3.3 Evaluation of suitable internal standard**

During investigations it was found that the SPE cartridges employed contained a hydrocarbon contamination (short carbon chains,  $\text{C}_8$  to  $\text{C}_{14}$ ) (see appendix). Which were noticed in SIM because the ions scanned for the internal standard decane, corresponded to those of the contaminations. Several batches of C8 (EC) cartridges were tested and the option of using a different supplier was evaluated as well. However, the problem persisted in all tested batches and was noted in the product of a different supplier as well. This made it necessary to use a different internal standard. It was decided to use the taste and odour compound trichloroanisole (TCA) at 50  $\mu\text{g L}^{-1}$ , due to its physico-chemical similarity to both 2-MIB and GSM.

#### **4.2.4 Optimised method for SPE**

Following analysis and optimisation of the key steps of SPE for 2-MIB and GSM the optimised solid phase extraction of samples is as follows: If required samples were vacuum filtered (GF/C Whatman filters, diameter 5.5 cm) to remove suspended solids. The sample (200 mL) was placed in a glass bottle (250 mL). Cartridges were conditioned with 2 mL of the following solvents in the order shown: hexane, acetone, and methanol, followed by 10 mL of Milli-Q. PTFE tubing was attached to the cartridges on the vacuum manifold and the glass bottles containing the samples. The samples were loaded onto the cartridges under -0.2 bar of pressure (approximate flow rate 5 mL min<sup>-1</sup>). Once the entire sample had passed through the cartridges, the PTFE tubing was removed and PTFE stoppers were placed on the cartridges to prevent sample loss by volatilisation. The cartridges were allowed to dry for 5 min and finally eluted with 500 µL of ethyl acetate into pre-weight GC vials already containing 50 µL of decane in ethyl acetate (375 µg L<sup>-1</sup>, for a final decane concentration of 35 µg L<sup>-1</sup>). The samples were then weight-adjusted to 550 µL with ethyl acetate and were then analysed by GC-MS (section 4.2.2).

#### **4.2.5 Analysis of environmental samples - Rescobie Loch and fishfarm**

Samples from Loch Rescobie had been collected the day prior to analysis, stored in glass bottles at approximately 4 °C overnight. The following day the samples were vacuum filtered, and then spiked with 0.5 µg L<sup>-1</sup> of the combined 2-MIB and GSM standard. The samples were then pre-concentrated by SPE (section 4.2.4) and analysed by GC-MS (section 4.2.2). The fishfarm samples were received from Pisces Engineering Ltd. fishfarm in glass bottles

(table 4.6). The samples were vacuum filtered to remove suspended solids and 200 mL of each sample was transferred to a clean glass bottle. For each sample SPE was carried out (section 4.2.4) with subsequent analysis by GC-MS (section 4.2.2.).

**Table 4.6:** Samples received from Pisces Engineering Ltd. and their origin.

<b>Origin</b>	<b>Sample</b>
Recirculation Tank 1 - Tank connected to regular recirculation system	Recirc 1
Recirculation Tank 2 - Tank connected to regular recirculation system	Recirc 2
Non-bio recirculation system - Tank connected to a recirculation system that does not employ biofilters	Non-Bio Recirc
Large recircled raceway in operation for > 2 years	Raceway
Artificial outdoor pond with recirculation system	Pond

#### **4.2.6 Stability of 2-MIB and GSM stored on SPE cartridges**

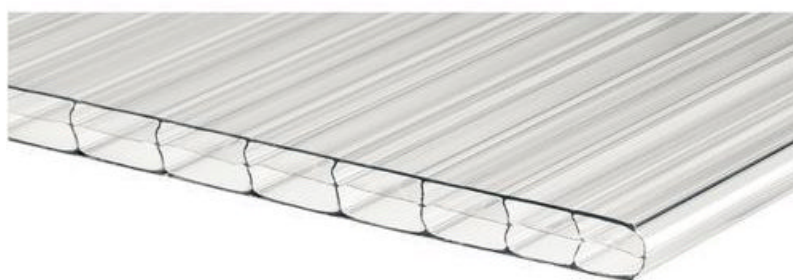
A further advantage of applying SPE as sample pre-concentration is the fact the solid phase extraction of environmental samples can be carried out *in situ* and the cartridges can then be stored to be transported to the location of analysis. To evaluate the stability of 2-MIB and GSM on the C8 (EC) cartridges from an environmental water source (Rescobie Loch), 200 mL of water sample was applied to the pre-conditioned C8 (EC) cartridges (section 4.2.4). One set of replicates (n=3) were immediately eluted and analysed by GC-MS (section 4.2.2). Storage of the cartridges was in the fridge (approximately 4 °C)

wrapped in aluminium foil. Further cartridges (triplicate) were analysed after 24, 48, and 72 h, one week, and two weeks storage.

## **4.2.7 Photocatalysis of 2-MIB and GSM**

### **4.2.7.1 Photocatalytic reactor Version 1 (V1)**

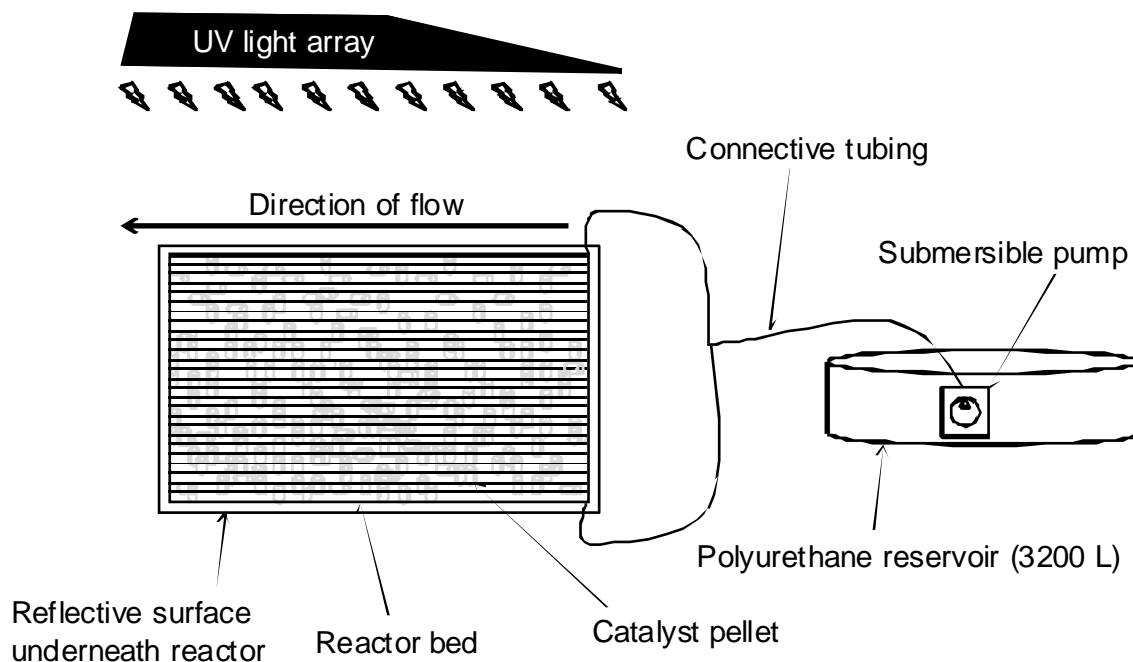
The first design of the photocatalytic reactor was built with commercially available triple walled polycarbonate sheeting (900 mm x 2000 mm x 10 mm; channel dimensions: 10 mm x 8 mm) (figure 4.2) and featured a straight flow through the length of the reactor.



**Figure 4.2:** Triple walled polycarbonate sheeting

The reactor was sealed at one end with a perforated length of polycarbonate capping end-piece (900 mm) (Wickes, UK) and then filled with approximately 20 kg of  $\text{TiO}_2$  catalyst in pellet form (Hombikat K01/C, Duisburg, Germany). Along the length of a 1000 mm, 25 mm bore, plastic tube slits of approximately 80 to 100 mm length were cut to facilitate water flow into the reactor (figure 4.3). This perforated tube was then attached, slits facing into the reactor, to the unsealed end of the sheet and sealed. A reflective acrylic sheet (1000 mm x 2100 mm) was attached to a board of marine ply wood of the same size and the reactor was placed on this assembly. The reflective sheet acted as a reflector behind the reactor when in operation. A

commercially available UV light array (sun bed for psoriasis treatment), consisting of a single bank of 12 UVB lamps (100 W each, spectral output: 280 to 330 nm) was used as light source.



**Figure 4.3:** Reactor V1 in operation for the determination of the photocatalytic efficiency of the degradation of 2-MIB and GSM.

To test reactor (V1), a submersible pump (max flow  $2.5 \text{ m}^3 \text{ h}^{-1}$ , Messner, Kalletal, Germany) was placed in a polyurethane reservoir (3200 L) filled with approximately 3000 L of tap water. A spiking solution of 2-MIB and GSM was produced by adding 1.5 mL of the combined 2-MIB and GSM standard ( $100 \text{ mg L}^{-1}$ ) to 10 L of tap water. This would achieve an approximate concentration of  $0.05 \text{ mg L}^{-1}$  of 2-MIB and GSM in the final testing solution. An initial sample was taken from the reservoir and the pump was switched on and allowed to pump water (flow rate  $2.5 \text{ m}^3 \text{ h}^{-1}$ ) without illumination for 15 minutes to ensure a stable, constant flow and for dark adsorption to take place. A sample was taken after this 15 min period and the lamps were switched on initially at

distance of 40 to 50 cm (differences due to curvature of lamp array) (figure 4.4). Following 10 minutes of constant illumination a sample was collected from the reactor outflow. The distance between the lamp and the UV array and the reactor was then reduced (10 – 20 cm; figure 4.5) to investigate the effect of higher illumination.

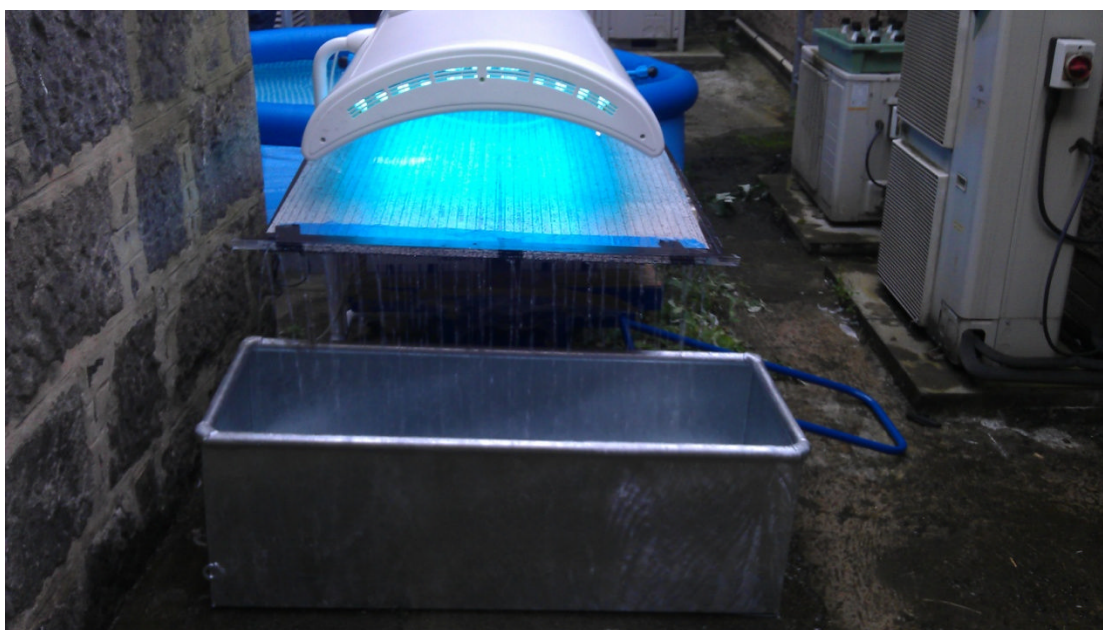
Further samples were then collected for analysis (table 4.7).

**Table 4.7:** Sampling regime during the photocatalytic destruction of 2-MIB and GSM over TiO<sub>2</sub> in continuous flow reactor V1.

<b><i>Sampling regime</i></b>	<b><i>Treatment</i></b>
Initial sample (T <sub>0</sub> <sub>1</sub> )	Sample taken from reservoir
Dark adsorption sample taken (T <sub>0</sub> <sub>2</sub> )	Sample taken after 15 min of flow without illumination
Sample taken from effluent	Sample taken after 10 minutes of illumination (40-50 cm distance)
Sample taken from effluent	Sample taken after additional 20 min of illumination (10-20 cm distance)
Sample taken from effluent	Sample taken after additional 10 minutes of illumination (10-20 cm distance)
Sample taken from reservoir to assess remaining 2-MIB and GSM concentrations	Sample taken from reservoir 1 h after T <sub>0</sub>



**Figure 4.4:** Reactor in operation with 40 to 50 cm distance of illumination



**Figure 4.5:** Reactor in operation with 10 to 20 cm distance of illumination

The samples were then pre-concentrated by SPE (section 4.2.4) and analysed by GC-MS (section 4.2.2). The spiking solution concentration was also analysed, by adding 10  $\mu\text{L}$  of the spiking solution to 30 mL of distilled water

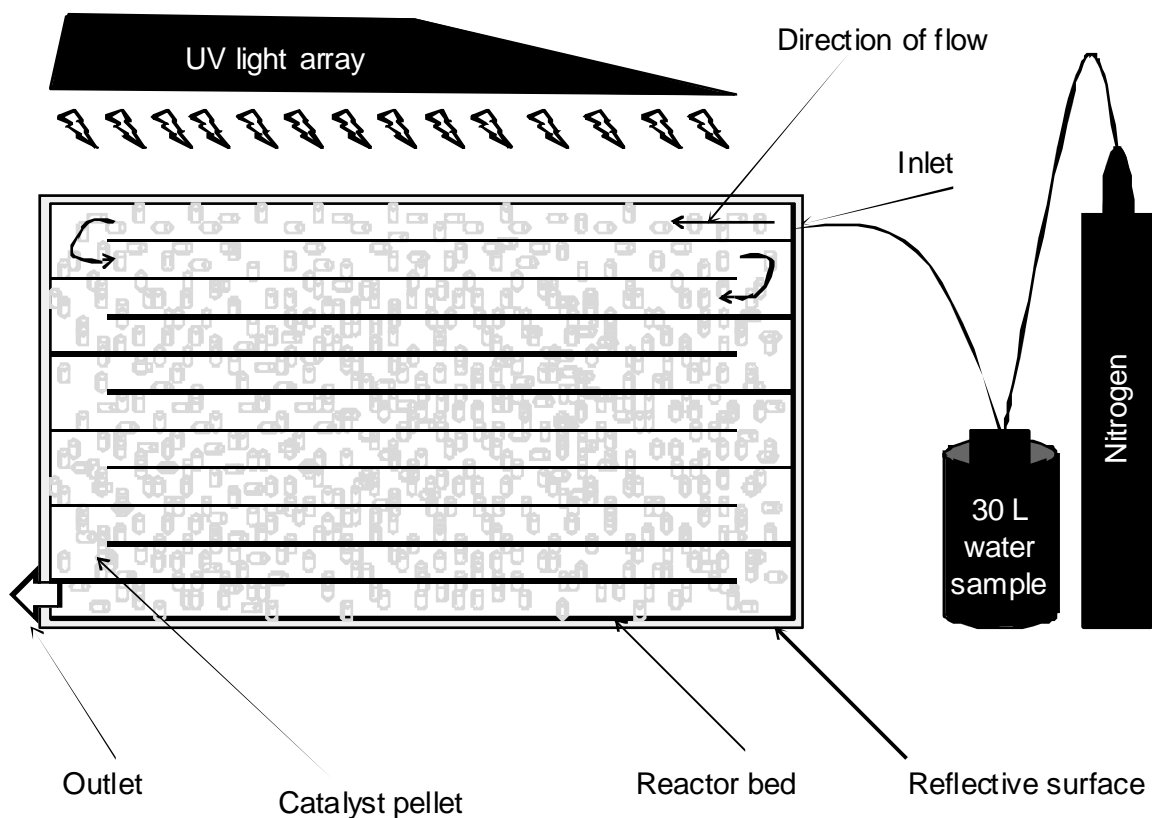


(thus achieving same concentration of analytes that was present in the reservoir:  $0.05 \mu\text{g L}^{-1}$ ), pre-concentration by SPE (section 4.2.4) and analysis by GC-MS (section 4.2.2) was carried out.

#### **4.2.7.2 Photocatalytic reactor Version 2 (V2)**

The performance evaluation of the photocatalytic efficiency of reactor V1 revealed considerable loss of analytes (97 %). The most likely cause was non-specific adsorption to the polyurethane of the water reservoir, used to store the spiked water prior to conveyance through the reactor and the polyurethane tubing of the reactor (Elhadi *et al.*, 2004). Furthermore the determination of the concentrations of 2-MIB and GSM did not demonstrate any evidence of analyte degradation, most likely due to the short residence time of the sample in the reactor, caused by the path length and flow rate employed. Therefore a modified reactor was designed that would address these limitations. The second reactor design was also built with commercially available polycarbonate sheeting (PLEXIGLAS ALTOP® SP, Evonik, Essen, Germany), with a guaranteed > 97 % UV light transmittance. The polycarbonate sheeting in this case was double walled and less compartmentalised than the previous material (channel dimensions 64 mm x 18 mm compared to 10 mm x 8 mm). This layout allowed for a different flow pattern and the new reactor was designed in such a fashion that the flow would move back and forth through the reactor allowing for a much longer resident time of the spiked water in the reactor. To facilitate this, 60 mm segments were removed from the inner vertical dividers on alternating end of the sheet. One side of the reactor was then sealed with the capping end-piece

(Wickes, UK). The end-piece covering the nearest channel to the edge of the sheet was perforated to allow the outflow of the effluent. The reactor was filled with the same type of catalyst as the previous design (Hombikat K01/C pellets). Then the other side was sealed with the capping end-pieces, only allowing one channel nearest the edge, diagonally opposite to the outlet, to remain open to receive the tubing that would introduce the spiked water into the reactor (figure 4.6).



**Figure 4.6:** Reactor V2 in operation for the determination of the photocatalytic efficiency of the degradation of 2-MIB and GSM.

To avoid sample loss due to non-specific binding stainless steel pressure cans were used. Four pressure cans were filled with 30 L each of Milli-Ro water that was spiked to achieve a concentration of  $0.1 \mu\text{g L}^{-1}$  in the final solution. Three

samples (200 mL) were taken from each of the pressure cans and treated as  $T_0$  sample. Nitrogen gas was used as propellant. The content of the first pressure can was passed through the reactor at approximately  $2 \text{ L min}^{-1}$  without illumination, three samples (200 mL) were taken. The next water samples were passed through the reactor at approximately the same flow rate under illumination. Samples were collected for each water aliquot (200 mL). Samples were pre-concentrated by SPE (section 4.2.4) and analysed by GC-MS (section 4.2.2). A second series of test was performed in the same manner as described above with the exception that water from the raceway at Pisces Engineering Ltd. was used (samples collected on 07.07.2012). The samples remained un-spiked.

## **4.2.8 Development of passive sampling for GSM and 2-MIB**

### **4.2.8.1 Pre-extraction of silicone**

Silicone (Laboratory, Translucent (Talc Free) AlteSil™ Silicone sheet- 0.5mm, Altec Products Limited, Bude, UK) was cut into 60 mm x 40 mm rectangles. The silicone rubber membranes (SRMs) were placed into a Soxhlet extractor, which was filled with approximately 300 mL of ethyl acetate to which was added a pinch of anti-bumping granules. Each batch of SRMs was extracted for 30 h. Then the SRMs were transferred into a bottle (500 mL) and stored in methanol. After extraction SRMs were only handled with forceps to avoid contamination.

### **4.2.8.2 Evaluation of uptake of 2-MIB and GSM onto SRMs**

A pre-extracted silicone rubber membrane was placed into a 70 mm screw top bottle (Kinesis, UK), to which each was added a spiked 2-MIB and GSM solution of Milli-Ro water (20 mL, 80  $\mu\text{g L}^{-1}$  of each analyte) in triplicate. A 0.5 mL aliquot of the spiked solution was retained for analysis ( $T_0$ ). The membrane was then placed on a shaker at 300 rpm for 24 h at 22 °C. After which the membrane was removed from the spiking solution, dried with tissue paper and transferred into an empty screw top vial and 20 mL of ethyl acetate added. The strip was then placed on the shaker for 1 h, after which the solvent was exchanged with another 20 mL of fresh ethyl acetate. Five sequential extractions were performed in this manner. A sample (0.5 mL) of the remaining spiked Milli-Ro solution was collected ( $T_{\text{final}}$ ). The  $T_0$  and  $T_{\text{final}}$  samples were passed through SPE (section 4.2.4), dried for 5 min, and eluted with 1 mL of ethyl acetate to facilitate a solvent exchange, no pre-

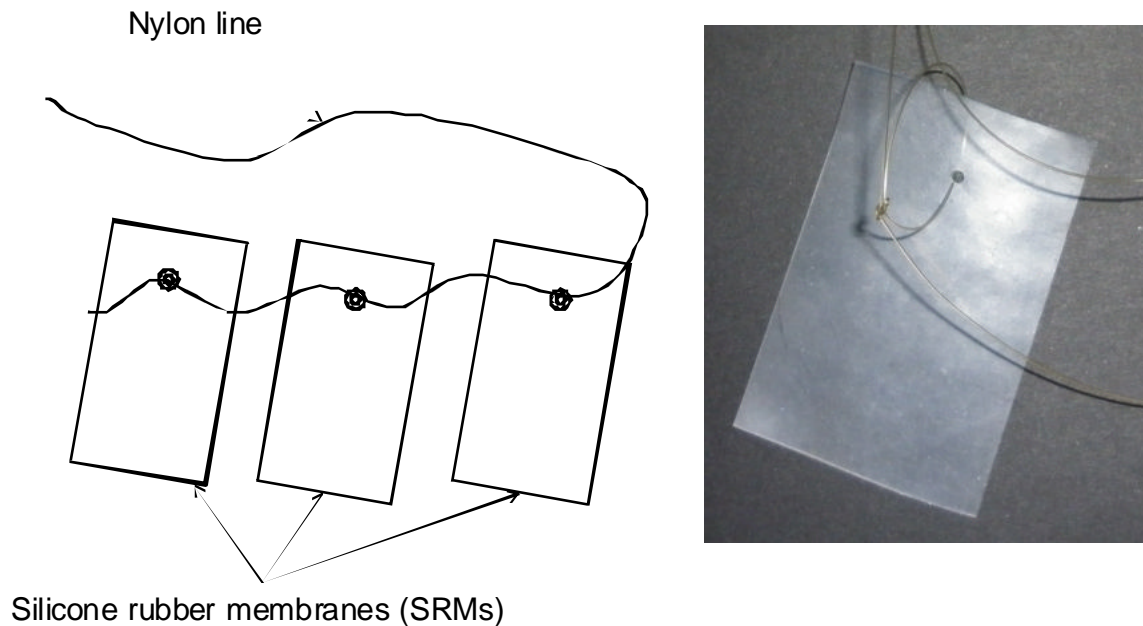
concentration was performed. All samples were analysed by GC-MS (section 4.2.2).

#### **4.2.8.3 Determination of the silicone rubber membrane water partition coefficient ( $K_{SRMW}$ ) of 2-MIB and GSM**

For this experiment five pre-extracted SRMs were placed into screw top bottles and covered with a spiked 2-MIB and GSM solution (20 mL Milli-Ro water, 80  $\mu\text{g L}^{-1}$  of each analyte) in triplicate. An aliquot (0.5 mL) was taken from each bottle ( $T_0$ ). The bottles were placed on a shaker at 300 rpm at 22 °C. Single membranes were removed from the shaker at the following intervals: 1, 2, 6, 12, and 24 h. At each sampling point an aliquot (0.5 mL) was retained for later analysis ( $T_{\text{final}}$ ). The membranes were extracted in two sequential extraction steps of 1 h each in ethyl acetate, as it was found that two extraction steps were sufficient. The  $T_0$  and  $T_{\text{final}}$  samples underwent a solvent exchange by SPE (section 4.2.4) and analysed along with the silicone membranes by GC-MS (section 4.2.2). After the last extraction step, the silicone strips were placed on aluminium foil in a fume cupboard and allowed to dry for approximately 1 h. When the strips were dry, they were placed on a balance and their weight was recorded as the weight of the strip was required for the determination of the partition coefficient of 2-MIB and GSM.

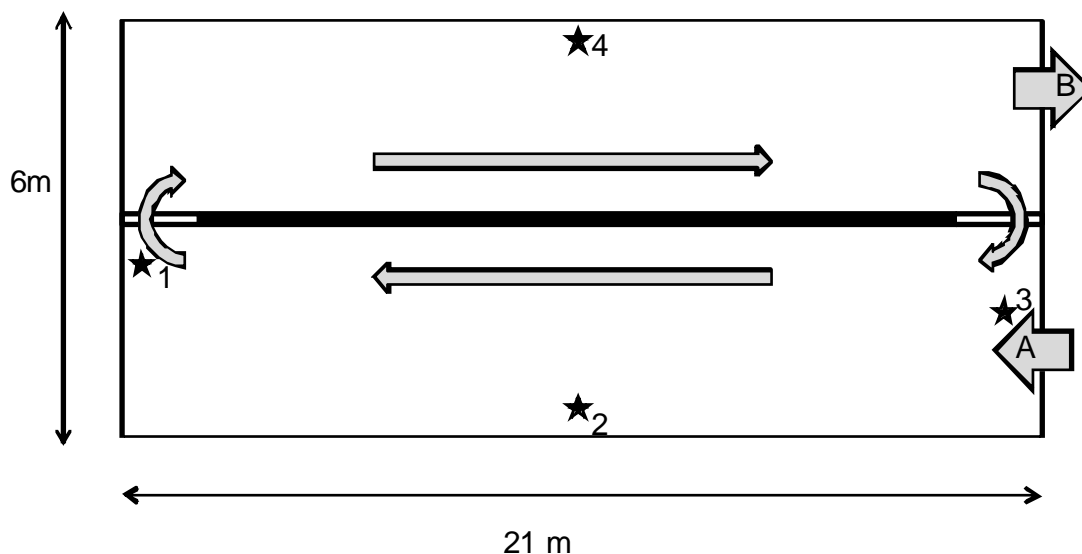
#### 4.2.8.4 Field testing of SRMs

For the field test, four passive samplers were assembled from nylon line and pre-extracted SRMs. To assemble a passive sampler three pre-extracted SRMs were attached to a length of nylon line (approximately 1.5 m) (figure 4.7).



**Figure 4.7:** The assembled passive sampling device with three silicone rubber membranes (SRMs) attached to a length of fishing line.

The passive samplers were deployed in a carp rearing raceway at Pisces Engineering Ltd. (figure 4.8). This raceway had been in operation for approximately 2.5 years and was known to exhibit detectable levels of 2-MIB and GSM.



**Figure 4.8:** Diagram of 2.5 year old raceway at Pisces Engineering Ltd. Grey arrows indicate direction of water flow. Large arrow A indicated the inlet from the recirculation system; large arrow B indicates outlet to recirculation system; ★ indicates deployment location for passive samplers. Pool depth: approximately 1.3 m (average).

The samplers were deployed and left *in situ* for 6 h, because equilibrium was known to be achieved at that point (section 4.2.8.3). Following exposure samplers were recovered, each strip was dried with tissue paper, detached from the sampling device and placed into a screw top bottle. Water samples were also taken at each sampling location to perform a SPE-GC-MS determination of the amounts of 2-MIB and GSM. This was done to be able to compare the results achieved by the passive samplers. Immediately after arriving in the laboratory the strips were extracted in ethyl acetate with the method described in section 4.3.9.2. Of the water samples taken at each sampling location, 200 mL aliquots were passed through SPE in triplicate (section 4.2.4) and eluted with 0.5 mL ethyl acetate. All samples were analysed by GC-MS (section 4.2.2).

#### **4.2.8.5 Determining stability of 2-MIB and GSM on SRMs**

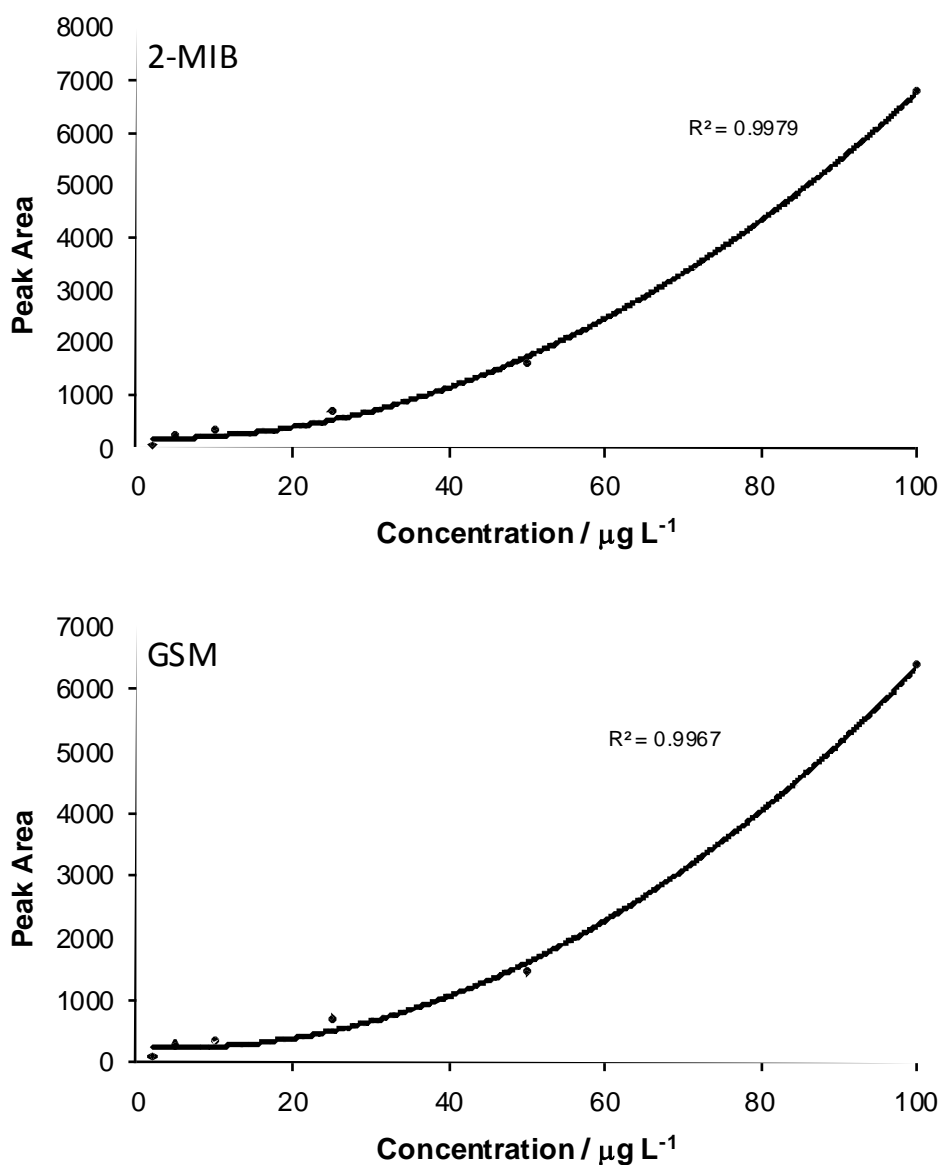
Three sets of passive samplers were assembled (section 4.2.8.4). They were deployed in the carp rearing raceway at Pisces Engineering Ltd. at sampling location 3 for 6 h. The samplers were recovered and each strip was dried with a tissue and placed into a screw-top bottle. Triplicates were stored for 68 h at room temperature, in the fridge (4 °C), and in the freezer (-20 °C). After the 68 h had elapsed the strips were extracted in sequential two extraction steps and analysed by GC-MS (section 4.2.2).



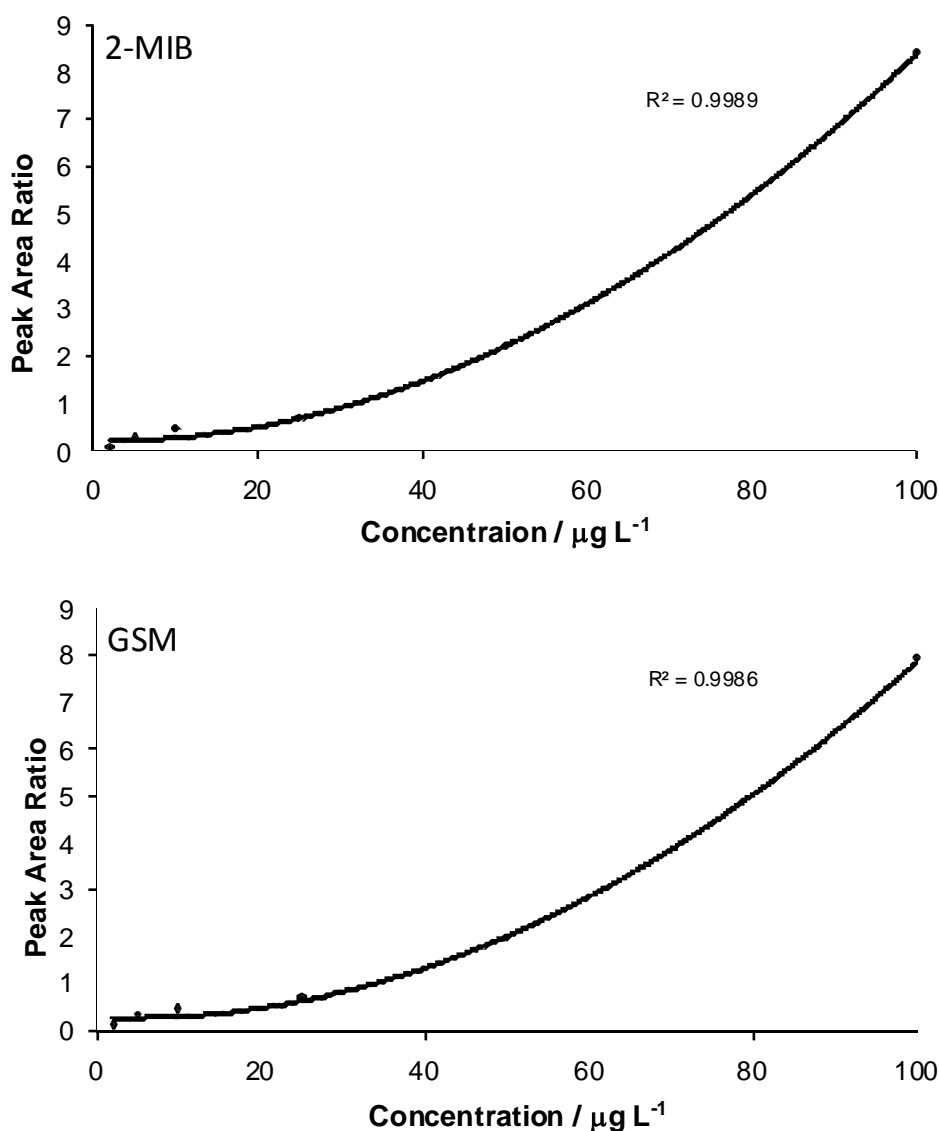
## 4.3 Results

### 4.3.1 Optimisation of GC-MS method

The external and internal calibrations for 2-MIB and GSM in ethyl acetate show good precisions (figures 4.9, 4.10).



**Figure 4.9:** External calibration (polynomial) for A) 2-MIB and B) GSM. Error bars=1 SD; n=3

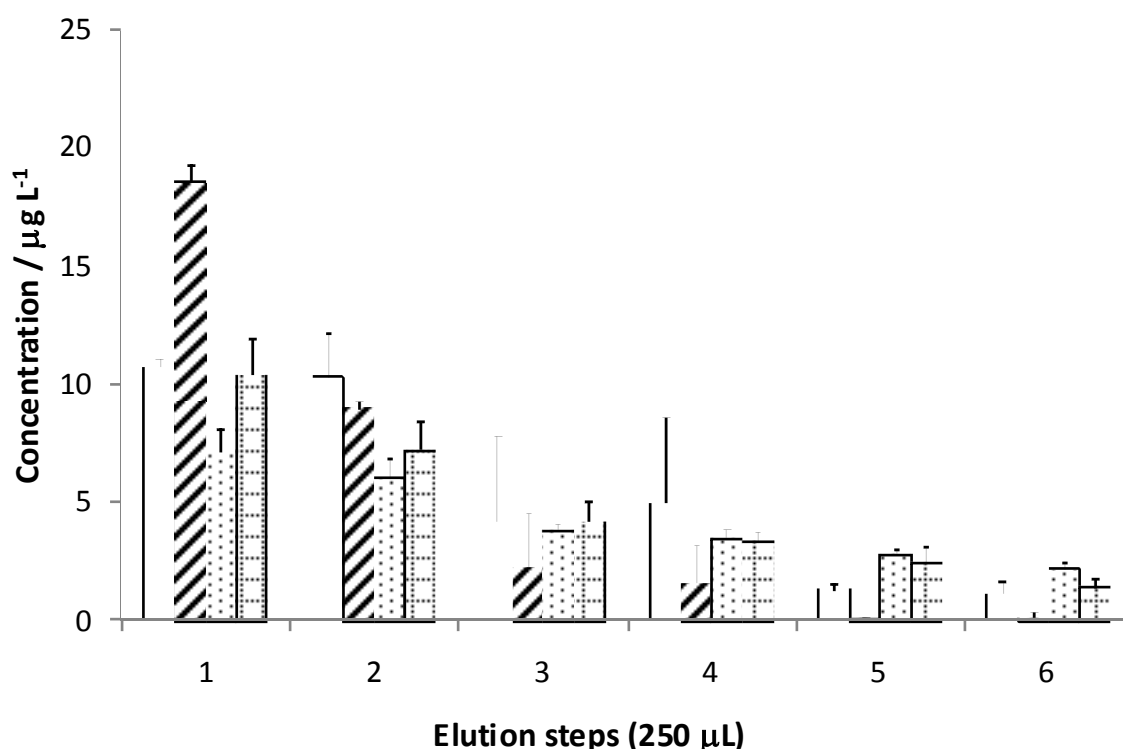


**Figure 4.10:** Internal calibration ( $35 \mu\text{g L}^{-1}$  decane) (polynomial). Error bars=1 SD;  $n=3$

As would be expected, slightly better precision is achieved with the internal calibration for both 2-MIB and GSM. However acceptable precision is also achieved without the use of an internal standard.

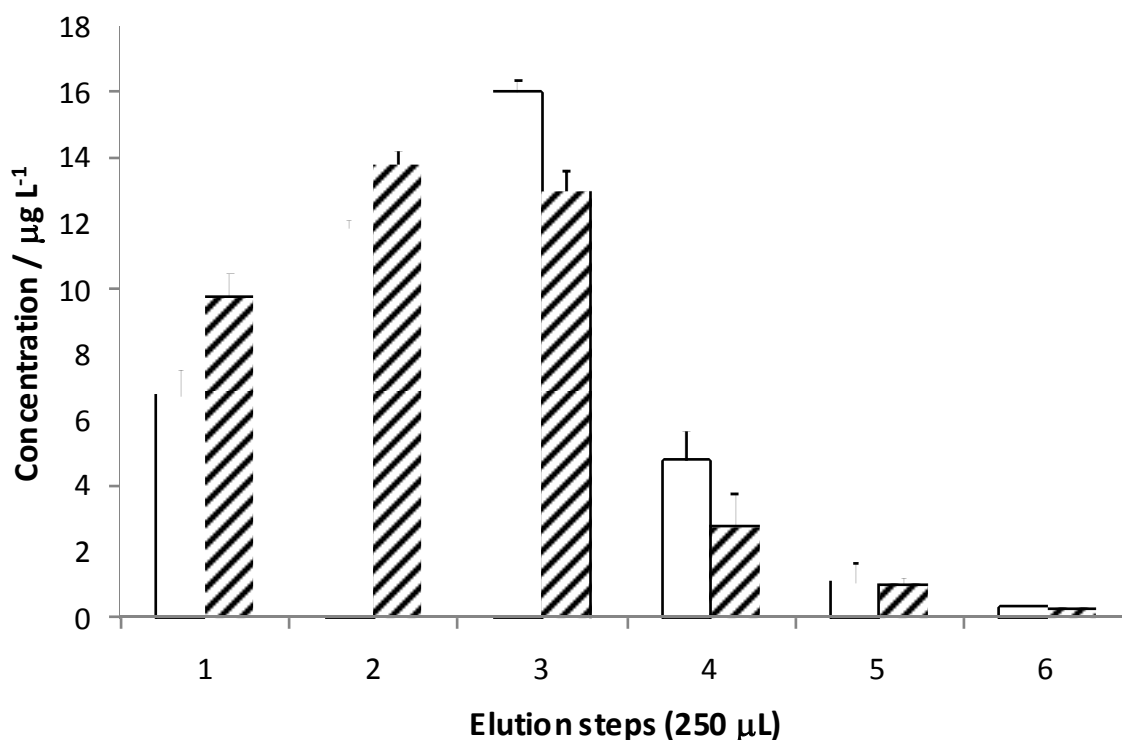
### 4.3.2 Optimisation of SPE method

Various factors concerning the solid phase extraction (SPE) of water samples containing 2-MIB and GSM were investigated. SPE is a useful tool that fulfils a number of roles; it serves to pre-concentrate the samples prior to analysis, and allows for a solvent exchange in one step. The first investigation was to determine the most suitable type of sorbent for 2-MIB and GSM. Commonly C18 cartridges are used (Conte *et al.*, 1996; Dzialowski *et al.*, 2009) for the solid phase extraction of 2-MIB and GSM, in this investigation C8 cartridges were also evaluated. The elution profile of the different cartridges showed that 2-MIB and GSM can be recovered from the C8 with less elution solvent than from the C18 cartridges (figure 4.11).



**Figure 4.11:** Elution profile of C18 (EC) and C8 (EC) cartridges for 2-MIB and GSM, elution performed with 250 µL isooctane. ▭ C8 2-MIB; ▨ C8 GSM; ▩ C18 MIB; ▪ C18 GSM. Error bars=1 SD, n=3

The C8 cartridges tested clearly performed better than the C18 ones and it was decided to proceed with the C8 cartridges for any further experiments (table 4.7). The recoveries for both 2-MIB and GSM were still relatively low (48 and 68 % respectively) and it was proposed that the amount of sorbent in the cartridge may play a role in how much of the 2-MIB and GSM would be retained and subsequently recovered. Hitherto 25 mg of sorbent material had been used, hence the effects of increasing the amount of the sorbent material four-fold to 100 mg were investigated (figure 4.12).



**Figure 4.12:** Elution profile of C8 (EC) 100 mg cartridges for 2-MIB and GSM, elution performed with 250 µL isooctane. ▭ 2-MIB; ▨ GSM

Comparing the results of the investigation of C8 25 mg sorbent load and 100 mg sorbent load, it can be observed that, all other factors remaining the

same, more of the 2-MIB and GSM was retained on the cartridges with the higher amount of sorbent material (table 4.8).

**Table 4.8:** Comparison of C8 (EC) and C18 (EC) cartridges and different sorbent loads

<b>Cartridge type</b>	<b>% Recovery</b>	
	<b>2-MIB</b>	<b>GSM</b>
C8 25 mg	48 ± 2	68 ± 4
C18 25 mg	28 ± 4	46 ± 2
C8 100 mg	84 ± 3	85 ± 2

While isooctane is ideal for gas chromatography due to its low expansion volume, it is less ideally suited to the elution of the 2-MIB and GSM from the SPE cartridges due to its low polarity (table 4.4). It requires a high elution volume, which means a lesser degree of pre-concentration. Therefore isooctane was mixed with a more polar solvent and tested (acetone). Considering the greater expansion volume of acetone a relatively low concentration of 20 % was chosen (table 4.4). The results show that GSM tends to display higher variability than 2-MIB and that generally less GSM is recovered (table 4.9).

**Table 4.9:** Investigation of drying times and elution solvents. Error=1 SD; n=3

	<b>% Recovery</b>					
	<b>Isooctane</b>			<b>Isooctane with 20 % acetone</b>		
	<i>5 min</i>	<i>15 min</i>	<i>30 min</i>	<i>5 min</i>	<i>15 min</i>	<i>30 min</i>
2-MIB	82 ± 8	76 ± 2	74 ± 1	82 ± 7	90 ± 1	89 ± 5
GSM	63 ± 9	67 ± 8	59 ± 3	75 ± 15	73 ± 3	81 ± 14

Furthermore, the effect of adding 20 % acetone to isooctane improved the recovery of 2-MIB and GSM. The results indicate that a more polar elution

solvent is capable of removing more 2-MIB and GSM from the sorbent than is a less polar solvent with an equal volume. This proved that the polarity of the elution solvent played an important role in the amounts recovered. A new investigation was devised to evaluate ethyl acetate as potential elution/GC-MS injection solvent. Ethyl acetate was chosen because it strikes a balance between having a relatively low expansion volume and being more polar than isooctane. The results of this experiment proved that ethyl acetate was a more suitable solvent than isooctane for the elution of the 2-MIB and GSM (table 4.10).

**Table 4.10:** Comparison of the efficiency of isooctane and ethyl acetate as elution solvents for 2-MIB and GSM from C8 (EC) 100 mg, 1 mL cartridges at different drying times. Error=1 SD; n=3

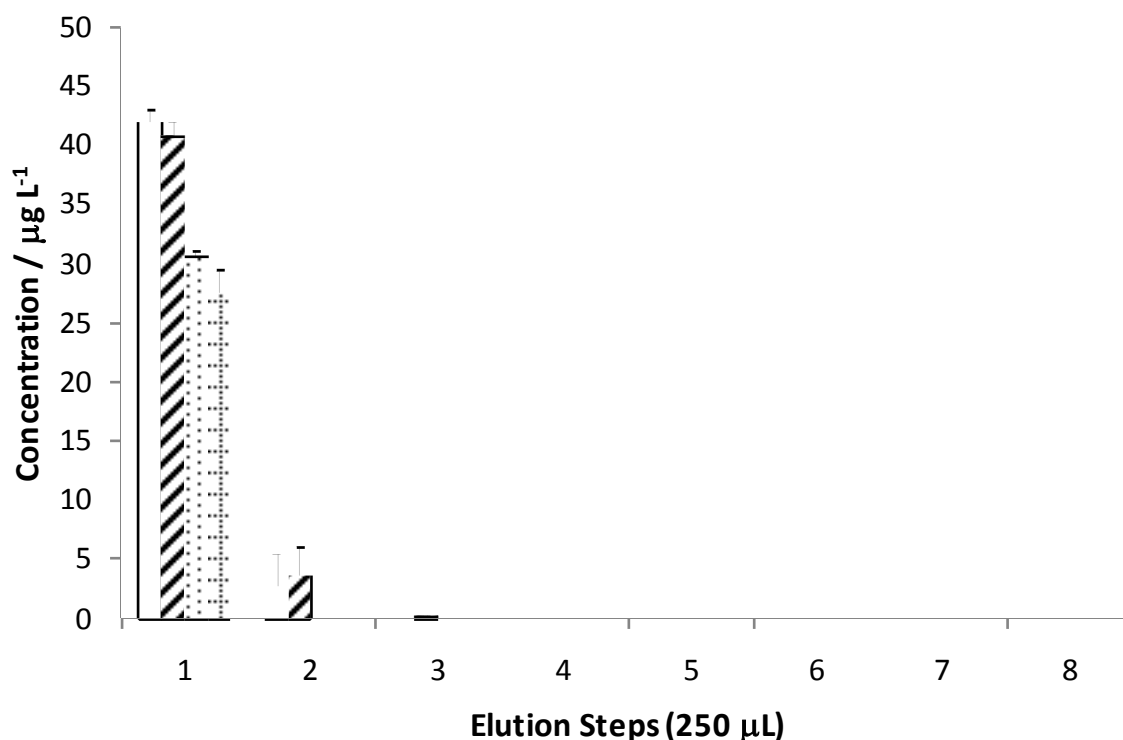
	<b>% Recovery</b>			
	<b>Isooctane</b>		<b>Ethyl acetate</b>	
	<i>5 min</i>	<i>30 min</i>	<i>5 min</i>	<i>30 min</i>
2-MIB (% recovery)	82 ± 8	74 ± 1	80 ± 2	70 ± 5
GSM (% recovery)	63 ± 9	59 ± 3	81 ± 1	72 ± 7

The number of fractions needed to completely remove all 2-MIB and GSM from the sorbent material was also investigated, results show that one fraction was sufficient to completely remove all of the 2-MIB and GSM from the cartridges (table 4.11).

**Table 4.11:** Result of the analysis of the four separate fractions (250  $\mu$ L) analysed after SPE of 2-MIB and GSM in C8 (EC) 100 mg, 1 mL cartridges with ethyl acetate as elution solvent. Error=1 SD; n=3

<b><i>Fraction</i></b>	<b><i>2-MIB (% recovery)</i></b>	<b><i>GSM (% recovery)</i></b>
1 <sup>st</sup>	80 $\pm$ 2	81 $\pm$ 3
2 <sup>nd</sup>	n/d	n/d
3 <sup>rd</sup>	n/d	n/d
4 <sup>th</sup>	n/d	n/d

It was also established that a drying time of 5 min was more beneficial to the recovery of both 2-MIB and GSM than drying for 30 minutes or more. This is due to the high volatility of these compounds. Having established ethyl acetate as elution/GC-MS injection solvent, focus was returned to the SPE cartridges. It had been established that C8 cartridges offered better recoveries than C18 cartridges. All cartridges used so far were end-capped, however, an investigation was carried out to assess whether end-capping had a beneficial effect on the recoveries of 2-MIB and GSM or not (figure 4.13 ; table 4.12).



**Figure 4.13:** Elution profile of C8 (EC) and C8 (Non-EC) cartridges for 2-MIB and GSM, elution performed with 250 µL ethyl acetate. □ C8 (EC) 2-MIB; ▨ C8 (EC) GSM; ▤ C8 (Non-EC) MIB; ▩ C8 (Non-EC) GSM. Error bars=1 SD, n=3

It was demonstrated that end-capping allows for a higher recovery of both 2-MIB and GSM from the cartridges allowing for higher recoveries. In the non-end-capped cartridges non-reversible binding of the analytes occurred resulting in a lower recovery.

**Table 4.12:** Results of the investigation on the effect of end-capping on C8 cartridges (100 mg, 1 mL). Error=1 SD; n=3

	<b>C8 end-capped (%)</b>	<b>C8 non end-capped (%)</b>
2-MIB	81 ± 3	57 ± 1
GSM	83 ± 2	52 ± 4

Initial optimisation tests were performed with relatively low volumes of testing solution to facilitate rapid processing, the degree of desired pre-concentration



needed for the analysis of the environmental samples meant that higher volumes would be needed to ensure that the concentrations of the pre-extracted samples fell within the LOD of the method. Furthermore, all samples were manually applied to the cartridges with the aid of Pasteur pipettes, which, while an arduous process, was achievable for samples of a volume no greater than 10 mL. This, however, would become unjustifiably time consuming with larger sample volumes and be contrary to the aim of a simple and rapid method. The use of polytetrafluoroethylene (PTFE) tubing to deliver the sample in to the cartridges was investigated. The concern with PTFE was the possibility of the 2-MIB and GSM adhering to the tubing resulting in poor analyte recoveries. A comparative study was designed where 100 mL of the spiked water was either pipetted into the cartridges or delivered into the cartridges by PTFE tubing (table 4.13).

**Table 4.13:** Comparison between manual feed and PTFE tube feed for the recovery of 2-MIB and GSM from C8 (EC) 100 mg, 1 mL cartridges. Error=1 SD; n=3

	<b>Manual Delivery (% recovery)</b>	<b>Delivery by PTFE tube (% recovery)</b>
2-MIB	93 ± 3	95 ± 2
GSM	93 ± 2	95 ± 1

The results for this investigation clearly show that the use of PTFE tubing does not negatively impact on the recoveries of neither 2-MIB nor GSM.

Further investigations were carried out to assess the optimum volume that could be applied to the selected cartridges without break-through occurring. In this investigation 250 mL of the spiked water was applied to SPE with GC-MS analysis. The use of a sample volume of 250 mL would mean an almost 450-

fold concentration of the sample, which would allow for the analysis of environmental samples well under the taste and odour threshold. The results of the experiment revealed that a significant amount of 2-MIB and GSM was lost (table 4.14).

**Table 4.14:** Testing C8 (EC), 100 mg, 1 mL cartridges with a sample volume of 250 mL for the recovery of 2-MIB and GSM. Error=1 SD; n=3

<b>Compound</b>	<b>Recovery (%)</b>
2-MIB	75 ± 7
GSM	79 ± 8

To ascertain whether actual break-through had occurred or whether sample loss had occurred due to different reasons, such as volatilisation, an investigation was devised. Two cartridges were placed on top of one another. In this configuration any of the 2-MIB and GSM that broke through the first cartridge would be retained by the second cartridge. The combined concentrations of both cartridges would then represent the entire amount recovered and should, relatively, closely correspond to the amount that the water was spiked with considering previous experiments yielded 95 % recovery. The results show a small amount of 2-MIB (4 %) had broken through the first cartridge (2-MIB recovery: 74 %; GSM recovery: 78 %), however, no GSM was detected on the second cartridge, suggesting that no break-through had occurred but that sample loss occurred by an alternative means.

However, the combined amounts recovered from both cartridges were not close to the expected yield of around 95 % from previous experiments. These results suggested that 250 mL was too large a sample volume, hence it was repeated with a lower volume (200 mL) (table 4.15). Another factor that was tested at the same time was whether vacuum filtering through glass fibre filters would negatively impact on the recoveries of 2-MIB and GSM. This would become important once environmental samples were investigated as the suspended solid in the samples would block the cartridges and increase the time needed for solid phase extraction, potentially allowing for parts of the 2-MIB and GSM to volatilise, or the cartridge to dry out during SPE. These factors would result in a decreased precision of the final analysis, which would be undesirable considering that samples with environmentally relevant concentrations of 2-MIB and GSM would be in the nano-gram range.

**Table 4.15:** Result of using a test solution volume of 200 mL for the recovery of 2-MIB and GSM from C8 (EC) 100 mg, 1 mL cartridges and the effects of glass fibre filtering the test solution prior to SPE. Error=1 SD; n=3

<b>Compound</b>	<b>200 mL unfiltered (%)</b>	<b>200 mL filtered (%)</b>
2-MIB	90 ± 1	89 ± 2
GSM	91 ± 2	92 ± 1

There was no significant loss in the recovery of 2-MIB and GSM when the test solution was vacuum filtered prior to SPE. The 200 mL spiked water sample gave acceptable recoveries (~ 90 %) and was adopted as the standard volume for SPE sample pre-concentration.

The instrumental and method limit of detection (LOD) and limit of quantification (LOQ) were determined by calculating three times and ten times

the signal to noise ratio of the lowest standard ( $2 \mu\text{g L}^{-1}$ ) respectively (table 4.16).

**Table 4.16:** Instrument and method limits of detection (LOD) and quantification (LOQ) for 2-MIB and GSM.

	<i>Instrument LOD (<math>\mu\text{g L}^{-1}</math>)</i>	<i>Instrument LOQ (<math>\mu\text{g L}^{-1}</math>)</i>	<i>Method LOD (<math>\text{ng L}^{-1}</math>)</i>	<i>Method LOQ (<math>\text{ng L}^{-1}</math>)</i>
2-MIB	0.35	1.16	0.99	3.22
GSM	0.36	1.17	0.99	3.19

The method limits of detection and quantification are based on a 200 mL sample loaded on SPE cartridges with a 0.55 mL final eluent volume.

#### 4.3.3 Analysis of environmental samples: Rescobie Loch and fishfarm

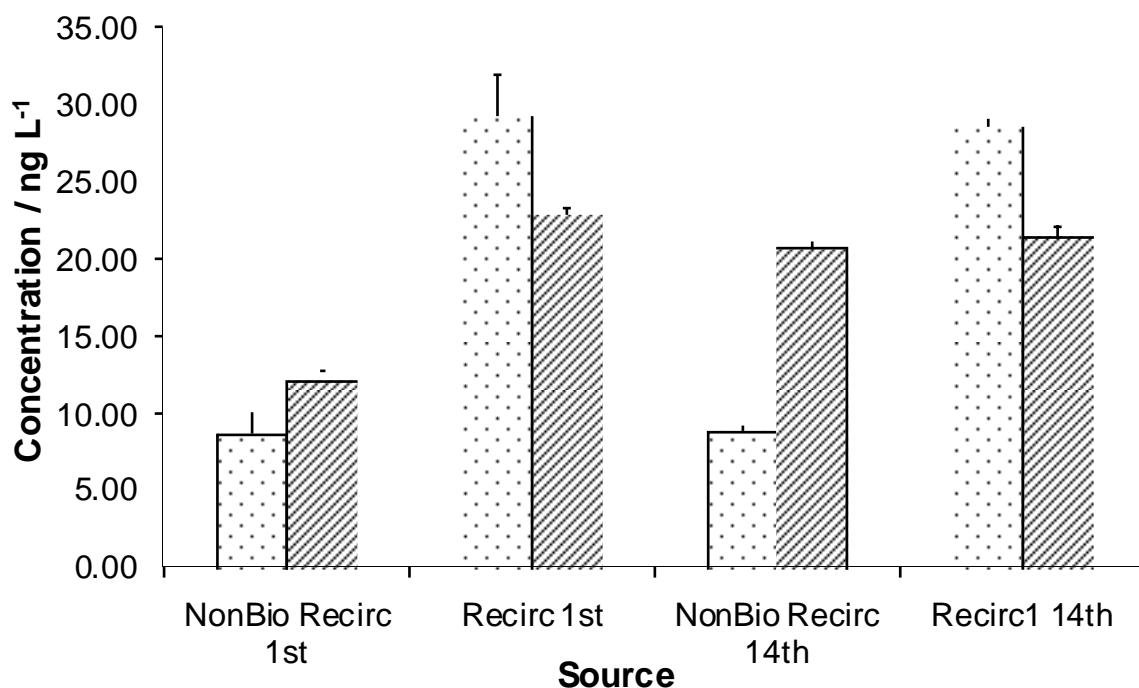
To evaluate the suitability of the SPE method for the detection and quantification of 2-MIB and GSM, two natural waters were selected. Samples were taken from Rescobie Loch in Angus, Scotland. Samples were collected from the north shore. The lake water was found to be containing 2-MIB and GSM, both compounds were close to the human taste and odour threshold (table 4.17).

**Table 4.17:** Determination of the presence of 2-MIB and GSM in Rescobie Loch, Angus, Scotland on 14.07.2011. Error=1 SD; n=3

	<i>MIB (<math>\text{ng L}^{-1}</math>)</i>	<i>GSM (<math>\text{ng L}^{-1}</math>)</i>
Rescobie Loch	$5.3 \pm 0.04$	$1.68 \pm 0.05$

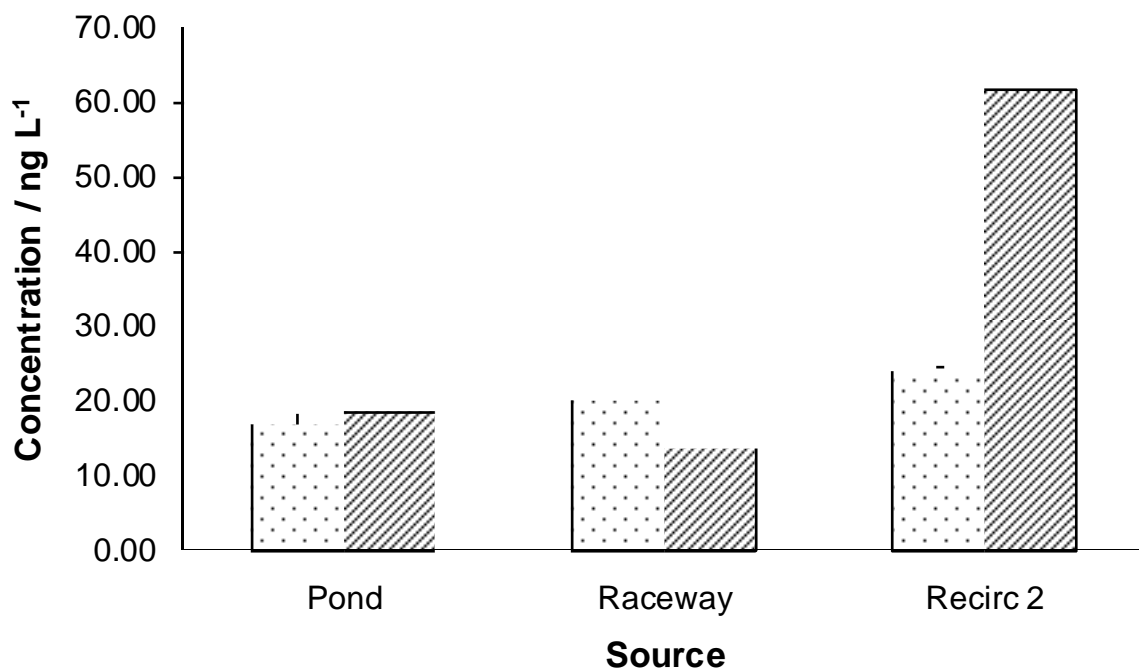
The other samples were received and collected from Pisces Engineering Ltd.. The first analysis was of the recirculation tank 1 (RT1) and the non-bio

recirculation system (NBR) with samples from two different sampling dates (figure 4.14).



**Figure 4.14:** Analysis of 2-MIB (▤) and GSM (▨) at Pisces Engineering Ltd. Analysis of Non-bio recirculation system (Non-Bio Recirc) and recirculation tank 1 (Recirc1) on two different sampling dates 01.07.2011 and 14.07.2011. Error bars=1 SD; n=3

The amount of 2-MIB on 01.07.2011 is almost half that in the tank attached to the non-bio recirculation system, compared to the tank with the regular recirculation system in place. A similar trend can be observed for GSM for that sampling point. Both 2-MIB and GSM levels are comparable in recirculation tank 1 on 14.07.2011 with the levels on 01.07.2011. There appears to be an increase in 2-MIB in the non-biological recirculation system on 14.07.2011 compared to 01.07.2011. In addition to the two types of recirculation systems, one other recirculation tank (recirc2), one carp rearing raceway, and one artificial outdoor pond were investigated as well as to the levels of 2-MIB and GSM they contained (figure 4.15).



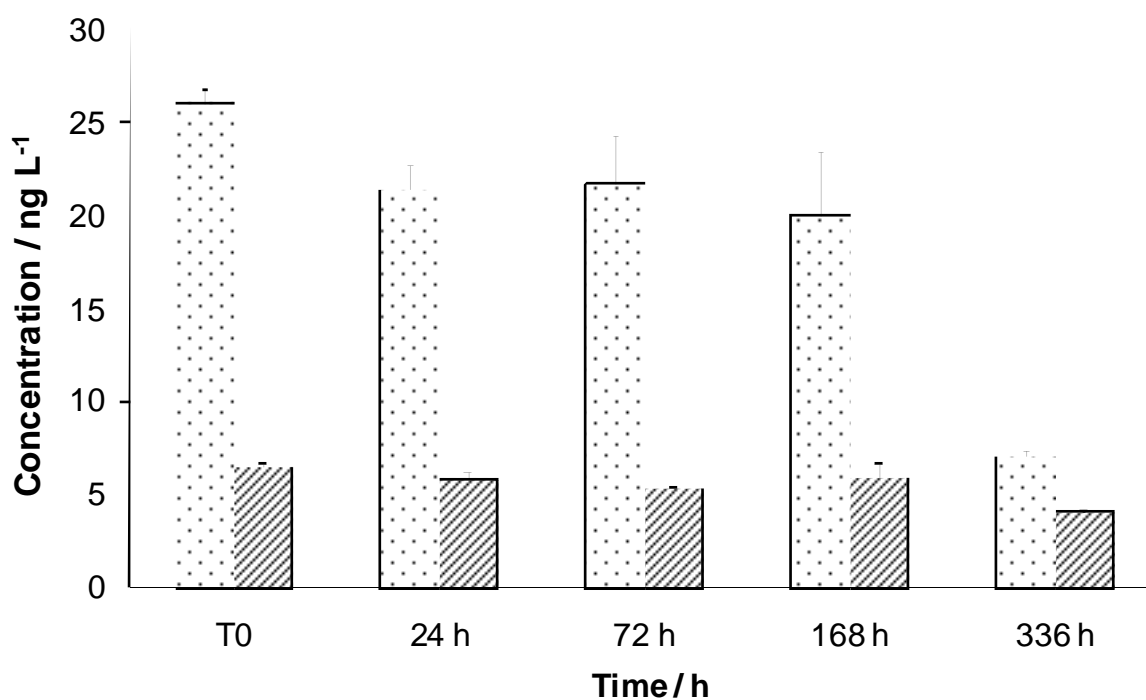
**Figure 4.15:** Analysis of the amounts of 2-MIB (▤) and GSM (▨) at Pisces Engineering Ltd. in outdoor pond, a carp rearing raceway, and a second recirculation tank (RT2). Error bars=1 SD; n=3

The outdoor pond shows comparatively low levels of 2-MIB and GSM. The carp rearing raceway that had been in operation for more than 2 years also showed comparatively low levels of 2-MIB and GSM, similar levels to the outdoor pond. Noteworthy is RT2, that, while showing similar levels of 2-MIB as the other tank with the regular recirculation system in operation, has almost three-fold the amount of GSM present.

#### 4.3.4 Stability of 2-MIB and GSM on SPE cartridges

Clients or researchers could carry out the solid phase extraction of the samples *in situ* and simply post or deliver the cartridges to the place of analysis. An investigation was carried out to assess the length of time 2-MIB

and GSM would be stable on the cartridges without significant loss. For this study environmental samples (Rescobie Loch) were evaluated. Five time points were examined:  $T_0$  (immediately after solid phase extraction), 24 , 72 , 168 (1 week), and 336 h (two weeks) (figure 4.16).

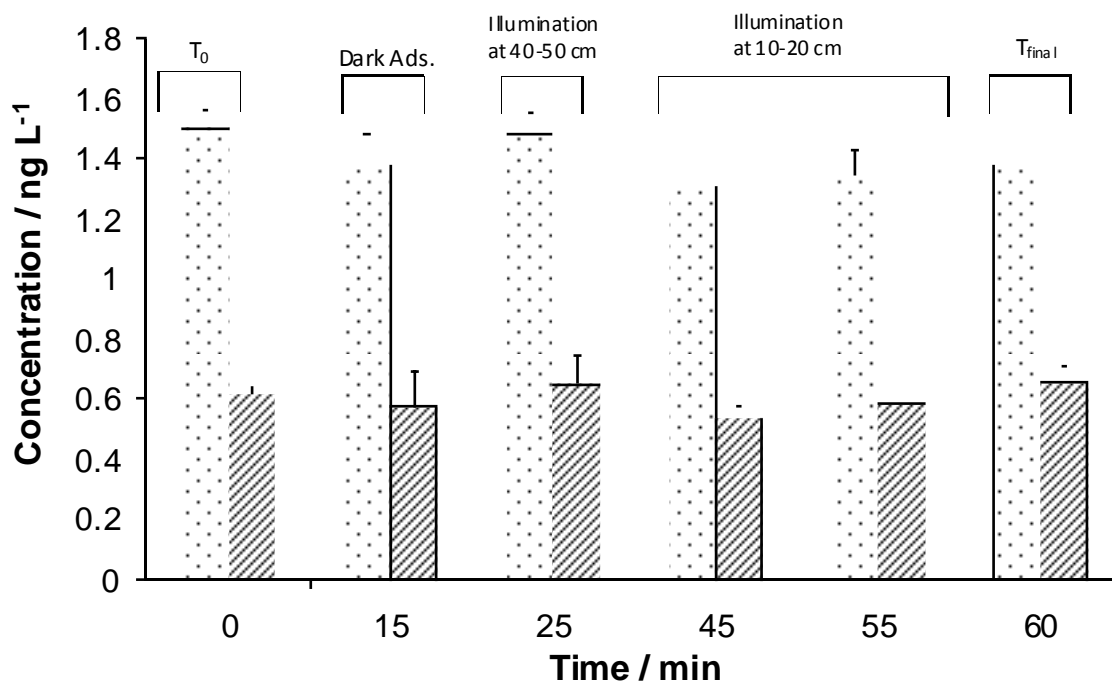


**Figure 4.16:** Stability of 2-MIB and GSM from environmental sample (Rescobie Loch) on C8 (EC) 100 mg, 1 mL Isolute cartridges stored at 4 °C (fridge) for different amounts of time. Error bars=1 SD; n=3

#### 4.3.5 Photocatalysis of 2-MIB and GSM

A photocatalytic reactor was designed and manufactured to be the final step in a recirculation system at a fishfarm. It was designed to be running continuously to eliminate 2-MIB and GSM as produced thus removing an additional depuration step in the production of fish for human consumption. During the preliminary test of the constructed reactor, water was fed from a

3000 L reservoir through the reactor and samples were taken at certain time points (figure 4.17).

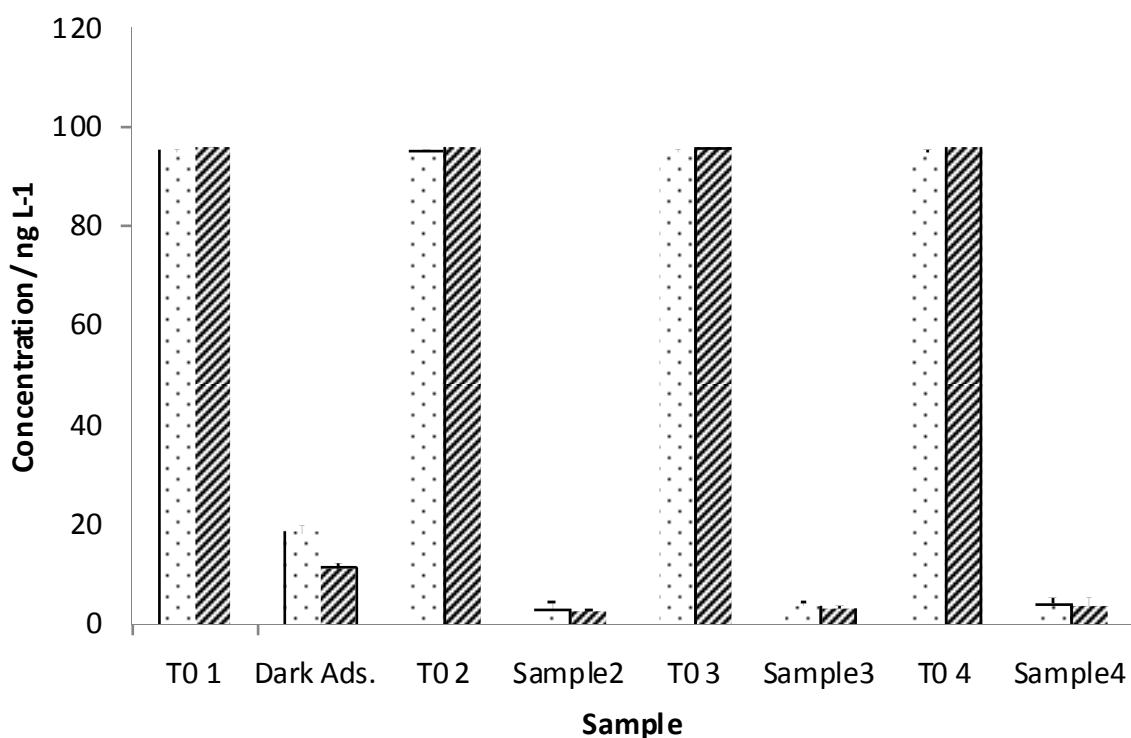


**Figure 4.17:** Laboratory test of the photocatalytic reactor V1. Initial concentration of 2-MIB and GSM: 50 ng L<sup>-1</sup>. Error bars=1 SD; n=3

The results show that very little of the initial 2-MIB and GSM concentration (50 ng L<sup>-1</sup>) was detected even at the initial sampling point. Concentrations remain constant for the entire duration of the experiment and the final concentration in the reservoir is virtually the same as the initial concentration in the reservoir. The second reactor design (V2) was tested with a total volume of 120 L of spiked Milli-Ro water split between four 30 L stainless steel pressure cans at a flow rate of approximately 2 L min<sup>-1</sup>, nitrogen was used as a propellant (figure 4.18). The first water sample was passed through the reactor without illumination to allow for initial binding (dark adsorption) of the



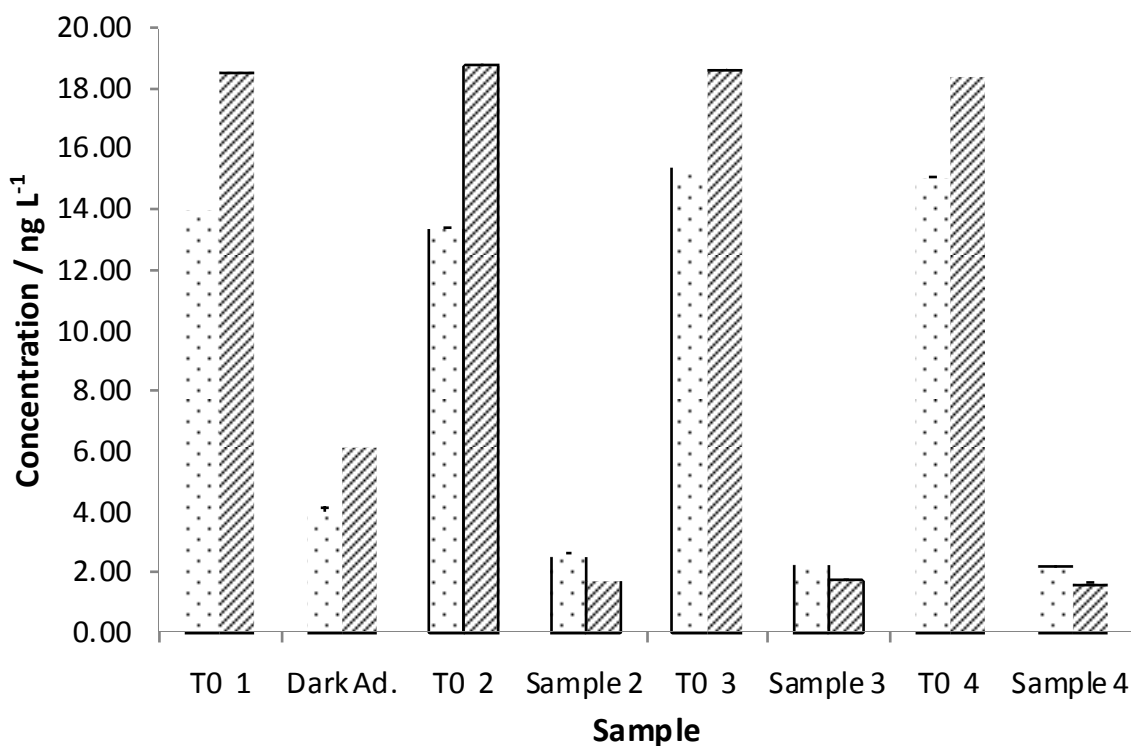
2-MIB and GSM to the titanium dioxide pellets. The following three water samples were passed through the reactor under illumination.



**Figure 4.18:** Laboratory test of photocatalytic reactor V2. 2-MIB (·) and GSM (▨) concentrations at  $T_0$  and after one pass through the photocatalytic reactor. Sample 1: no irradiation, samples 2-4: irradiation. Initial concentration of 2-MIB and GSM:  $100 \text{ ng L}^{-1}$ . Error bars=1 SD;  $n=3$

The second design provides much improved results over the first design, albeit at a considerably lower flow rate. Furthermore, the reservoir for the spiked solution has changed from one of plastic to metal, so that initial losses could be avoided. A high amount of the removal is accounted for by the dark adsorption to the catalyst (approximately 80 % for 2-MIB and 85 % for GSM). In the samples that were illuminated degradation occurred with taste and odour compound levels reduced to as little as 3 – 4 % (3 - 4  $\text{ng L}^{-1}$ ) of the original concentration. After the successful test of the spiked Milli-Ro water, samples were taken at Pisces Engineering Ltd. Four pressure cans were filled

with water from the raceway that has been in operation for more than two years and was known to contain naturally occurring amounts of 2-MIB and GSM. The samples were passed through the reactor at the same flow rate as the above experiment. The first 30 L were again passed through without illumination and all consecutive ones with illumination (figure 4.19). The reactor successfully removed the majority of the 2-MIB and GSM present in the fishfarm samples. The dark adsorption is lower compared to the tested spiked water samples (2-MIB: 72 %, GSM: 67 % compared to 2-MIB: 80 % and GSM: 85 %).

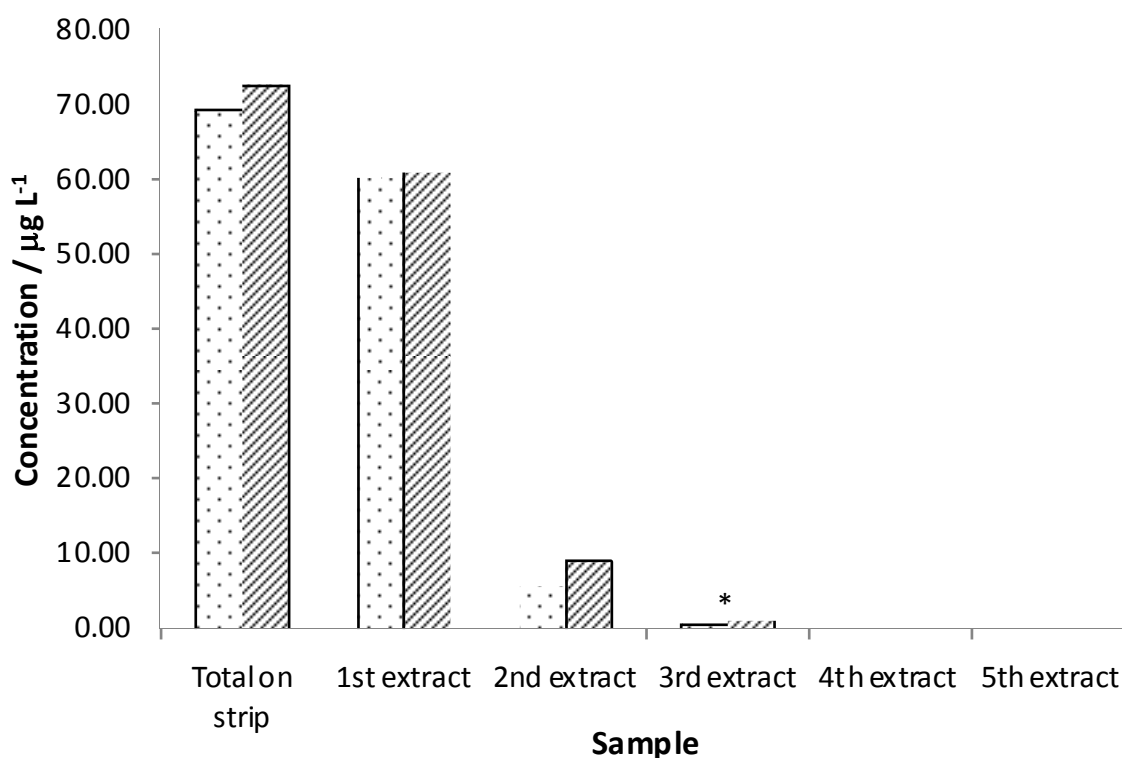


**Figure 4.19:** Results of the fishfarm test of the second photocatalytic reactor design. 2-MIB (▨) and GSM (▩) concentrations at  $T_0$  and after one pass through the photocatalytic reactor. Sample 1: no irradiation, samples 2-4: irradiation. Error bars=1 SD; n=3

### 4.3.6 Development of passive sampling for 2-MIB and GSM

#### 4.3.6.1 Evaluation of the uptake of 2-MIB and GSM onto SRMs

This investigation was carried out to assess the feasibility of employing silicone rubber membranes (SRM) as passive samplers for the detection of 2-MIB and GSM (2-MIB and GSM). The SRMs were pre-extracted to remove any residual chemicals from the manufacturing process (Booij *et al.*, 2002), then shaken for 24 h in Milli-Ro water that was spiked with 2-MIB and GSM ( $80 \mu\text{g L}^{-1}$ ). Following the incubation period they were extracted in five sequential steps with ethyl acetate (figure 4.20).



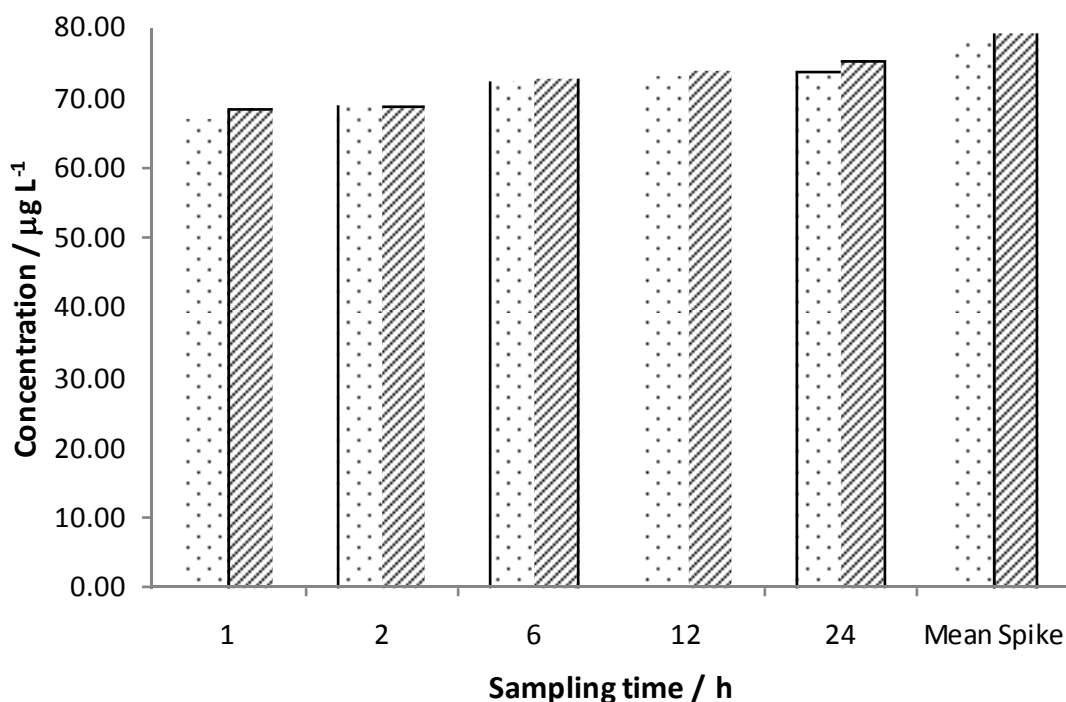
**Figure 4.20:** Result of testing the feasibility of SRMs as passive samplers for 2-MIB (▨) and GSM (▩). \* samples were below LOQ but above LOD. Initial concentration of 2-MIB and GSM:  $80 \mu\text{g L}^{-1}$  Error bars=1 SD; n=3

The results clearly indicate that SRMs can be successfully employed as passive samplers for both 2-MIB and GSM (figure 4.20). The majority of the spiked

amount was taken up by the strips after 24 h. The results also show that two extraction steps suffice to remove approximately 97 and 98 % of 2-MIB and GSM respectively from the strips. Based on the results it was decided to forego a third extraction step in future experiments. Considering that after 24 h most of the present 2-MIB and GSM had adsorbed to the SRMs it is safe to assume that isothermic equilibrium was reached within that time frame. A time course experiment was set up to investigate when exactly that equilibrium was reached.

#### **4.3.6.2 Determination of the silicone rubber membrane water partition coefficient ( $K_{SRMW}$ ) of 2-MIB and GSM**

To determine when the isothermic equilibrium was reached a time course investigation was carried out with SRMs exposed to an aqueous 2-MIB and GSM solution ( $80 \mu\text{g L}^{-1}$ ) with membranes removed at 1, 2, 6, 12, and 24 h and analysed by GC-MS (figure 4.21).



**Figure 4.21:** Concentrations of 2-MIB (▨) and GSM (▩) after different lengths of exposure. The mean spike concentration was determined by SPE of the spiked solution. Initial concentration of 2-MIB and GSM: 80 µg L<sup>-1</sup>. Error bars=1 SD; n=3

It was apparent that within a relatively short amount of time (1 h) the majority (86 % for both 2-MIB and GSM) of the 2-MIB and GSM adsorbs to the SRMs. The isothermic equilibrium is reached at around 6 h. The partition coefficient ( $K_{SRMW}$ ) of silicone rubber membrane and water for 2-MIB and GSM was calculated to be 305 L kg<sup>-1</sup> and 312 L kg<sup>-1</sup> respectively (log  $K_{SRMW}$  2-MIB: 2.63; GSM: 2.69) (equation 4.1).

$$K_{SRMW} = C_{SRM} / C_W$$

**Equation 4.1:** Equation to calculate the partition coefficient for 2-2-MIB AND GSM and silicone rubber. Where:

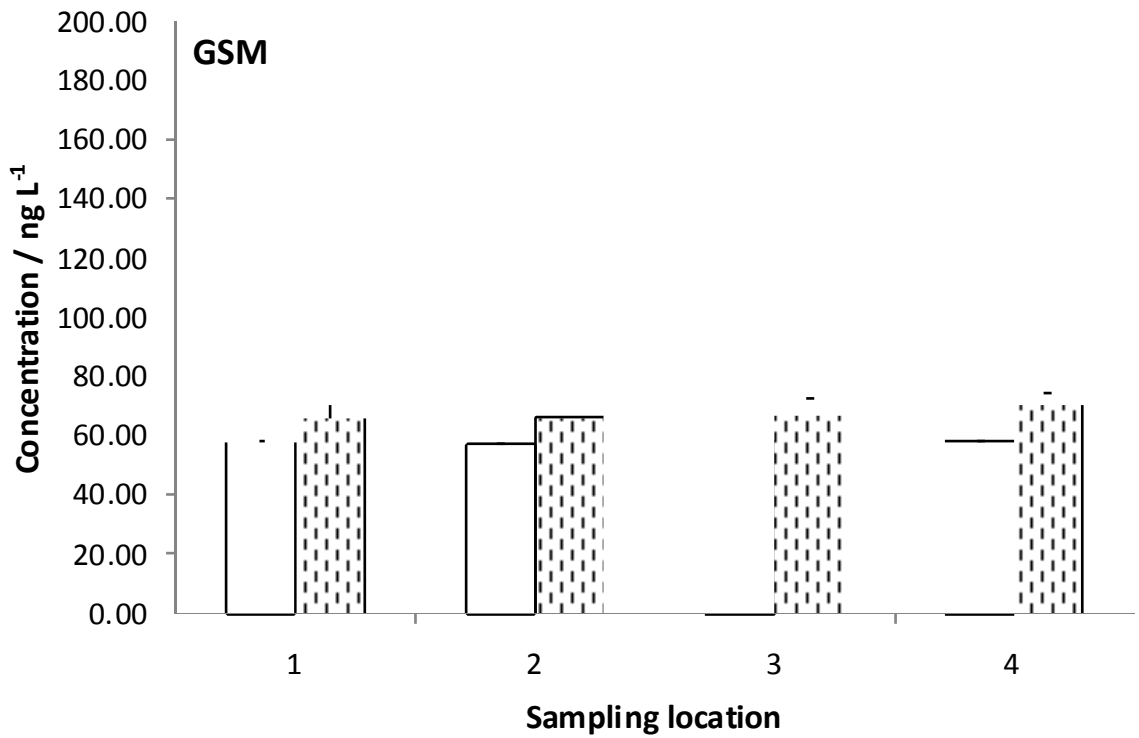
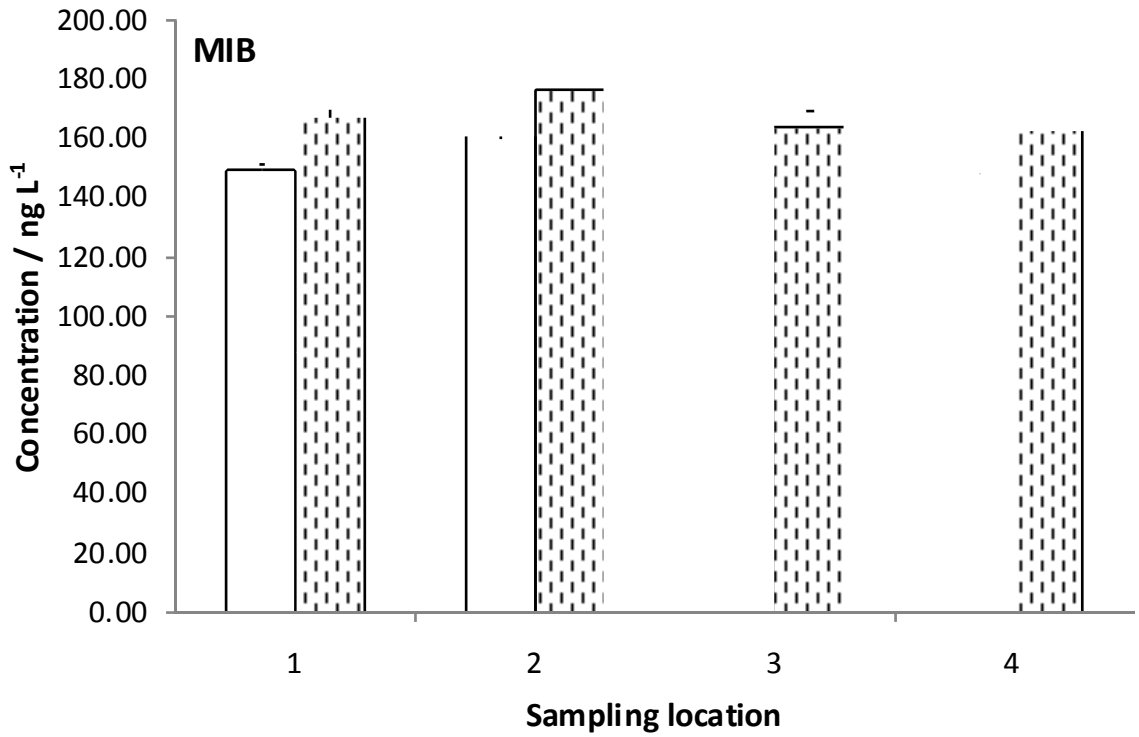
$K_{SRMW}$  = partition coefficient

$C_{SRM}$  = concentration of analyte on silicone rubber (w/w)

$C_W$  = concentration of remaining analyte in solution (w/v)

#### **4.3.6.3 Field testing of SRMs**

To test the feasibility of SRMs in an *in vivo* setting the SRMs were assembled into passive sampling devices that were deployed at Pisces Engineering Ltd. The strips were exposed for 6 h, when equilibrium between the aqueous phase and the silicone rubber of the SRM is reached, as determined by the previous experiment (section 4.3.6.2) (figure 4.22). The passive sampling devices were deployed at four different locations in a carp rearing raceway that had been in operation for more than 2 years. The results show that through the agitation supplied by the influx from the recirculation filtration system the levels of 2-MIB and GSM are evenly distributed throughout the raceway. The data from the SPE determination shows a close correlation with the data obtained from the SRMs, bearing in mind that the concentrations determined by SPE only represent approximately 90 to 95 % of the actual concentration. It can be assumed, as was also seen from the results in section 4.3.6.2, that nearly 100 % of the actual concentration of 2-MIB and GSM in a water source can be recovered.



**Figure 4.22:** Deployment of SRM passive samplers at four locations in a raceway at Pisces Engineering Ltd.; (□) SPE determination of samples taken at respective sampling point; (▨) SRM passive sampler determination. Error bars=1 SD; n=3

#### 4.3.6.4 Determining the stability of 2-MIB and GSM on SRMs

An important criterion for passive samplers is the ability to retain the target analyte for a prolonged period of time (24-72 h), ideally at room temperature, without loss of analysis response. To investigate this aspect of the SRMs and 2-MIB and GSM, three passive samplers were deployed at Pisces Engineering Ltd. at sampling location 3 (figure 4.8), exposed for 6 h and stored for 68 h at either RT, 4 °C (fridge), or -20 °C (freezer) prior to analysis (table 4.16).

**Table 4.18:** Determination of the stability of 2-MIB and GSM on SRMs after 68 h storage at different temperatures in the dark. Results of SPE determination and immediate analysis included for reference. Error=1 SD, n=3

<b>Compound (ng L<sup>-1</sup>)</b>	<b>Immediate analysis</b>		<b>Storage of SRM for 68 h</b>		
	<b>SPE</b>	<b>SRM</b>	<b>Room Temperature</b>	<b>4 °C (fridge)</b>	<b>-20 °C (freezer)</b>
2-MIB	148 ± 0	164 ± 5	25 ± 22	N/D	14 ± 24
GSM	58 ± 0	67 ± 6	48 ± 8	38 ± 7	34 ± 2

N/D=not detected

The results show that GSM and 2-MIB, especially, display poor stability on the SRMs. The storage conditions appear not to make a marked difference.



#### 4.4 Discussion

Cyanobacterial taste and odour compounds, especially 2-methylisoborneol (2-MIB) and geosmin (GSM) pose a nuisance in drinking water and can have significant negative impacts in aquaculture (Izaguirre *et al.*, 1982; Robertson *et al.*, 2006). Failing to control cyanobacterial blooms and the release of their secondary metabolites into the water, it is necessary to develop means of removing 2-MIB and GSM due to the financial and aesthetic impact they can have (Hanson, 2003). Previous studies have suggested that one means to deal with 2-MIB and GSM in water is by photocatalysis with a semi-conductor under UV irradiation (Lawton *et al.*, 2003; Bellu *et al.*, 2008; Robertson *et al.*, 2011). These studies have utilised batch reactors, however, flow-reactors are more desirable because reactors of that type would allow online treatment of contaminated water during water treatment of potable water and could be incorporated into the recirculation systems employed in aquaculture applications (Svrcek and Smith, 2004). The photocatalytic treatment could be utilised prophylactic or as and when required to reduce cost. Furthermore, successful monitoring of 2-MIB and GSM to ensure the applied photocatalytic treatment successfully removes both 2-MIB and GSM to levels below the taste and odour threshold or as an indicator when to incorporate photocatalysis into the recirculation/treatment regime, would be immensely useful. The deployment of silicone rubber membranes (SRMs) as passive samplers could fill that role appropriately. What is required for both the successful monitoring of 2-MIB and GSM and controlling them is an analytical method that is sensitive enough to determine 2-MIB and GSM levels towards the lower end or below the human taste and odour threshold.

Because of their inherent volatility gas-chromatography coupled with mass spectroscopy is the usual means of analysis (Watson *et al.*, 2000). Due to the low taste and odour threshold in humans a very sensitive technique is required, GC-MS by itself cannot meet that demand, which makes a pre-concentration step necessary. There are various means of preconcentration, but some require costly specialist equipment and most are time-consuming allowing only for a comparatively small sample throughput (Lloyd *et al.*, 1998; Bennanou *et al.*, 2003; Zhang *et al.*, 2006; Corteda *et al.*, 2010). Solid phase extraction (SPE) combined with GC-MS has been used before to achieve limits of quantification near the human taste and odour threshold limit for geosmin only (Dzialowski *et al.*, 2009), however Dzialowski *et al.* (2009) quote an unpublished PhD thesis for their method, so no comparison with the present study can be made. SPE has inherent advantages over other pre-concentration techniques, because it is low in cost and allows for a high sample throughput. The ideal analytical method to monitor levels of 2-MIB and GSM, would incorporate SPE for sample pre-concentration making the most of the possibility of processing a high amount of samples day<sup>-1</sup> and that technique's cost-effectiveness, combined with a GC-MS method that allows for a method of LOD in the very low nano gram to high pico gram range.

The GC-MS method employed here shows good precision and accuracy over the range tested (0.5 to 100 µg L<sup>-1</sup>). Slightly better accuracy and precision is achieved by the use of an internal standard (R<sup>2</sup> 2-MIB: 0.9989 ; GSM: 0.9986) (figure 4.10) compared to an external calibration (R<sup>2</sup> 2-MIB: 0.9979 ; GSM:

0.9967) (figure 4.9). The external calibration, however, still achieves acceptable accuracy and precision. In fact most of the application investigations were analysed without the use of an internal standard due to the contamination encountered in the SPE cartridges (section 4.2.3.3). Trichloroanisole was evaluated as a potential substitute for decane as internal standard, however, results are still pending.

In order to achieve a suitably sensitive method, pre-concentration by SPE had to be developed. In most studies the sorbent of choice was C18 (Conte *et al.*, 1996; Ikai *et al.*, 2003; Cole *et al.*, 2003; Ma *et al.*, 2007), this was tested here as well as C8 which had been successfully used by Bellu *et al.* (2008) (table 4.8). Conte *et al.* (1996) used C18 cartridges to determine 2-MIB concentrations in catfish pond waters. They applied 1 L of sample through the SPE cartridge (sorbent load not stated). They achieved recoveries of  $92 \pm 13$  % with a method detection limit of  $\sim 11 \text{ ng L}^{-1}$ . Their method displays a high amount of variability and the limit of detection of  $11 \text{ ng L}^{-1}$  is still above the human taste and odour threshold in water. Ikai *et al.* (2003) also used 1 L of water (spiked with 1 ng each 2-MIB and GSM standard), SPE was performed with C18 (500 mg sorbent load). They report recoveries of 104 % (6 % RSD) for GSM and recoveries of 117 % (8 % RSD) for 2-MIB and a detection limit of  $0.1 \text{ ng L}^{-1}$ . The analytical method used to obtain these results was head-space GC-MS, which adds an additional preparation step and requires specialist equipment. Ma *et al.* (2007) also used a C18 column (sorbent load not stated) and applied 200 mL of spiked water to it (range of concentration 50 – 300 ng L<sup>-1</sup> of both analytes), recoveries for both 2-MIB and GSM were below 50 %

across all concentrations with per cent relative standard deviations of approximately 20. Results obtained for spiked environmental samples were similar. Bellu *et al.* (2008) only applied the SPE as a means for solvent exchange (water to methanol) for injection in GC-MS, so no direct comparison is possible. It was observed that the cartridges with the C8 sorbent achieved better recoveries than those containing the C18 sorbent. Furthermore, the elution profile of both cartridge types shows that C8 cartridges require less solvent to successfully elute 2-MIB and GSM from the cartridges (figure 4.11). Moreover the sorbent load had an effect on the recoveries of both 2-MIB and GSM with 100 mg of C8 higher recoveries were achieved compared with 25 mg of that sorbent. In addition the elution profile of the higher sorbent mass cartridges shows that less solvent is required compared to the lower sorbent mass cartridges of the same type (figure 4.12).

The initial investigation was carried out with isooctane as elution solvent due to the need to have a solvent with low expansion volume to allow for an increased injection volume in the GC-MS determination. Isooctane is non-polar and therefore not ideal as an SPE elution solvent. By mixing isooctane with acetone, a more polar solvent, it was hoped to achieve improved recoveries of both 2-MIB and GSM (table 4.9). Furthermore the duration of the drying step was investigated, as it was hypothesised that a longer duration of drying might contribute to sample loss by volatilisation. It was found that mixing acetone with isooctane indeed achieved higher recoveries for both compounds but also impacted negatively on the precision of the analysis, especially for GSM. This may be due to acetone's comparatively large expansion volume (375:1) (table 4.4), causing back-flash and thus decreasing analysis precision.

As can be seen from the results of this investigation a more polar elution solvent was desirable. Ethyl acetate was proposed as an alternative due to its increased polarity compared to isooctane and its comparatively lower vapour expansion volume (233:1) compared to acetone, furthermore, it had been successfully used by Conte *et al.* (1996), who demonstrated that 1 mL of ethyl acetate was sufficient to remove 98 % of MIB from C18 cartridges, with a second volume of 1 mL removing > 99 %. Different drying times were also investigated for ethyl acetate even though different durations of drying did not appear to have a significant effect in the previous investigation.

As can be seen from the obtained results ethyl acetate appears to be striking the ideal balance between low vapour expansion and polarity to work both as SPE elution solvent and GC-MS injection solvent (table 4.10). The increased expansion volume compared to isooctane was mitigated for by the injection method (pulsed split-less); the pulsed carrier gas prevented any back-flash from occurring. Elution in four sequential fractions and separate analysis of each fraction found that ethyl acetate was able to successfully elute most of the 2-MIB and GSM from the C8 cartridges, as approximately 80 % and 81 % of 2-MIB and GSM, respectively, could be recovered in the first fraction, but no detectable amounts were identified in the second, third and fourth fraction analysed (table 4.11).

The effect of end-capping (EC) on the retention and subsequent recovery of 2-MIB and GSM was evaluated. An end-capped bonded stationary phase in chromatography has its accessible silanol groups replaced with trimethylsilyl groups, which could serve to improve the retention of the 2-MIB and GSM by limiting the amount of irreversible binding of the analyte to the stationary

phase (Sudo, 1996). Unfortunately the cartridges used were not directly comparable as the non-EC cartridges had a larger cartridge volume with the same sorbent load with the result that the sorbent bed was much thinner than it was in the EC cartridges. The results obtained appear to be indicating that EC has a beneficial effect on the recoveries of both 2-MIB and GSM, which appears to be supported by the elution profile of both cartridges suggesting that end-capping allows for several elution steps, indicating that the binding of 2-MIB and GSM is not irreversible (figure 4.13). The only elution fraction that yielded 2-MIB and GSM from the non-EC cartridges was the first which would indicate irreversible binding of both compounds to the sorbent material (table 4.12). It appears that the physical thickness of the sorbent bed can impact negatively on the retention and recoveries if it is too thin. As stated before, environmentally relevant concentrations of 2-MIB and GSM require pre-concentration, one means of archiving this is by increasing the amount of sample that passes through the cartridge. With larger volumes, however, manual loading becomes unfeasible, therefore the effect of polytetrafluoroethylene (PTFE or Teflon™) tubing on the recoveries of 2-MIB and GSM was tested (table 4.13). The test solution volume of 100 mL was loaded onto the cartridge without significant losses when compared to the manual loading. None of the studies involving the solid phase extraction of 2-MIB and GSM (Conte *et al.*, 1996; Ikai *et al.*, 2003; Cole *et al.*, 2003) describe how the sample was physically loaded onto the cartridges or investigated the effect of tubing on recoveries. However, Elhadi *et al.* (2004) determined that only PTFE tubing guaranteed no system loss when pumping 2-MIB and GSM through tubing. In that study Elhadi *et al.* (2004) tested several materials

including Pharmed™ (thermoplastic elastomer material), Viton™ (fluoroelastomer) and Teflon™ (PTFE). The smallest amount of sample loss was observed with PTFE tubing, GSM: 19 % and 2-MIB: 13 % after four days storage, compared to GSM losses of 47 and 56% and 2-MIB losses of 41 and 52 % in Pharmed™ and Viton™ respectively. Having established that tubing has no negative impact on the recoveries of the 2-MIB and GSM, it was investigated how much test solution could be loaded onto the cartridges before break through occurred. A high volume of sample is desirable because assuming an unchanging elution volume, the greater the volume of sample loaded onto the cartridges without sample loss, the greater the factor of concentration (table 4.19). The sample volume in different studies varies widely from 1 mL (Bellu *et al.*, 2008) and 1000 mL (Conte *et al.*, 1996), depending on the application and focus of the study. If environmental samples are used generally a large sample volume is used (Conte *et al.*, 1996; Ikai *et al.*, 2003). Conte *et al.* (1996) passed 1 L of pond water through C18 cartridges of unknown sorbent load with a pump at a flow rate of approximately 40 mL min<sup>-1</sup> and report recoveries of near 90 %. No comment is made about potential break through or other system loss (due to tubing or length of extraction). Ikai *et al.* (2003) also applied 1 L to C18 cartridges (500 mg) and used a vacuum pump with a flow rate of 15 mL min<sup>-1</sup>, achieving recoveries in excess of 100 % for both 2-MIB and GSM. Therefore a test solution volume of 250 mL was investigated, it was found, however, that this resulted in decreased recoveries of both 2-MIB and GSM (table 4.14). There are several possible ways which could have contributed to the sample loss such as volatilisation of the sample during the solid phase extraction and break

through. Due to the relatively low flow rate of approximately 5 mL min<sup>-1</sup> it could be possible for the 2-MIB and GSM to evaporate from the vessel containing the test solution. This, however, is relatively unlikely as the vessels are covered with parafilm. Another possible reason for the sample loss was break-through.

**Table 4.19:** Examples of SPE sample volumes and the corresponding concentration factors, and resulting hypothetical combined (both 2-MIB and GSM) LOQ assuming an elution volume of 0.55 mL as used in the proposed method.

<b>Sample volume (mL)</b>	<b>Concentration factor (assuming 0.55 mL elution)</b>	<b>Hypothetical combined LOQ (ng L<sup>-1</sup>)</b>
10	18	50
100	181	5
200	363	3.3
250	455	2.9
500	909	0.5
1000	1818	0.3

To test whether break-through had occurred two SPE cartridges were placed on top of each other and 250 mL of test solution was passed through the cartridges. The reasoning was that any 2-MIB and/or GSM breaking through the first cartridge would be retained by the second. The results of this investigation, however, show that only a very small amount of 2-MIB (4 %) and no GSM broke through the first cartridge. The recoveries of both compounds was comparatively low (2-MIB: 74 % recovery, GSM: 78 % recovery), as observed in the previous investigation (table 4.14). This means that the 2-MIB and GSM either volatilised during the solid phase extraction, which was deemed unlikely, adhered to plastic of the SPE cartridge, or, as previous experimentation had shown that one elution step is sufficient to remove all of the 2-MIB and GSM from the sorbent material (table 4.11), and



simply irreversibly bound to the sorbent material in the cartridge which concurs with the findings of Elhadi *et al.* (2004) who observed non-specific binding of both 2-MIB and GSM to similar materials. A decreased sample volume (200 mL) was investigated. At the same time the effect of vacuum filtering with GF/C (5.5 diameter) filters was investigated. The rationale for evaluating the effects of filtration on the recoveries arose from the fact that the ultimate application of the proposed method was the analysis of environmental samples. As environmental samples routinely contain suspended solids, filtration of the samples was important to avoid blockage of the cartridges and PTFE tubing. It can be seen that a test solution volume of 200 mL achieves satisfactory recoveries for both 2-MIB ( $90 \pm 1 \%$ ) and GSM ( $91 \pm 2 \%$ ) (table 4.15). A test solution volume of 200 mL corresponds to the pre-concentration factor of 363. Furthermore, the filtration of the test solution through GF/C filters does not appear to impact negatively on the recoveries (2-MIB  $89 \pm 2 \%$ ; GSM  $92 \pm 1 \%$ ) (table 4.15), this is corroborated by Conte *et al.* (1996), Elhadi *et al.* (2004), and Ikai *et al.* (2003), in whose studies samples were filtered through glass wool or GF/A filters prior to SPE/analysis.

With the optimised SPE parameters (table 4.20) the method limits of detection and quantification can be stated as 0.99 and 3.22 ng L<sup>-1</sup> respectively for 2-MIB and 0.99 and 3.19 ng L<sup>-1</sup> respectively for GSM (table 4.16). The achieved method limits of quantification compare favourably with the other published methods of detection (table 4.2). The LODs achieved are lower than those achieved by SPE-GC-MS by Dzialowski *et al.* (2009) who achieved 5 ng L<sup>-1</sup> for GSM (2-MIB was not investigated), and by SPME-GC-MS by Lloyd *et al.*

(1998), who achieved 10 ng L<sup>-1</sup> for each of the two analytes. Conte et al (1996) achieved 11 ng L<sup>-1</sup> for 2-MIB, which is also higher than what was achieved with the presented method. Ikai *et al.* (2003) achieved a lower LOQ (0.1 ng L<sup>-1</sup> for both analytes), however, used specialist equipment in their investigation. The other studies (table 4.2) that achieved lower LODs all used specialist equipment which have limitations or require trained operators (as discussed in section 4.1). Furthermore, it is the lowest limit of quantification achieved by the combination of simple solid phase extraction and gas chromatography.

**Table 4.20:** Optimised SPE method for the pre-concentration of 2-MIB and GSM

<b><i>SPE parameter</i></b>	<b><i>Applied in this method</i></b>
Sorbent material	C8
Sorbent load	100 mg
Cartridge volume	1 mL
End-capped	Yes
Conditioning	2 mL: Hexane, Acetone, Methanol; 10 mL: Milli-Q
Mode of loading	PTFE tubing
Sample volume	200 mL
Drying time	5 min
Elution solvent	Ethyl acetate
Elution solvent volume	0.5 ml (+0.05 mL TCA internal standard)
Pre-concentration achieved	363:1

The fitness for purpose of the method was tested with environmental samples, to this end samples from Rescobie Loch and waters from a fishfarm were investigated.

Rescobie Loch has a history of cyanobacterial blooms (Sano *et al.* 2005) and is associated both with cyanotoxins (microcystin) and 2-MIB and GSM. The

results of samples collected on the 14.07.2011 show relatively low concentrations of both analytes in the water (2-MIB:  $5.3 \pm 0.04 \text{ ng L}^{-1}$ ; GSM:  $1.68 \pm 0.05 \text{ ng L}^{-1}$ ). The results indicate that the method is capable of determining the levels at and below the human taste and odour threshold in environmental samples with good reproducibility. In addition to the water samples from Rescobie Loch, SPE-GC-MS determinations of different water samples from a fishfarm were carried out. These investigations were performed to further test the method with field samples. The different waters tested (table 4.6) were sampled at different time points and stored in glass bottles at 4 °C until analysis. The results indicate the suitability of the method for a range of concentrations (figure 4.14; figure 4.15). The concentration in all samples tested was well over  $10 \text{ ng L}^{-1}$  and thus above the human taste and odour threshold in water. As mentioned before (section 4.1) it is difficult to exactly relate the amount of 2-MIB and GSM in the water with amounts present in fish, due to the involvement of a number of factors, such as the amount of time the fish have spent in contaminated water, the body weight of the fish, the meat-to-fat ratio of the fish, the oil content of the fish, the species of fish and the concentration in the water (Howgate, 2004). It is interesting to see that, in general the concentrations of 2-MIB and GSM are at approximately the same levels, with the exception of recirculation tank 1 (Recirc1) at the sampling on 14.07.2011, which displayed more 2-MIB than GSM present. The recirculation tank 2 (Recirc2), and the non-bio recirculation system (NonBioRecirc) at 14.07.2011 exhibited both increased GSM levels compared to the 2-MIB levels. In Recirc1 and Recirc2 this was most likely due to the makeup of 2-MIB- and GSM-producing biota on the biofilters, as Auffret

*et al.* (2011) have shown that 2-MIB and GSM production is strain and species specific in actinomycetes, the most likely 2-MIB- and GSM-producers in recirculation systems. A similar reason can be found for NonBioRecirc at 14.07.2011, while this system does not employ biofilters there will very likely be bacteria at other points within the system. The NonBioRecirc system at Pisces Engineering Ltd. was specifically designed to remove the source of 2-MIB and GSM producing bacteria by removing the habitat (biofilters) of these producers. If the system is new, the low levels of 2-MIB and GSM detected could also be due to non-specific binding to the parts of the system. This non-specific binding does occur until an equilibrium is reached and the parts are saturated and then the concentration of both 2-MIB and GSM, over time, would increase again. There are other sources of 2-MIB and GSM than actinomycetes, however, cyanobacteria, which are also capable of producing both off-flavour compounds, could be present in the water. Furthermore, eliminating the 2-MIB and GSM producers from the filtration system still leaves potential producers in the tank itself. The outdoor pond shows comparatively low levels of 2-MIB and GSM, though this might be due to exposure to the elements and the outside weather conditions.

It has been shown that the method can successfully detect both 2-MIB and GSM in environmental samples. Following on from this a means of controlling the amount of 2-MIB and GSM was investigated, using the analytical tool developed. The advanced oxidation process of titania assisted photocatalysis was employed in a continuous flow reactor. Two designs were built and tested (V1 and V2). The testing of the V1 reactor was not very successful, it

displayed a number of design issues, including the use of polyethylene/polyurethane components (thus allowing non-specific binding to these parts), a short path length (and thus a reduced residence time of the test solution in the reactor), and the use of a material of unknown UV transmittance. The non-specific binding to the polyethylene/polyurethane parts is problematic only when attempting to measure the amount of removal by photocatalysis. In operation at a fishfarm for example, non-specific binding, to a degree, can contribute to the removal of 2-MIB and GSM in the water. However, when attempting to measure removal of these two compounds all sources of non-specific binding need to be eliminated/reduced to a minimum to assess actual removal by the method tested. The data shows only very low amounts of 2-MIB and GSM present in the initial samples ( $\sim 1.6 \text{ ng L}^{-1}$ ; figure 4.15) even though the initial spike was  $50 \text{ ng L}^{-1}$ ; this would support the theory of non-specific binding of 2-MIB and GSM to the polyurethane/polyethylene parts as observed in Elhadi *et al.* (2004). The reactor appears not to have an effect on the amount of the 2-MIB and GSM. There are a number of reasons why this may have occurred, a large volume reservoir (3200 L) was employed and the 2-MIB and GSM stock was added as it was filled to ensure good mixing, however, due its size the filling of the reservoir took approximately 3.5 h, allowing for non-specific binding to the plastic components of the reactor, the pump, the tubing, and the reservoir, to occur. The most likely reason for the poor photocatalytic performance in the destruction of 2-MIB and GSM of the reactor could have been the relatively short residence time of the test solution in the reactor itself. With a flow rate of approximately  $2.5 \text{ m}^3 \text{ h}^{-1}$ , the time it would take a given amount of water is

about 0.5 sec (equation 4.2, equation 4.3, equation 4.4). Because the reactor's path is rectangular, the rectangular area first needs to be converted to its equivalent diameter (equation 4.2).

$$\begin{aligned}
 &= 1.3 \times \frac{( \times ) \cdot}{( + ) \cdot} \\
 &= 1.3 \times \frac{(13.5 \times 10) \cdot}{(13.5 + 10) \cdot} \\
 &= 14.5
 \end{aligned}$$

**Equation 4.2:** Conversion of the area of a square pipe to a circular diameter.

Where:  $d_e$ =equivalent diameter  
 $a$ =length of major side (13.5 mm)  
 $b$ =length of minor side (10 mm)

Once the rectangular area has been converted to its equivalent diameter it can be input into the equation that will yield the velocity of the flow inside the reactor (equation 4.3).

$$= \frac{\times}{\times ( \quad )}$$

$$= \frac{4 \times 2.5 \quad /h}{\times (0.0145 \quad )}$$

$$= \frac{4 \times 6.9 \times 10 \quad /}{6.6 \times 10}$$

$$= 4.18 \quad /$$

**Equation 4.3:** Calculation of the velocity of flow in the photocatalytic reactor

Where: flowrate =  $2.5 \text{ m}^3 \text{ h}^{-1}$  and pipe diameter = 25 mm (0.025 m)

With the acquired velocity of flow the residence time can be calculated with the length of the reactor bed (equation 4.4).

$$= \frac{\quad}{\quad}$$

$$= \frac{2}{4.18}$$

$$= 0.48$$

**Equation 4.4:** Calculation of the time needed for a given amount of water to flow through the photocatalytic reactor

Where: length of reactor bed = 2 m and velocity =  $1.4 \text{ m s}^{-1}$

While all of the above reasons will have contributed to the ineffectiveness of the V1 reactor in the degradation of 2-MIB and GSM, the most pertinent

reason for the fact that no measurable photocatalytic breakdown occurred at all is the fact that the triple walled polycarbonate sheeting used in the construction of the reactor has unknown UV transmittance. This would render the use of a catalyst inside inefficient as only a fraction of the energy required to excite the photocatalyst actually reaches it. The second design attempted to remove all sources of non-specific binding by the use of metal (stainless steel) parts and polycarbonate sheeting with a guaranteed UV transmittancy (table 4.21). The material chosen for this design was from Degussa with a guaranteed 97 % UV transmittance, the flow-path of the test solution was altered from a straight flow along the length of the reactor to a flow that would lead the test solution to and fro through the reactor until exiting from a point diagonally opposite of the point of entry (thus increasing the resident time in the reactor by increasing the path length 14-fold). While most likely not an issue with the previous design the amount of catalyst added was also slightly increased from approximately 20 kg to approximately 22 kg.



**Table 4.21:** List of differences between photocatalytic reactors V1 and V2.

<b>Component</b>	<b>1<sup>st</sup> design</b>	<b>2<sup>nd</sup> design</b>
UV transmittance	unknown	95 %
Path length	2 m	28m
Tubing diameter	25 mm	60 mm
Catalyst load	~20 kg	~22 kg
Flow rate	2.5 m <sup>3</sup> h <sup>-1</sup>	2 x 10 <sup>-3</sup> m <sup>3</sup> h <sup>-1</sup>
Resident time of solution in reactor	0.48 s	560 s
Breakdown of 2-MIB and GSM (including dark adsorption)	No breakdown detected	> 95 % of both 2-MIB and GSM

The improved design of the V2 reactor greatly enhanced the photocatalytic destruction of both 2-MIB and GSM (figure 4.18). It is capable of removing > 95 % of the 2-MIB and GSM present ( $\leq 4 \text{ ng L}^{-1}$  for 2-MIB and GSM). The relatively high amount of dark adsorption observed is remarkable, with 80 % for 2-MIB and 88 % for GSM. The trade-off for the increased destruction of 2-MIB and GSM is the flow rate. What has to be considered, however, is the fact that the V2 reactor is a prototype that was built with commercially available parts. A custom built version, with custom built parts would be able to achieve a much higher flow rate, due to an increased structural integrity. Bellu (2007) has also observed that the destruction of GSM in a flow-through reactor is dependent on the flow rate applied. In Bellu's (2007) design the lowest flow rate ( $0.05 \text{ L min}^{-1}$ ) only achieved 67 % removal of the original spike ( $100 \text{ ng L}^{-1}$ ) for GSM with the same type of catalyst (Hombikat K01/C). The path length

of Bellu's (2007) reactor is difficult to determine as a glass coil was used, the coil length was 1.2 m, but the actual path length would be greater than that. However, in their batch reactor (Hombikat K01/C) Bellu *et al.* (2008) achieved complete degradation for GSM in 25 minutes, which in itself was an improvement over the removal of GSM reported in Lawton *et al.* (2003) which employed P25 (nanoparticulate powder catalyst), where total degradation was only achieved in 60 minutes. The V2 design achieves > 95 % removal with one pass through the reactor, which takes 9.3 minutes. These results are obviously not directly comparable as both of these studies were conducted in batch reactors. Furthermore, the initial concentration in the Bellu study was considerably higher ( $1 \text{ mg L}^{-1}$ ) than it was in this investigation. The Lawton *et al.* (2003) study also investigated the photocatalytic destruction of 2-MIB and found that P25 successfully degraded > 99 % of 2-MIB within 30 minutes of irradiation of titania. The concentrations used in this investigation were  $9.16 \mu\text{g L}^{-1}$  (2-MIB) and  $5.54 \mu\text{g L}^{-1}$  (GSM), which again were much higher than the concentrations used in the current experiment ( $0.1 \mu\text{g L}^{-1}$ ).

Having proven the photocatalytic efficiency of the reactor in a laboratory test, the V2 reactor was applied to fishfarm water (figure 4.19). The concentration of the water from Pisces Engineering Ltd. was found to contain moderate levels of both 2-MIB ( $14 \text{ ng L}^{-1}$ ) and GSM ( $18 \text{ ng L}^{-1}$ ). As in the laboratory test the dark adsorption was found to be significant (2-MIB: 71 %, GSM: 68 %), but decreased compared to the laboratory test (2-MIB: 80 %, GSM: 88 %) which can be explained with the presence of natural organic matter (NOM) in the fishfarm samples. Newcombe *et al.* (2002a, 2002b) have conducted a

study that investigated the competition of 2-MIB and natural organic matter (NOM) for binding sites on activated carbon. It was found that NOM actively competes with 2-MIB for binding places on the activated carbon, a similar process is very likely to be happening with 2-MIB and GSM and NOM in the fishfarm samples and the titanium dioxide particles. Bellu (2007) found that their flow reactor design applied to waters of a Danish eel farm could only remove 33 % of the GSM present ( $7 \text{ ng L}^{-1}$ ) in one pass through their reactor. Bellu (2007) also propose NOM as a competitor for the photocatalytic decomposition of GSM.

Because of the negative financial impact both 2-MIB and GSM can have on both the potable water industry and aquaculture, it is important to have in place a means of detecting the presence of 2-MIB and GSM (Hanson, 2003). A practical and cost effective way to achieve this is the deployment of passive samplers in the bodies of water in question. Silicone rubber membranes (SRMs) have been successfully employed to measure polyaromatic hydrocarbons and polychlorinated biphenyls (Booij *et al.*, 2002). A series of investigations was launched to determine the suitability of SRMs as passive samplers for the 2-MIB and GSM. In the first test SRMs were exposed to a combined 2-MIB and GSM spiked solution. After allowing 24 h for adsorption to occur the SRMs were extracted in several steps and analysed. The data revealed that a significant amount of the 2-MIB and GSM adhered to the silicone rubber (2-MIB: 90 %, GSM: 97 %) (figure 4.20). Employing ethyl acetate as desorption solvent allowed for desorption of > 98 % of the adsorbed material to be desorbt again. The SRMs allowed for good precision

showing that there is little difference between different membranes. This investigation also illustrated that a desorption step of 2 h is sufficient. This is comparable to a similar experiment described by Liu *et al.* (2011), where a polypropylene glycol coated hollow fibre membrane was employed as a passive sampler for 2-MIB and GSM, and a desorption time of 24 h was stated, with the remark that 4 h and 10 h desorption time significantly decreased GC-MS response and precision. It has to be considered, however, that Liu *et al.* used a much lower starting concentration ( $0.4 \mu\text{g L}^{-1}$ ) and that desorption in their study took part statically. They also explain that with 20 minutes sonication they achieve similar results compared to 24 h static desorption. Following on from the investigation regarding the suitability of SRMs as passive sampling devices, the partition coefficient of the silicone rubber and water ( $K_{\text{SRMW}}$ ) for both 2-MIB and GSM had to be determined. This investigation would reveal when the isothermic equilibrium between the concentration in the water and the concentration on the membrane would be reached, thus determining for how long the SRMs would need to be exposed to the contaminated water. The experiment was performed much like the previous ones, except that samples at different points in time were taken and the concentration on the membranes at each specific time point was determined (figure 4.21). It was found that an exposure of six hours is sufficient for the isothermic equilibrium to be reached. An exposure for longer than six hours does not significantly increase the concentration of the 2-MIB and GSM on the membranes. The  $\log K_{\text{SRMW}}$  for 2-MIB and GSM was determined to be 2.49 for both compounds. Even though Booij *et al.* (1998, 2002) have argued that SRMs are unsuitable for compounds with  $\log K_{\text{ow}}$

(octanol/water) lower than 3.9, 2-MIB and GSM work with a log  $K_{SRMW}$  of around 2.49, of course these values are not directly comparable. Having determined the point of equilibrium the membranes were field tested at Pisces Engineering Ltd., where they were exposed for six hours in the carp rearing raceway (figure 4.21). In addition to the membranes spot samples in glass bottles were also taken and analysed with SPE-GC-MS to compare the determinations of both methods. The results indicate that the SPE-GC-MS determination and the determination with the SRMs correlate well. This shows that the SRMs can determine the concentration of both 2-MIB and GSM accurately. This corresponds to the finding of Liu *et al.* (2011) who found that the recoveries of their environmental samples (pond and lake water from Wuxi, Jiangsu province, China) were in the range of 87 to 110 %. From the results of both investigations, Liu *et al.* and the current investigation, it would appear that the presence of NOM does not negatively impact on the amount of 2-MIB and GSM adsorbed to the SRMs. In parallel to the exposure of the SRMs to the raceway water to determine the concentration present, three additional sets of membranes were exposed to determine the stability of both of the 2-MIB and GSM on the SRMs during storage at three different temperature conditions. One of the greatest limitations with passive sampling devices employed to determine volatile compounds is the fact that storage of the device in a fridge or even immersion in liquid nitrogen is required to avoid sample loss (Liu *et al.*, 2011). The investigation revealed that after 68 h of storage a considerable amount of sample loss can be observed for both 2-MIB and GSM regardless of the storage conditions (table 4.18). These results are markedly different from what Liu *et al.* (2011) found in their investigation. In

their study both 2-MIB and GSM displayed stability over 72 h at room temperature without a tangible loss of analysis response. Even after 2 week's storage at 4 °C their passive samplers produced reliable results in the analysis of both 2-MIB and GSM. One possible explanation for the success of Liu *et al.* is the fact that their environmental samples were spiked with 0.5 or 1 µg L<sup>-1</sup> of both 2-MIB and GSM, which presented them with results in the low µg L<sup>-1</sup> range for 2-MIB and high ng L<sup>-1</sup> to low µg L<sup>-1</sup> for GSM, where the loss of 100 nano grams would not necessarily negatively skew their analytical response. In this study, however, the relatively low amounts on the strip might simply have volatilised and greatly affected the analytical response. The data argues against biological degradation of the 2-MIB and GSM by the biota present in the raceway, because loss of sample occurs at all three temperatures. Biological degradation would be hindered at 4 °C and completely stopped at -20 °C. The data also suggests that GSM is more stable on the SRMs than 2-MIB. A possible solution to circumvent the issue of degradation/loss of sample during storage would be to utilise the Liu *et al.* (2011) and Korth *et al.* (1992) approach of storing the strips in an organic solvent such as methanol or ethyl acetate prior to analysis. It is remarkable that the SRMs do not seem to be as pertinent in regarding 2-MIB and GSM as the SPE cartridges appear to be, where significant losses can only be observed after three day's storage at 4 °C and more severe losses only after 1 or 2 weeks. Arguably the SPE cartridge present a more protected environment for the 2-MIB and GSM than the SRM does.

Geosmin and 2-methylisoborneol cause considerable expenses in both potable water treatment and aquaculture, therefore controlling and monitoring these compounds are of importance. It has been shown that controlling the presence of both 2-MIB and GSM by photocatalysis over titanium dioxide is a feasible approach. The flow reactor design may easily be applied to both settings allowing degradation of 2-MIB and GSM to below human taste and odour threshold levels. SRMs can offer a cost effective means of monitoring levels 2-MIB and GSM. The short exposure and desorption times allow for a quick turnaround of samples, allowing for concentration determination within the same day. An additional rapid means of determining the concentration of the 2-MIB and GSM in point samples has been developed. The SPE-GC-MS determination of water samples also allows for a high turnaround of samples. The pre-concentration achieved by the solid phase extraction allows for the determination of the concentration of 2-MIB and GSM well below the human taste and odour threshold. Which of the methods is employed depends on the application at hand. In a setting, such as on a research vessel or a location with laboratory facilities attached, where sample processing with SPE is feasible, that approach can be taken. In a different setting, where no such facilities are accessible, a commercial fishfarm for example, deployment of pre-extracted passive samplers with subsequent conveyance to a lab to desorb the samplers and conduct the analysis might be more fit for purpose.

# Conclusions



## **5 Conclusions**

### **5.1 Introduction**

The problems caused by cyanobacterial secondary metabolites in potable water as well as aquaculture are well documented, and as current water treatments are inefficient at removing and mitigating their impact on potable water and aquaculture produce, alternative treatment methods need to be explored.

The aim of this thesis was to explore means of monitoring and controlling cyanobacterial metabolites. The metabolites under investigation were microcystins and nodularin, a group of potent hepatotoxic compounds produced by a range of cyanobacteria, and the off-flavour compounds 2-methylisoborneol (2-MIB) and geosmin (GSM) that are responsible for earthy-muddy flavours in water and aquaculture produce.

### **5.2 5.2 Pheromonal activity of microcystin-LR in the control of microcystins in water**

The biological role of microcystins and nodularin remains unclear. One of the proposed functions is that of a semiochemical (signalling compound). Microcystin-LR evaluated in regards to putative pheromonal activity by the use of stable isotope labelling with <sup>15</sup>N. The effects of MC-LR as a pheromone were examined in *Microcystis aeruginosa* PCC 7820. It was found that the addition of exogenous MC-LR limited *de novo* MC production, a statistically significant impact was observed independent of the dose of exogenously added MC-LR. The effects observed were more pronounced when adding 10 µg mL<sup>-1</sup>

compared to adding  $1 \mu\text{g mL}^{-1}$ , however, the effect was still observable and was statistically significant. In addition to the toxin synthesis limiting effect a culture growth stimulating effect was also observed in the cultures treated with exogenous toxin. This effect was dose-independent and resulted in 15 % increased culture size at the end of the experiments (10 days). Furthermore the distribution of the *de novo* toxin between the intra- and extra-cellular matrices was affected by the addition of exogenous MC-LR. Treated cultures released less MC-LR into the extra-cellular matrix compared to the control cultures. This effect appears to be dose-dependent, with a higher degree of toxin retained intra-cellularly in cultures treated with higher amounts ( $10 \mu\text{g mL}^{-1}$ ) of exogenous toxin. The fate of the exogenously added toxin remains unknown, only small amounts are taken up by, or are associated with, the cyanobacterial cells ( $\sim 4 \%$ ).

In addition to the putative pheromonal effects of MC-LR the effect of the density of the cyanobacterial cultures on MC synthesis was investigated. It was found that a high initial cell inoculum negatively impacts on the amount of toxin produced  $\text{cell}^{-1} \text{ day}^{-1}$ . The reasons for this remain unestablished. Two possible explanations have been proposed: the physical density of the cultures shades individuals and limits these individuals to focus their energy on photosynthesis and survival as opposed to the production of secondary metabolites, or the physical density promotes the release of semiochemicals that limit MC synthesis as a high cell density can be equated with favourable growth conditions thus limiting the necessity of MC production.

An observation made during all experiments where exogenous toxin was added to cultures of *M. aeruginosa* was that the amount detected at the first sampling point after inoculation never reflected the original spiked amount. The reasons for this remain unestablished.

Future research needs to be directed towards determining the fate of the exogenously added toxin. Furthermore, the effects of more environmentally relevant concentrations (0.25 – 10  $\mu\text{g L}^{-1}$ ) need to be explored and it needs to be established whether the dose-dependent effects established in this work are still observable at these concentrations. The observed phenomenon of the initial decrease in exogenous toxin requires further exploration.

### **5.3 Photocatalytic water treatment**

One of the difficulties of applying photocatalysis in water treatment thus far has been a trade-off between ease of removal of the catalyst and the photocatalytic efficiency. Powder suspensions are highly effective but difficult to remove while pellet presentations offer ease of removal at reduced photocatalytic efficiency. The novel Photospheres™ offer to combine ease of removal with photocatalytic effectiveness at the level of powder suspensions. Photospheres™ were applied in the photocatalytic destruction of MC-LR and found to be performing at the level of powder suspensions with complete MC-LR degradation of higher than naturally occurring concentrations. Photospheres™ have been shown to be reusable for at least ten photocatalytic cycles and were effective in removing 11 MC analogues as well as nodularin in five minutes or less.

To address the issue of the financial impact posed by the use of high power UV light arrays, a pilot reactor applying UV light emitting diodes (LEDs) was designed. The photocatalytic destruction of > 75 % MC-LR over Photospheres™ was achieved in ten minutes. The energetic output of the LEDs represents a 20,000-fold reduction compared to the high power Xenon lamp that was used to achieve the previous results. Even though the LED reactor was not optimised it still achieved a high degree of removal illustrating that the use of UV LEDs in photocatalysis is a viable and economically feasible option.

For the Photospheres™ to be employed successfully in potable water treatment, it had to be demonstrated that their applicability is not limited to the removal of cyanobacterial secondary metabolites. The photocatalytic efficiency of the Photospheres™ was tested on four common waste water pollutants (2-chlorophenol, Acid Orange 74, *p*-cresol, and trichloroethylene). The photocatalytic efficiency of the Photospheres™ was compared to P25, a well studied powder catalyst. The Photospheres™ were successful in completely removing Acid Orange 74 and trichloroethylene. More than 70 % removal of 2-chlorophenol and approximately 25 % removal of *p*-cresol were achieved. The performance of the Photospheres™ compared favourably to that of P25.

Various aspects of this work would benefit from further research. The effect of natural organic matter (NOM) and other organic chemicals on the

Photospheres™ remains to be established. Furthermore, testing of the Photospheres™ in a complex matrix with a mix of pollutants/cyanobacterial metabolites would elucidate further their fitness for purpose. The application of UV LEDs in photocatalysis is another area that requires further work. Optimisation of a system that applies UV LEDs would be beneficial, taking full advantage of the opportunities that LEDs offer (longevity, flexibility in deployment and configuration, low heat release, cost effectiveness, and robustness). The incorporation of a duty cycle with on-off phases could further enhance the photocatalytic efficiency of LEDs.

#### **5.4 Monitoring and controlling of the cyanobacterial metabolites 2-MIB and GSM**

Off-flavour compounds produced by cyanobacteria constitute a nuisance factor in potable water and aquaculture and can have a significant financial impact in both sectors due to customer rejection of the product due to taste and odour. A sensitive gas chromatographic (GC-MS) method coupled with mass spectroscopic analysis that allows for the rapid, robust, and economical determination of samples at environmentally relevant concentrations was designed. Sample pre-concentration by solid phase extraction (SPE) offers a reproducible, fast, and economical means of sample concentration enabling the analysis of both 2-MIB and GSM in the low nano gram range. It has been demonstrated that apart from spiked purified water samples, also environmental samples (loch water and fishfarm water) could be determined successfully.

The development of this method was instrumental for the further research, as it allowed the rapid analysis of a large amount of samples. One area that benefitted from this was the development of a photocatalytic flow reactor that facilitates the destruction of both 2-MIB and GSM in water to below the human taste and odour threshold for these compounds. In spiked water samples the amounts of 2-MIB and GSM were successfully degraded to , 5 % of the original concentration ( $100 \text{ ng L}^{-1}$ ). The reactor was also successfully applied to the removal of both compounds from fishfarm water reducing the amounts of 2-MIB and GSM by 95 %.

A further area that benefitted from the rapid analysis method was the evaluation of silicone rubber membranes (SRMs) as passive sampling devices. It was demonstrated that SRMs are suitable samplers for both 2-MIB and GSM. The partition coefficient ( $K_{\text{SRMW}}$ ) of silicone rubber and water for 2-MIB and GSM were successfully determined, and it was further established that the isothermic equilibrium of the samplers and the analytes was reached after 6 h. The suitability of SRMs as passive samplers for 2-MIB and GSM was further demonstrated when they were deployed at a fishfarm and were able to correctly predict the concentration of both compounds in the sampled water (confirmation by SPE-GC-MS). It was also shown that the presence of other organic matter did not negatively impact on the recoveries of either 2-MIB or GSM and, due to the short exposure time, biofouling did not pose a problem. The stability of both 2-MIB and GSM on SRMs was also evaluated under different storage conditions. However, it was found that neither compound

remained stable under the conditions tested. The reasons for this remain unestablished.

In the future enhancing the design of the flow reactor to allow a higher flow rate and thus a higher through-put needs to be evaluated, the relatively low flow rate of  $2 \text{ L min}^{-1}$  ( $120 \text{ L h}^{-1}$ ) is unsuitable in either a potable water treatment or an aquaculture setting. The limiting factor in the presented study was the structural integrity of the connection of the reactor to the feed hose. If this limitation can be addressed a potential application in water treatment or aquaculture could be feasible, possibly in combination with UV LEDs to reduce the cost of operation. Further development of the SRMs as passive samplers is also required. At this point the only solution to the stability issue is the placement of the exposed SRMs in vials with extraction solvent to prevent analyte loss. Options for the use of the GC-MS method in the application in other fields presents another avenue of investigation, for example contamination of wine with GSM is a known problem and a rapid analysis method would present a useful tool in developing means of preventing contamination of this produce.

# **References**



## 6 References

ABDOLLAHI, Y., Abdullah, A.H., Zakaria, A., Zainal, Z., Reza, H., Yusof, N.A., (2012) *Photocatalytic degradation of p-cresol by zinc oxide under UV irradiation*. International Journal of Molecular Sciences, 13 (1), pp. 302-315

ADAMS, D. (1997) *Cyanobacteria*, in J. Shapiro and M. Dworkin (eds) *Bacteria as multicellular organisms*. Oxford University Press: New York, pp. 109-48

ATSDR (2010) *Minimal risk levels (MRLs) for hazardous substances*. [online] Agency for Toxic Substances And Disease Registry  
<http://www.atsdr.cdc.gov/mrls/mrllist.asp#30tag> [accessed on 26 January 2011]

AGRAWAL, S. and SINGH, V. (2002) *Viability of dried filaments, survivability and reproduction under water stress, and survivability following heat and UV exposure in Lyngbya martensiana, Oscillatoria agardhii, Nostoc calcicolam Hormidium fluitans, Spirogyra sp and Vaucheria geminata*. Folia Microbiologica, 47 (1), pp. 61-67

AGUS, E., Lim., M., Zhang, L., Sedlak, D. (2011) *Odorous compounds in municipal wastewater effluent and potable water reuse systems*. Environmental Science and Technology, 45, pp. 9347-9355

ANDERSON, R., Luu, D., Chen, C., Holmes, M., Kent, M., Le Blanc, F., Taylor, J., Williams, D. (1993) *Chemical and biological evidence links microcystins to salmon nepten liver disease*. *Toxicon*, 31, pp. 1315–1323

BANSAL, P., Singh, D., Dhiraj, S., (2010) *Photocatalytic degradation of azo dye in aqueous TiO<sub>2</sub> suspension: Reaction pathway and identification of intermediates products by LC/MS*. *Separation and Purification Technology*, 72, pp. 357-365

BÁRTOVÁ, K., Hilscherová, K., Babica, P., Maršálek, B. (2011) *Extract of Microcystis water bloom affects cellular differentiation in filamentous cyanobacterium Trichormus variabilis (Nostocales, Cyanobacteria)*. *Journal of Applied Phycology*, 23, pp. 967-973

BAUERSACHS, T., Speelman, E., Hopmans, E., Reichart, G., Schouten, S., Damste, J. (2010) *Fossilized glycolipids reveal past oceanic N<sub>2</sub> fixation by heterocystous cyanobacteria*. *Proceedings of the National Academy of Sciences of the United States of America*, 107 (45), pp. 19190-19194

BERNHARDT, H. and Clasen, J. (1991) *Flocculation of microorganisms*. *AQUA*, 40 (2), pp. 76-87

BERTELLI, M. and SELLI, E., (2006) *Reaction paths and efficiency of photocatalysis on TiO<sub>2</sub> and of H<sub>2</sub>O<sub>2</sub> photolysis in the degradation of 2-chlorophenol*. *Journal of Hazardous Materials*, B138, pp. 46-52

BERTHELOT and ANDRE (1892) Chapitre XIV: *Sur l'odeur proper de la terre*. In Berthelot and Marcellin (eds) *Chimie végétale et agricole*. Masson: Paris, pp. 227-230

BLAHA, L., Sabater, S., Babica, P., Vilalta, E., Maršálek, B. (2004) *Geosmin occurrence in riverine cyanobacteria mats: is it causing a significant health hazard?*. *Water Science & Technology*, 9, pp. 307-312

BRIAND, E., Bormans, M, Quiblier, C., Salençon, M., Humbert, J. (2012) *Evidence of the cost of the production of microcystins by *Microcystis aeruginosa* under differing light and nitrate environmental conditions*. *PLOS ONE*, 7 (1), pp. 1-10

BRUCHET, A, Bernazeau, F., Baudin, I., Pieronne, P. (1998) *Algal toxins in surface waters: analysis and treatment*. *Water Supply* 16 (1-2), pp. 619-623

BUDAVARI, S. (2001). *The Merck index: an encyclopedia of chemicals, drugs, and biological*. Merck & Co: Whitehouse Station, NJ

BYRNE, J., Eggins, B., Brown, N., McKinney, B., Rouse, M. (1998) *Immobilisation of TiO<sub>2</sub> powder for the treatment of polluted water*. *Applied Catalysis B: Environmental*, 17 (1-2), pp. 25-36

CARMICHAEL, W. (1994) *Toxins of Cyanobacteria*. *Scientific American*, 270 (1), pp. 78-86

CARMICHAEL, W. (1997) *The cyanotoxins*. Advanced Botany Research, 27, pp. 212-256

CARMICHAEL, W., Azevedo, S., An, J., Molica, R., Jochimsen, E., Lau, S., Rinehard, K., Shaw, G., Eaglesham, G. (2001) *Human fatalities from cyanobacteria: chemical and biological evidence for cyanotoxins*. Environmental Health Perspectives, 109 (7), pp. 663-668

CARP, O., Huisman, C., Reller, A. (2004) *Photoinduced reactivity of titanium dioxide*. Progress in Solid State Chemistry, 32, pp. 33-177

CASTENHOLZ, R. and WATERBURY, J. (1989) In: J. Stanley, M. Bryant, N. Pfennig, J. Holt, (eds) *Bergey's Manual of Systematic Bacteriology*, Williams and Wilkins: Baltimore, pp. 1710-1727

CHESTNUTT, J., Bach, M., Mazyck, D. (2007) *Improvement of thermal reactivation of activated carbon for the removal of 2-methylisoborneol*. Water Research, 41, pp. 79-86

CHORUS, I. and BARTRAM, J. (Editors) (1999) *Toxic Cyanobacteria in water: a guide to their public health consequences, monitoring, and management*. E & FN Spon: New York

CHOW, C., Panglisch, S., House, J., Drikas, M., Burch, M., Gimbel, R. (1997) *A study of membrane filtration for the removal of cyanobacterial cells*. AQUA, 46 (6), pp. 324-334

CHRISTOFFERSEN, K., Lyck, S., Winding, A., (2002) *Microbial activity and bacterial community structure during degradation of microcystins*. Microbial Ecology, 27 (2), pp. 125-136

COOK, D. and NEWCOMBE, G. (2002) *Removal of microcystin variants with powdered activated carbon*. Water Science and Technology: Water Supply, 2 (5-6), pp. 201-207

CORNISH, B., Lawton, L. A., Robertson, P.J.K. (2000) *Hydrogen peroxide enhanced photocatalytic oxidation of microcystin-LR using titanium dioxide*. Applied Catalysis B: Environmental, 25, pp. 59-67

COUSINS, I., Bealing, D., James, H., Sutton, A. (1996) *Biodegradation of microcystin-LR by indigenous mixed bacterial populations*. Water Research, 30 (2), pp. 481-485

DAWSON, R. (1998) *The Toxicology of microcystins*. Toxicon, 36 (7), pp. 953-962

DE FIGUEIREDO, D., Azeiteiro, U., Esteves, S., Gonçalves, F., Pereira, M. (2004) *Microcystin-producing blooms – a serious global public health issue*. *Ecotoxicology and Environmental Safety*, 59, pp. 151-163

DEVLIN, J., Edwards, O., Gorham, P., Hunter, M., Pike, R., Stavric, B. (1977) Anantoxin-a, a toxic alkaloid from *Anabaena flos-aquae* NCR-44h. *Canadian Journal of Chemistry*, 55, pp. 1367-1371

DIOGINI, C., Lawlor, T., McFarland, J., Johnsen, P. (1993) *Evaluation of geosmin and 2-methylisoborneol on the histidine dependence of TA98 and TA100 Salmonella typhimurium tester strains*. *Water Research*, 27 (11), pp. 1615-1618

DONATI, C., Drikas, M., Hayes, R., Newcombe, G. (1994) *Microcystin-LR adsorption by powdered activated carbon*. *Water Research*, 29 (8), pp. 1735-1742

DOW, C. and SWOBODA, U. (2000) *Cyanotoxins*. In: B. WHITTON and M. POTTS (eds.), *The Ecology of Cyanobacteria*. Kluwer Academic Publishers: The Netherlands, pp. 613–632

DRIKAS, M., Chow, C., House, J., Burch, M. (2001a) *Using coagulation, flocculation, and settling to remove toxic cyanobacteria*. *American Water Works Association Journal*, 93 (2), pp. 100-111

EDWARDS, C., Lawton, L.A., Coyle, S.M., Ross, P. (1996) *Laboratory scale purification of microcystins using flash chromatography and reversed phase high-performance liquid chromatography*. *Journal of Chromatography A*, 734, pp. 163-173

EDWARDS, C. and LAWTON, L. (2009) *Bioremediation of Cyanotoxins*. In: Allen, I., Laskin, S., Geoffrey, M. (Eds.) *Advances in Applied Microbiology*. Academic Press: London, pp, 109-129

EDWARDS, C. and LAWTON, L. (2010) *Assessment of microcystin purity using charged aerosol detection*. *Journal of Chromatography A*, 1217, pp. 5233-5238

ENGEL, E., Ulrich, H., Vasold, R., König, B., Landthaler, M., Süttinger, R., Bäuml, W. (2008) *Azo Pigments and a Basal Cell Carcinoma at the Thumb*. *Dermatology*, 216 (1), pp. 76–80

ENGELKE, C., Lawton, L., Jaspars, M. (2003) *Elevated microcystin and nodularin levels in cyanobacteria growing in spent medium of Planktothrix agardhii*. *Archiv für Hydrobiologie*, 158 (4), pp. 541-550

FAWELL, J., Hart, J., James, H., Parr, W. (1993) *Blue-green algae and their toxins: analysis, toxicity, treatment, and environmental control*. *Water Supply*, 11 (2-4), pp. 109-121

FERRAO-FILHO, A., Azevedo, S., DeMott, W. (2000) *Effects of toxic and non-toxic cyanobacteria on the life history of tropical and temperate cladocerans*. *Freshwater Biology*, 45, pp. 1-19

FIENG, X.G., Rong, F., Fu, D.G., Yuan, C.W., Hu, Y. (2006) *Photocatalytic degradation of trace level Microcystin-LR by nano-film of titanium dioxide*. *Chinese Science Bulletin*, 51 (10), pp. 1191-1198

FISHER, R. and WOLK, C. (1976) *Substance stimulating the differentiation of spores of the blue-green alga *Cylindrospermum lichenforme**. *Nature*, 259, pp. 394-399

FOSTER, R., Kuypers, M., Vagner, T., Paerl, R., Musat, N., Zehr, J. (2011) *Nitrogen fixation and transfer in open ocean diatom-cyanobacterial symbioses*. *ISME Journal*, 5 (9), pp. 1484-1493

FRANCHE, C., Lindström, K., Elmerich, C. (2009) *Nitrogen-fixing bacteria associated with leguminous and non-leguminous plants*. *Plant Soil*, 321, pp. 35-59

FRANCIS, G. (1878) *Poisonous Australian Lake*. *Nature*, 18, pp. 11-12



FROSCIO, S., Humpage, A., Burcham, P., Falconer, I. (2003)

*Cylindrospermopsin-induced protein synthesis inhibition and its dissociation from acute toxicity in mouse hepatocytes.* Environmental Toxicology, 18, pp. 243-251

GAGNÉ, F., Ridal, C., Blaise, B., Brownlee, J. (1999) *Toxicological effects of geosmin and 2-methylisoborneol on rainbow trout hepatocytes.* Bulletin of Environmental Contamination and Toxicology, 63, pp. 174-180

GALINDO, C., Jacques, P., Kalt, A., (2001) *Photooxidation of the phenylazonaphthol AO20 on TiO<sub>2</sub>: kinetic and mechanistic investigations.* Chemosphere, 45, pp. 997-1005

GALVIN, R. and MELLADO, J. (1998) *Potassium permanganate as pre-oxidant in a reverse osmosis water plant.* Water SA (Pretoria), 24 (4), pp. 361-363

GAN, N., Xiao, Y., Zhu, L., Wu, Z., Liu, J., Hu, C., Song, L. (2011) *The role of microcystins in maintaining colonies of bloom-forming Microcystis spp..* Society for Environmental Microbiology, Blackwell Publishing, pp. 1-13

GASH, D.M. (2008) *Trichloroethylene: Parkinsonism and complex 1 mitochondrial neurotoxicity.* Annals of Neurology, 63 (2), pp. 184-192

GERARD, C. and POULLAIN, V. (2005) *Variation in the response of the invasive species Potamopyrgus antipodarum (Smith) to natural (cyanobacterial toxin) and anthropogenic (herbizide atrazine) stressors*. Environmental Pollution, 138, pp. 28-33

GERBER, N. and LECHEVALIER, H. (1965) *Geosmin, an earth-smelling substance isolated from actinomycetes*. Applied Microbiology, 13 (6), pp. 935-938

GHADOUANI, A., Pinel-Alloul, B., Prepas, E. (2003) *Effects of experimentally induced cyanobacterial blooms on crustacean zooplankton communities*. Freshwater Biology, 48, pp. 363-381

GILBERT, J. (1990) *Differential effects of Anabaena affinis on cladocerans and rotifers: mechanisms and implications*. Ecology, 71, pp. 1727-1740

GILROY, D., Kauffman, K., Hall, R., Huang, X., Chu, F. (2000) *Assessing potential health risks from microcystin toxins in blue-green algae dietary supplements*. Environmental Health Perspectives, 108 (5), pp. 435-439

GLAZE, W., Kang, J., Chapin, D. (1987) *The chemistry of water treatment processes involving ozone, hydrogen peroxide and ultraviolet radiation*. Ozone: Science and Engineering, 9 (4), pp. 335-352

GLAZE, W.H., Kenneke, J.F., Ferry, J.L., (1993) *Chlorinated byproducts from the TiO<sub>2</sub>-mediated photodegradation of trichloroethylene and tetrachloroethylene in water*. Environmental Science and Technology, 27, pp. 177-184

GLÖCKNER, F., Zaichikov, E., Belkova, N., Denissova, L., Pernthaler, J., Pernthaler, A., Amann, R. (2000) *Comparative 16S rRNA Analysis of Lake Bacterioplankton Reveals Globally Distributed Phylogenetic Clusters Including an Abundant Group of Actinobacteria*. Applied and Environmental Microbiology, 66 (11), pp. 5053-5065

GOLDBERG, J., Huang, H., Kwon, Y., Greengard, P., Nairn, A., Kuriyan, J. (1995) *Three-dimensional structure of the catalytic subunit of protein serine/threonine phosphatase-1*. Nature, 376, pp. 745-753

GRAHAM, J., Loftin, K., Meyer, M., Ziegler, A. (2010) *Cyanotoxin mixtures and taste-and-odour compounds in cyanobacterial blooms from the Midwestern United States*. Environmental Science and Technology, 44, pp. 7361-7368

GROSS, E., Wolk, C., Jüttner, F. (1991) *Fischerellin, a new allelochemical from the freshwater cyanobacterium Fischerella muscicola*. Journal of Phycology, 27, pp. 686-692

HAGMAN, L. and JÜTTNER, F. (1996) *Fischerellin A, a novel photosystem II-inhibiting allelochemical of the cyanobacterium Fischerella muscicola with antifungal and herbicidal activity*. Tetrahedon Letters, 37 (36), pp. 6539-6542

HANNAOR, D. and SORRELL, C. (2011) *Review of the anatase to rutile phase transformation*. Journal of Material Science, 46, pp. 855-874

HANSON, T. (2003) *Economic Impact of Off-Flavor to the U.S. Catfish Industry*. ACS Symposium Series 848 Off Flavours in Aquaculture, pp. 13-29

HARADA, K. and TSUJI, K. (1998) *Persistence and decomposition of hepatotoxic microcystins produced by cyanobacteria in natural environment*. Journal of Toxicology: Toxin Reviews, 17 (3), pp. 385-403

HART, J., Fawell, J., Croll, B. (1998) *The fate of both intra- and extracellular toxins during drinking water treatment*. Water Supply, 16 (1-2), pp. 611-616

HASHIMOTO, K., Irie, H., Fujishima, A. (2005) *TiO<sub>2</sub> Photocatalysis: a Historical Review and Future Prospects*. Japanese Journal of Applied Physics, 44 (12), pp. 8269-8285

HATTORI, K. (1988) *Water treatment systems and technology for the removal of odor compounds*. Water Science and Technology, 20 (8-9), pp. 237-244

HAVENS, K. (2005) *Cyanobacteria blooms: effects on aquatic ecosystems*. In: Hudnell, K. (editor) *International Symposium of Cyanobacterial Harmful Algal Blooms*, September 6-10 2005, Triangle Park, NC, USA

HEALTH CANADA (2002) *Cyanobacterial toxins – microcystin-LR* [online]. Health Canada, Federal-Provincial Subcommittee on Drinking Water, supporting documents for the Guidelines for Canadian Drinking Water Quality. Ottawa, Ontario. Available from [http://www.hc-sc.gc.ca/ewh-semt/pubs/water-eau/cyanobacterial\\_toxins/toxin-toxines-eng.php](http://www.hc-sc.gc.ca/ewh-semt/pubs/water-eau/cyanobacterial_toxins/toxin-toxines-eng.php) [accessed 18 April 2012]

HEPPLEWHITE, C., Newcombe, G., Knappe, D. (2004) *NOM and MIB, who wins in the competition for activated carbon adsorption sites?* *Water Science & Technology*, 49 (9), pp. 257-265

HIMBERG, K., Keijola, A., Hiisvirta, L., Pyysalo, H., Sivonen, K. (1989) *The effect of water treatment processes on the removal of hepatotoxins from Microcystis and Oscillatoria cyanobacteria: a laboratory study.* *Water Research*, 23 (8), pp. 979-984

HO, L. and NEWCOMBE, G. (2005) *Effect of NOM, turbidity and floc size on the PAC adsorption of MIB during alum coagulation.* *Water Research*, 39 (15), pp. 3668-3674

HOFFMAN, J. (1976) *Removal of Microcystis toxins in water purification processes.* *Water SA (Pretoria)*, 2 (2), pp. 58-60

HOFFMANN, M., Martin, S., Choi, W., Bahnemann, D. (1995) *Environmental applications of semiconductor photocatalysis.* *Chemical Reviews*, 95, pp. 69-96

HOWGATE, P. (2004) *Tainting of farmed fish by geosmin and 2-methyl-isoborneol: a review of sensory aspects and of uptake/depuration*. *Aquaculture*, 234 (1-4), 155-181

ILISZ, I., Dombi, A., Mogyorosi, K., Farkas, A., Dekany, I. (2002) *Removal of 2-chlorophenol from water by adsorption combined with TiO<sub>2</sub> photocatalysis*. *Applied Catalysis B: Environmental*, 39, pp. 247-256

IMANISHI, S. and HARADA, K. (2004) *Proteomics approach on microcystin binding proteins in mouse liver for investigation of microcystin toxicity*. *Toxicon*, 43, pp. 651-659

ISOC-HAB (2005) Hudnell, K. (editor) *International Symposium of Cyanobacterial Harmful Algal Blooms*, September 6-10 2005, Triangle Park, NC, USA

ITO, E., Kondo, F., Terao, K., Harada, K. (1997) *Neoplastic nodular formation in mouse liver induced by repeated intraperitoneal injections of microcystin-LR*. *Toxicon*, 35, pp. 1453-1457

IZAGUIRRE, G., Hwang, C., Krasner, S., McGuire, M. (1982) *Geosmin and 2-methylisoborneol from cyanobacteria in three water supply systems*. *Applied and Environmental Microbiology*, 43 (3), pp. 708-714

JACOBY, J., Collier, D., Welch, E., Hardy, F., Crayton, M. (2000) *Environmental factors associated with a toxic bloom of Microcystis aeruginosa*. Canadian Journal of Fisheries and Aquatic Sciences, 57 (1), pp. 231-240

JÄHNICHEN, S., Long, B., Petzoldt, T. (2011) *Microcystin production by Microcystis aeruginosa: Direct regulation by multiple environmental factors*. Harmful Algae, 12, pp. 95-104

JANG, M., Ha, K., Takamura, N. (2007) *Reciprocal allelopathic responses between toxic cyanobacteria (Microcystis aeruginosa) and duckweed (Lemna japonica)*. Toxicon, 49, pp. 727-733

JARDINE, C., Gibson, N., Hrudehy, S. (1999) *Detection of odour and health risk perception of drinking water*. Water Science and Technology, 40 (6), 91-98

JIA, J., Chu, W., Ling, Y. (2009) *The photodegradation of trichloroethylene with or without the NAPL by UV irradiation in surfactant solutions*. Journal of Hazardous Materials, 161 (1), pp. 196-201

JO, C., Dietrich, A., Tanko, J. (2011) *Simultaneous degradation of disinfection byproducts and earthy-musty odorants by the UV/H<sub>2</sub>O<sub>2</sub> advanced oxidation process*. Water Research, 45, pp. 2507-2516

JONES, B. (1987) *Lake Okeechobee eutrophication research and management*. Aquatics, 9, pp. 21-26

JONES, G. and ORR, P. (1994) *Release and degradation of microcystin following algicide treatment of a Microcystis aeruginosa bloom in a recreational lake, as determined by HPLC and protein phosphatase inhibition assay*. Water Research, 28 (4), pp. 871-876

JONES, G., Falconer, I., Wilkins, R. (1995) *Persistence of cyclic peptide toxins in dried Microcystis aeruginosa crusts from lake Mokoan, Australia*. Environmental Toxicology and Water Quality, 10, pp. 19-24

JUANG, R., Lin, S., Hsueh, P. (2010) *Removal of binary azo dyes from water by UV-irradiated degradation in TiO<sub>2</sub> suspensions*. Journal of Hazardous Materials, 182 (1-3), pp. 820-826

JUNG, S., Baek, K., Yu, M. (2004) *Treatment of taste and odor material by oxidation and adsorption*. Water Science & Technology, 49 (9), pp. 289-295

KAEBERNICK, M. and NEILAN, B. (2001) *Ecological and molecular investigations of cyanotoxin production*. FEMS Microbiology Ecology, 35, pp. 1-9

KAEBERNICK, M., Neilan, B., Börner, T., Dittmann, E. (2000) *Light and transcriptional response of the microcystin biosynthesis gene cluster*. Applied and Environmental Microbiology, 66 (8), pp. 3387-3392



KANN, J. and SMITH, V. (1999) *Estimating the probability of exceeding elevated pH values critical to fish populations in a hypereutrophic lake.* Canadian Journal of Fisheries and Aquatic Sciences, 56, pp. 2262–2270

KARNER, D., Standridge, J., Harrington, G., Barnum, R. (2001) *Microcystin algal toxins in source and finished drinking water.* American Water Works Association Journal, 93 (8), pp. 72-81

KARETNIKOVA, E.A., Chaikovskaya, O.N., Sokolova, I.V., Nikitina, L.I., (2008) *Sequential degradation of p-cresol by photochemical and biological methods.* Applied Biochemistry and Microbiology, 44 (5), pp. 493-501

KARUNAKARAN, C. and DHANALAKSHMI, R., (2008) *Semiconductor-catalyzed degradation of phenols with sunlight.* Solar Energy Materials and Solar Cells, 92, pp. 1315-1321

KASARSKIS, E.J. (2008) *Clinical aspects of ALS in Gulf War Veterans.* Amyotrophic Lateral Sclerosis, 16, pp. 1-7

KAYA, K. and SANO, T. (1998) *A photodetoxification mechanism of the cyanobacterial hepatotoxin microcystin-LR by ultraviolet irradiation.* Chemical Research in Toxicology, 11 (3), pp. 159-163

KEATING, K. (1978) *Blue-green algal inhibition of diatom growth: transition from mesotrophic to eutrophic community structure.* Science, 199, 971-973

KEIJOLA, A., Himberg, K., Esala, A., Sivonen, K., Kiisvirata, L. (1988) *Removal of cyanobacterial toxins in water treatment processes: laboratory and pilot plant experiments*. Toxicity Assessment, 3, pp. 643-656

KIELY, G. (1998). Environmental Engineering, Irwin/McGraw-Hill

KOCH, B., Gramith, J., Dale, M., Ferguson, D. (1992) *Control of 2-Methylisoborneol and Geosmin by ozone and peroxone: A pilot study*. Water Science & Technology, 25 (2), pp. 291-298

KRIENITZ, L., Bock, C., Kotut, K., Luo, W. (2012) *Picocystis salinarum (Chlorophyta) in saline lakes and hot springs of East Africa*. Phycologia, 51 (1), pp. 22-32

KU, Y., Leu, R.M., Lee, K.C., (1996) *Decomposition of 2-chlorophenol in aqueous solution by UV irradiation with the presence of titanium dioxide*. Water Research, 30 (11), pp. 2569-2578

LAMBERT, T., Holmes, C., Hrudey, S. (1996) *Adsorption of microcystin-LR by activated carbon and removal in full scale water treatment*. Water Research, 30 (6), pp. 1411-1422

LAWTON, L. A. and EDWARDS, C. (2001) *Purification of microcystins*. Journal of Chromatography A, 912 (2), pp. 191-209

LAWTON, L.A., Robertson, P.K.J., Cornish, B.J.P.A., Marr, I.L., Jaspars, M., (2003) *Processes influencing surface interaction and photocatalytic destruction of microcystins on titanium dioxide photocatalysts*. *Journal of Catalysis*, 213, pp. 109-113

LAWTON, L. A. and ROBERTSON, P.J.K. (1999) *Physico-chemical treatment methods for the removal of microcystins*. *Chemical Society Reviews*, 28 (4), 217-224

LAWTON, L., Edwards, C., Codd, G. (1994) *Extraction and high performance liquid chromatographic method for the determination of microcystins in raw and treated waters*. *Analyst*, 119, 1525-1530

LEÃO, P., Vasconcelos, M., Vasconcelos, V. (2009) *Allelopathy in freshwater cyanobacteria*. *Critical Reviews in Microbiology*, 35 (5), pp. 271-282

LEHTINIEMI, M., Engstrom-Ost, J., Karjalainen, M., Kozlowsky-Suzuki, B., Viitasalo, M. (2002) *Fate of cyanobacterial toxins in the pelagic food web: transfer to copepods or to fecal pellets?* *Marine Ecology Progress Series*, 241, pp. 13-21

LETTERMAN, R. (Editor) (1999) *Water quality and treatment: a handbook of community water supplies*. 5<sup>th</sup> ed. American Water Works Association, McGraw Hill, Inc.: New York

LEVINE, L.H., Richards, J.T., Coutts, J.L., Soler, R., Maxik, F., Wheeler, R.M., (2011) *Feasibility of ultraviolet-light-emitting diodes as an alternative light source for photocatalysis*. Journal of the Air and Waste Management Association, 61 (9), pp. 932-940

LI, Y., Chen, L., Guo, Y.L., Sun, X.G., Wei, Y (2012) *Preparation and characterization of WO<sub>3</sub>/TiO<sub>2</sub> hollow microsphere composites with catalytic activity in the dark*. Chemical Engineering Journal, 181, pp. 734-739

LIRAS, V., Lindberg, M., Nystrom, P., Annadotter, H., Lawton, L., Graf, B. (1998) *Can ingested cyanobacteria be harmful to the signal crayfish (Pacifastacus leniusculus)?* Freshwater Biology, 39 (2), pp. 233-242

LIU, I., Lawton, L.A., Bahnemann, D., Liu, L., Proft, B., Robertson, P. (2009) *The photocatalytic decomposition of microcystin-LR using selected titanium dioxide materials*. Chemosphere, 76, pp. 549-553

LIU, I., Lawton, L.A., Cornish, B.J.P.A, Robertson, P.K.J. (2002) *Mechanistic and toxicity studies of the photocatalytic oxidation of microcystin-LR*. Journal of Photochemistry and Photobiology A: Chemistry, 148, pp. 349-354

LIU, I., Lawton, L.A., Bahnemann, D.W., Robertson, P.K.J. (2005) *The photocatalytic destruction of the cyanotoxin, nodularin using TiO<sub>2</sub>*. Applied Catalysis B: Environmental, 60, pp. 245-252

LIU, Y., Li, X., Jia, R., Huang, L., Zhou, Y., Gao, Y. (2011) *Effects of biological soil crusts on soil nematode communities following dune stabilization in the Tengger Desert, Northern China*. *Applied Soil Ecology*, 49, pp. 118-124

LIU, J., Tao, Y., Sun, J., Jiang, G. (2011) *Development of polypropylene glycol coated hollow fibre membranes as passive sampler for field equilibrium sampling of odorous compounds in environmental waters*. *Analytical Methods*, 3, pp. 696-702

LOVELL, R. Lelana, I., Boyd, C., Armstrong, M. (1986) *Geosmin and muddy-musty flavour compounds in pond-raised channel catfish*. *Transactions of the American Fisheries Society*, 115, pp. 485-489

LUKAC, M. and AEGERTER, R. (1993) *Influence of trace-metals on growth and toxin production of Microcystis aeruginosa*. *Toxicon*, 31 (3), pp. 293-305

LUMPKIN, T. and PLUCKNETT, D. (1980) *Azolla: botany, physiology, and use as a green manure*. *Economic Botany*, 34, pp. 111-153

MAGALHAES, V., Soares, R., Azevedo, S. (2001) *Microcystin contamination in fish from Jacarepagua Lagoon: ecological implication and human health risk*. *Toxicon*, 39, pp. 1077-1085

MARTÍNEZ, L., Morán, A., García, A. (2012) *Effect of light on Synechocystis sp. and modelling of its growth rate as a response to average irradiance.* Journal of Applied Phycology, 24, pp. 125-134

MATSUMOTO, A. and TSUCHIYA, Y. (1988) *Earthy-musty odor-producing cyanophytes isolated from five water areas in Tokyo.* Water Science & Technology, 20 (8-9), 179-183

MATSUNAGA, H., Harada, K., Senma, M., Ito, Y., Yasuda, N., Ushida, S., Kimura, Y. (1999) *Possible cause of unnatural mass death of wild birds in a pond in Nishinomiya, Japan: sudden appearance of toxic cyanobacteria.* Natural Toxins, 7, pp. 81-84

MAZUR-MARZEC, H., Torunska, A., Blonska, M., Moskot, M., Plinski, M., Jakóbkiewicz-Banecka, J., Wegrzyn, G. (2009) *Biodegradation of nodularin and effects of the toxin on bacterial isolates from the Gulf of Gdansk.* Water Research, 43, pp. 2801-2810

MCELHINEY, J. and LAWTON, L. (2005) *Detection of the cyanobacterial hepatotoxins microcystins.* Toxicology and Applied Pharmacology, 203, pp. 219-230

MCGUIRE, M. (1995) *Off-flavor as the consumer's measure of drinking water safety.* Water Science and Technology, 31 (11), pp.1-8

MCGUIRE, M. and GATSON, J. (1988) *Overview of technology for controlling off-flavors in drinking water*. *Water Science and Technology*, 20 (8-9), pp. 215-228

MIKHAILOV, A., Harmala-Brasken, A., Hellman, J., Meriluito, J., Eriksson, J. (2003) *Identification of ATP-synthase as a novel intracellular target for microcystin-LR*. *Chemico-Biological Interactions*, 142, pp. 223-237

MILLER, M. and FALLOWFIELD, H. (2001) *Degradation of cyanobacterial hepatotoxins in batch experiments*. *Water Science and Technology*, 43 (12), pp. 229-232

MILLS, A. and LE HUNTE, S. (1997) *An overview of semiconductor photocatalysis*. *Journal of Photochemistry and Photobiology A: Chemistry*, 108 (1), pp. 1-35

MILLS, A., Davies, R., Worsley, D. (1993) *Water purification by semiconductor photocatalysis*. *Chemical Society Reviews*, 45, pp. 417-425.

MINERO, C. and ALIBERTI, C. (1991) *Kinetic studies in heterogeneous photocatalysis. 6. AM1 Simulated Sunlight photodegradation over titania in aqueous media: a first case of fluorinated aromatics and identification of intermediates*. *Langmuir*, 7, pp. 928-936

MOHAMED, Z. and SHEHRI, A. (2009) *Microcystin-producing blooms of Anabaenopsis arnoldi in a potable mountain lake in Saudi Arabia*. FEMS Microbiology Ecology, 69, pp. 98-105

MOISANDER, P., Ochiai, M., Lincoff, A. (2009) *Nutrient limitation of Microcystis aeruginosa in Northern California Klamath River Reservoirs*. Harmful Algae, 8 (6), pp. 889-897

MOUCHET, P. and BONNÉLYE, V. (1998) *Solving algae problems: French expertise and world-wide applications*. AQUA, 47 (3), pp. 125-141

MUNTISOV, M. and TRIMBOLI, P. (1996) *Removal of algal toxins using membrane technology*. Journal of the Australian Water Association, 23 (3), p. 34

MUR, L., Skulberg, O., Utkilen, H. (1999) *Cyanobacteria in the environment*. In: I. Chrous and J. Bartram (eds) *Toxic cyanobacteria in water: a guide to their public health consequences, monitoring and management*. E & FN Spon: New York, pp. 113-132

NAKAJIMA, M., Ogura, T., Kusama, Y., Iwabuchi, N., Imawaka, T., Araki, A., Sasaki, T., Hirose, E., Sunairi, M. (1996) *Inhibitory effects of odor substances, geosmin and 2-methylisoborneol, on early development of sea urchins*. Water Research, 30 (10), pp. 2508-2511



NATIONAL GEOGRAPHIC (2012) *Brown-throated three-toed sloth* (*Bradypus vagriegatus*) [online]. National Geographic stock images, available from <http://www.nationalgeographicstock.com/ngsimages/explore/explore.jsf> [accessed 18 April 2012]

NEGORO, T., Ando, M., Ichikawa, N. (1988) *Blue-green algae in Lake Biwa which produce earthy-musty odors*. *Water Science & Technology*, 20 (8-9), pp. 117-123

NERENBERG, R., Rittmann, B., Soucie, W. (2000) *Ozone/biofiltration for removing MIB and geosmin*. *American Water Works Association Journal*, 92 (12), pp. 85-95

NEUMAN, J. and WECKESSER, H. (1998) *Elimination of microcystin peptide toxins from water by reverse osmosis*. *Environmental Toxicology and Water Quality*, 13 (2), pp. 143-148

NG, C., Losso, J., Marshall, W., Rao, R. (2002) *Freundlich adsorption isotherms of agricultural by-product-based powdered activated carbons in a geosmin-water system*. *Bioresource Technology*, 85 (2), pp. 131-135

NHMRC and ARMCANZ (2011) *Australian drinking water guidelines* [online]. National Health and Medical Research Council (NHMRC) and the Agriculture and Resource Management Council of Australia and New Zealand (ARMCANZ), Canberra, Australia. Available from [http://www.nhmrc.gov.au/\\_files\\_nhmrc/publications/attachments/eh52\\_aaus\\_drinking\\_water\\_guidelines\\_120323\\_0.pdf](http://www.nhmrc.gov.au/_files_nhmrc/publications/attachments/eh52_aaus_drinking_water_guidelines_120323_0.pdf) [accessed 18 April 2012]

O'ROURKE, C. and MILLS, A. (2010) *Adsorption and photocatalytic bleaching of acid orange 7 on P25 titania*. *Journal of Photochemistry and Photobiology A: Chemistry*, 216, pp. 261-267

ORR, P., Jones, G., Hamilton, G. (2004) *Removal of saxitoxins from drinking water by granular activated carbon, ozone and hydrogen peroxide - implications for compliance with the Australian drinking water guidelines*. *Water Research*, 38 (20), pp. 4455-4461

PAERL, H. (1988) *Nuisance phytoplankton blooms in coastal, estuarine and inland waters*. *Limnology and Oceanography*, 33, pp. 823-847

PAERL, H. and HUISMAN, J. (2008) *Blooms like it hot*. *Science*, 320, pp.57-58

PAPKE, U., Gross, E., Francke, W. (1997) *Isolation, identification and determination of the absolute configuration of Fischerellin B. A new algicide from the freshwater cyanobacterium Fischerella muscicola (Thuret)*. *Tetrahedon Letters*, 38 (3), pp. 379-382

PEARSON, L., Hisbergues, M., Börner, T., Dittmann, E., Neilan, B. (2004) *Inactivation of an ABC transporter gene, mcyH, results in loss of microcystin production in the cyanobacterium Microcystis aeruginosa PCC 7806*. Applied and Environmental Microbiology, 70 (11), pp. 6370-6378

PEIRO, A.M., Ayllon, J.A., Peral, J., Domenech, X. (2001) *TiO<sub>2</sub>-photocatalyzed degradation of phenol and ortho-substituted phenolic compounds*. Applied Catalysis B: Environmental, 30, pp. 359-373

PERSSON, P. (1982) *Muddy odour: a problem associated with extreme eutrophication*. Hydrobiologia, (1-32), pp. 161-164

PESTANA, C. (2008) *Applying a novel stable labelling method to assess the impact of cyanobacterial signalling compounds on microcystin synthesis in Microcystis aeruginosa*. Unpublished thesis (MSc), Robert Gordon University, Aberdeen, Scotland

PIRBAZI, M., Borow, H., Craig, S., Ravindran, V., McGuire, M. (1992) *Physical chemical characterization of five earthy-musty-smelling compounds*. Water Science and Technology, 25 (2), pp. 81-88

POBLETE, R., Otal, E., Vilches, L.F., Vale, J., Fernandez-Pereira, C. (2011) *Photocatalytic degradation of humic acids and landfill leachate using a solid industrial by-product containing TiO<sub>2</sub> and Fe*. Applied Catalysis B: Environmental, 102, pp. 172-179

POULOPOULOS, S.G., Nikolaki, M., Karampetsos, D., Philippopoulos, C.J. (2008) *Photochemical treatment of 2-chlorophenol aqueous solutions using ultraviolet radiation, hydrogen peroxide and photo-Fenton reaction*. Journal of Hazardous Materials, 153 (1-2), pp. 582-587

PREPAS, E., Kotak, B., Campbell, L., Evans, J., Hrudehy, S., Holmes, C. (1997) *Accumulation and elimination of cyanobacterial hepatotoxins by the freshwater clam Anodonta grandis simpsoniana*. Canadian Journal of Fisheries and Aquatic Sciences, 54, pp. 41-46

RANTALA, A., Fewer, D., Hisbergues, M., Rouhiainen, L., Vaitomaa, J., Borner, T., Sivonen, K. (2004) *Phylogenetic evidence for the early evolution of microcystin synthesis*. Proceedings of the National Academy of Sciences of the United States of America, 101, pp. 568-573

RAPALA, J. and SIVONEN, K. (1997) *Assessment of environmental conditions that favour hepatotoxic and neurotoxic Anabaena spp. strains cultured under light limitation at different temperatures*. Microbial Ecology, 36, pp. 181-192

RAPALA, J., Lahti, K., Sivonen, K., Niemelä, S. (1994) *Biodegradability and adsorption on lake sediments of cyanobacterial hepatotoxins and anatoxin-a*. Letters in Applied Microbiology, 19 (6), pp. 423-428

RASHID, M.M. and SATO, C. (2010) *Photolysis, sonolysis, and photosonolysis of trichloroethane (TCA), trichloroethylene (TCE), and tetrachloroethylene (PCE) without catalyst*. *Water Air Soil Pollution*, 216, pp. 429-440

RAVEN, J. and ALLEN, J. (2003) *Genomics and chloroplast evolution: what did cyanobacteria do for plants?*. *Genome Biology*, 4 (3), article 209

REISS, R., Taylor, J., Robert, C. (1999) *Surface water treatment using nanofiltration – pilot testing results and design considerations*. *Desalination*, 125, pp. 97-112

RIDEH, L., Wehrer, A., Ronze, D., Zoulalian, A. (1997) *Photocatalytic degradation of 2-chlorophenol in TiO<sub>2</sub> aqueous suspension: modeling of reaction rate*. *Industrial and Engineering Chemistry Research*, 36, pp. 4712-4718

RINEHART, K. , Harada, K., Namikoshi, M., Chen, C., Harvis, C. (1988) *Nodularin, microcystin, and the configuration of Adda*. *Journal of the American Chemical Society*, 110, pp. 8557-8558

ROBERTSON, P., Lawton, L., Munch, B., Rouzade, J. (1997) *Destruction of cyanobacterial toxins by semiconductor photocatalysis*. *Chemical Communications*, 4, pp. 393-394

ROBERTSON, R., Hammond, A., Jauncey, K., Beveridge, M., Lawton, L. (2006) *An investigation into the occurrence of geosmin responsible for earthy-musty taints in UK farmed rainbow trout, Onchorchynchus mykiss*. *Aquaculture*, 259, pp. 153-163

ROHRLACK, T. and HEYENSTRAND, P. (2007) *Fate of intracellular microcystins in the cyanobacterium Mircocystis aeruginosa (Chroococcales, Cyanobphyceae)*. *Phycologia*, 46 (3), pp. 277-283

ROSENFELDT, E., Melcher, B., Linden, K. (2005) *UV and UV/H<sub>2</sub>O<sub>2</sub> treatment of methylisoborneol (MIB) and geosmin in water*. *AQUA*, 54 (7), pp. 423-434

ROSITANO, J. and NICHOLSON, B. (1994) *Water treatment techniques for removal of cyanobacterial toxins from water*. Australian Centre for Water Quality Research, Salisbury, South Australia

ROSITANO, J., Newcombe, G., Nicholson, B., Sztajn bok, P. (2001) *Ozonation of NOM and algal toxins in four treated waters*. *Water Research*, 35 (1), pp. 23-32

ROSITANO, J., Nicholson, B., Pieronne, P. (1998) *Destruction of cyanobacterial toxins by ozone*. *Ozone: Science and Engineering*, 20, pp. 223-238

SAN MIGUEL, G., Lambert, S., Graham, N. (2001) *The regeneration of field-spent granular-activated carbons*. *Water Research*, 35 (11), pp. 2740-2748

SANO, T., Takagi, H., Nagano, K., Nishikawa, M., Kaya, K. (2011) *Accurate LC-MS analyses for microcystins using per-<sup>15</sup>N-labelled microcystins*. *Analytical and Bioanalytical Chemistry*, 399, pp. 2511-2516

SCHATZ, D., Keren, Y., Vardi, A., Sukenik, A., Carmeli, S., Börner, T., Dittmann, E. (2007) *Towards clarification of the biological role of microcystins, a family of cyanobacterial toxins*. *Environmental Microbiology*, 9 (4), pp. 965-970

SCHEFFER, M., Hosper, S., Meijer, M., Moss, B., Jeppesen, E. (1993) *Alternative equilibria in shallow lakes*. *Trends in Ecology and Evolution*, 8, pp. 275-279

SCHMIDT, W., Willmetzer, H., Bornmann, K., Pietsch, J. (2002) *Production of drinking water from raw water containing cyanobacteria – pilot plant studies for assessing the risk of microcystin break-through*. *Environmental Toxicology*, 17 (4), pp. 375-385

SEGER, R. and KREBS, E. (1995) *The MAPK signalling cascade*. *FASEB Journal*, 9, pp.726-735

SHEPHARD, G.S., Stockenstrom, S., de Villiers, D., Engelbrecht, W.J., Wesels, G.F.S. (2002) *Degradation of microcystin toxin in a fallin film photocatalytic reactor with immobilized titanium dioxide catalyst*. *Water Research*, 36 (1), pp. 140-146

SHI, L., Carmichael, W., Miller, I. (1995) *Immunogold localization of hepatotoxins in cyanobacterial cells*. Archives of Microbiology, 163 (1), pp. 7-15

SHIE, J.L. and PAI, C.Y. (2010) *Photodegradation kinetics of toluene in indoor air at different humidities using UVA, UVC and UVLED light sources in the presence of silver titanium dioxide*. Indoor and Built Environment, 19 (5), pp. 503-512

SHIE, J.L., Lee, C.H., Chiou, C.S., Chang, C.T., Chang, C.C., Chang, C.Y. (2008) *Photodegradation kinetics of formaldehyde using light sources of UVA, UVC and UVLED in the presence of composed silver titanium dioxide photocatalyst*. Journal of Hazardous Materials, 155, pp. 164-172

SIVONEN, K. (1996) *Cyanobacterial toxins and toxin production*. Phycologia, 35 (6) pp. 12-24

SIVONEN, K. and JONES, G. (1999) *Cyanobacterial toxins*. In: I. Chorus and J Bartram (eds) *Toxic cyanobacteria in water: a guide to their public health consequences, monitoring, and management*. E & FN Spon: New York, pp. 41-111



SMITH, D., Levine, A., Mody, A., MacLeod, B., Simpson, M. (2003) *Factors influencing selection of nanofiltration membranes for removal of organics from surface water*. AWWA Water Quality Technology Conference, Philadelphia, Pennsylvania

SOBCZYŃSKI, A. and DOBOSZ, A. (2001) *Water purification by photocatalysis on semiconductors*. Polish Journal of Environmental Studies, 10 (4), pp. 195-205

STANIER, R., Kunisawa, R., Mandel, M., Cohen-Bazire, G. (1971) *Purification and properties of unicellular blue-green algae (order Chroococcales)*. Bacteriological Reviews, 35, pp. 171-205

SU, Z., Sheets, M., Ishida, H., Li, F., Barry, W. (2004) *Saxitoxin Blocks L-Type ICa*. Journal of Pharmacology and Experimental Therapeutics, 308, pp. 324-329

SUDO, Y. (1996) *End-capping of octadecylsilylated silica gels by high temperature silylation*. Journal of Chromatography A, 737, pp. 139-147

SUFFET, I., Khiari, D., Bruchet, A. (1999) *The drinking water taste and odor wheel for the millennium: Beyond Geosmin and 2-Methylisoborneol*. Water Science and Technology, 40 (6), pp. 1-13

SUIKKANEN, S., Fistarol, G., Granéli, E. (2004) *Allelopathic effects of the Baltic cyanobacteria Nodularia Spumigena, Aphanizomenon flos-aquae and Anabaena lemmermannii on algal monocultures*. Journal of Experimental Marine Biology and Ecology, 308, pp. 85-101

SUMITOMO, H. (1992) *Biodegradation of 2-Methylisoborneol by gravel sand filtration*. Water Science & Technology, 25 (2), pp. 191-198

SUMMONS, R., Jahnke, L., Hope, J., Logan, G. (1999) *2-Methylhopanoids as biomarkers for cyanobacterial oxygenic photosynthesis*. Nature, 400, pp. 554-557

SURYAMAN, D. and HASEGAWA, K. (2010) *Biological and photocatalytic treatment integrated with separation and reuse of titanium dioxide on the removal of chlorophenols in tap water*. Journal of Hazardous Materials, 183, pp. 490-496

SVCRCCEK, C. and SMITH, D. (2004) *Cyanobacteria toxins and the current state of knowledge on water treatment options: a review*. Journal of Environmental Engineering and Science, 3, pp. 155-185

TSUJI, K., Nalto, S., Kondo, F., Ishikawa, N., Wantanabe, M., Suzuki, M., Harada, K. (1994) *Stability of microcystins from cyanobacteria: effect of light on decomposition and isomerisation*. Environmental Science and Technology, 28 (1), pp. 173-177

TSUJI, K., Watanuki, T., Kondo, F., Watanabe, M., Suzuki, S., Nakazawa, H., Suzuki, M., Uchida, H., Harada, K. (1995) *Stability of microcystins from cyanobacteria – II. Effect of UV light on decomposition and isomerisation*. *Toxicon*, 33 (12), pp. 1619-1631

TUNG, S., Lin, T., Liu, C., Lai, S. (2004) *The effect of oxidants on 2-MIB concentration with the presence of cyanobacteria*. *Water Science & Technology* (9), pp. 281-288

TURCHI, C. and OLLIS, D. (1990) *Photocatalytic degradation of organic water contaminants: Mechanisms involving hydroxyl radical attack*. *Journal of Catalysis*, 122 (1), pp. 178-192

U.S. EPA (1998) *Drinking water contaminant candidate list*. United States Environmental Protection Agency, Washington, D.C., EPA 815-F-98-002

VACELET, J. (1971) *Étude en microscopie électronique de l'association entre une cyanophycée chroococcale et une éponge du genre Verongia*. *Journal de Microscopie*, 12, pp. 363-380

VAN APPELDOORN, M., Vab Egmond, H., Speijers, G., Bakker, G. (2007) *Toxins of cyanobacteria*. *Molecular Nutrition and Food Research*, 51, pp. 7-60

VARIN, T., Lovejoy, C., Jungblut, A., Vincent, W., Corbeil, J. (2011) *Metagenomic analysis of stress genes in microbial mat communities from Antarctica and the High Arctic*. Applied and Environmental Microbiology, 78 (2), pp. 549-559

VELDHUIS, M. and KRAAY, G. (2000) *Application of flow cytometry in marine phytoplankton research: current applications and future perspectives*. Scientia Marina, 64 (2), pp. 121-134

VELEGRAKI, T., Poullos, I., Charalabaki, M., Kalogerakis, N., Samaras, P., Mantzavinos, D. (2006) *Photocatalytic and sonolytic oxidation of acid orange 7 in aqueous solution*. Journal of Photochemistry and Photobiology A: Chemistry, 62, pp. 159-168

VIEIRA, J., Azevedo, M., Azevedo, S., Honda, R., Correa, B. (2003) *Microcystin production by Radiocystis fernandoi (Chroococcales, Cyanobacteria) isolated from a drinking water reservoir in the city of Belem, PA, Brazilian Amazonia region*. Toxicon, 42, pp. 709-713

WARHURST, A., Ragget, S., McConnachie, G., Pollard, S., Chipofya, V., Codd, G. (1997) *Adsorption of the cyanobacterial hepatotoxin microcystin-LR by a low-cost activated carbon from the seed husks of the pan-tropical tree, Moringa oleifera*. Science of the Total Environment, 207 (2-3), pp. 207-211

WARNER, M.A., Harper, J.V., Miller, J. (1985) *Cardiac dysrhythmias associated with chemical peeling with phenol*. *Anesthesiology*, 62 (3), pp. 366–367.

WHO (1998) *Guidelines for drinking water quality*. 2<sup>nd</sup> ed. World Health Organisation, Geneva, Switzerland

WHO (2003) *Guidelines for Drinking-water Quality*. 3<sup>rd</sup> ed. [online] World Health Organisation, Geneva. Available from:

[http://www.who.int/water\\_sanitation\\_health/dwq/fulltext.pdf](http://www.who.int/water_sanitation_health/dwq/fulltext.pdf)

[accessed on 26 January 2011]

WHO (2008). *Guidelines for safe recreational water environments*. [online] World Health Organisation, Geneva. Available from:

<http://whqlibdoc.who.int/publications/2003/9241545801.pdf>

[accessed on 26 January 2011]

WIEDNER, C., Visser, P., Fastner, J., Metcalf, J., Codd, A., Mur, R. (2003) *Effects of light on microcystin content of Microcystis strain PCC 7806*. *Applied and Environmental Microbiology*, 69 (3), pp. 1475-1481

WIEGAND, C. and PFLUGMACHER, S. (2005) *Ecotoxicological effects of selected cyanobacterial secondary metabolites a short review*. *Toxicology and Applied Pharmacology*, 203, pp. 201-218

WOOD, S., Mountfort, D., Selwood, A., Holland, P., Puddick, J., Cary, C. (2008) *Widespread distribution and identification of eight novel microcystins in Antarctic cyanobacterial mats*. Applied and Environmental Microbiology, 74 (23), pp. 7243-7251

WUJECK, D. and Lincoln, T. (1988) *Ultrastructure and taxonomy of Oscillatoria pilicola, a new species of bluegreen alga from sloth hairs*. Brenesia, 16 (12-34), pp. 190-207

YAGI, M., Kajino, M., Matsuo, U., Ashitani, K., Kita, T., Nakamura, T. (1983) *Odor problems in Lake Biwa*. Water Science & Technology, (6-7), pp. 311-321

YAGI, M., Nakashima, S., Muramoto, S. (1988) *Biological degradation of musty odor compounds, 2-methylisoborneol and geosmin, in a bio-activated carbon filter*. Water Science & Technology, 20 (8-9), pp. 255-260

YOUNG, F., Morrison, L., James, J., Codd, G. (2008) *Quantification and localisation of microcystins in colonies of a laboratory strain of Microcystis (Cyanobacteria) using immunological methods*. European Journal of Phycology, 43 (2), pp. 217-225

YOUNG, F., Thomson, C., Metcalf, J., Lucocq, J., Codd, G. (2005) *Immunogold localisation of microcystins in cryosectioned cells of Microcystis*. Journal of Structural Biology, 151, pp. 208-214

YU, S. 1989. *Drinking water and primary liver cancer*. In: *Primary Liver Cancer*, Z.Y. Tang, M.C. Wu and S.S. Xia, Ed. China Academic Publishers: New York, pp. 30-37

YU, S., Chen, W., Li, J. (1995) *The prospective research of risk factors of primary liver cancer in Nanhui County, Shanghai*. *Zhonghua Liu Xing Bing Xue Za Zhi*, 16, pp. 22-24

YURKOWSKI, M. and TABACHEK, J. (1974) *Identification, analysis, and removal of geosmin from muddy-flavoured trout*. *Journal of the Fisheries Research Board of Canada*, 31, pp. 1851-1858

ZHOU, H. and SMITH, D. (2001) *Advanced technologies in water and waste water treatment*. *Canadian Journal of Civil Engineering*, 28 (1), pp. 49-66

ZILLIGES, Y., Kehr, J., Meissner, S., Ishida, K., Mikkat, S., Hagemann, M., Kaplan, A., Börner, T., Dittmann, E. (2011) *The cyanobacterial hepatotoxin Microcystin binds to proteins and increases the fitness of Microcystis under oxidative stress conditions*. *PLOS ONE*, 6 (3), pp. 1-11

ZILLIGES, Y., Kehr, J., Mikkat, S., Bouchier, C., de Marsac, N., Börner, T., Dittmann, E. (2008) *An extracellular glycoprotein is implicated in cell-cell contacts in the toxic cyanobacterium Microcystis aeruginosa PCC 7806*. *Journal of Bacteriology*, 190 (8), pp. 2871-2879

ZOHARY, T., Paismadeira, A., Robart, R., Hambright, K. (1995) *Cyanobacteria-phytoplankton dynamics of a hypertrophic African lake*. *Water Science and Technology*, 32 (4), pp. 103-104

ZURAWELL, R. (2002) *An initial assessment of microcystin in raw and treated municipal drinking water derived from eutrophic surface waters in Alberta*. Prepared for Alberta Environment, Science and Standards Branch, Edmonton, Alberta, Canada



## Appendix

---

## **7 Appendix**

As mentioned in chapter 4, the selected internal standard (decane) for the analysis of the cyanobacterial off-flavour compounds 2-MIB and GSM could ultimately not be employed for GC-MS due to contaminations in the solid phase extraction cartridges. These contaminations originated from the manufacture and have since been identified and rectified. Attached are GC-MS chromatograms from different batches of cartridges, different manufacturers, intact cartridges and the constituent cartridge parts tested separately, all indicating the contaminations.

Note: All data shown collected using a hydrocarbon scanning method m/z: 57, 71, 85.

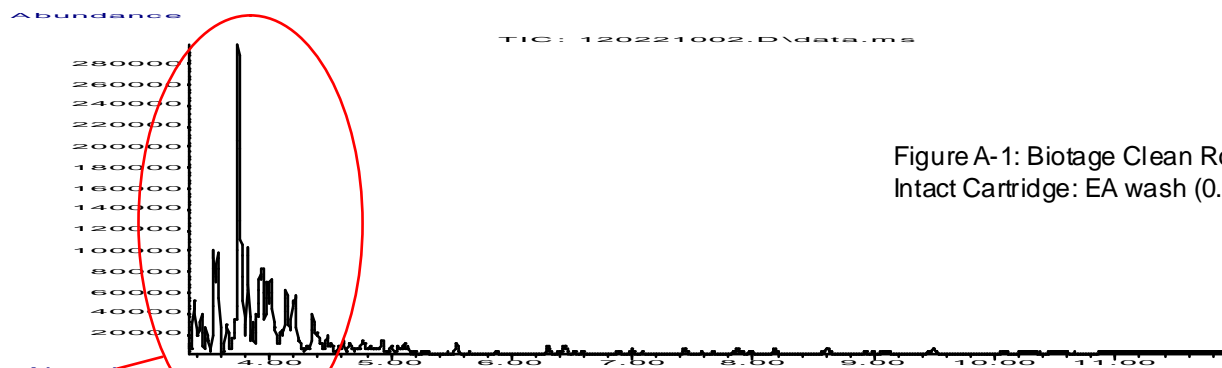


Figure A-1: Biotage Clean Room Sample  
Intact Cartridge: EA wash (0.5ml)

Hydrocarbon  
contamination

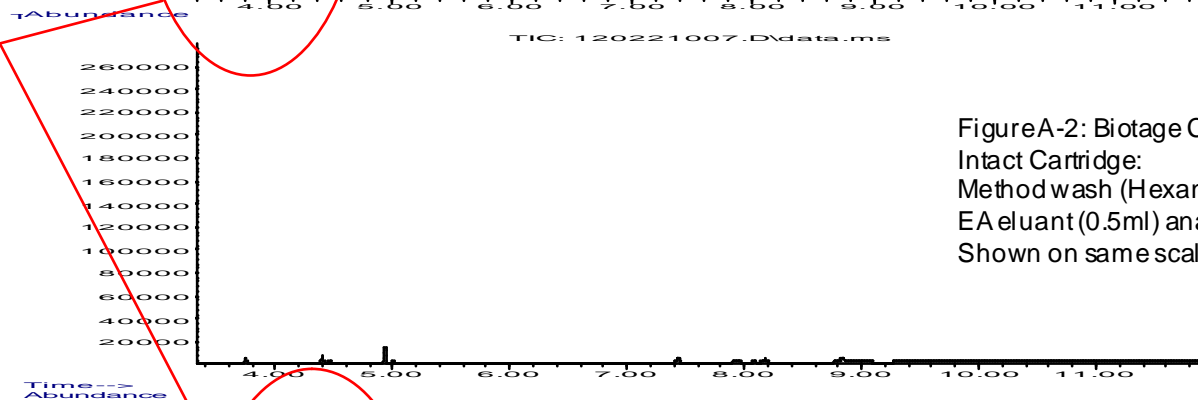


Figure A-2: Biotage Clean Room Sample  
Intact Cartridge:  
Method wash (Hexane – MeOH – MilliQ)  
EA eluant (0.5ml) analysed  
Shown on same scale as Figure A-1

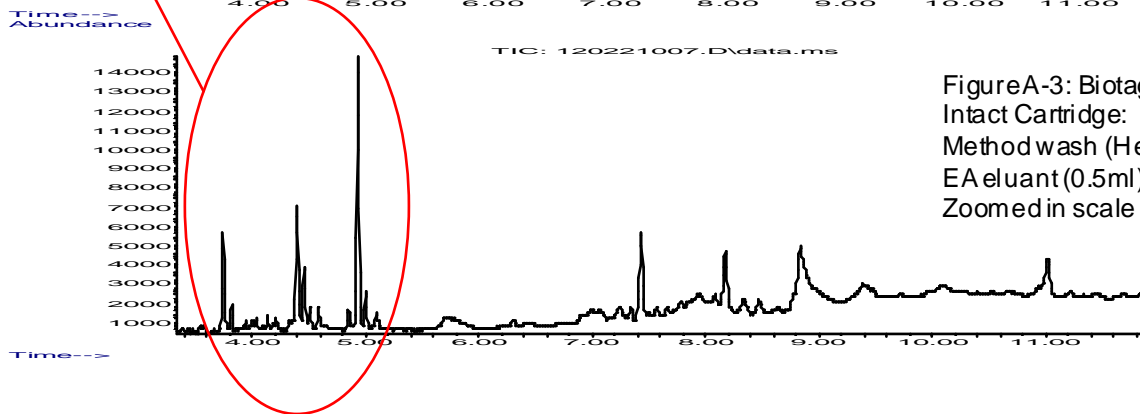
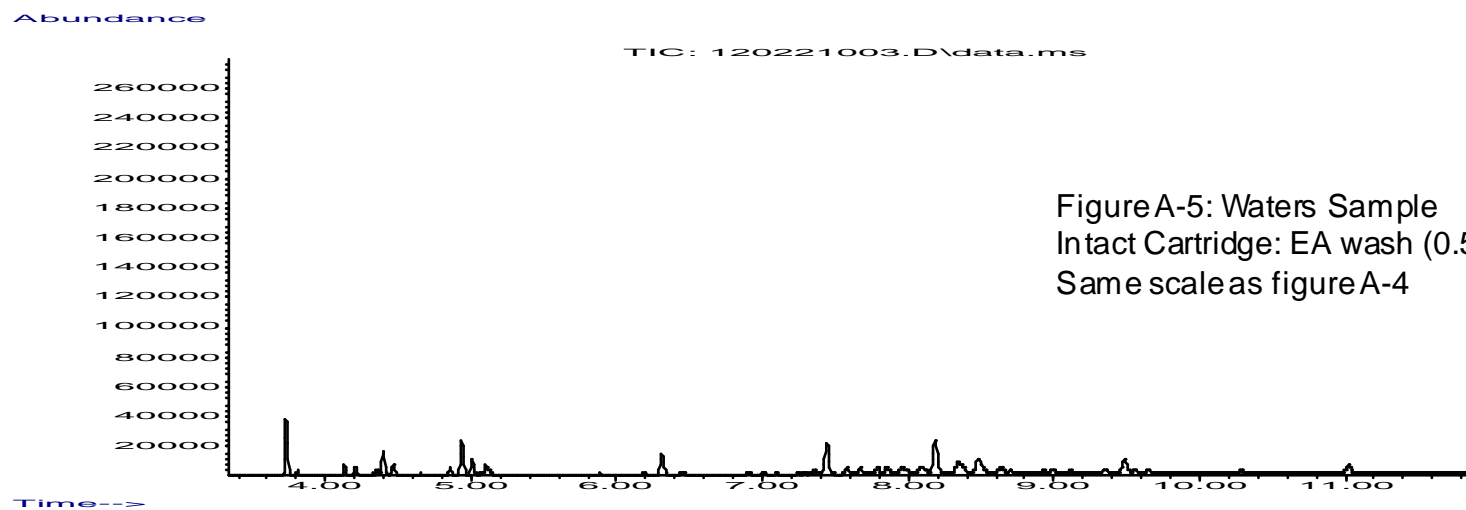
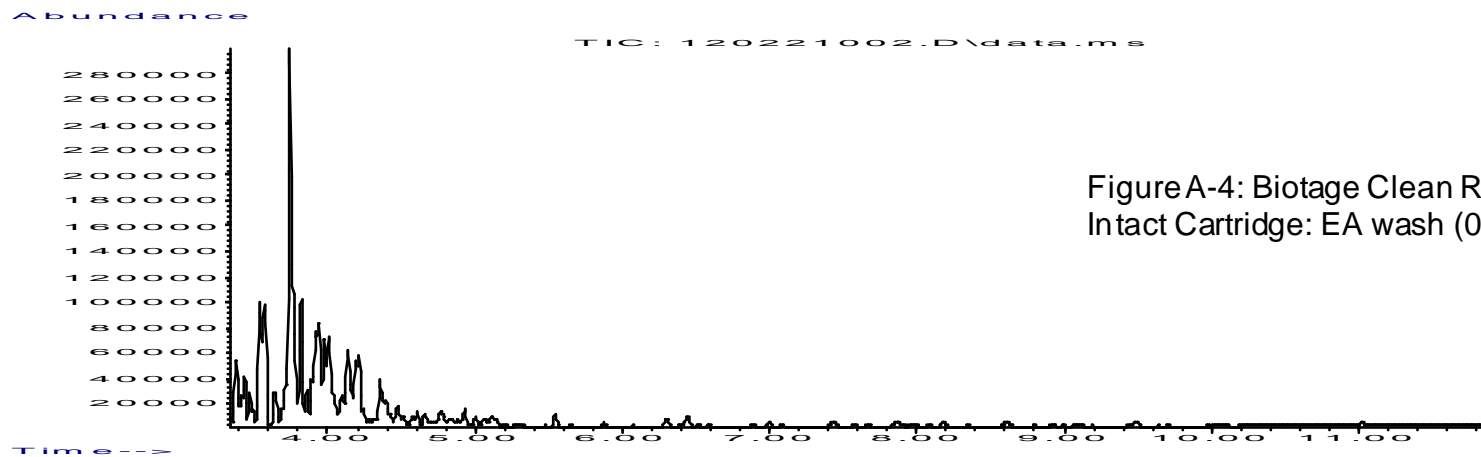


Figure A-3: Biotage Clean Room Sample  
Intact Cartridge:  
Method wash (Hexane – MeOH – MilliQ)  
EA eluant (0.5ml) analysed  
Zoomed in scale



Abundance

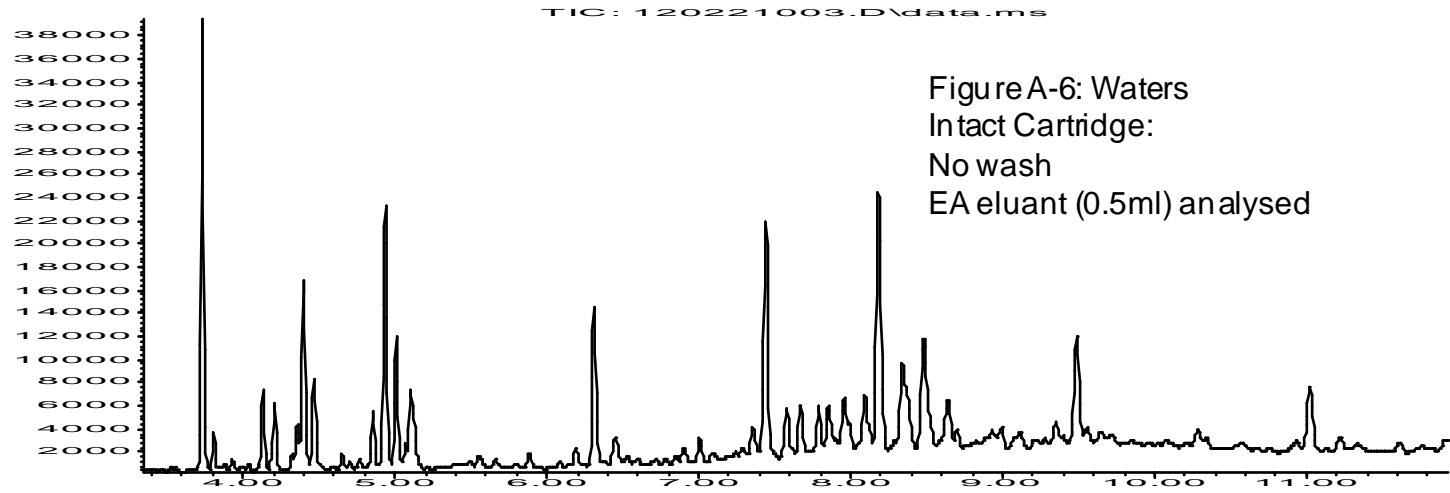


Figure A-6: Waters  
Intact Cartridge:  
No wash  
EA eluant (0.5ml) analysed

Abundance

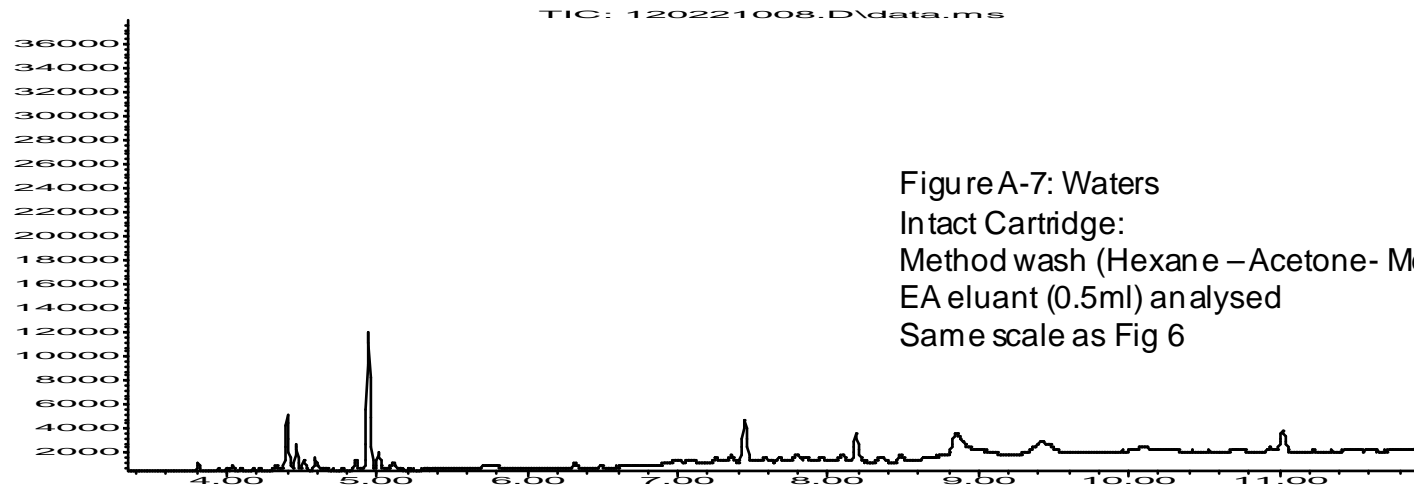
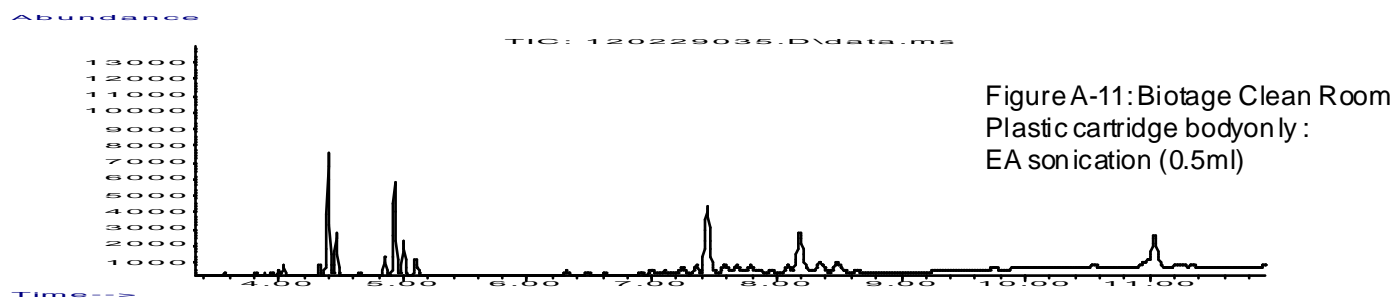
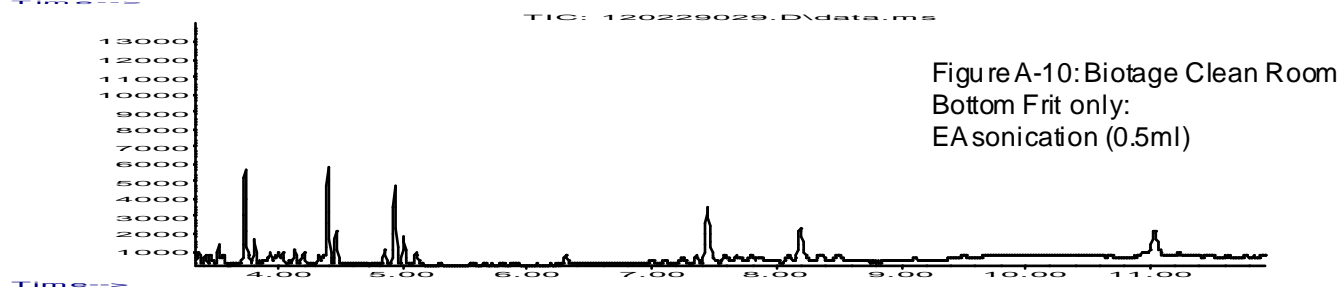
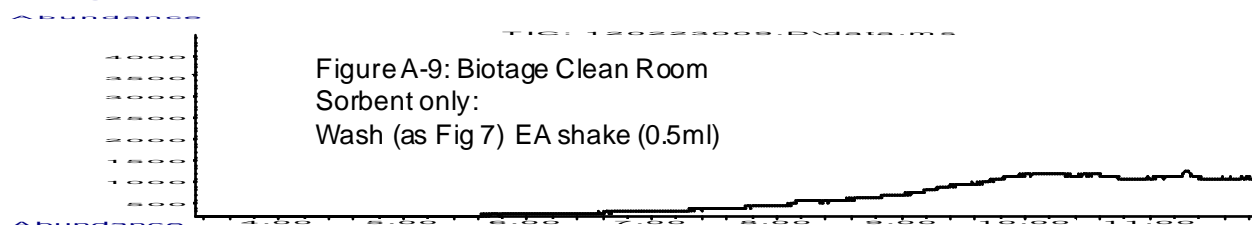
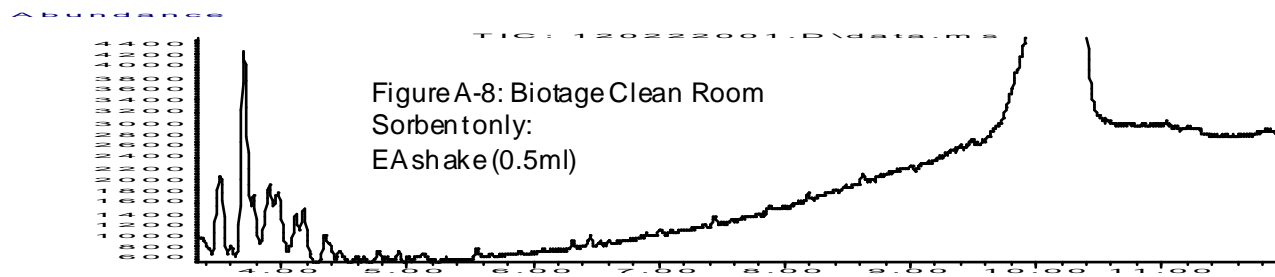


Figure A-7: Waters  
Intact Cartridge:  
Method wash (Hexane – Acetone- MeOH – MilliQ)  
EA eluant (0.5ml) analysed  
Same scale as Fig 6

Time-->



Abundance

TIC: 120229030.D\data.ms

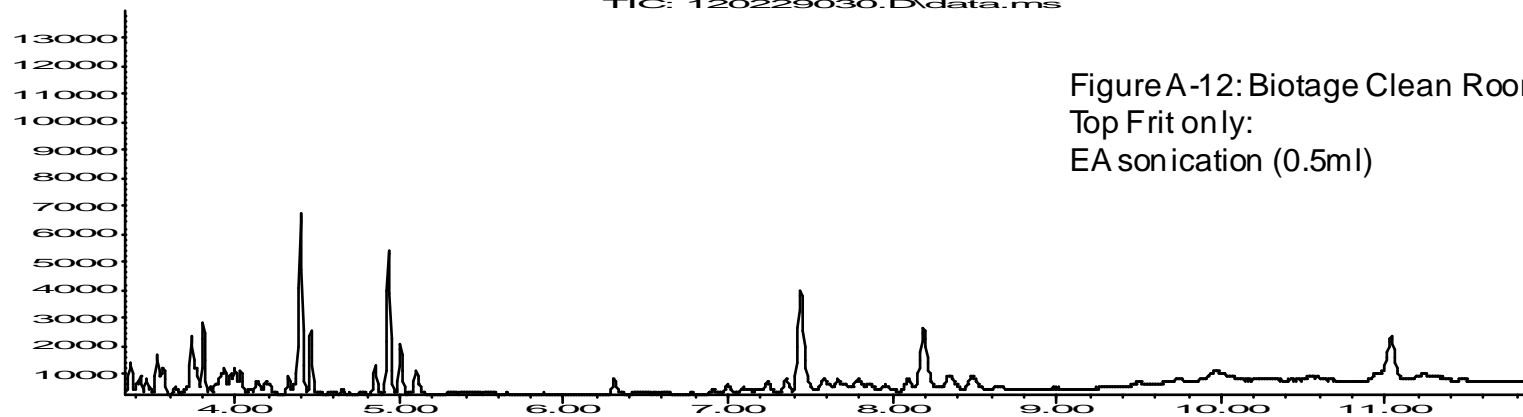


Figure A-12: Biotage Clean Room  
Top Frit only:  
EA sonication (0.5ml)

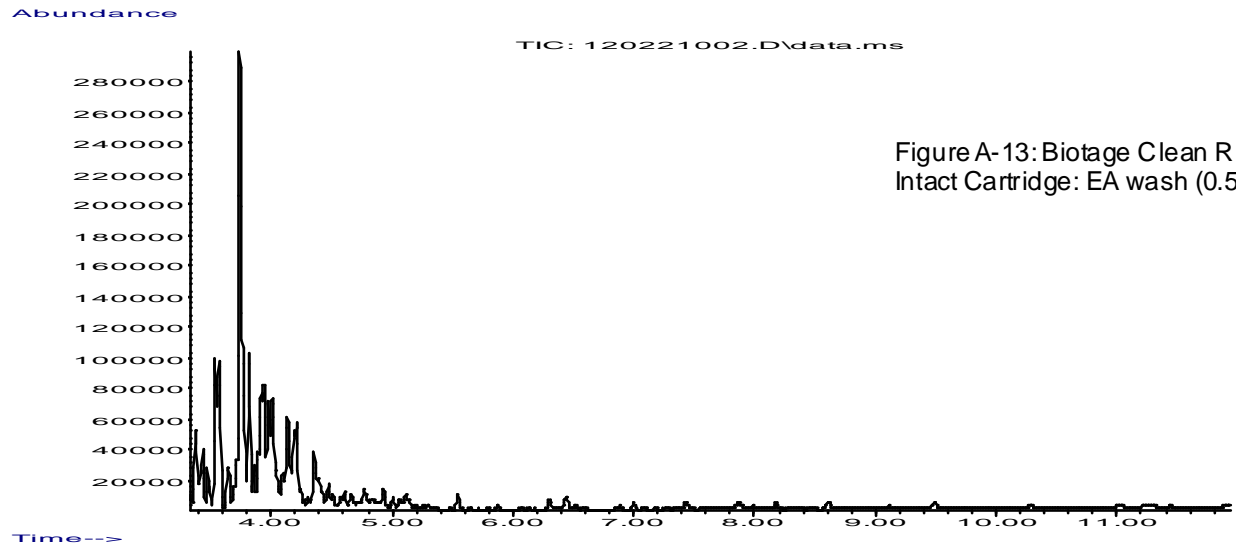


Figure A-13: Biotage Clean Room Sample  
Intact Cartridge: EA wash (0.5ml)

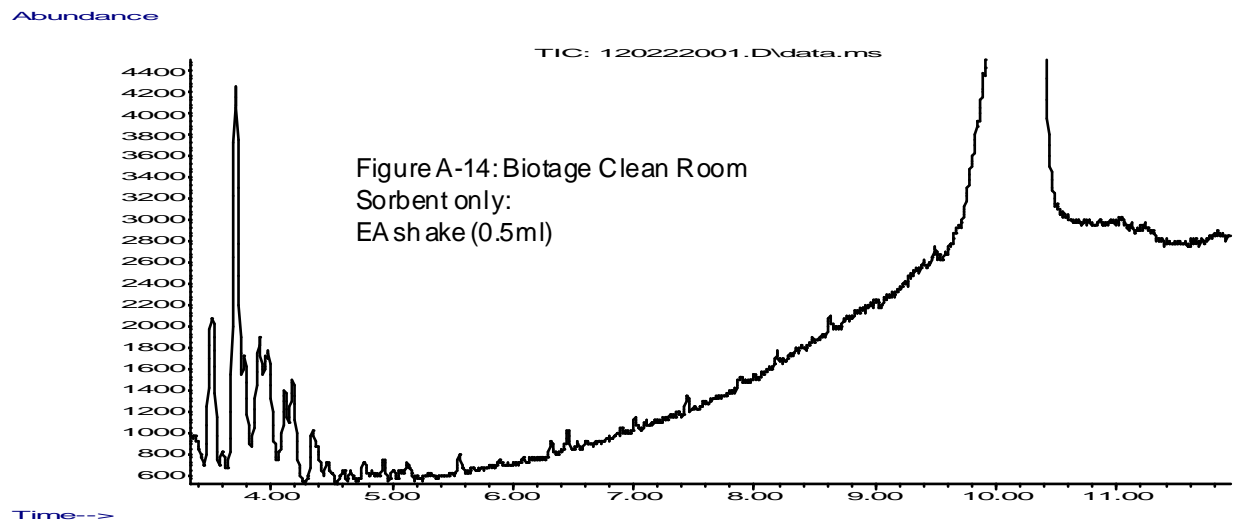
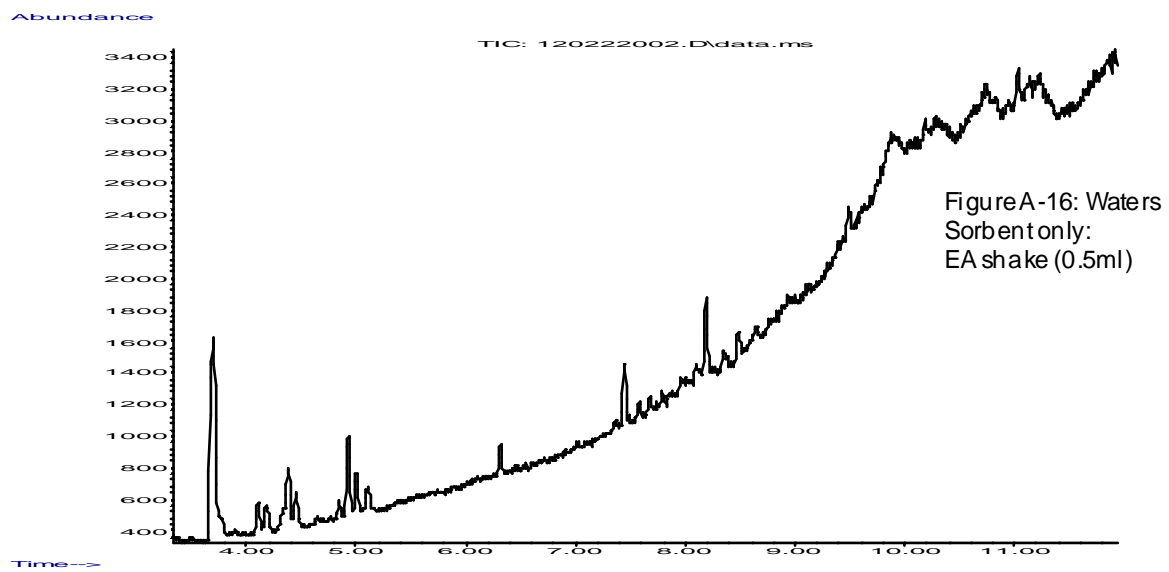
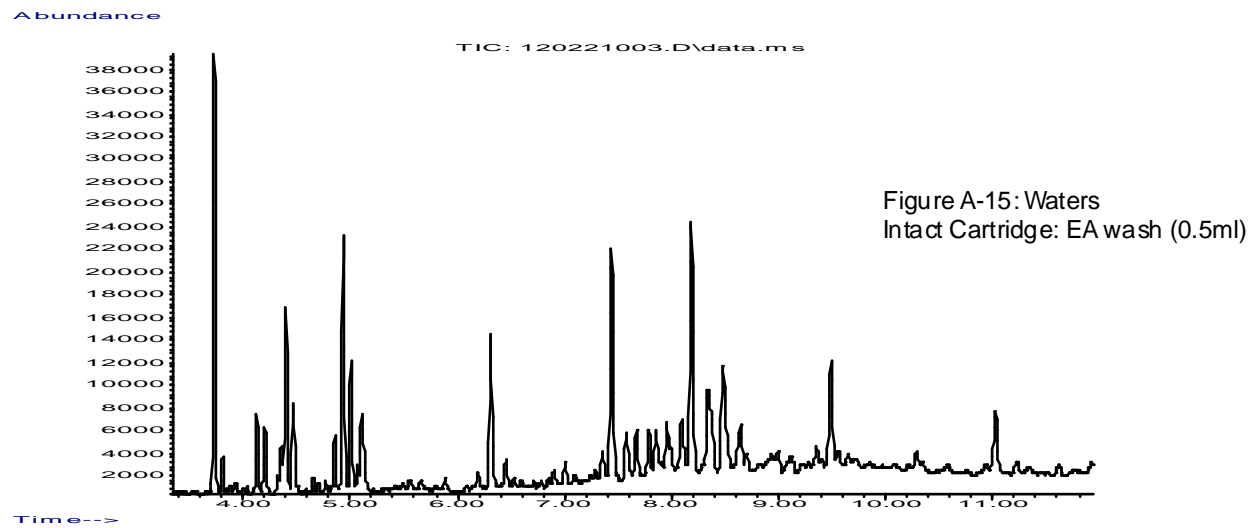
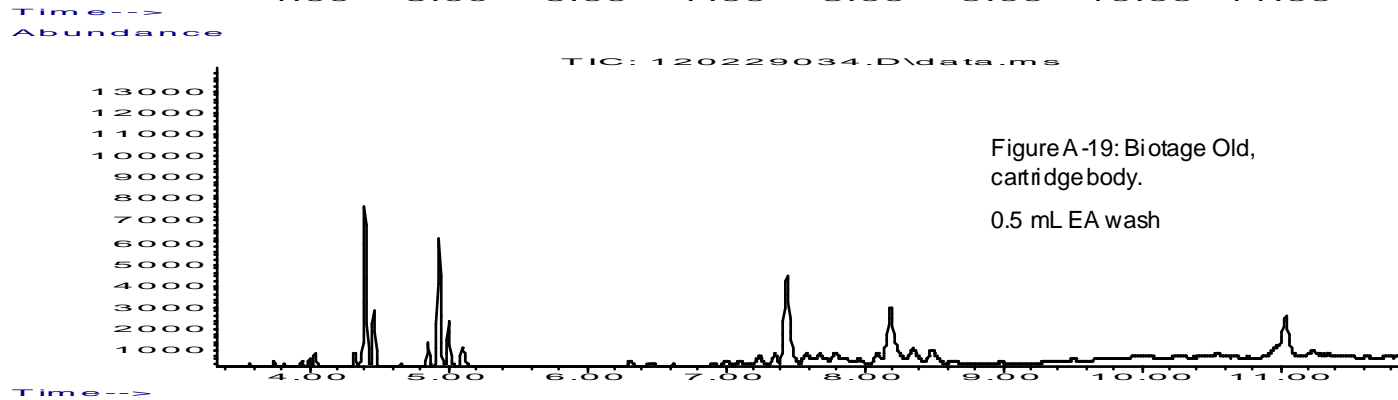
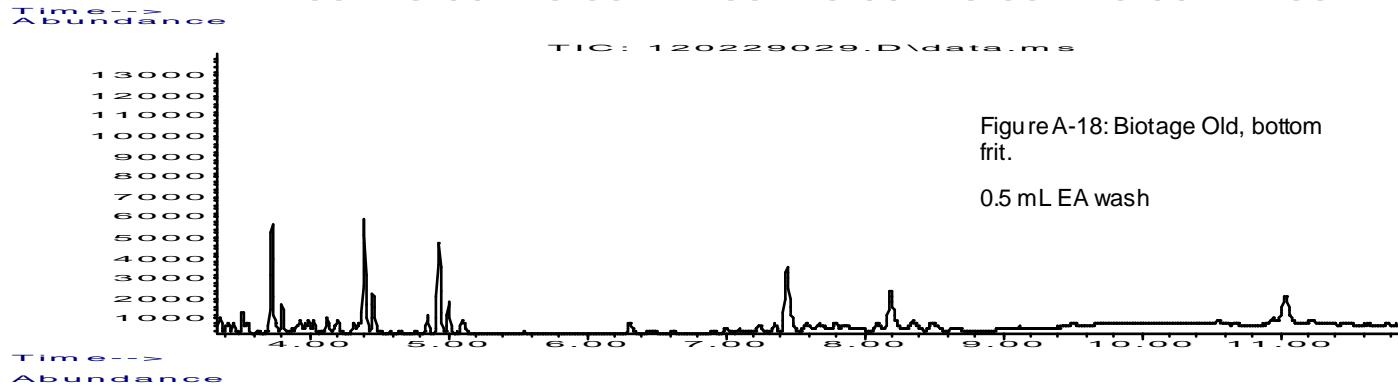
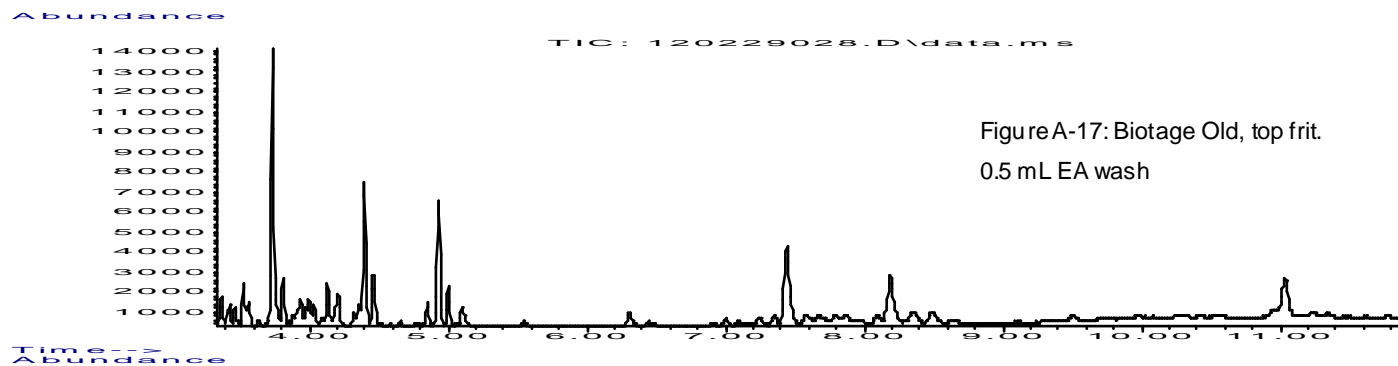


Figure A-14: Biotage Clean Room  
Sorbent only:  
EA shake (0.5ml)







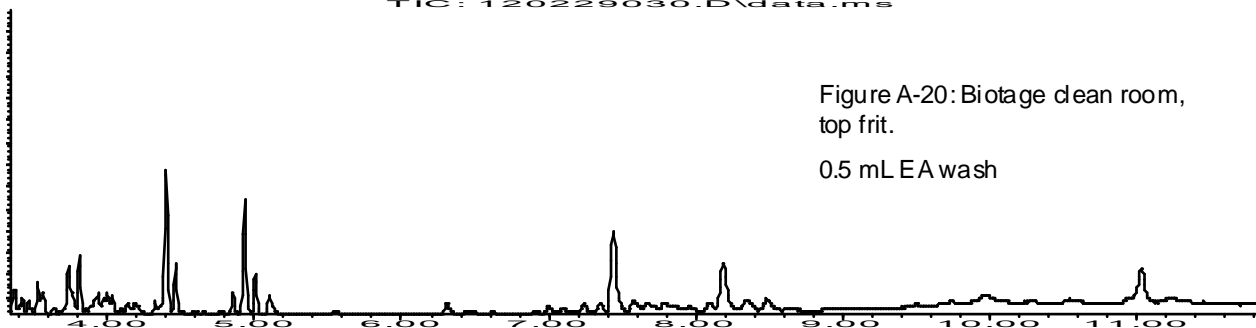
Abundance

TIC: 120229030.D\data.ms

13000  
12000  
11000  
10000  
9000  
8000  
7000  
6000  
5000  
4000  
3000  
2000  
1000

Figure A-20: Biotage clean room,  
top frit.

0.5 mL EA wash



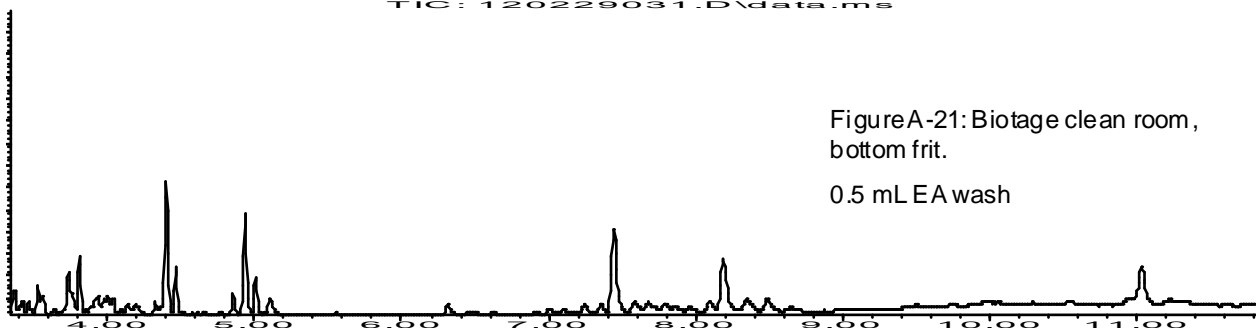
Time-->  
Abundance

TIC: 120229031.D\data.ms

13000  
12000  
11000  
10000  
9000  
8000  
7000  
6000  
5000  
4000  
3000  
2000  
1000

Figure A-21: Biotage clean room,  
bottom frit.

0.5 mL EA wash



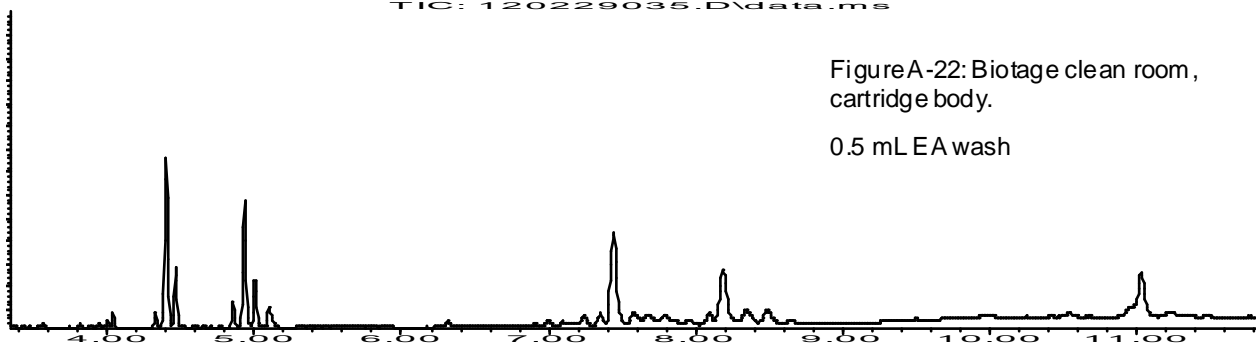
Abundance

TIC: 120229035.D\data.ms

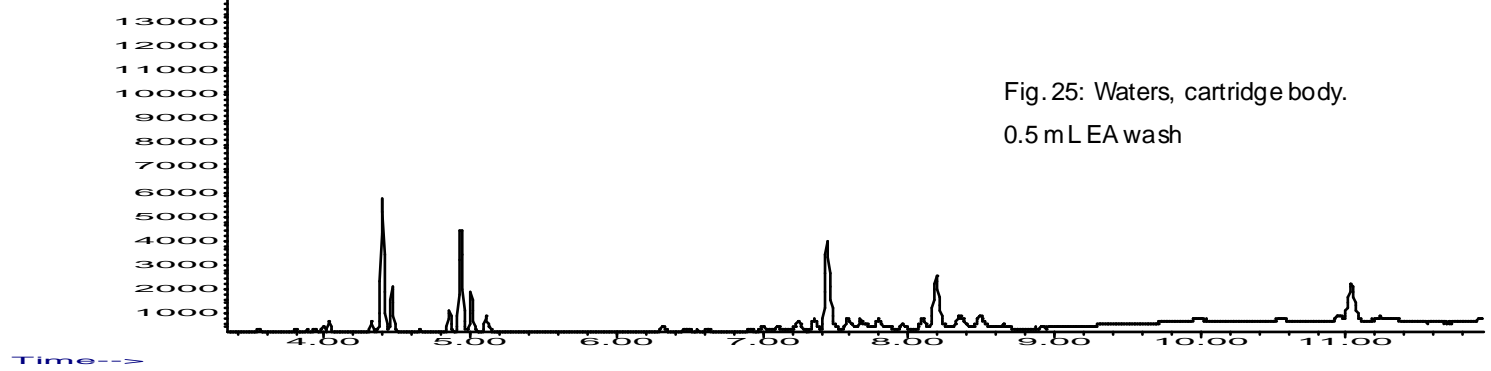
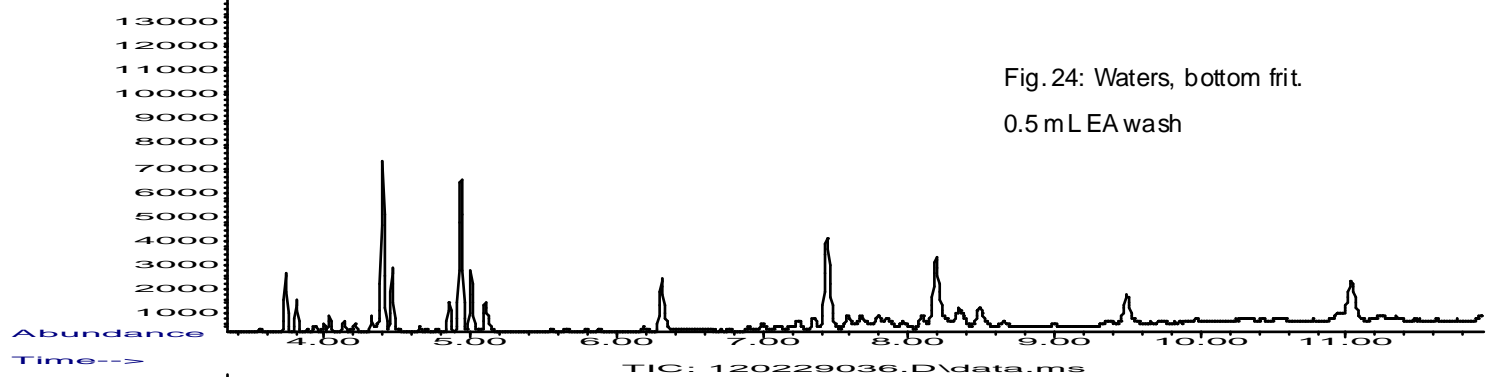
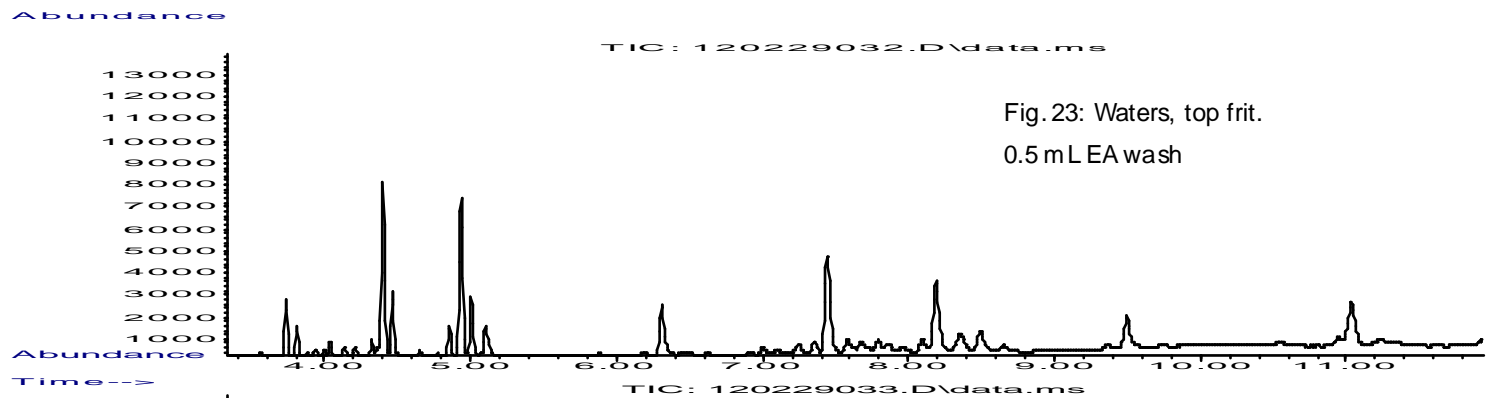
13000  
12000  
11000  
10000  
9000  
8000  
7000  
6000  
5000  
4000  
3000  
2000  
1000

Figure A-22: Biotage clean room,  
cartridge body.

0.5 mL EA wash



Time-->



## Scientific Output

---

## 8 Scientific Output

**PESTANA, C.**, Prabhu, R., Robertson, P., Lawton, L., Banks, M., Johnston, T. (2011) *Photocatalytic degradation properties of Photospheres™ for waste water treatment*. International Conference on Photocatalytic and Advanced Oxidation Technologies for the Treatment of Water, Air, Soil and Surfaces. 4-8 July 2011, Gdansk, Poland

MCKENZIE, C., **Pestana, C.**, Buksh, E., Edwards, C., Lawton, L. (2011) *The rapid analysis of geosmin and 2-methylisoborneol from aqueous samples and solid sample extracts using solid phase extraction and pulsed splitless injection gas chromatography-mass spectroscopy*. 9<sup>th</sup> IWA Symposium on Off-flavours in the Aquatic Environment. 14-19 August 2011, Aberdeen, Scotland

BAWDEN, B., McKenzie, C., **Pestana, C.**, Edwards, C., Lawton, L. (2011) *Novel treatment technology for removal of T&O compounds in recirculating aquaculture systems*. 9<sup>th</sup> IWA Symposium on Off-flavours in the Aquatic Environment. 14-19 August 2011, Aberdeen, Scotland

PRABHU, R., **Pestana, C.**, Lawton, L., Robertson, P., Johnston, T. (2011) *Application of Photospheres™ in waste water treatment*. 9<sup>th</sup> IWA Symposium on Off-flavours in the Aquatic Environment. 14-19 August 2011, Aberdeen, Scotland

**PESTANA, C.**, Lawton, L., Edwards, C. (2010) *A novel approach for the removal of microcystins from water by photocatalysis: Microspheres*. 8<sup>th</sup> International Conference on Toxic Cyanobacteria, 2-9 September 2010, Istanbul, Turkey

**PESTANA, C.**, Lawton, L., Edwards, C. (2009) *Cyanobacterial signalling compounds and water safety*. Research Student Symposium, Robert Gordon University, 10 October 2009

**PESTANA, C.**, Lawton, L., Edwards, C. (2009) *Unravelling cyanobacterial signalling compounds*. Society for General Microbiology, autumn meeting. 7-12 September 2009, Edinburgh, Scotland